UNIVERSITÀ DEGLI STUDI
DI MILANO

FACOLTÀ DI SCIENZE DEL FARMACO

*Department of Pharmaceutical Science*

**DOCTORATE SCHOOL IN CHEMICAL SCIENCE AND TECHNOLOGIES**

*Curriculum*

***Pharmaceutical Sciences (XXVII Cycle)***

**CHIM/08**

# SYNTHESIS AND STRUCTURE-ACTIVITY RELATIONSHIP OF NEW SUBTYPE SELECTIVE KA RECEPTOR LIGANDS

**Federica Mastronardi**
**R09585**

*Tutor*: Prof. Paola Conti
*Coordinator*: Prof. Ermanno Valoti

Academic year 2013/2014

# Summary:

# ABBREVIATIONS

| | |
|---|---|
| **AMPA** | (*S*)-2-amino-3-(3-hydroxy-7,8-dihydro-6*H*-cyclohepta[*d*]-4-isoxazolyl)proprionic acid |
| **AMPAR** | AMPA receptor |
| **ATD** | amino terminal domain |
| **ATP** | adenosine triphosphate |
| **CNS** | central nervous system |
| **CTD** | carboxy terminal domain |
| **DA** | domoic acid/domoate |
| **DH** | dysiherbaine |
| **DHKA** | dihydrokainate |
| **EAAT** | excitatory amino acid transporter |
| **EPSC** | excitatory postsynaptic current |
| **ER** | endoplasmic reticulum |
| **GABA** | gamma-aminobutyric acid |
| **GDH** | glutamate dehydrogenase |
| **Gln** | glutamine |
| **Glu** | glutamate |
| **GLS** | glutaminase |
| **iGluR** | ionotropic glutamate receptor |
| **KA** | kainate |
| **KAR** | kainate receptor |
| **LBD** | ligand binding domain |
| **LTP** | long term potentiation |
| **MW** | molecular weight |
| **mGluR** | metabotropic glutamate receptor |
| **NMDA** | N-Methyl-D-aspartic acid |
| **NMDAR** | NMDA receptor |

# CHAPTER 1. INTRODUCTION

## 1.1 PHYSIOLOGICAL ROLE OF GLUTAMIC ACID

The excitatory action of L-Glutamic acid (Glu) (*Figure 1.1*) in the mammalian brain and spinal cord has been known since the 1950s, however it was not until the late 1970s that it became widely recognized that glutamate is the principal excitatory transmitter within the mammalian central nervous system (CNS).[1] It has been proved that Glutamate is released by neuron terminals in a calcium dependent manner, in response to depolarization. Nowadays, it is well known that glutamate synaptic release is involved in the modulation of many physiological processes, i.e. sensations and pain perception and cognitive functions regulation. Furthermore, Glu plays a key role in synaptic plasticity.[2] This plasticity is manifested mainly through the phenomenon of long-term potentiation (LTP), which was firstly discovered in the hippocampus but has subsequently been demonstrated in many regions of the cortex. LTP is a long-lasting strengthening in signal transmission between two neurons that are activated synchronously and is widely considered one of the major cellular mechanisms that underlie learning and memory.[3,4]

Together with GABA, these neurotransmitters are responsible for the activation and the inhibition of the entire brain and their balance is the basis of CNS functionality.

***Figure 1.1.*** L-Glutamic acid

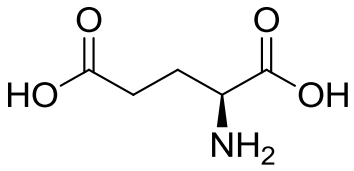

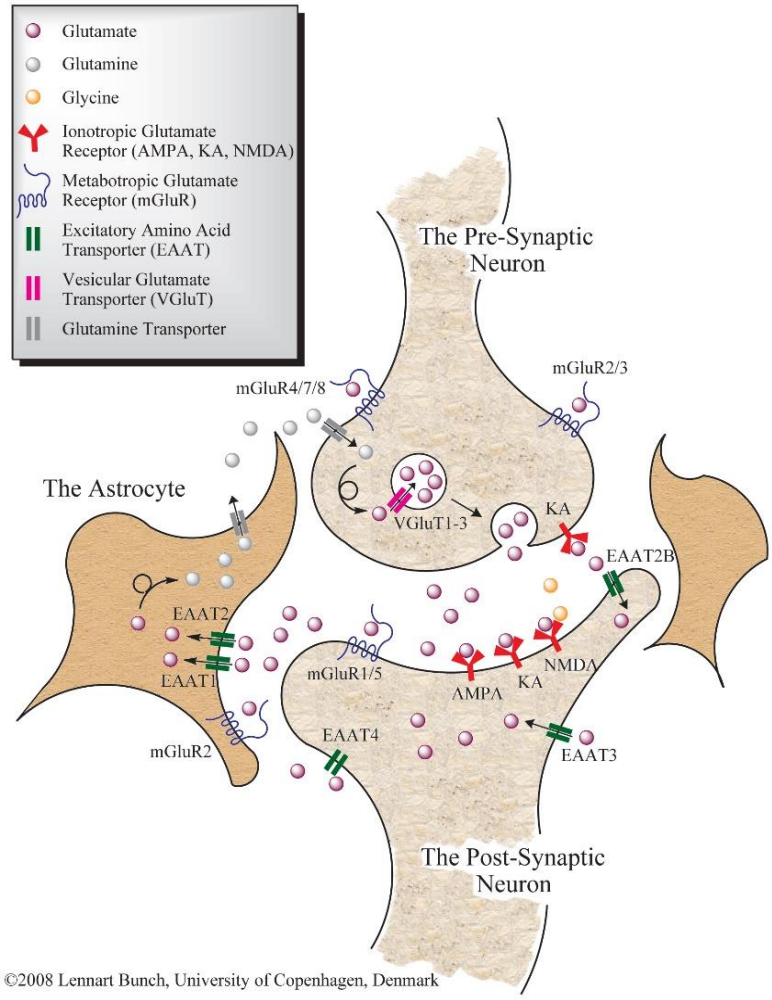


***Figure 1.2.*** Synaptic transmission of glutamate in the CNS. From Lennart, 2008.

## 1.2 BIOSYNTHESIS

Glutamate is a non-essential amino acid, which means that mammalian body can synthesize it without any dietary intake. As glutamate plays many roles in mammalian metabolism, there are no unique synthetic ways to produce it. In nerve terminals, L-Glu can be synthesized from α-ketoglutarate (deriving from gluconeogenesis and the tricarboxylic acid cycle) by the enzyme glutamate dehydrogenase (GDH), and from glutamine by the phosphate-activated enzyme glutaminase (GLS).

## 1.3 STORAGE AND RELEASE

L-Glu is stored in the cytoplasm of neurons in specific synaptic vesicles. The family of vesicular glutamate transporters in mammals is comprised of three homologous proteins: VGLUT1-3. These work using a proton gradient that they create by hydrolysing adenosine triphosphate (ATP) and thus creating a pH gradient across the membrane. Consequently, the anionic L-Glu is carried into the interior of the vesicles, where it can reach a concentration of 100 mM or more.[5]

Upon activation of the presynaptic neurons, the level of the internal $Ca^{2+}$ increases and this event triggers the fusion of the vesicles with the plasmatic membrane; therefore, glutamate is released into the synaptic cleft and can interact with different targets comprising receptors, transporters and enzymes. When glutamate is released in the synaptic cleft its concentration can vary from 2 to 1000 µM (*Figure 1.2*).[6]

## 1.4. REUPTAKE: EXCITATORY AMINO ACID TRANSPORTERS (EAATs)

Glutamate is removed from the synaptic cleft by the excitatory amino acid transporters (EAATs). Five types of high-affinity Glu transporters (EAAT1–5) have been identified. These proteins are located in the plasma membrane of the neurons (EAAT3-4), in the glial cells (EAAT1-2) and the latter type in rod photoreceptors and bipolar cells of the retina. The transporters EAAT1 and EAAT2 in glial cells are responsible for the majority of Glu uptake, while neuronal EAATs appear to have specialized roles at particular types of synapses. Dysfunction of EAATs is implicated in neurodegenerative conditions such as amyotrophic lateral sclerosis, epilepsy, Huntington's disease, Alzheimer's disease and ischemic stroke injury and thus the modulation of EAAT function may prove beneficial in these disorders.[7]

When reuptake is due to EAAT1-2, glutamate is converted first to glutamine (Gln), which is later taken up by the presynaptic neurons and transformed into Glu. Instead, when glutamate is removed by transporters settled in the presynaptic membrane, it is directly stored into the vesicles. In this way the concentration of Glu in the synaptic cleft is kept under control at physiological conditions, because high levels of this neurotransmitter cause pathological conditions.

## 1.5 GLUTAMATE RELATED DISEASES

Due to the close correlation between glutamate excitatory activity and its neurotoxicity, in 1968 Onley formulated the so-called "Excitotoxicity" hypothesis, affirming that the neuronal degeneration is due to a prolonged activation of the same post-synaptic receptors responsible for Glutamate excitatory activity: persistent concentrations in the range of 50-100 µM provoke a serious condition named excitotoxicity (*Figure 1.3*). In this situation, glutamatergic neurons are over-activated and the resulting membrane depolarization causes an abnormal influx of sodium and calcium into the cells. The increase of intracellular sodium leads to the activation of the $Na^{+}$-$Ca^{2+}$ transporter, which promotes a further entry of calcium. This is the ascribed ion for the excitotoxicity process: high levels determine the activation of caspases, an increase of the oxidative stress and the enhancement of the synthesis of nitric oxide (NO). This molecule, in turn, is a retrograde messenger that exacerbates neurons excitability enhancing the glutamate release in presynaptic neurons and it is also involved in the impairment of the antioxidant status of the cells. The final result is neuron death due to apoptosis and necrosis (*Figure 1.3*).[8]

Over-stimulation of the glutamatergic system can be caused by a facilitation of glutamate release from nerve terminals but it can also be produced by a reduced functionality of glutamate transporters.

Excitotoxicity is a common mechanism found in a plethora of striking neuropatological conditions, such as stroke, Alzheimer's disease, Huntington's disease, multiple sclerosis, Parkinson's disease and epilepsy.[9,10]. Moreover, an imbalance between glutamatergic neurotransmission and others is responsible for many mental and neurologic disorders. For example, one of the causes of epilepsy is a prevalence of the glutamatergic system over the GABAergic one and one of the principal determinants of schizophrenia is a diminished functionality of the NMDA receptors that, in turn, contribute to a reduced inhibitory capacity of GABAergic neurons (glutamatergic hypothesis of schizophrenia).[11]

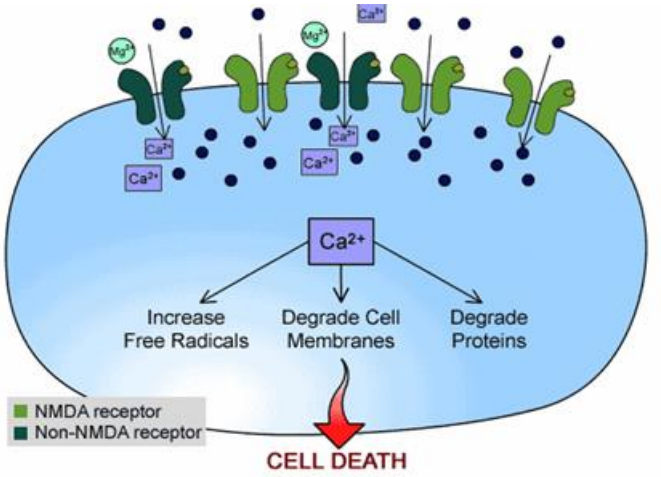


***Figure 1.3.*** Excitotoxicity

Because excitotoxicity may be involved in several neurodegenerative pathologies and neurologic disturbances, the glutamatergic system is recognized as an important therapeutic target. A major goal for medicinal chemists is undoubtedly to identify subtype-selective Glu receptor ligands capable of selectively activating, blocking or modulating the various receptor subtypes, which are characterized by a different CNS distribution and physiological functions. Such ligands would represent essential pharmacological tools and may be further developed into therapeutically useful drugs with minimized side effects.

## 1.6 GLUTAMIC ACID RECEPTORS

Glutamate and other excitatory amino acids operate through different classes of receptors. Their classification is based on pharmacological studies regarding the interaction with selective agonists and antagonists. Glu receptors are divided in two big families, depending on the signal transduction mechanism: ionotropic Glu receptors (iGluRs) and metabotropic Glu receptors (mGluRs), which are G-protein coupled receptors[12]. Eight subtypes of mGluRs have been characterized (mGluR1-8) and they have been subclassified in mGluRI (mGluR1,5), which stimulates phospholipase C, mGluRII (mGluR2,3) and mGluRIII (mGluR4,6-8), which both inhibit adenylyl cyclase enzyme.[13]

Ionotropic Glu receptors (iGluRs) are ligand gated ion channels that, upon activation, trigger the influx of cations ($Na^+$, $K^+$, $Ca^{2+}$), which in turn determines fast depolarization of the post-synaptic

membrane. iGluRs are tetrameric and are composed by four subunits forming the transmembrane ionic channel permeable to $Na^+$, $K^+$ and $Ca^{2+}$ ions. The membrane depolarization generates at last the postsynaptic excitatory stimulus.

The three heterogeneous classes of iGluRs are:

- *N*-methyl-D-aspartic acid (NMDA) receptors
- (*RS*)-2-amino-3-(3-hydroxy-5-methyl-4-isoxazolyl)propionic acid (AMPA) receptors
- kainic acid (KA) receptors [14,15]

This classification is based on the specific interaction with the selective ligands above mentioned (*Figure 1.4*).

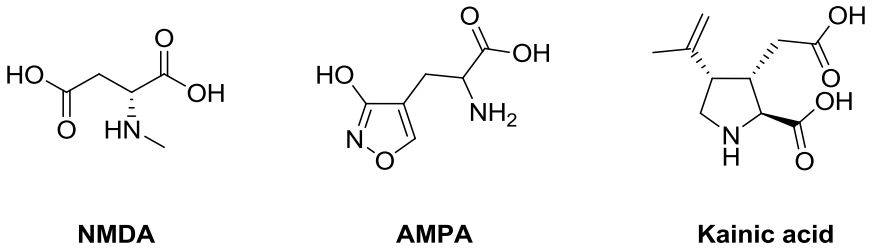


***Figure 1.4.*** iGluRs selective substrates

Each receptor class is formed by various receptor subtypes, depending on subunits assembly. On the basis of sequence homologies, the Glu receptor subunits can be divided into six groups: [16]

- GluA1-GluA4 (previously: GluR1-GluR4), AMPA receptors subunits
- GluK1-GluK3 (previously: GluR5-GluR7), low affinity KA receptors subunits
- GluK4 e GluK5 (previously: KA1 e KA2), high affinity KA receptors subunits
- GluN1 (previously: NR1), NMDA receptors subunits
- GluN2A-2D (previously: NR2A-NR2D), NMDA receptors subunits
- GluN3A-B (previously: NR3A-NR3B), NMDA receptors subunits

A seventh group consists of two orphan subunits, $\delta$1 and $\delta$2, but these subunits do not form channels activated by Glu, nor do they assemble with any of the other Glu receptor subunits. Mutations on these subunits are associated with schizophrenia.[17]

Evidence derived from different studies is consistent with a predominantly postsynaptic localization of NMDA and AMPA receptors. They are co-expressed in most excitatory terminals, but some terminals only express NMDA receptors and would require membrane depolarization to allow activation.[18] Early lesion studies combined with [$^3$H]-KA binding suggested that a substantial number of KA receptors were located at presynaptic terminals.[19] Activation of presynaptic KA receptors seems to have a regulative action on glutamate release. Employing the GluK1 partial selective antagonist LY294486, it was demonstrated that GluK1 containing receptors are also involved in the reduction of evoked GABA (inhibitory neurotransmitter) release from hippocampal pre-synaptic neurons by a G-protein coupled mechanism.[20] Moreover, KA receptors are also located at postsynaptic terminals.

## 1.7 IONOTROPIC RECEPTORS

The iGluRs topology was debated for a long time, especially because of the difficulty of crystallizing a receptor, with or without a ligand. The elevate similitude grade of the various Glu receptors subunits suggests that NMDA, AMPA and KA receptors have similar architecture.

The family of iGluRs is composed by tetrameric membrane proteins, all of which consist of four subunits (> 900 residues) assembled together to form the inner ion channel pore. Each subunit can be divided into four different domains: the extracellular amino terminal domain (ATD), the extracellular ligand binding domain (LBD), the transmembrane domain and the intracellular carboxyl-terminal domain (CTD). The receptors have an overall 2-fold symmetry perpendicular to the membrane plane (*Figure 1.5*).

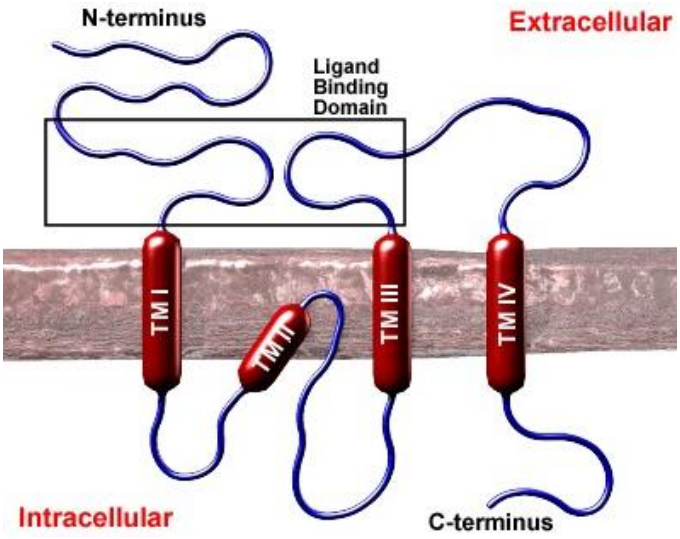


***Figure 1.5.*** Schematized iGluR structure

It should be pointed out that, due to technical difficulties in expressing and crystallizing multimeric membrane proteins, the majority of the structural studies have been done on isolated domains of iGluRs and thus crystallographic studies have been carried out focusing on the complex between a ligand and the LBD of the receptor. This has been possible because it was validated that the agonist binding site in the soluble LBD resembles very well the binding site of intact receptors.[21]

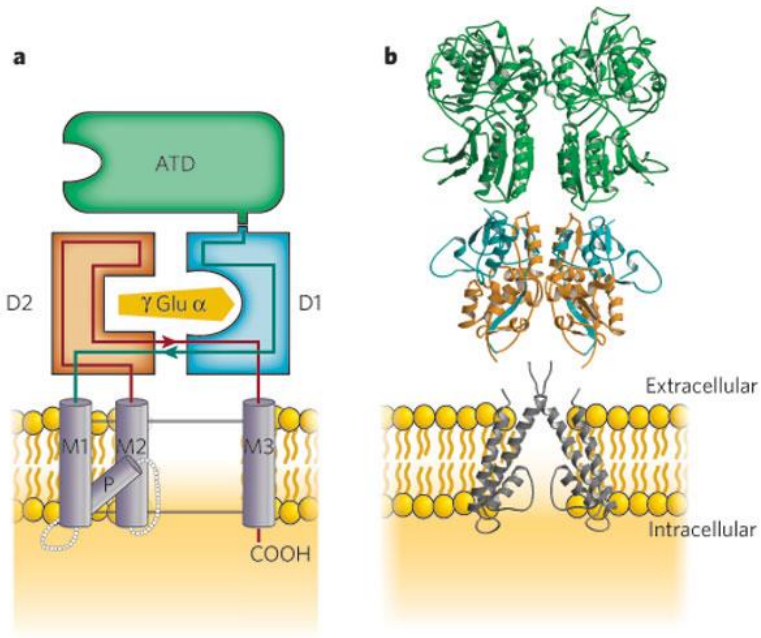


***Figure 1.6.*** Modular structure of a glutamate receptor.[22]

The ATD seems to have a regulatory role and it is involved in receptor trafficking, localization and subunits dimerization, which is probably the initial step of receptor assembly process. Moreover, the ATD is the site of action of a certain number of molecules that modulate the receptors.[23] Like the LBD, also the ATD adopts a clamshell like conformation, consisting by R1 and R2 lobes, and assembles as dimers.[24] After the first structure of ATD of GluA2 was solved, more and more crystal structures of this domain are emerging, providing further insight into its influence over the dynamic of the full-length receptor. The LBD adopts a clamshell like conformation and the agonist binding site is located within the cleft between two lobes, D1 and D2.[25]

In particular the D1-lobe is mainly constituted by the S1 segment, while the D2-lobe contains most of the S2 segment (*Figure 1.6*).

The glutamate binding site is conserved throughout the iGluRs and, among them, also in subtype-specific subunits. This is due to chemical interactions between conserved amino acids that are crucial for the activation of glutamate receptors; in particular, these are the salt bridge formed by the $\alpha$-carboxylate of glutamate and the arginine residue in lobe D1, the salt bridge between the glutamate residue in the lobe D2 and the $\alpha$-ammonium group of the bound glutamate and the salt bridge between a Thr690 residue of the lobe D2 and the distal carboxylate of the bound glutamate (*Figure 1.7*).[26,27]

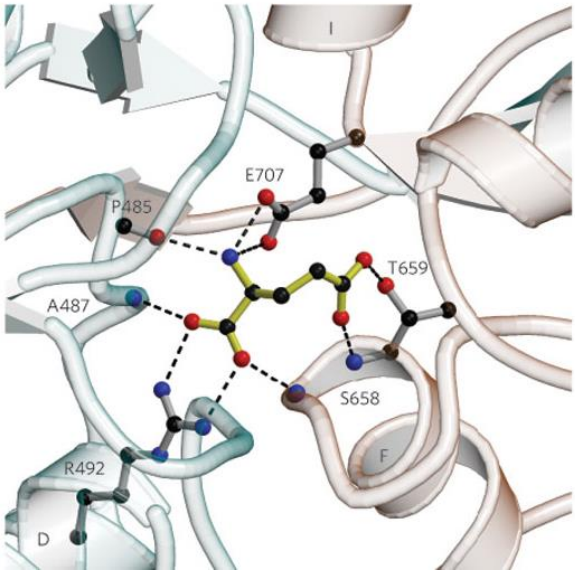


***Figure 1.7.*** Conserved amino acid residues in the ligand binding site. The Arg (R492), Glu (E707) and Thr (T659) side chains bind glutamate. Dashed lines indicate hydrogen bonds. The ligand binding site of GluK2 is showed.[22]

It has been established that the degree of domain closure is directly linked to the receptor activation.[28] Indeed, upon the binding of an agonist, the D2 domain moves towards D1, causing the cleft closure to occur and this movement is followed by conformational changes in the transmembrane domain. This conformational change induces a specific degree of domain closure that varies among different agonists (*Figure 1.8*).

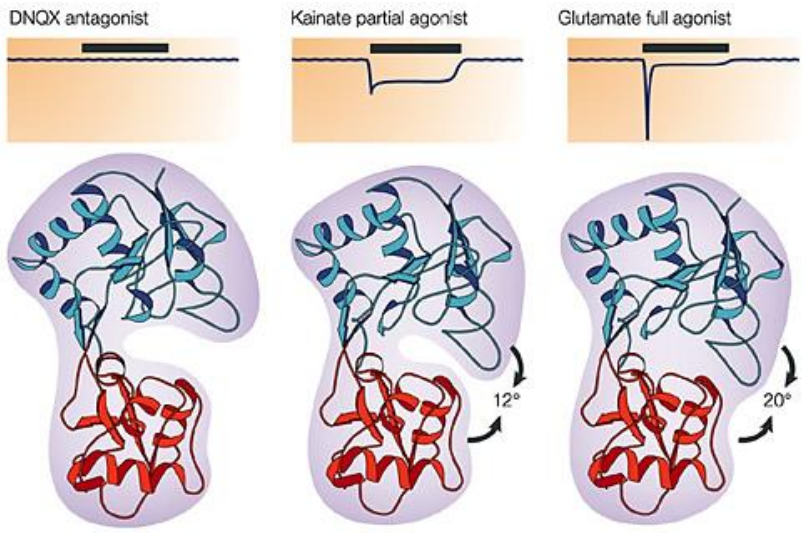


***Figure 1.8.*** Cleft closure upon the binding of different ligands. Structures of the S1S2 domain are showed[29]

The movement of D1 and D2 relative to each other provokes instability at the TMD and at the LBD dimer interface. Stability can be restored by LBD reopening, that is the first step of agonist dissociation. Alternatively, this reduced stability can lead to a rearrangement of the dimer interface of the receptor, resulting, as we see later, in a desensitized state.[30]

When an antagonist is bound, the movement of D2 lobe is prohibited, that means that the LBD is stabilized in the open conformation and the channel remains closed (*Figure 1.8*).

The arrangement of the D1 and D2 lobe is also critical for the kinetics of receptors; when a receptor is in the resting (apo) state can bind an agonist, which in turn will determine the closure of the clamshell and the opening of the channel pore. In this case, the D2 lobes of each monomer of the LBD dimer move away from each other. Depending on the agonist, the receptor can subsequently adopt a desensitized closed state, in which the ion channel remains closed. When

the agonist unbinds the receptor, it enters a desensitized open state (ion channel closed) that in turn undergo conformational changes into an apo state (*Figure 1.9*).[31]

Desensitization by definition is a reduction in response in the presence of a sustained stimulus and thus the ion channel remains closed even though stimulated by an agonist. The desensitization process is fast in AMPA and kainate receptors, occurring within 20 ms and implying a reduction of 90% in current amplitudes.[32]

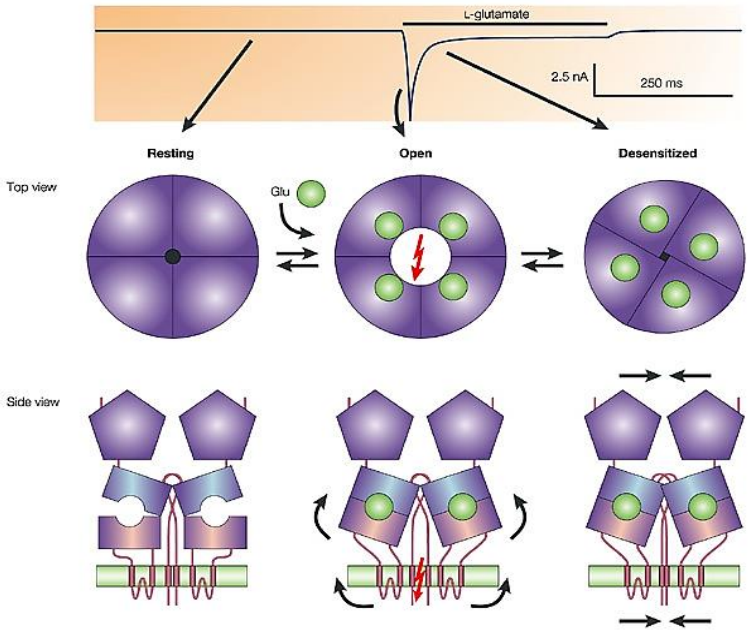


***Figure 1.9.*** Activation and desensitization in iGluRs. Red lightning arrow shows flux of ions inside the cannel pore (open conformation). Grey arrows indicate the movements of the different domains.[29]

It has been established that, during receptor assembly, two LBDs form a dimer and further two of these dimers couple together to form a tetramer in a dimer-of-dimers manner.

The TMD is composed of four membrane segments (M1-4) and it is the domain forming the ion channel pore. The TMD is connected to the LBD through three short linkers. Three helical segments (M1, M3, M4) completely cross the bilayer, whereas M2 segment is a reentrant loop. Depending on the amino acidic residues of the reentrant loop, this site determines calcium permeability and sensitivity to the intracellular polyamines.[33] The properties of the GluA2 subunit and of the GluK1 and GluK2 subunits are modified post-transcriptionally by RNA editing at the Gln codon in the apex of the reentrant M2 loop (QRN site).

The CTD is the only domain entirely placed in the intracellular region and exhibits a great diversity in length and amino acid sequence among the different iGluRs. This domain is of particular interest because it contains important binding sites for cytosolic proteins interacting with iGluRs and displays numerous consensus sites for phosphorylation.[34] The CTD is thought to be involved in receptor trafficking, post-translational modifications and targeting for the degradation. Little is known because no crystal structures are available yet.

### 1.7.1 NMDA RECEPTORS

The NMDA subtype has been extensively studied and it is the target for the only drug towards iGluRs currently used in Alzheimer's disease: memantine.[35]

These receptors require glycine as co-agonist and they are sensitive to voltage-dependent $Mg^{2+}$ inhibition.[36,37] For this reason, NMDARs can be defined as 'coincidence' receptors. Due to $Mg^{2+}$ block of the channel pore, NMDARs can participate to the excitatory post-synaptic current (EPSC) only when the membrane potential of the neuron reaches more positive voltages. Indeed, at the beginning the EPSC induced by glutamate is mediated by non-NMDARs, especially AMPARs: because of the fast AMPARs-mediated membrane depolarization that relieves the magnesium block, NMDARs can be activated (in the presence of both glutamate and glycine).

In agreement with the requirement of both glycine and Glu for activation, NMDA receptors are heterotetrameric ion channels composed of two copies each of the obligatory glycine-binding GluN1 subunit and the Glu-binding GluN2 and/or GluN3 subunits. The four distinct GluN2 subunits (A–D) combine with the splice variants of the N1 subunit to convey multiple subtypes with distinct ion channel properties and spatial and temporal expression patterns. The molecular diversity of the Glu binding site might be a potential target for competitive subtype specific drugs.

The opening of NMDA receptor ion channels results in influx of cations, including $Ca^{2+}$, into the postsynapse and activates signal transduction cascades that control synaptic strength. This coincidental integration of chemical and electrical information into a $Ca^{2+}$ signal is crucial for activity-dependent synaptic plasticity underlying neuronal development and memory formation. In contrast, dysfunction of NMDA receptors is implicated in numerous neurological diseases and disorders, including seizure, stroke, Parkinson's disease, Alzheimer's disease, and schizophrenia.

The architecture of NMDA receptors, like the other subfamily members of iGluRs, is modular and is composed of multiple domains with distinct functional roles. The large extracellular region of iGluRs is partitioned into two domains, an amino-terminal domain (ATD) and a ligand-binding domain (LBD) (S1-S2). The S1-S2 LBD binds glutamate and glycine and elicits opening of the ion channel pore formed by the transmembrane domains (TM) in the heterotetrameric assembly (*Figure1.10*). In the S1-S2 domain, NMDA receptors and non-NMDA receptors have rather high sequence similarity (≈ 50% similar) and similar overall architectures as revealed by recent crystallographic studies.

In contrast, ATDs of NMDA receptors and non-NMDA receptors have little or no sequence homology. Most importantly, although there is no ATD-targeted ligand or evidence for the ATD-mediated functional regulation in non-NMDA receptors, there is a rich spectrum of small ligands that bind the ATD of NMDA receptors and allosterically modulate ion channel activity. These ligands are small molecules and ions including polyamines, phenylethanolamines, or $Zn^{2+}$ that bind to ATD in a subunit-specific manner. [38]

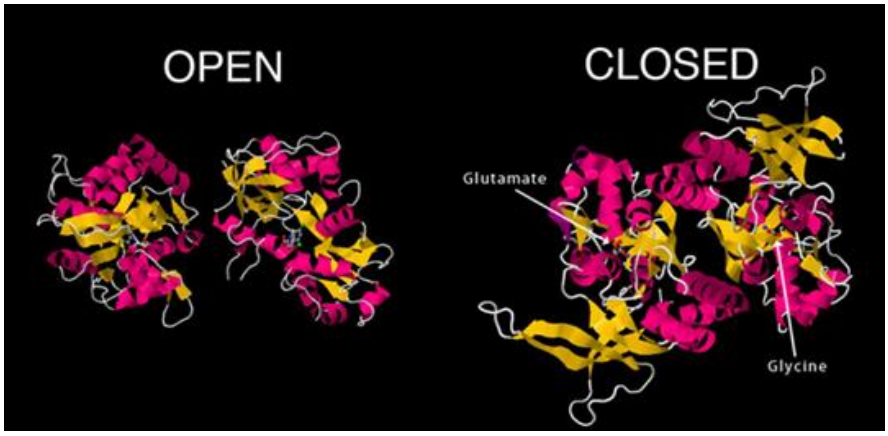


***Figure 1.10.*** NMDAR in open conformation (left) and closed conformation (right, in presence of the agonist Glu and the co-agonist Gly).

Recent evidence has highlighted the role of NMDA in peripheral non neuronal tissues and organs, as founds with the autocrine and paracrine systems. Interestingly, blocking NMDA receptors is shown to enhance appetite and food intake and the effect is attenuated by using capsaicin to

destroy small unmyelinated vagus nerves. NMDA receptors, thus, may regulate gastric motility by interacting with cholinergic transmission linked to the vagus nerve.

### 1.7.1.1 Molecular structure of NMDA agonists

The synthetic amino acid NMDA (*Figure 1.11*), which is a very selective agonist at NMDA receptors, has been available for more than 30 years. In addition to this, a large number of very potent and selective NMDA agonists have been developed during the past two decades and the availability of these compounds has greatly facilitated studies of the physiological and pathophysiological roles of NMDA receptors.[39,40] From a structure-activity point of view, NMDA, which has (*R*)-configuration at the amino acidic center, is quite unique: it is the only *N*-methylated acidic amino acid showing an affinity for NMDA receptors similar to that of its unmethylated form.

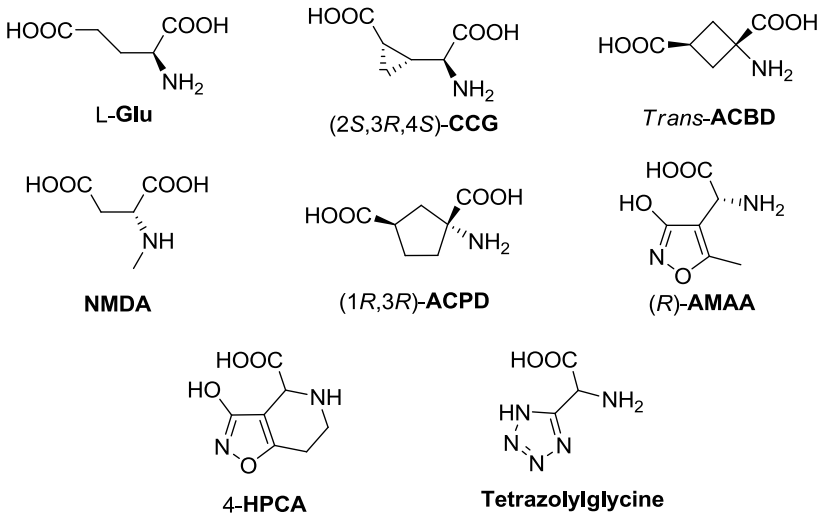


***Figure 1.11.***

*N*-Methyl-(*S*)-Glu and, in particular, *N*-methyl-(*R*)-Glu interact much less potently with NMDA receptor sites than does (*S*)-Glu. Although (*R*)-Glu is much weaker than (*S*)-Glu as an NMDA agonist, NMDA is more potent than its (*S*)-form. Despite its high potency, NMDA binds to NMDA receptor sites with very low affinity and attempts to use radioactive NMDA as a ligand for binding studies have been unsuccessful.[41]

These properties of NMDA are shared by AMAA (*Figure 1.11*), another potent NMDA agonist.

Three carbocyclic acidic amino acids, in which different parts of the molecule of Glu have been conformationally restricted, have been shown to be very potent NMDA agonists, namely the (2*S*,3*R*,4*S*)-enantiomer of CCG,[42] (1*R*,3*R*)-ACPD,[43] and *trans*-ACBD (*Figure 1.11*).[44]

### 1.7.1.2 Molecular structure of competitive NMDA antagonists

Using (*R*)-2-aminoadipic acid and, in particular, the phosphonate analogue (*R*)-AP5, as lead structures, a very large number of potent and selective competitive NMDA antagonists have been developed (*Figure 1.12*).

Most of these NMDA antagonists are phosphono amino acids, in which the α-carboxylate and the distal phosphonate groups are typically separated by four or six atoms. Not all of these compounds have been resolved, but for those that are available in stereochemically pure forms, the NMDA antagonist effect resides in the (*R*)-enantiomer, though a few exceptions from this rule have been described.[45] The phosphono amino acids (*R*)-CPP,[46] (*R*)-CPPene, and LY235959[47] are among the most potent competitive NMDA antagonists described and these compounds have been extensively studied pharmacologically.[48] Substitution of the phosphono group with a tetrazole group afforded the NMDA antagonist (±)-cis-LY 233053 (*Figure 1.12*), with only limited loss of activity.[49]

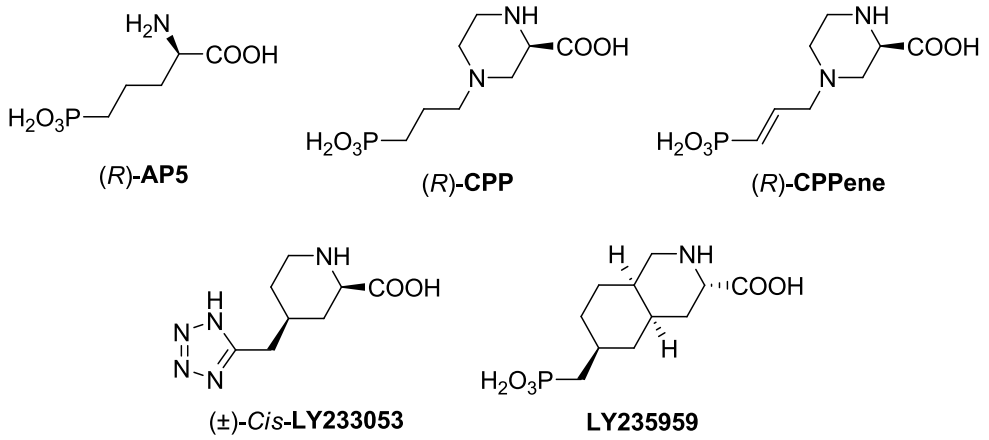


***Figure 1.12.***

### 1.7.1.3 Molecular structure of non-competitive NMDA antagonists

Non-competitive antagonists such as PCP, ketamine, MK-801 and memantine (*Figure 1.13*) behave as channel blockers interacting with the binding site for $Mg^{++}$, located inside the channel, and blocking it in an agonist-dependent way. Memantine has been approved by the European Union and the U.S. Food and Drugs Administration (FDA) for the treatment of Alzheimer's disease.

Open-channel block is so far the most appealing strategy for therapeutic intervention during excessive NMDARs activation as this action of blockade requires prior activation of the receptor. This property, in theory, leads to a higher degree of channel blockade in the presence of excessive levels of Glu and lesser degree of blockade at relatively lower levels, for example, during physiological neurotransmission. Clinical use has corroborated the prediction that memantine is well tolerated. Besides Alzheimer's disease, memantine is currently in trials for additional neurological disorders, including other forms of dementia, depression, glaucoma and severe neuropathic pain.

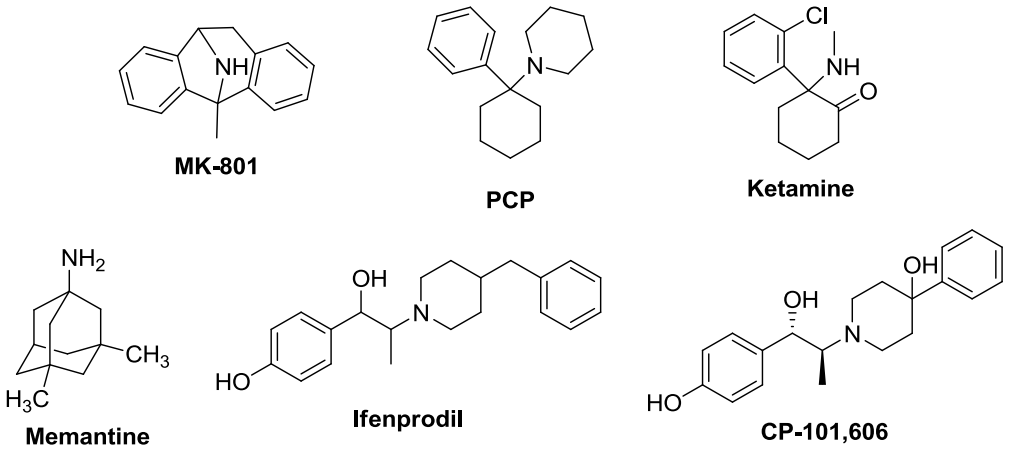


***Figure 1.13.***

Another approach to antagonize the NMDA receptors is the use of non-competitive antagonists acting at the polyamine binding site, such as Ifenprodil and its analogues, e.g., CP-101,606 (*Figure 1.13*). These molecules have recently received much attention because of the subtype selectivity and the mode of action, which is an activity-dependent blockade of N2B containing NMDA receptors.[50,51] Ifenprodil inhibits GluN1/N2B receptors ($IC_{50}$: 0.3 $\mu$M) and is at least 150-fold

weaker against GluN1/ N2C or GluN1/N2D receptors.[52]

## 1.7.2 AMPA RECEPTORS

AMPA receptors (AMPARs), ion channels permeable to $Na^+$ and $Ca^{2+}$, are the main ionotropic glutamate receptors that mediate fast excitatory synaptic transmission in mammalian brain (*Figure 1.14*). AMPARs are tetrameric assemblies of highly homologous subunits, i.e. GluA1-4, encoded by four different genes. The AMPA receptor subunits are expressed in different variants due to splicing and RNA editing. All subunits occur in two alternative spliced forms where the C-terminal part of the binding segment can be in either a *flip* or a *flop* form. The *flip* forms are predominantly expressed before birth and desensitize slowly and less strongly to Glu when compared to the *flop* forms. The *flop* forms are generally expressed at the same level as the *flip* forms in adults.

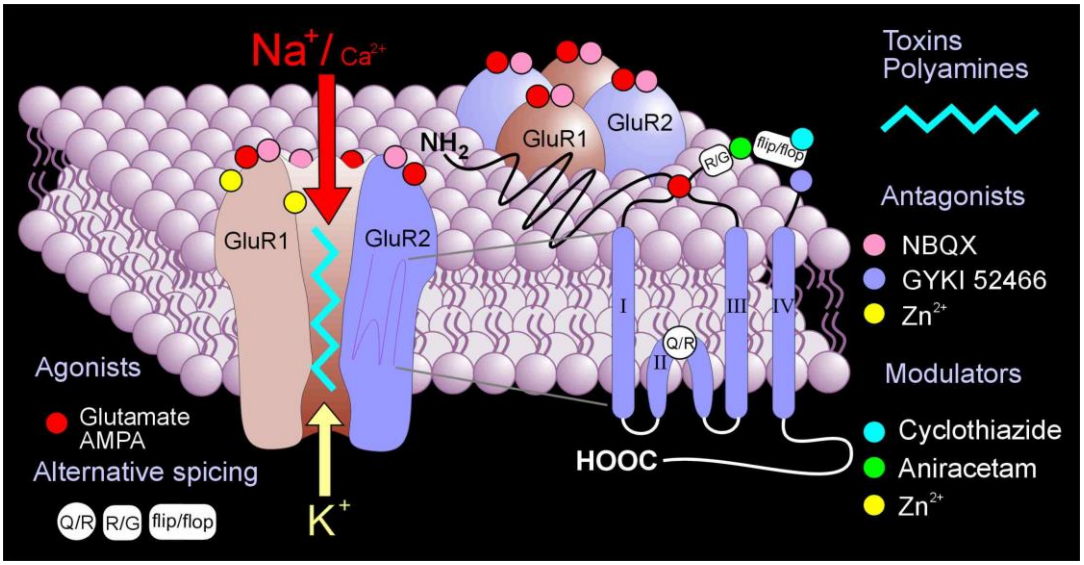


***Figure 1.14.*** AMPA receptor

Expression of the various forms of the AMPA receptor subunits in heterologous systems shows that the most significant pharmacological and physiological differences depend on the presence of GluA2 in the complex or the type of splice variant in the individual subunits. The presence of an arginine, i.e. on GluA2 subunit in the receptor complex, at that position in the pore abolishes $Ca^{2+}$

permeability and changes the rectifying properties.[53]

AMPA receptors are involved in synaptic plasticity and Long Term Potentiation (LTP) phenomena.[54] An increase of the post-synaptic response to a stimulation is achieved by an increment of AMPA receptors expression or by an higher conductance of already present channels.[55,56]

### 1.7.2.1 Molecular structure of AMPA agonists and functional partial agonists

The introduction of [$^3$H]-AMPA as a radioligand, greatly facilitated the pharmacological characterization of AMPA receptors and the development of new AMPA receptor ligands, including the very potent AMPA agonists trifluoro-AMPA, (*S*)-5-chloro-6-azawillardine, and (*S*)-ACPA (*Figure 1.15*). Like ACPA, 4-AHCP actually is a homologue of Glu, and both these compounds are highly potent agonists at AMPA receptors. (5*S*)-CIP-A, which is a semirigid analogue of (*S*)-Glu showing potent agonist effect at AMPA receptors, is a useful tool for the development of AMPA agonist pharmacophore(s)

Analogues of AMPA having different substituents in the 5-position of the isoxazole ring have been synthesized and used in structure-activity studies on the AMPA receptors. A prerequisite for the development of practically useful therapies along these lines obviously is the availability of agonists and competitive antagonists capable of penetrating the BBB. In this regard, (*S*)-APPA and (*R*)-APPA have been studied in a drug discrimination model, showing (*R*)-APPA to have antagonistic effects toward the central stimulus properties of ATPA, whereas no agonist (substituting) effect was observed with (*S*)-APPA.

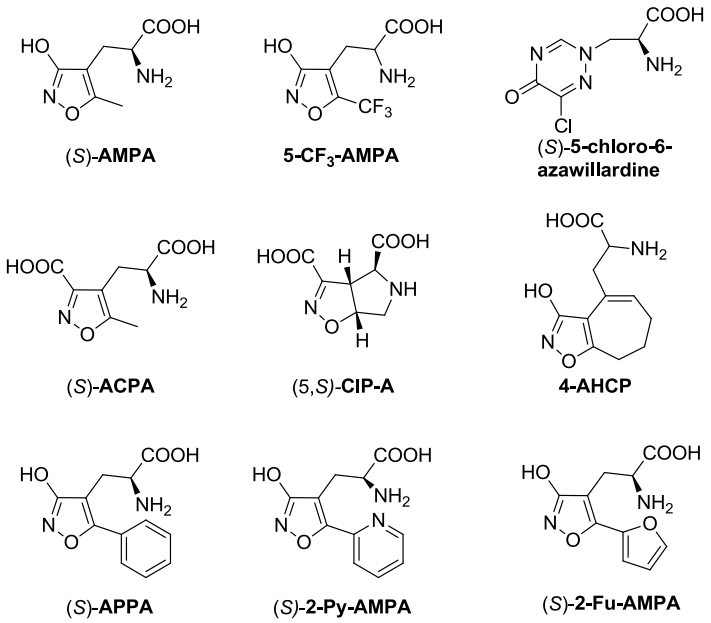


***Figure 1.15.*** AMPA Receptors Antagonists

## 1.7.2.2 Molecular structure of competitive AMPA antagonists

Different series of competitive AMPA receptor antagonists have been developed. Early pharmacological studies on AMPA and KA receptors were hampered by the lack of selective and potent antagonists. CNQX (*Figure 1.16*) and related compounds offered a breakthrough in this respect, being quite potent antagonists, though nonselective. Subsequently, NBQX was shown to have improved AMPA receptor selectivity compared to CNQX. A large number of compounds have been developed with the quinoxalinedione structure, not only as AMPA receptor antagonists, but also as compounds showing effects at other Glu receptor sites, notably glycine-B antagonists. YM90K shows high potency compared to NBQX as an AMPA receptor antagonist and is systemically active. Within this family of compounds the highly selective AMPA antagonist, Ro 48-8587, has been radiolabeled and shown to be a very useful tool for studies of AMPA receptors. A number of isatin oximes, such as NS-257, have shown antagonist activity, and these compounds, like YM90K and Ro 48-8587, show higher water solubility than NBQX, and they have been shown to be systemically active anticonvulsants. One group of AMPA receptor antagonists contain the acidic amino acid structure generally found in Glu receptor agonists, whereas another group of antagonists are acidic amino acids containing a longer backbone. One member of the latter group is the tricyclic compound LY293558, which shows significant antagonist effects at KA receptors in

addition to the potent AMPA receptor blocking effects. The AMPA receptor antagonists (*S*)-AMOA and (*S*)-ATPO, which have been developed using AMPA as a lead structure, also have carbon backbones longer than that normally found in AMPA agonist molecules. For LY293558, (*S*)-AMOA, and (*S*)-ATPO, the (*S*)-form has been shown to be the more potent enantiomer. Recently, the carbon analogue of (*S*)-AMOA, ACMP, has shown improved AMPA antagonist potency compared to (*S*)-AMOA. Within the group of AMPA antagonists having "agonist chain lengths", the (*R*)-form is generally the active enantiomer, as exemplified by (*R*)-APPA, (*R*)-2-Py-AMPA, and (*R*)-ATAA. These antagonists are remarkable because, despite their "agonist-like" structure and AMPA antagonist activity, they show very low receptor affinity in the [$^3$H]-AMPA binding assay.

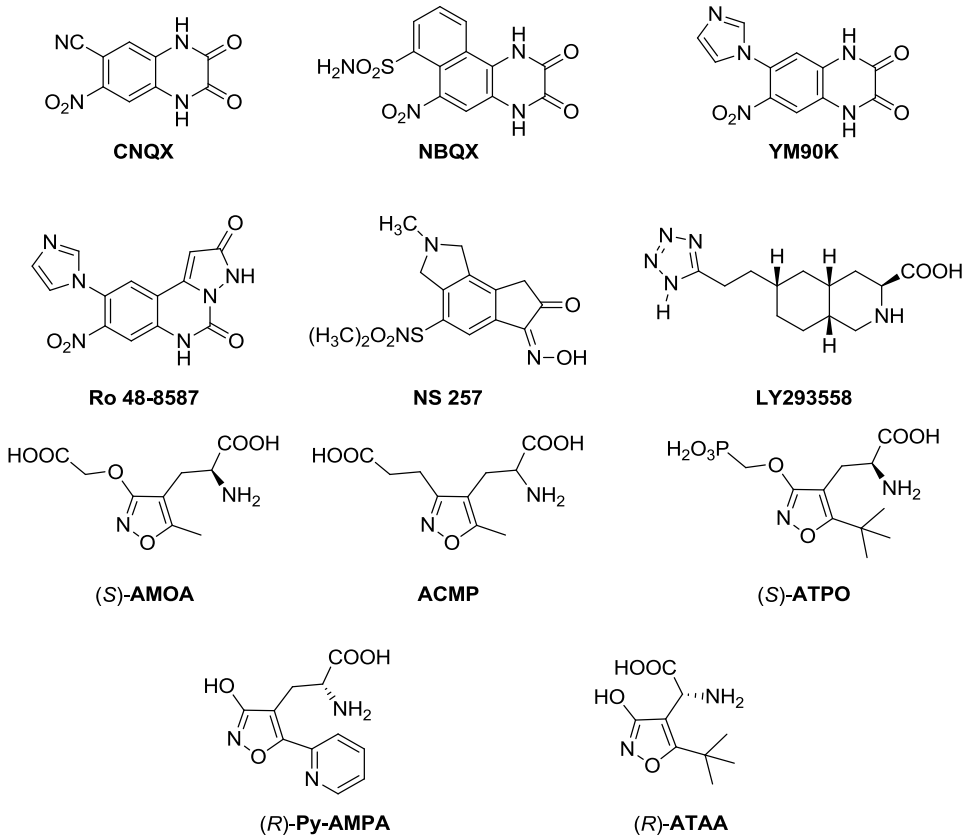


***Figure 1.16.*** Structures of some Competitive AMPA Antagonists

## 1.7.2.3 Molecular structure of non-competitive AMPA antagonists and modulatory agents

Like the NMDA receptors, the AMPA receptors appear to be biomolecular complexes comprising a number of binding sites in addition to the Glu recognition sites. Whereas philanthotoxins, normally

block iGluRs with a low degree of selectivity, a number of 2,3-benzodiazepines such as GYKI 52466 and GYKI 53655 (*Figure 1.17*) have been characterized as potent and selective non-competitive AMPA antagonists. The noncompetitive nature of these antagonists, assumed to interact with an allosteric receptor site, suggests that they may be capable of inhibiting AMPA receptor functions in the presence of high levels of Glu. Within this group of compounds, Talampanel is under clinical evaluation.

The rapid agonist induced desensitization of AMPA receptors can be markedly inhibited by a number of structurally dissimilar compounds including cyclothiazide, the related sulfonamide IDRA-21, and aniracetam, a group of compounds named "Ampakines".

These compounds essentially block AMPA receptor desensitization and, consequently, enhance excitatory activity several-fold, depending on the initial level of desensitization observed for the individual agonist.

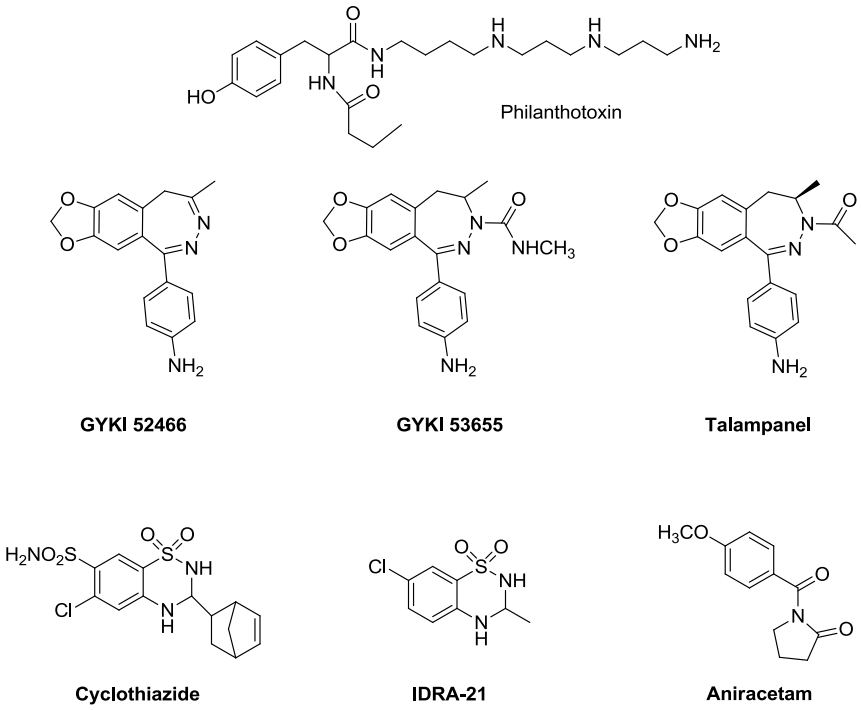


***Figure 1.17.*** Structures of Non-competitive AMPA Receptors Antagonists and AMPA Receptors modulatory agents

## 1.7.3 KAINATE RECEPTORS

First of all, kainate is derived from the seaweed known as "kaininso" in Japanese and it is a mixed agonist that can also activate AMPARs. Kainate receptors are the least studied iGluRs and one of

the reasons is the lack of specific compounds to activate or block them. Like AMPARs and NMDARs, KARs are tetrameric combinations of a number of subunits; in this case, five types of subunits exist, named GluK1, GluK2, GluK3, GluK4 and GluK5 (previously known as GluR5-GluR7 and KA1 and KA2, respectively).[57]

GluK1-3 subunits share a 75-80% homology, and GluK5 and GluK6 are 68% homologous. Homology between GluK1-3 and GluK4,5, however, is just 45%. GluK1-3 can bind glutamate and kainate with low nanomolar affinities and GluK4-5 with very high nanomolar affinities. Moreover, glutamate activates homomeric GluK1 and GluK2 receptors with a low micromolar value of $EC_{50}$, whereas for GluK3 this value is in the low mM range.[58] [59]

GluK1-3 can form homomeric and heteromeric receptors, while GluK4-5 can generate functional receptors only when partnering any of the GluK1-3 subunits. This is due the fact that the GluK5 subunit possesses an endoplasmic reticulum retention signal in the C-terminus, which prevents surface cell expression. Instead, this signal is shielded when GluK5 is assembled with GluK1, 2 or 3, allowing cell surface expression of these heteromeric receptors.[60]

KARs framework is further extended by editing of the GluK1 and GluK2 receptor subunit pre-mRNA at the so-called Q/R site of the second membrane domain (*Figure 1.18*). More isoforms also originate from the alternative splicing of GluK1-3 subunits, while GluK4-5 are not object of this process. Kainate receptors seem to have also a presynaptic action and, in addition to their conventional pathway as ion channels, some of these proteins are associated in some way with G proteins to pain and fear memory and other CNS disorders.[61]

Because of all these features, KARs are thought to have a neuromodulatory role and this aspect make them an attractive therapeutic target.

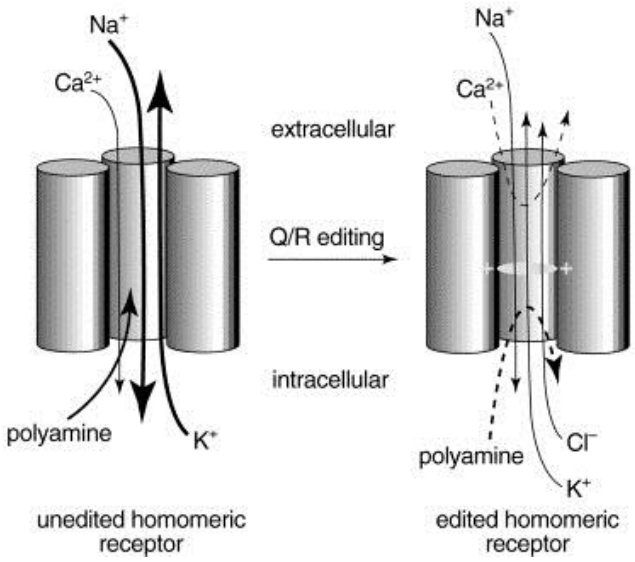


***Figure 1.18.*** Q/R editing of homomeric GluK1 and GluK2 and effects on the channel ion permeations. Because of the introduction of arginine at the Q/R site the channel pore obtains a positive charge, this leads to a reduction of single cation conductance (as indicated by the thickness of the arrows) and to the introduction of $Cl^-$ permeability. Moreover, polyamines interaction is prevented. From Chittajallu (2009). [62]

## LOCALIZATION

Even if KARs are widely distributed within the CNS, they are present at fewer synapses. Due to the absence of specific antibodies against different KAR subunits, subunit distribution has become a challenging feature. Nevertheless, on the basis of mRNA detection studies, GluK1 is highly abundant in the hippocampal and cortical interneurons, as well as in sensory neurons and in Purkinje cells; GluK2 is mostly expressed in the cerebellum granule cells, while GluK3 is less expressed than the other subunits and it can be found in the neocortex and hippocampus. GluK4 is highly abundant in the hippocampus (CA3 pyramidal cells) and, finally, GluK5 is the most commonly KA subunit found in the brain and is highly abundant in the neocortex, hippocampus, and cerebellum.[63]

## PROPERTIES OF KAR SUBUNITS

It has been found that some diseases are associated to a specific KAR subunit; thus, it is useful to go deep into the understanding of each KAR in term of pharmacology, structure and function. To

date, this is not possible yet due to the complicated connection between diseases and their causes and because not all the subunits are known at the same level.

GluK1 counts for the higher number of selective compounds available. This is because of the larger ligand binding pocket of this subunit compared to the ones of the other KARs and also to GluA2. The availability of selective ligands targeting this subunit led to the success of GluK1 structural studies: 75% of the 40 structures of GluK1 and GluK2 deposited in Protein Data Bank (PDB) are of the GluK1 subunit. The GluK1 LBD has been crystallized in complex with different agonists and it is the only KAR subunit to have been crystallized with antagonists. GluK1 is associated with pain and epilepsy and GluK1 antagonists show to eliminate seizures and demonstrate the involvement of this subunit in pain pathways in animal models.[64 65]

GluK2 contributes to the onset of many neurodegenerative disorders linked with the other KARs and they seem also to be involved in autism.[66]

The GluK3 subunit has a unique physiological role, because its $EC_{50}$ is 10-100 time higher compared to other iGluRs (it is in the millimolar range) and for this reason at the beginning of KAR research it was thought that GluK3 was a non-functional subunit. Now it is known that to be activated GluK3 need to be close to the glutamate release sites or to be in certain conditions in which there is high concentration of glutamate, as shown in reports in which agonists were applicated in the millimolar concentration range.[41] The high $EC_{50}$ for glutamate appears to be linked to the S1 region of the LBD of GluK3 receptors, as validated by studies with chimeras and mutated GluK3.[67]

Moreover, it was demonstrated that GluK3 is an essential subunit of presynaptic KARs autoreceptors[68] and GluK3 knock-out mice display markedly reduced short- and long-term synaptic potentiation.[50]

Now the structures of GluK3 in complex with glutamate (*Figure 1.19*), kainate and three other agonists are available; they reveal a conserved glutamate binding mode and a water molecule network similar to that of GluK1, even if the domain closure induced upon kainate binding is similar to that seen for GluK2. The volume of the glutamate binding pocket is of intermediate size between those of GluK1 and GluK2. This is because of the presence of bulkier residues (Asn722 and Thr742) in GluK3 in comparison to the corresponding amino acids in GluK1 (Ser721 and

Ser741) and due to the presence of a bulkier phenylalanine in GluK2, where in GluK3 there is a leucine.[24]

There are two splice variants of GluK3: GluK3a and GluK3b. The first one is efficiently expressed in the plasma membrane thanks to its C-terminal motif that is identical to the one found in GluK2, whereas the latter is mostly retained in the ER.

GluK3 is associated with depressive disorder, schizophrenia and bipolar disorder.[69] GluK4 and GluK5 subunits can exist only in heteroreceptors in association with the subunits GluK1-3. GluK2/GluK5 is the most prevalent combination found in the CNS.

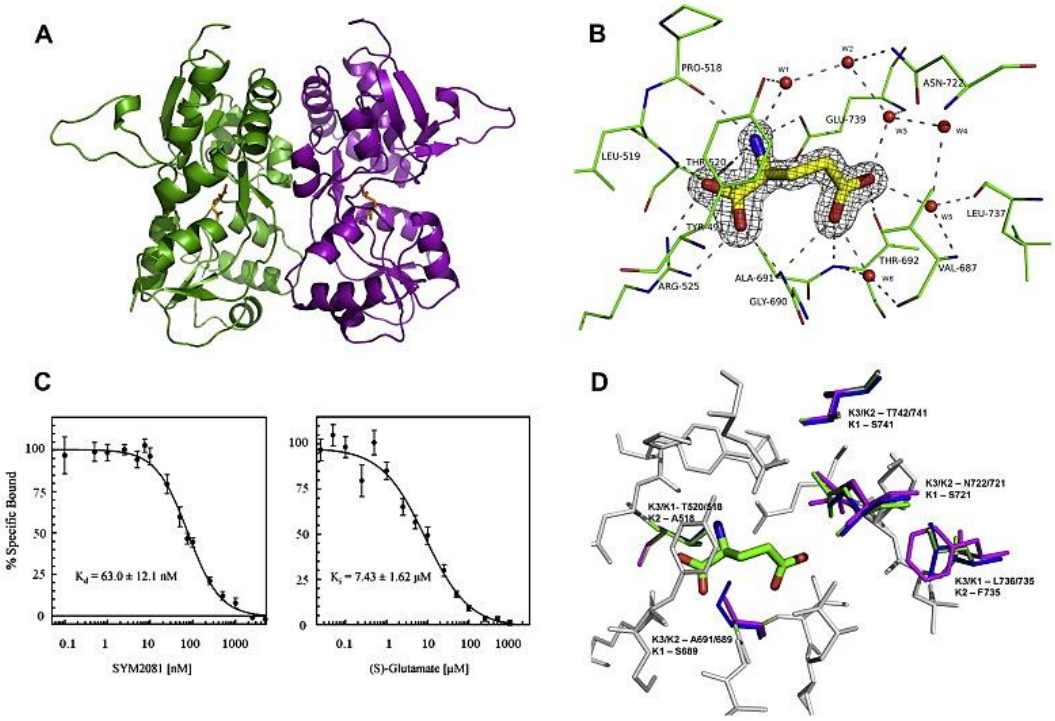


***Figure 1.19.*** Ligand binding site of GluK3. (A) Crystal structure of GluK3 dimer LBD in complex with glutamate (orange). (B) Zoom on one LBD with glutamate (yellow) Dashed lines indicate hydrogen bonds to water molecules (red spheres). (C) Affinities of SYM2081 and glutamate at purified GluK3 LBD. (D) Illustration of the differing amino acids in the LBD of GluK1 (blue), in the LBD of GluK2 (magenta) and in the LBD of GluK3 (green). From Venskutonytè (2011).[24]

## INTERACTING PROTEINS

A series of proteins have been found to interact with the C-terminal tail of KAR subunits and they have shown to have influence on the receptor trafficking and kinetics. Besides, the understanding

of the contribution of these proteins elucidates the discrepancies between native and recombinant receptor properties. Among them, PDZ-motif containing proteins such as PSD-95, PICK1 and GRIP are thought to contribute to the stabilization of KARs at the synaptic membrane.[70]

Recently, two integral membrane proteins have been discovered to have an important action on KARs: Neuropillin Tolloid-like 1 (Neto1) and Neuropillin Tolloid-like 2 (Neto2).[71] It was demonstrated that the coexpression of these proteins with KARs in recombinant systems decelerates the onset of the desensitization of kainate-evoked responses and accelerates the recovery from the desensitized state. As a result, the agonist-induced current persists for longer period. Another striking feature is that KAR-mediated EPSCs are accelerated in Neto1 KO mice, approaching the AMPA kinetics (*Figure 1.20*).[72]

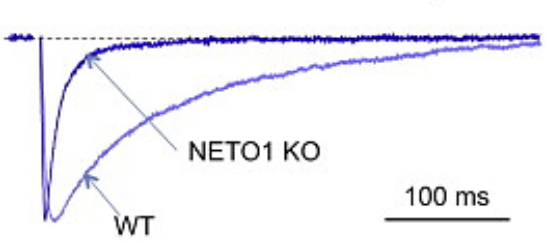


***Figure 1.20.*** Influences of NETO proteins on KAR kinetic. KAR-mediated EPSCs are accelerated in the Neto1 KO mice, approaching the characteristics of the AMPA-mediated component. From Lerma (2013)[lxxii].

## UNCONVENTIONAL PATHWAY

Unlike AMPA and NMDA receptors, KARs seem to have a remarkable component of their signalling based upon an unconventional metabotropic mechanism (*Figure 1.21*). This was first observed in the hippocampus and later confirmed in other preparations. This noncanonical signalling occurs by receptor coupling to G proteins and is independent of ion flux. Moreover, the unconventional pathway is involved in both the presynaptic control of neurotransmitter release and the postsynaptic excitability. Unfortunately, none of the KAR-interacting proteins so far identified show to act as a linker between KARs and a G protein, so this intermediary element still remains to be identified.[73] [74]

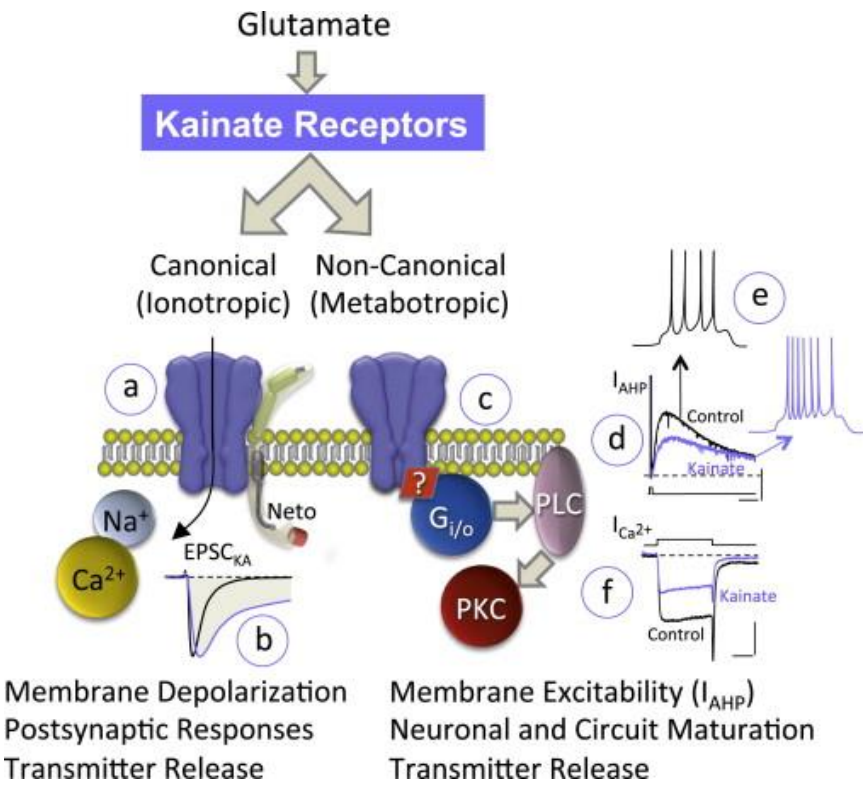


***Figure 1.21.*** KARs different signalling. a) Ionotropic pathway. These receptors account for ancillary proteins, like NETO. b) EPSC mediated by KARs. c) unconventional pathway through G proteins. The intermediate protein to couple to G proteins is missing. d-e-f) Effects of noncanonical pathway: increase of neuronal excitability (e) that leads to an increase of the firing frequency and modulation of calcium currents (f) which in turn act on the facilitation and inhibition of transmitter release. From Lerma (2013).[lxii]

## ION-DEPENDENT KAR GATING

Another important difference between KARs and the other iGluRs is that KARs require external monovalent cations and anions for channel opening.[75] This feature has been confirmed by crystallographic studies, which have shown the presence of an ion binding pocket in KAR subunits.[76]

One aspect connected to such a strict ion dependence is that activation of KARs under intense neuronal activity would be limited, because the external levels of $Na^+$ would drop under these circumstances. Consequently, tissue damage due to excitotoxicity would be contained. Moreover, as KAR function only when the external ion site is occupied, it could be possible to regulate KAR activity by targeting this site.

## POSTSYNAPTIC KARs

The activation of postsynaptic KARs provokes small amplitude EPSCs, with slow activation and

deactivation kinetics compared to AMPARs (*Figure 1.22*).[77] [78]

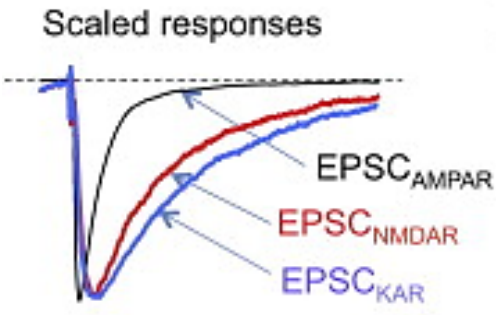


***Figure 1.22.*** Kinetics between iGluRs. Responses mediated by AMPAR are much faster than the KAR and NMDAR ones. From Lerma (2013). [lxii]

Thus, $EPSC_{KAR}$ acts as an integrative element to glutamate neurotransmission, adding its contribute to the other glutamate receptors. Nevertheless, $EPSC_{KAR}$ are important components of the excitatory synapse, as shown by experiments that have demonstrated that long term potentiation was impaired in GluK3 KO mice.

PRESYNAPTIC KARs

It is now established that presynaptic KARs modulate GABA and glutamate release in a bidirectional manner. Indeed, in the hippocampus KARs inhibit GABA release at interneuron-pyramidal cell connections and in experiments carried out in vivo infusion of glutamate provokes a drop of inhibition, conducing to an epileptic state. Together with the activation of postsynaptic KARs, this KAR mediated-inhibition of GABA release has a relevant role in the acute epileptogenic effect. It was also postulated that KARs participates in presynaptic activity with a metabotropic pathway rather than ion flux.[79] [80]

### 1.7.3.1 Molecular structure of KA agonists

Kainoids are a series of ligands sharing a common trisubstituited pyrrolidine skeleton. Two natural compounds of this class have been discovered by extraction from marine algae: kainate and domoate. Even though they bind to KARs with high affinity, they still bind AMPA with lower $K_d$ and for this reason they cannot be used in receptors-selective binding studies. Both of these natural kainoids are partial agonist on KARs, apart from domoate at GluK3, where it does not display any

agonistic effect. Example of kainate analogues are dihydrokainate (DHK), kainoids with thiazole moiety and 2-carboxypyrrolidine-3-acetic acid (CPPA). DHT is the compound that possesses the higher affinity towards GluK3 so far described in literature (*Figure 1.23*).

Willardine is another natural compound and it binds to AMPA and KA receptors as a partial agonist. It was found that 5-halo-substituted analogues bind KARs to different extents and, in particular, 5-iodowillardine shows an improved selectivity and affinity at the GluK1 subunit.[81 82]

Further the compound (*S*)-CPW399 was designed from the willardine scaffold and it has good selectivity towards GluK1.[83 84]

Another class of agonists that is active on KARs was developed from the structure of the dysiherbaine (DH) and of neodysiherbaine (NDH) (*Figure 1.23*).

Moreover, it was found that 4-substituted glutamate analogues have high affinity at KARs. (2*S*,4*R*)-4-methylglutamate (SYM2081) shows high selectivity at KARs and, among them, towards the GluK1 subunit. [85]

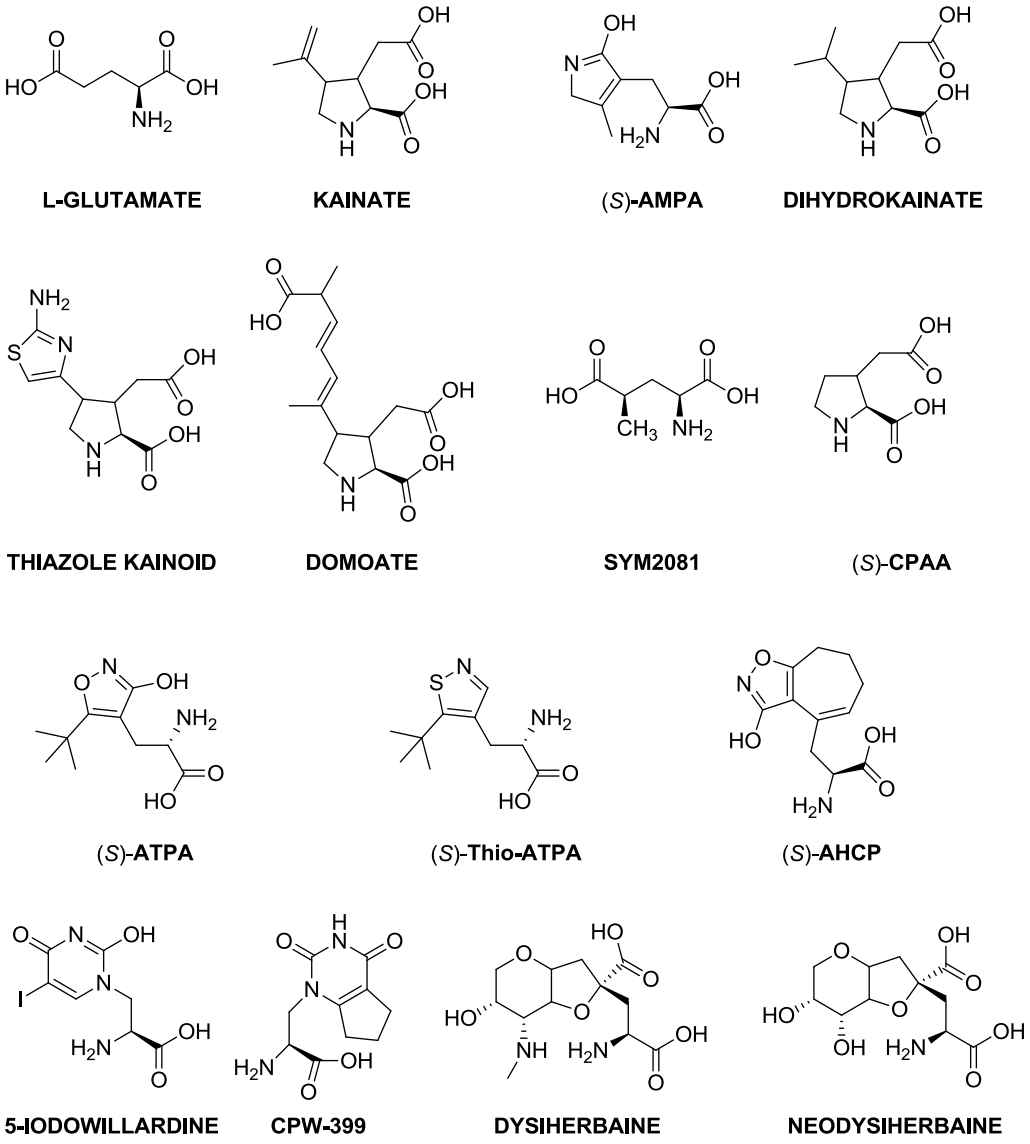


***Figure 1.23.*** Structures of KA receptor agonists.

## 1.7.3.2 Molecular structure of KA antagonists

Many efforts have been done to develop antagonists towards a specific type of glutamate receptor and, among them, toward a specific KARs subtype. Unfortunately, to date selectivity has been achieved only towards GluK1, due to its larger ligand binding cavity that allows the binding of bulkier compounds.

As mentioned before, willardine is a natural compound that after chemical modifications can bind to different extents to AMPARs and KARs. It was demonstrated that the introduction of a bulky

acidic group at the $N^3$ position of the uracil ring determines an antagonist profile at iGluRs. In this way, medicinal chemists attained the series of UBP compounds (*Figure 1.25*), which has revealed a useful tool to provide insight into KARs. The introduction of a thiophene moiety at the $N^3$ position of the uracil ring led to a compound with an increased selectivity and potency at GluK1 receptors (UBP304).[86]

The crystal structure of the 5-methyl analogue of the latter compound (UBP310) in complex with GluK1 revealed the presence of an unoccupied hydrophobic cavity in the binding domain (Figure *1.24*). This suggestion led to the synthesis of ACET, that possesses a phenyl ring at the 5-position of the thiophene moiety. ACET displays the best selectivity and potency towards GluK1 so far obtained.[87]

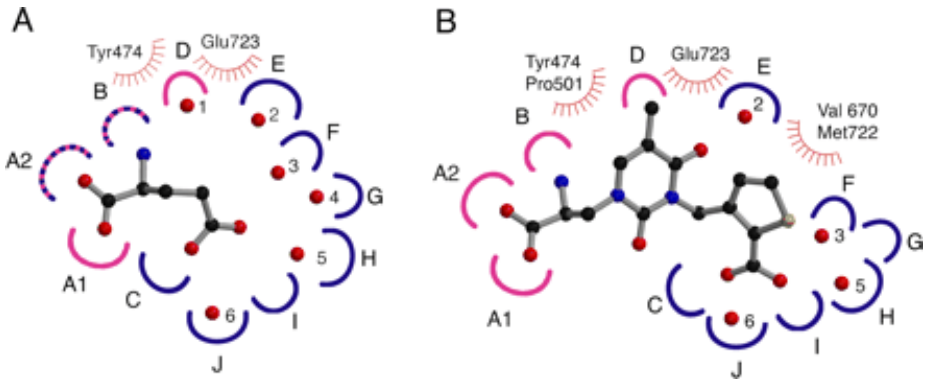


***Figure 1.24.*** Subsite map of the GluK1 ligand-binding pocket occupied by (S)-glutamate (A) and UBP310 (B). Ion pair sites and hydrogen bonds generated by domains 1 and 2 are colored in blue and pink, respectively; stripes indicate site generated by both domains; hatched curved lines indicate sites of van der Waals contacts. From Mayer (2006).[88]

Another class of KAR antagonists consists in skeleton series of decahydroisoquinoline derivatives. Pharmacological studies shown that this series has a neuroprotective action in cerebral ischemia models. The most remarkable compound is LY382884, which shows high selectivity at GluK1 (*Figure 1.25*). [89]

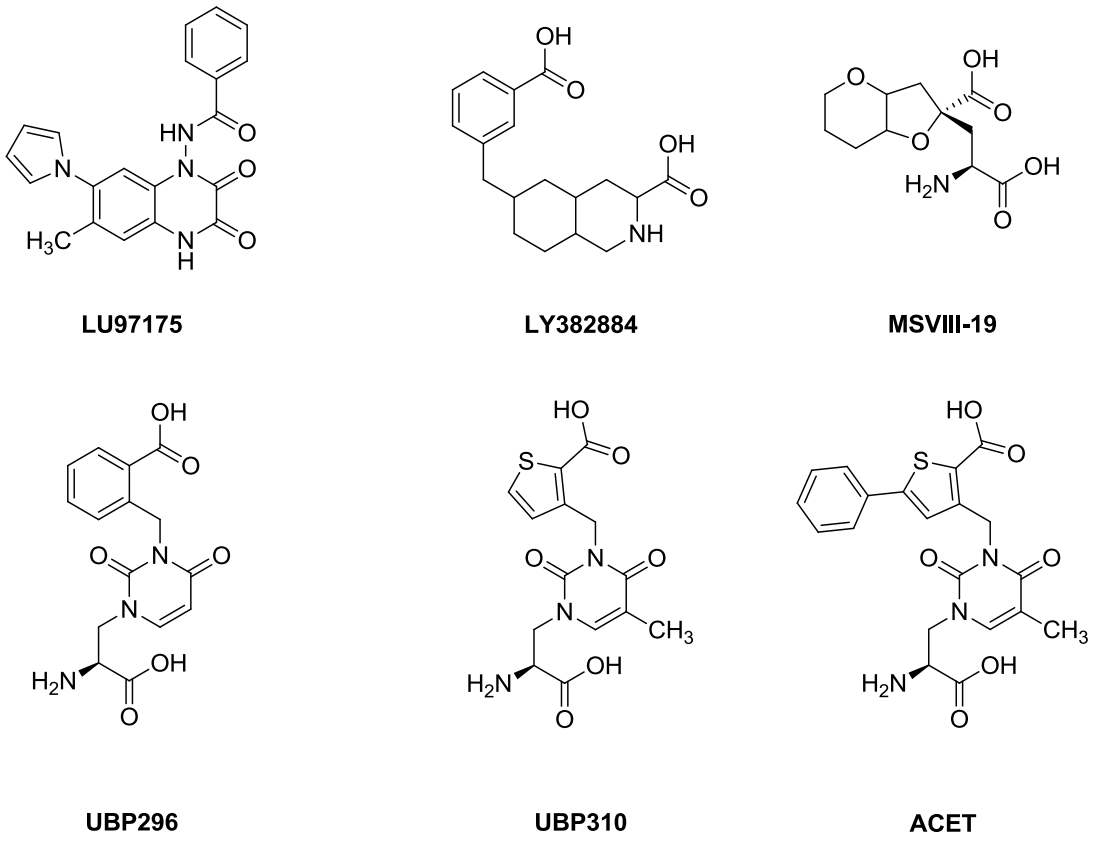


***Figure 1.25.*** Structures of KA receptor antagonists

## 1.8 METABOTROPIC RECEPTORS

The mGluRs belong to the superfamily of G-protein coupled receptors (GPCRs) as judged by their signal transduction pathways and hydropathy plots revealing seven transmembrane (7TM) segments (*Figure 1.26*). The eight presently cloned mGluRs can be divided into three groups on the basis of their sequence homology (receptors within a group show more than 60% sequence identity, whereas there is 40-50% sequence identity between the groups), signal transduction pathways, and selectivity for specific agonists and antagonists.[90]

Group I receptors mGluR1 and mGluR5 stimulate phospholipase C (PLC), causing an increase in intracellular inositol phosphates (IPs) and $Ca^{2+}$ levels. Group II consists of mGluR2 and mGluR3 while Group III includes mGluR4, mGluR6, mGluR7 and mGluR8, all of which inhibit adenylate cyclase (AC) causing a decrease in intracellular cAMP levels.[91,92]

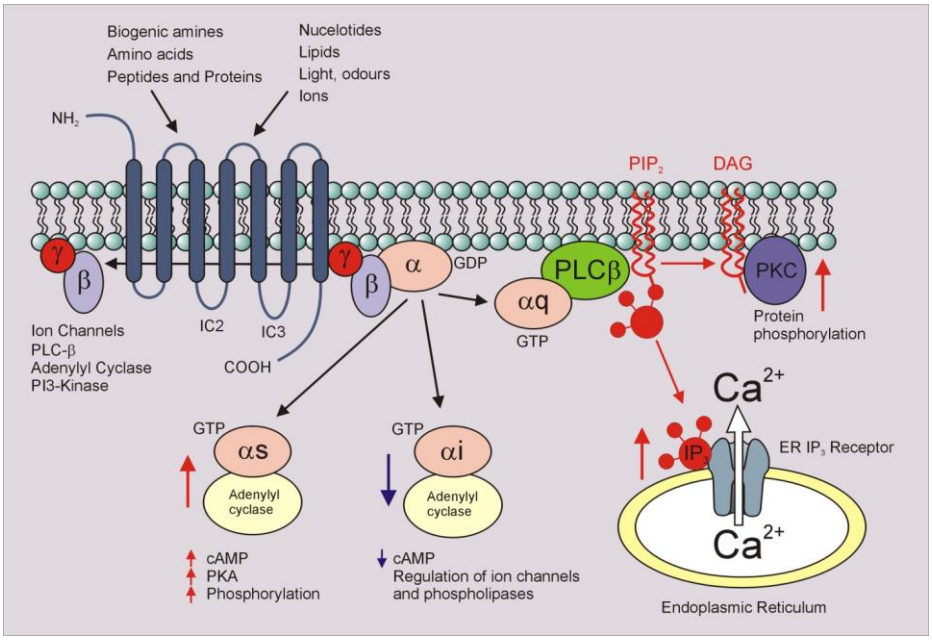


***Figure 1.26.*** mGluRs

Although the mGluRs possess seven transmembrane domains, there are important differences between these receptors and other G-protein-coupled receptors, i.e. the rhodopsin-like receptors.[93] For example, the third intracellular loop is important for determining the specificity of G-protein coupling in most G-protein-coupled receptors examined, whereas the C-terminal end of the second intracellular loop is critical in the mGluRs. Moreover, all mGluRs have a very large N-terminal extracellular domain (about 65 kDa in mGluR5), constituting about one-half of the protein, whereas most G-protein-coupled receptors do not. The glutamate binding domain is believed to lie in this extracellular region, not within the bundle of membrane-spanning domains, as is typical of the rhodopsin-like receptors. Three-dimensional crystal structures have indicated that this site is composed of two distinct globular domains with a ligand binding cleft between them, forming the Venus Flytrap Domain (VDF).[94] The glutamate binding induces the closure of the two domains and a conformational modification of the transmembrane domain. These conformational changes determine the intracellular GPCR activation.

In addition to the orthosteric binding site above illustrated, there is evidence for allosteric binding sites, located in a very distinct region of the receptor i.e. the transmembrane-spanning domains.[95] Since the glutamate-binding site is highly conserved across all mGluR subtypes, allosteric modulators offer the possibility to achieve subtype selectivity.[96]

# CHAPTER 2. AIM OF THE PROJECT

## 2.1 STRATEGIES FOR THE DESIGN OF KA RECEPTOR LIGANDS ON A RATIONAL BASIS

The discovery of highly selective ligands is of extreme importance for understanding the therapeutic potentials of KARs. From this assumption, the goal of this project is to design, synthesize and pharmacologically test potential subunit-selective compounds. Moreover, another aim is to attain selective compounds with an antagonist profile, as such molecules could be useful for the treatment of pathological conditions like depressive disorder, pain perception, schizophrenia and bipolar disorder.

In the present project, with this aim, classical medicinal chemistry approaches were applied on non selective AMPA/KA ligands: the **conformational rigidification**, the **bioisosteric substitution**, in particular on the distal carboxylic group, which can be efficaciously substituted with various group, e.g. phosphonate, tetrazole and 3-hydroxyisoxazole, and the **amino acidic chain homologation**, utilized to modify a ligand profile from agonist to antagonist. Finally, another strategy to improve the ligand selectivity is the **increase of the molecular complexity**.

### 2.1.1 CONFORMATIONAL RIGIDIFICATION

Glutamic acid chain is highly flexible and has nine energetically stable rotamers. With the aim of investigating the hypothesis that different Glu receptors are activated by a specific conformation of the endogenous ligand, Shimamoto and Ohfune[97] have studied the pharmacological profile of a series of L-2-(2-carboxy-cyclopropyl) glycines. The results suggested that the activation of metabotropic receptors requires an extended conformation *anti-anti*, while glutamic acid interacts at the ionotropic receptors in a (+) *gauche*-(+) *gauche* folded conformation (*Figure 2.1*).

Very interestingly, a further increase in the conformational constraint caused a dramatic increase in the selectivity for group II receptors affording (1*S*,2*S*,5*R*,6*S*)-2-aminobicyclo[3.1.0]hexane-2,6-dicarboxylic acid (LY354740)[98,99,100] which displays low nanomolar agonist potency for mGluR2 and mGluR3, low micromolar agonist potency for mGluR6 and mGluR8, while it is not active at the remaining mGlu receptors (*Figure 2.1*).

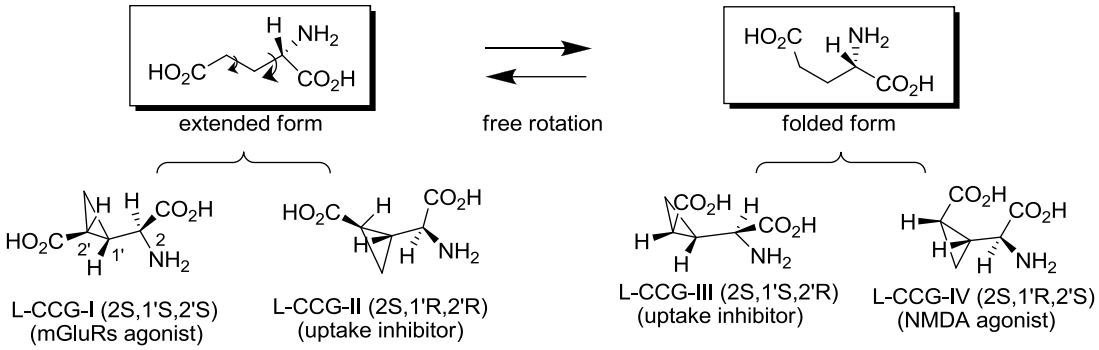


***Figure 2.1.*** Structures of L-2-(carboxycyclopropyl)glycines CCG-I–IV. From Shimamoto (1996)[i]

## 2.1.2 HOMOLOGATION OF THE AMINO ACIDIC CHAIN

Chain homologation of Glutamic acid leads to an increase of selectivity and to a switch of pharmacological profile strictly related to the absolute configuration of the amino acidic C-α atom. Homologation of *S*-Glu leads to *S*-amino adipic acid, which selectively activates mGluR2 and mGluR6, whereas it has no effect on mGluR1, mGluR4, or mGluR5.[,101,102]

On the other hand, while *R*-Glu is inactive, the *R* enantiomer of amino adipic acid behaves as a competitive NMDA receptor antagonist, even if with low potency. Very interestingly, a simple bioisosteric substitution of the distal carboxylic acid with a phosphonic acid group led to a potent and selective competitive antagonists for the NMDA receptor, i.e. (*R*)-2-amino-5-phosphonopentanoic acid (*R*-**AP-5**). Further extension of the backbone chain length gives another potent NMDA antagonist, i.e. (*R*)-2-amino-5-phosphonoeptanoic acid (*R*-**AP-7**) (*Figure 2.2*).

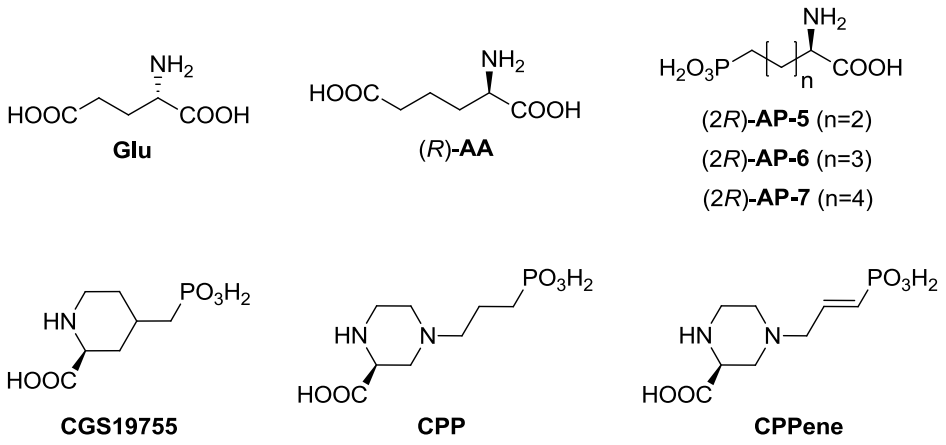


***Figure 2.2.***

## 2.1.3 INCREASE OF THE MOLECULAR COMPLEXITY

Kainate receptors possess a larger ligand binding pocket in comparison to AMPARs, due to the presence of less hindered amino acid residues. Consequently, the presence of a new functional group, usually in a non-pharmacophoric portion of the molecule can determine selectivity for KA *vs* AMPA receptors and may also bring about selectivity for specific KAR subtypes, due to the establishment of additional bond interactions with the binding pocket of the target receptor subunit, and/or causing the exclusion from undesired binding sites, for example due to steric clashes, with specific amino acidic residues.

For example, in Willardine the introduction of a bulky phenyl or thiophene moiety (UBP296 and UBP310) at the $N^3$ position of the uracil ring led to antagonists with an increased selectivity and potency at GluK1 receptors. The further insertion in ACET of a phenyl ring at the 5-position of the thiophene moiety determines the best selectivity and potency towards GluK1 so far obtained (*Figure 2.3*).

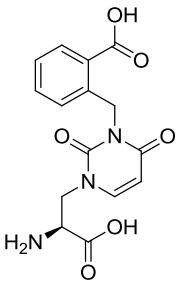


UBP296

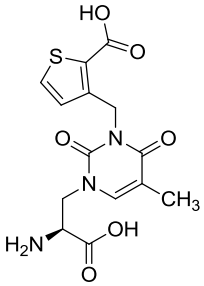


UBP310

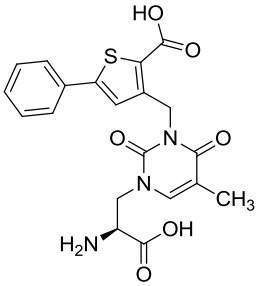


ACET

***Figure 2.3.***

## 2.2. DESIGN AND SYNTHESIS OF SELECTIVE KA ANTAGONISTS

The previously described strategies were applied on the structure/backbone to non selective AMPA/KA agonists for the design of new selective KAR antagonists possibly endowed with selectivity across the different KA receptor subtypes. In particular, I focused my attention on the following model compounds:

1. The endogenous ligand L-Glutamate
2. The natural compound L-Tricholomic acid
3. The synthetic compound CIP-AS

### 2.2.1. Design and synthesis of L-Glutamate homologues

Starting from the endogenous ligand L-Glu, I planned the synthesis of a series of γ-glutamyl-dipeptides, built by condensing the distal carboxylate of L-Glu to a series of differently functionalized amino acids. Such derivatives represent easy to synthesize ligands, featuring as ideal tools for rapidly probing the stereo-electronic properties of iGluRs, in the search for subtype-selective antagonists. Indeed, γ-glutamyl-dipeptides are acidic amino acids characterized by a 6-atom spacer connecting the proximal and the distal acidic functions and by different side chains useful to confer an increasing degree of molecular complexity on the molecules, making possible the establishment of additional interaction/steric occlusion with the binding pocket.

In detail, L-Glu was coupled to glycine and to a series of L-and D-amino acids shown in *Figure 2.4*. The coupling reaction was performed taking advantage of the innovative methodology of *flow chemistry*.

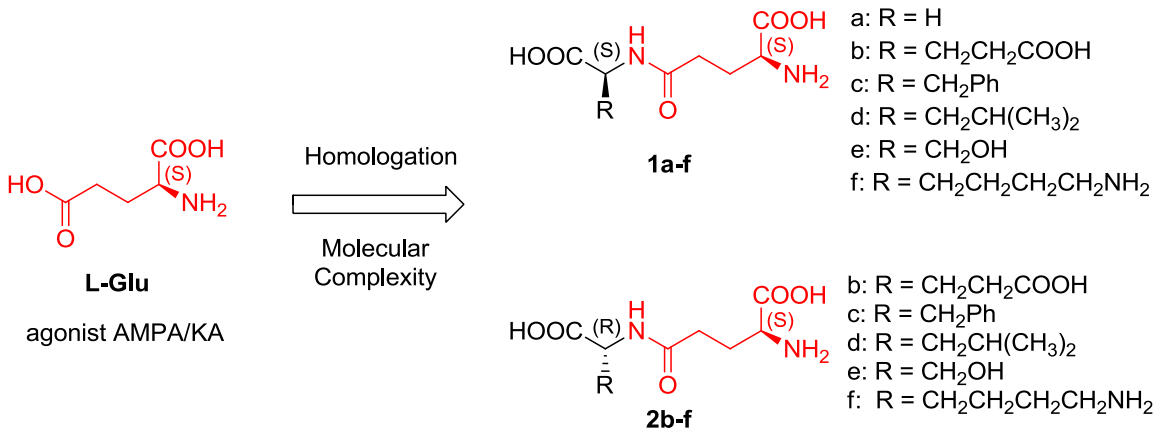


***Figure 2.4.***

Since reduction of the conformational freedom can be another efficient strategy to increase the receptor selectivity, I have also planned to synthesize a series of unusual isoxazoline containing β and ɣ dipeptides as higher homologues of L-Glu (*Figure 2.5*).

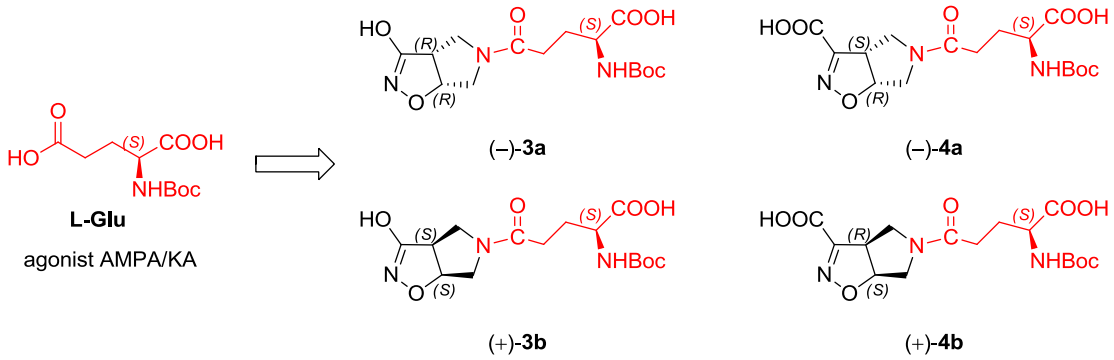


***Figure 2.5***

The ɣ-carboxylate of L-Glu was efficiently coupled with the isolated enantiomers of two rigid bicyclic scaffolds to give the conformationally constrained derivatives **3** and **4**. It has to be underlined that the bicyclic scaffold carries the distal acidic function, i.e. a carboxylate (compounds (–)-**4a**/(+)-**4b**) or a 3-hydroxy-isoxazoline (compounds (–)-**3a**/(+)-**3b**), which represent a bioisostere of the COOH group.

All the designed derivatives have been synthesized and pharmacologically characterized through the evaluation of their binding affinity for both native ionotropic glutamate receptors and for recombinant homomeric GluK1-3 receptors. Since it is known that the molecular complication of the aspartate/glutamate skeleton may generate molecules that act as blockers of the EAATs, we have also tested our derivatives **1a-f** and **2b-f** as potential inhibitors of glutamate transporters EAAT1-3.

## 2.2.2 Design and synthesis of L-Tricholomic acid analogues

L-Tricholomic acid is a natural compound extracted from the poisonous mushrooms *Tricholoma muscarium*, *Amanita strobiliformis* and *Ustilago maydis*. It is a partially rigidified analogue of the endogenous ligand L-Glu, in which the distal carboxylic group is bioisosterically replaced by the 3-hydroxy-isoxazoline ring. Its biological activity has been evaluated in the past in rat cortical giant neurons of *Achatina fulica* and resulted very similar to L-Glu. A recent study[103] has demonstrated that L-Tricholomic acid is an agonist at the AMPA and KA receptors ($IC_{50}$= 0.95 µM and 0.29 µM respectively) while its D-enantiomer interacts selectively with the NMDA receptors ($K_i$= 0.67 µM); moreover both the L-*threo* and D-*threo* diasteroisomers are weak and non-selective GluR ligands.

With the aim of increasing the affinity for the KA receptor and to switch the profile from agonist to antagonists, starting from L-Tricholomic acid, I have planned the synthesis of both *eritro* and *threo* stereoisomers (α*S*, 5*S*)-**5a-c** and (α*S*, 5*R*)-**6a-c** (*Figure 2.6*), characterized by the presence of bulky phenyl ring linked to the 3-position of the isoxazoline core. The hindered aromatic moiety was functionalized in the *ortho*, *meta* or *para* position with a carboxylic acid, realizing both an increase of the molecular complexity and an increase of the distance between the distal and the proximal carboxylate.

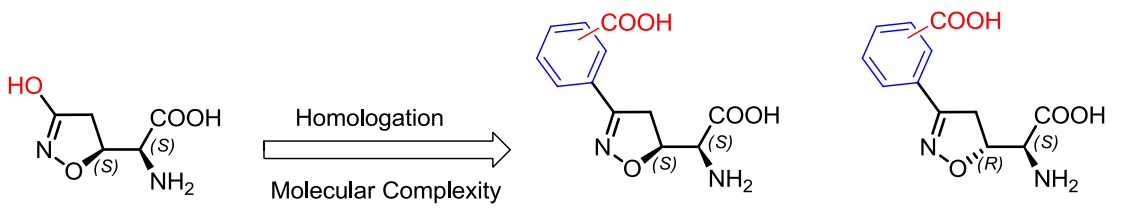


**L-Tricholomic acid**
agonist AMPA/KA

(α*S*,5*S*)-**5a:** 2-COOH
(α*S*,5*S*)-**5b:** 3-COOH
(α*S*,5*S*)-**5c:** 4-COOH

(α*S*,5*R*)-**6a:** 2-COOH
(α*S*,5*R*)-**6b:** 3-COOH
(α*S*,5*R*)-**6c:** 4-COOH )

***Figure 2.6.***

With the aim of investigating the effect of introducing a bulky moiety in different positions and with different spatial orientation, I substituted the isoxazoline ring with a pyrazoline bearing a benzyl group on the $N^1$. In analogy with the previously described amino acids **5a-c** and **6a-c**, the aromatic moiety was functionalized in the *ortho*, *meta* or *para* position with a further acidic function. Unfortunately, the *ortho*-substituted derivative resulted not stable in bases since it underwent lactamization due to the reaction of the aromatic carboxylate with the $N^2$ of the pyrazoline, forming a stable six-membered ring.

In order to facilitate the synthetic pathway, the starting point for the synthesis of the planned molecules was D,L-Serine. The final amino acids (±)-**7a**/(±)-**7b** and (±)-**8a**/(±)-**8b** (*Figure 2.7*) were initially tested on iGluRs as racemic mixture of diasteroisomers, with the purpose of repreparing and testing the isolated enantiomers only if any interesting biological activity was observed.

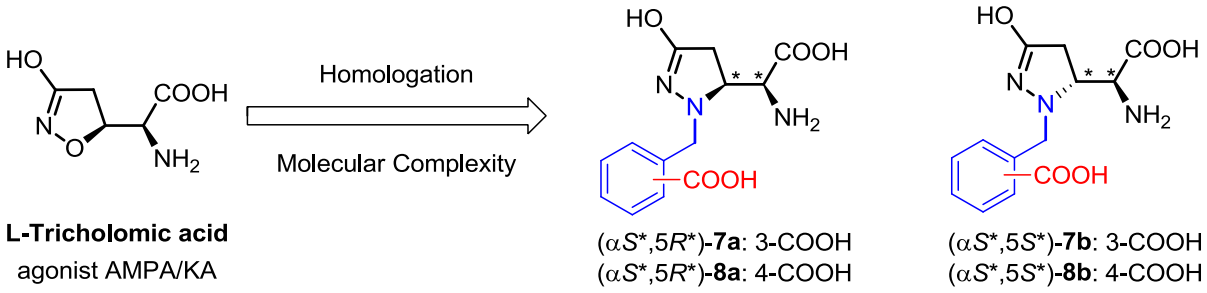


**L-Tricholomic acid**
agonist AMPA/KA

(αS*,5R*)-**7a**: 3-COOH
(αS*,5R*)-**8a**: 4-COOH

(αS*,5S*)-**7b**: 3-COOH
(αS*,5S*)-**8b**: 4-COOH

***Figure 2.7.***

The new derivatives were compared to the model compound L-*erythro* Tricholomic acid in terms of affinity and selectivity for the different ionotropic receptors. It was also evaluated the interaction of our new ligands with human recombinant EAAT subtypes EAAT1-3.

## 2.2.3. Design and synthesis of CIP-AS analogues

Only a few GluK1 selective antagonists have been discovered to date. Among these, considerably interesting are Willardine derivatives. The natural compound Willardine is a partial agonist at AMPA and KA receptors and has been extensively used as a lead structure to design novel neuroprotective agents: the introduction of a halogen (5-iodowillardine) in the uracil ring increases the affinity for activating KARs containing homomeric or heteromeric GluK1 subunit. On the contrary, the presence of a further acidic function linked through an aromatic spacer to the $N^3$ position of the ring (UBP 302, UBP 310, ACET) switches the activity from agonist to antagonist.

By applying a strategy similar to that used for the design of UBP and ACET derivatives, I have designed new potential KARs antagonists by modifying the structure of CIP-AS, a potent non-selective AMPA/ KA agonist previously reported by P. Conti et al.[104](*Figure 2.8*). The aromatic group (phenyl or thiophene) was used as a spacer to add a further acidic function in order to favor possible additional/alternative ionic or hydrogen bonding interactions within the binding pocket.

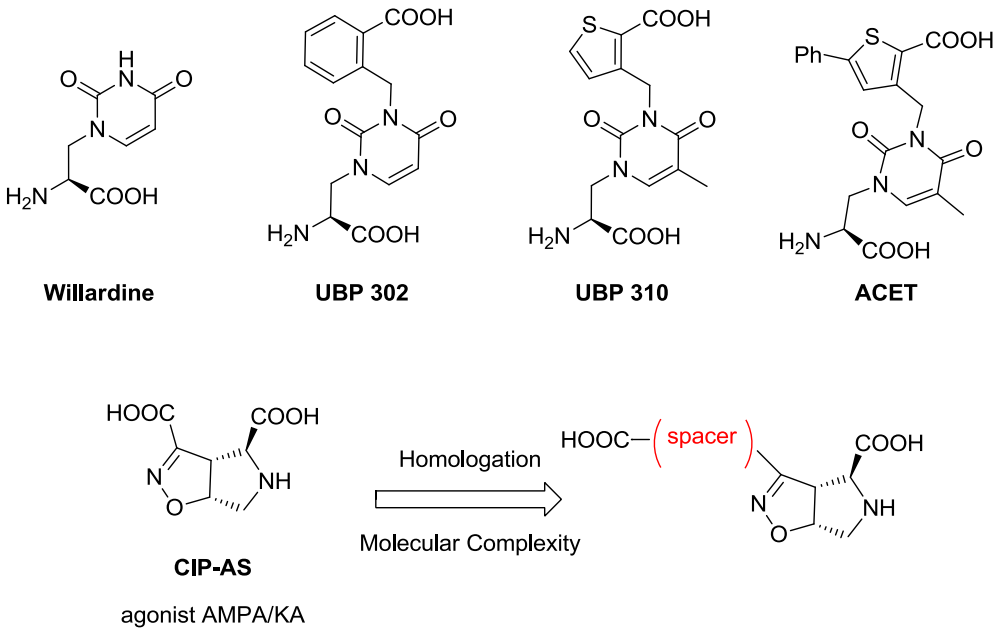


***Figure 2.8.***

Derivatives **9a** and **9d** (*Figure 2.9*) were designed in close analogy with model compounds UBP302 and UBP310. Moreover, in order to study the structure-activity relationships of this new class of KAR antagonists, amino acids **9b** and **9c**, having the acidic group in the *meta* or *para*-position of the phenyl ring, were synthesized. In addition, also the orientation of the carboxylic function on the thiophene ring was modified (derivatives **9e,f**) (*Figure 2.9*).

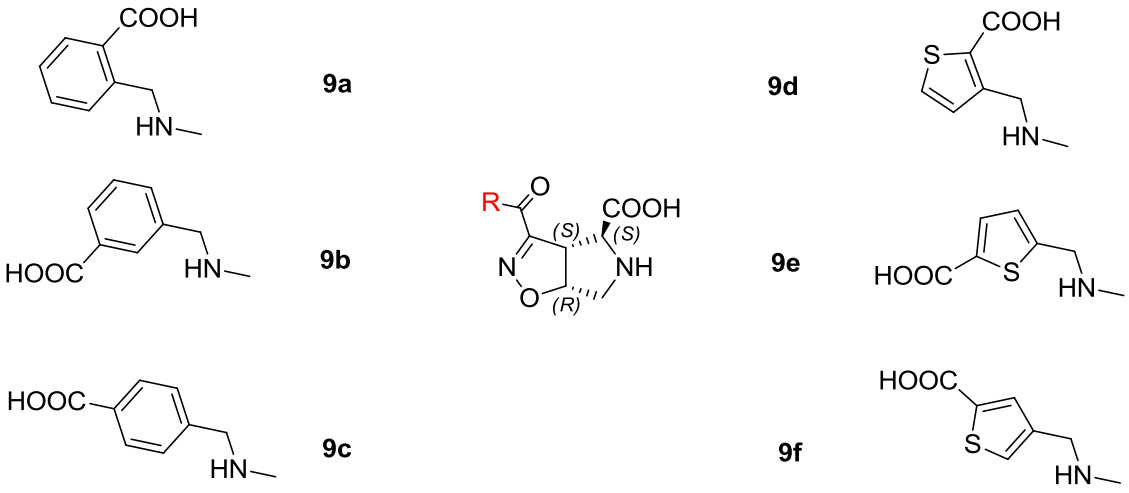


***Figure 2.9.***

Final compounds **9a-f** were pharmacologically characterized in order to evaluate their affinity for native iGluRs and for recombinant homomeric GluK receptors. Moreover, we have also tested our new derivatives as potential inhibitors of glutamate transporters EAAT1-3.

# CHAPTER 3. L-GLUTAMATE HOMOLOGUES

## 3.1 CHEMISTRY

### 3.1.1 Synthesis of γ-glutamyl-dipeptides

The first part of my work involved the synthesis of γ-glutamyl dipeptides, which are higher homologs of the natural ligand (*S*)-Glu. As explained in Chapter 2, the medicinal chemistry strategy of elongating the glutamate amino acidic chain, associated with an increase of steric hindrance, leads to compounds **1a-f** and **2b-f** with an increased likelyhood to be antagonists selectively targeting kainate receptors or even a specific KA receptor subtype (*Figure 3.1*).

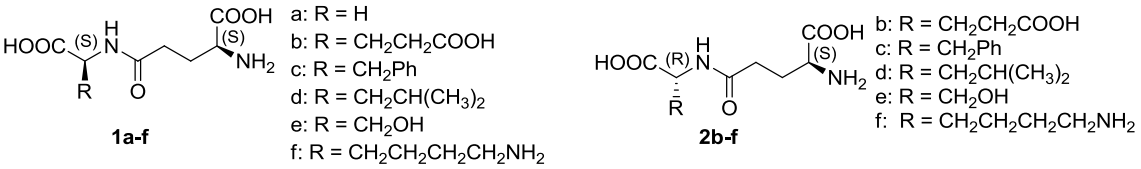


***Figure 3.1.***

(*S*)-Glu was used as starting point for the synthesis of the suitably protected amino acid (+)-**13**.The carboxylic functions of L-Glu were functionalised using protecting groups with orthogonal stability: the distal carboxylic acid function was initially protected as benzyl ester, whereas the α-carboxylic acid was protected as ethyl ester. This strategy allowed me to obtain compound (+)-**12**, which was finally submitted to a catalytic hydrogenation in the presence of 5% Pd/C to give the key intermediate (+)-**13** in 84% yield and high purity (*Figure 3.2*).

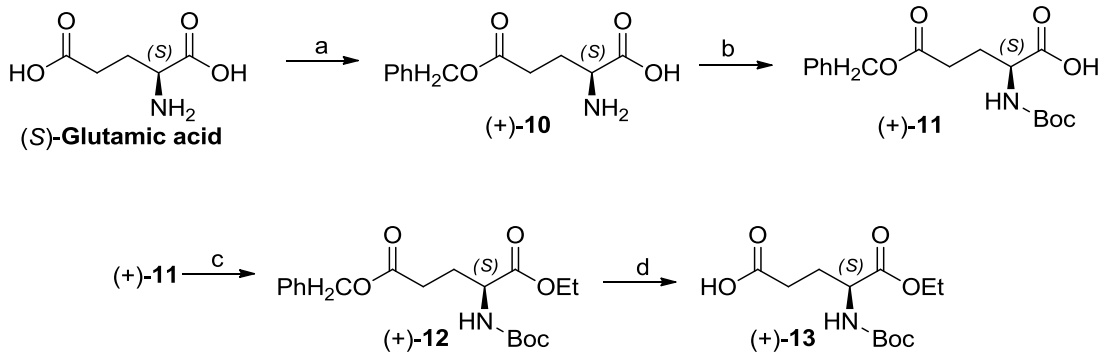

***Figure 3.2.*** a) BnOH, HCl conc. b) $(Boc)_2O$, $NaHCO_3$, $H_2O$, THF c) DCC, DMAP, EtOH, $CH_2Cl_2$ d) $H_2$, 5% Pd/C, EtOH

Each amino acid used in the coupling reaction was protected as methyl ester at the carboxylic function. This step was carried out using thionyl chloride in MeOH and the corresponding ester was obtained in a quantitative yield as a hydrochloride salt (*Figure 3.3*).

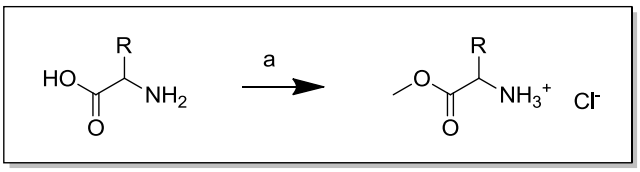


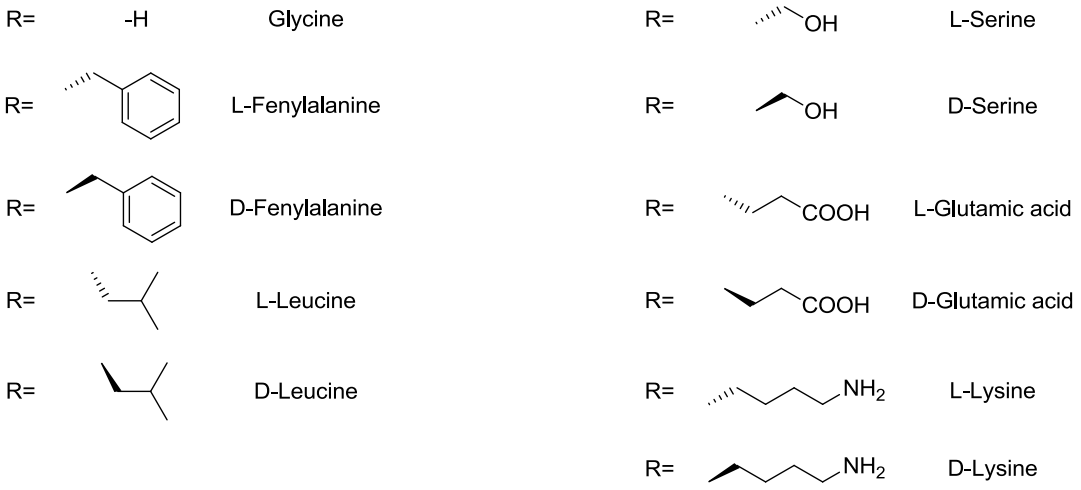


***Figure 3.3.*** a) $CH_3OH$, $SOCl_2$

The amino acids Lys, Glu and Ser were further protected at the side chain functional groups. In the case of Glutamic acid, both the carboxylates were protected using the same procedure described above.

For Lysine, the more reactive distal amino function was selectively protected with the Boc group using 1 equivalent of $(Boc)_2O$ (*Figure 3.4*).

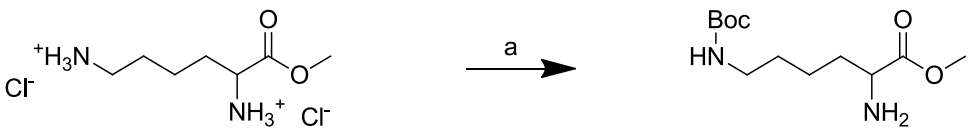


lysine methylester * 2HCl lysine methylester N-Boc

***Figure 3.4.*** a) $(Boc)_2O$, TEA, $CH_3OH$, $CH_2Cl_2$

For the amino acid Serine, it was necessary to protect the hydroxyl function with the trytil group, which can be easily removed in the same strongly acidic conditions as the Boc group. Thus, I synthesized first the methyl ester and protected both the hydroxyl and the amine function with triphenylchloromethane in the presence of triethylamine (TEA). Subsequently, the amine function was selectively deprotected using a 1% trifluoroacetic acid (TFA) solution in $CH_2Cl_2$ and the product was isolated as free amine after extraction from a basic aqueous solution (*Figure 3.5*).

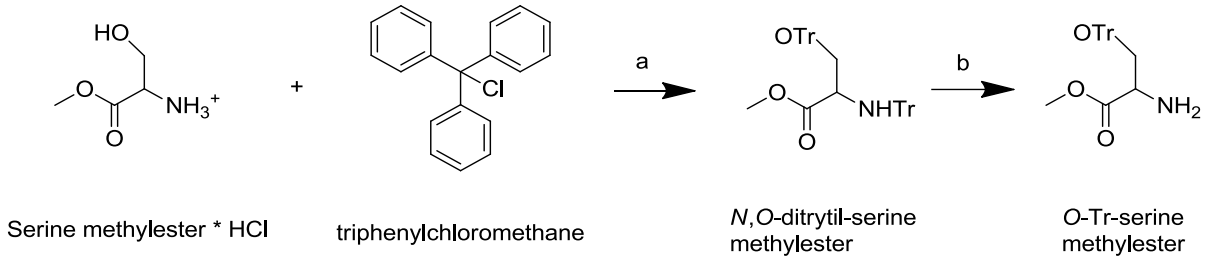


***Figure 3.5.*** a) TEA, $CHCl_3$ b) 1% TFA in $CH_2Cl_2$

The optimal conditions for the coupling reactions between the key intermediate (+)-**13** and the different methyl ester amino acids were reached using hydroxybenzotriazole (HOBt) and *N,N,N',N'*-tetramethyl-O-(1*H*-benzotriazol-1-yl)uronium hexafluorophosphate (HBTU) as coupling reagents and *N,N*-diisopropylethylamine (DIPEA) as base, in THF (*Figure 3.6*). The reaction took place in 24 hours and required an aqueous work-up and a column chromatography to afford the desired products **14**-**24**.

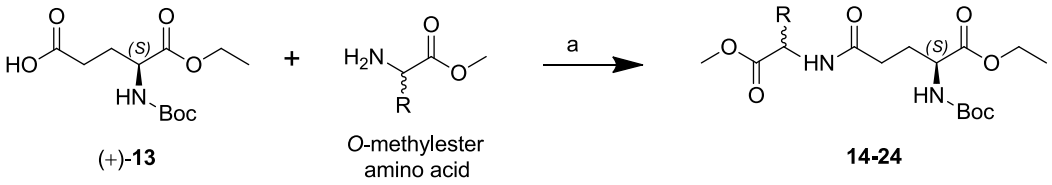


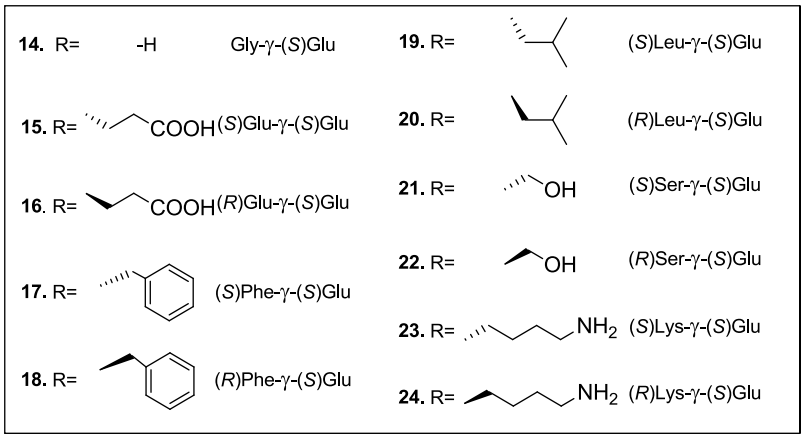


***Figure 3.6.*** a) HOBt, HBTU, DIPEA, THF

Consequently, the coupling reaction was optimized exploiting a Vapourtec R2+/R4 *flow chemistry* reactor.

First, the carboxylic acid (+)-**13** was activated through the linkage to polymer supported HOBt (PS-HOBt). To this aim PS-HOBt was packed into a glass column (Ø:6.6mm; h: 100 mm), then a solution of the carboxylic acid (+)-**13**, DIPEA and of bromo-tris-pyrrolidino phosphoniumhexafluorophosphate (PyBroP) in DMF was fluxed (150 µL/min) for 1 hour through the column (*Figure 3.7*). PyBroP is a peptide coupling reagent that promotes the activation of (+)-**13**, with a consequent facilitated linkage to PS-HOBt.

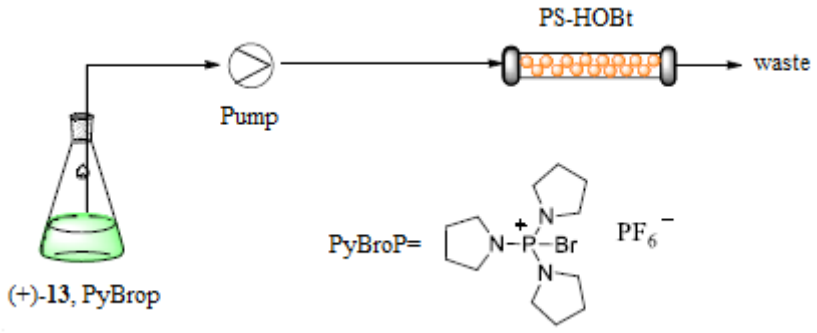


***Figure 3.7.***

At this point I set up the proper reactor configuration to perform the coupling reaction.

The reactor was configured as follows:

1) a glass column packed with Amberlyst A-21, a resin bearing a dimethylamino function;

2) the column containing the activated (+)-**13**;

3) a column packed with Amberlyst A-15, a sulphonic acid resin.A solution of the desired amino acid methylester hydrochloride salt in DMF (1 mmol, 0.2 M) was fluxed into the column containing A-21 to liberate the free amine, which was then fluxed into the column containing the activated acid (+)-**13** linked to the resin (*Figure 3.8*), where the coupling took place. The exiting flow stream was finally directed into a column filled with A-15 to perform an in-line purification, by removing any unreacted amine.

Exploiting this innovative approach, it was possible to obtain the desired dipeptides **14-24** in high yield (75-95%) and with a significant reduction of time (residence time: 10 min). Moreover, the products were obtained in high purities (> 95%) without any aqueous work up or column chromatography.

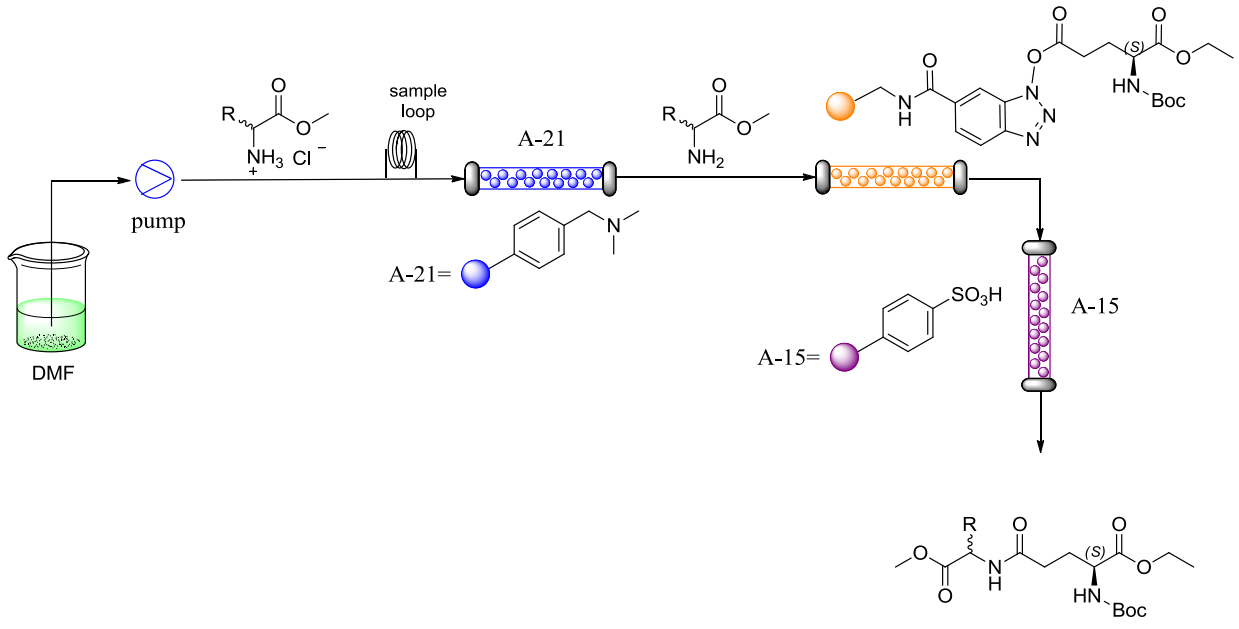


***Figure 3.8***

The final compounds **1a-f** and **2b-f** were obtained after deprotection of the carboxylate and amine

functions of intermediates **14**-**24**. These steps were easily carried out in batch, hydrolysing the esters with 1N NaOH in MeOH and removing the Boc protecting groups in acidic conditions using a 30% trifluoroacetic acid solution in $CH_2Cl_2$ (*Figure 3.9*).

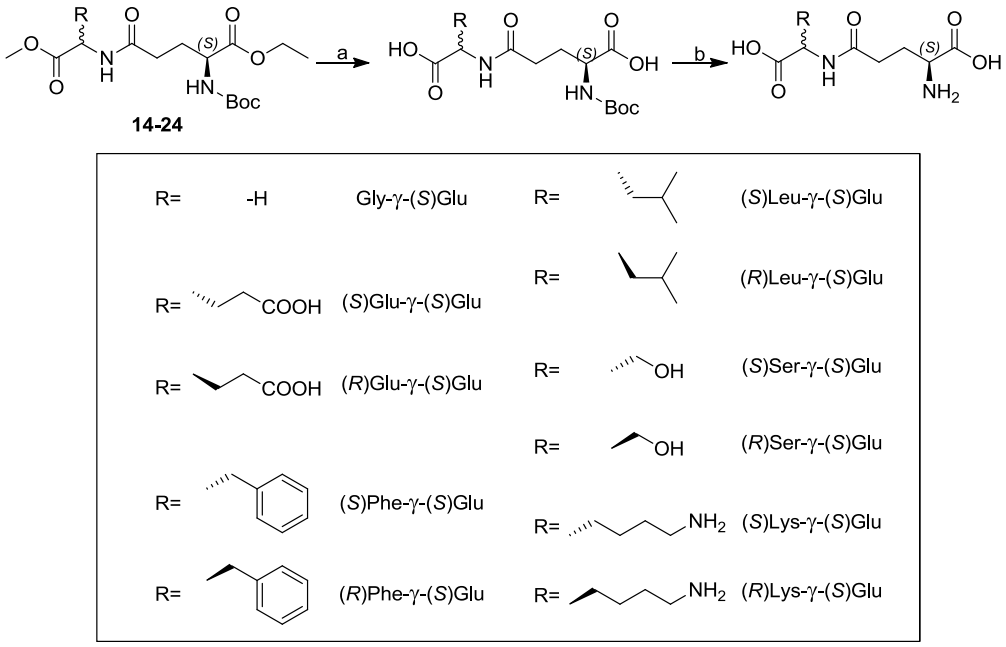


***Figure 3.9.*** a) 1N NaOH, MeOH; b) 30% TFA in $CH_2Cl_2$

In the case of the compounds **23** and **24**, which possess the distal amino function of Lys, the acidic ion exchange resin Amberlite IR-120 was used to eliminate the salt formed between the distal amine and the TFA. The final product was then released from the resin using a 1N ammonia solution.

## 3.1.2 Synthesis of unusual isoxazoline-containing β and γ dipeptides

Still using L-Glu as a model compound I have then applied a design approach which combined chain homologation and reduction of the conformational freedom**,** the latter being an efficient strategy to increase the receptor selectivity.

Therefore, I planned the synthesis of dipeptides (−)-**3a**, (+)-**3b** and (−)-**4a**, (+)-**4b** in which the distal carboxylate of glutamic acid was condensed to unconventional isoxazoline-containing beta or gamma amino acids, thus generating partially constrained glutamic acid higher homologues, of different length, possessing the suitable characteristic to be considered potential selective Glu receptor antagonists (*Figure 3.10*).

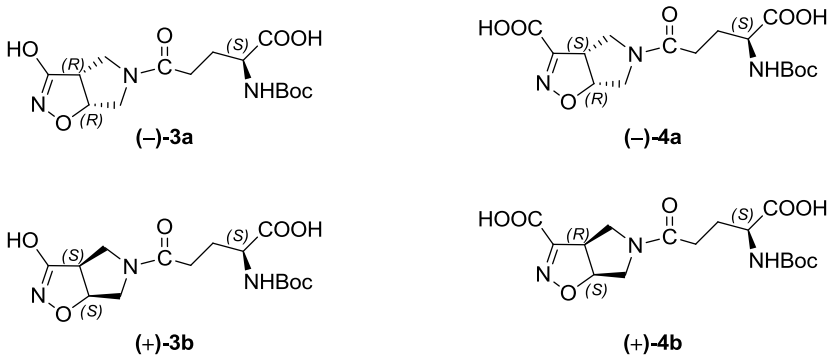


***Figure 3.10.***

The γ-carboxylate of L-Glu (+)-**13** was efficiently coupled with the isolated enantiomers of two rigid bicyclic scaffolds to give the conformationally constrained derivatives **3** and **4**.

Amino acids (−)-**3a** and (+)-**3b** were obtained from intermediates (−)-**26** and (+)-**26**, obtained after resolution of the racemic mixture (±)-**26**. The cycloadduct (±)-**26** was prepared through a 1,3-dipolar cycloaddition reaction of the dipolarophile **25** with bromoformonitrile oxide, generated *in situ* by treatment of 2,2-dibromoformaldoxime with a base (*Figure 3.11*). The reaction takes place in a heterogeneous phase, using $NaHCO_3$ as base and EtOAc as solvent. This method is used with very sluggish dipolarophiles to reduce the formonitrileoxide formation rate and the consequent undesired dimerization to furoxan.

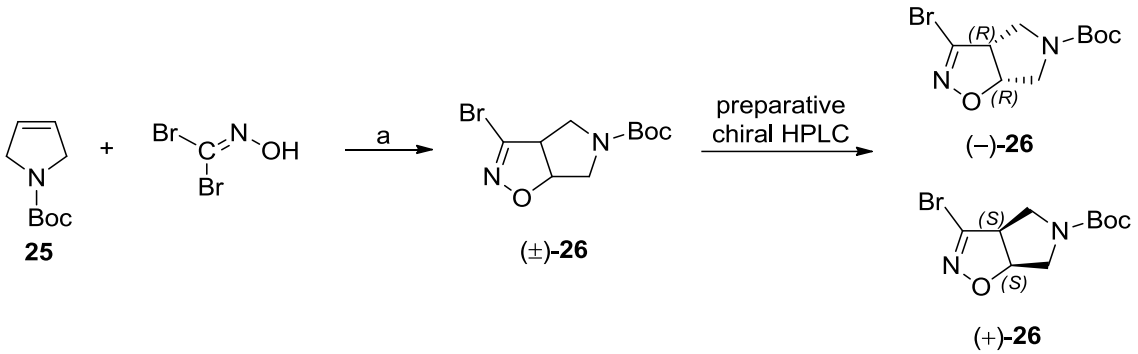


***Figure 3.11.*** a) $NaHCO_3$, EtOAc

In order to find the suitable conditions to resolve the racemic mixture, a small quantity of (±)-**26**, was analysed by chiral HPLC *(Figure 3.11*). To this aim, I explored a number of differently functionalized cellulose-and amylose-based phases in combination with various eluent solutions and flow rates. An excellent enantiomeric separation was obtained using tris-(3,5-dimethyl-phenyl)carbamoyl amylose as chiral stationary phase and 95/5 n-hexane/iPrOH as eluent mixture at a flow rate of 1mL/min. (α = 1.4; Rs = 2.5; see chapter 6.3). Semi-preparative chiral HPLC on compound (±)-**26** (injection volume: 1 ml, concentration: 100 mg/ml) allowed me to collect substantial amounts of the two enantiomers (–)-**26** and (+)-**26** with high enantiomeric excess (e.e. >99%).

The absolute configuration of the stereogenic centers for derivatives (+)-**26** and (–)-**26** was unequivocally determined by single crystal X-Ray analysis performed on the enantiomerically pure (+)-**26**. Thanks to the anomalous scattering of the bromine atom, the absolute configuration was unequivocally determined as (+)-(*S*,*S*)-**26** (*Figure 3.12*).

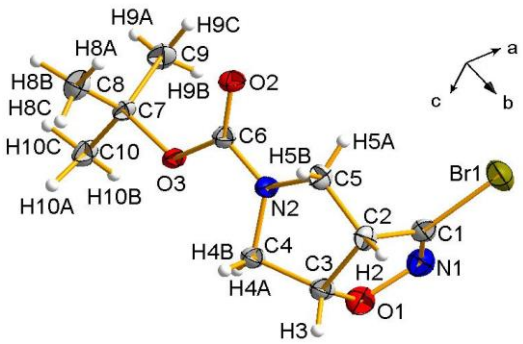


***Figure 3.12.*** Perspective view of the molecular structure with numbering for compound (+)-(*S*,*S*)-2**6**

The two enantiomers (–)-**26** and (+)-**26** were then in parallel submitted to *N*-Boc deprotection reaction using a 30% solution of trifluoroacetic acid in $CH_2Cl_2$ (*Figure 3.13*). The corresponding secondary amines, (–)-**27** and (+)-**27** respectively, were then submitted to the coupling reaction with the previously prepared protected-L-Glu derivative (+)-**13** using HOBt and HOBTU as coupling reagents and DIPEA as base in $CH_2Cl_2$.

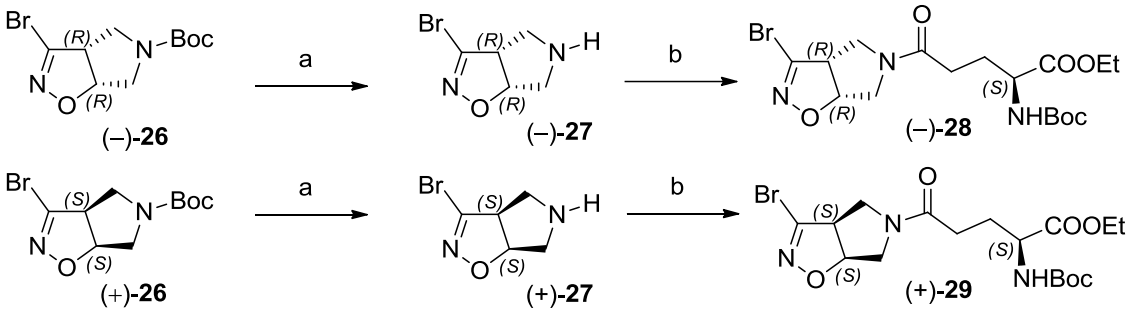


***Figure 3.13.*** a) 30% TFA in $CH_2Cl_2$: b) (+)-**13**, HOBt, HBTU, DIPEA, $CH_2Cl_2$

Starting from intermediates (–)-**28** and (+)-**29**, the initially planned synthetic step was the hydrolysis of the amino acidic ester group and the nucleophilic substitution of the 3-Br isoxazoline to give the corresponding 3-OH derivative. To this aim compounds (–)-**28** and (+)-**29** were treated with a 1N NaOH aqueous solution at room temperature. Unfortunately, under these reaction conditions only the ester hydrolysis was accomplished, whereas the nucleophilic substitution of the 3-Br isoxazoline did not take place. Therefore, I increased the temperature up to 60 °C, but in this case hydrolysis of the amide bond occurred (*Figure 3.14*).

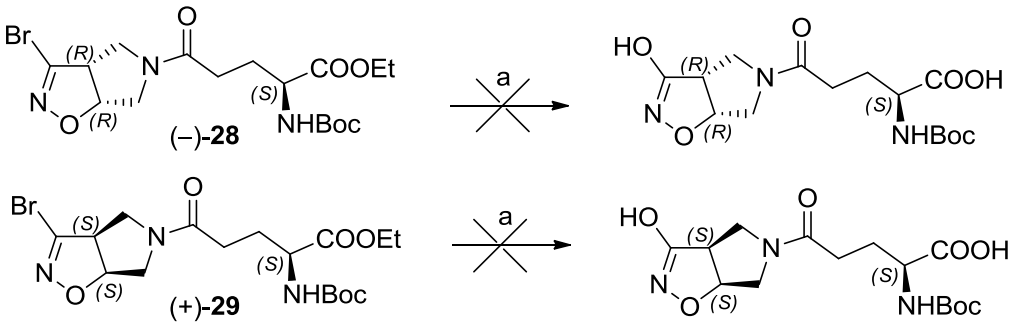


***Figure 3.14.*** a) 1N NaOH/Dioxane 20-60 °C

Consequently, the synthetic strategy was revised: enantiomers (–)-**26** and (+)-**26** were submitted to a nucleophilic substitution at the C-3 in the presence of benzyl alcohol and NaH in THF at room temperature. The reaction produced the desired 3-benzyloxy-substituted intermediates (–)-**30** and (+)-**30,** respectively, in very high yield (94%).

On both enantiomers the *N*-tert-butyl carbamate protecting group was removed by treatment with 30% trifluoroacetic acid solution in $CH_2Cl_2$ to give the free amines (–)-**31** and (+)-**31** (*Figure 3.15*) that were used for the coupling reaction with the protected- L-Glu derivative (+)-**13**. The reaction was performed under the already optimised condition described above to give with 70% yield the desired adducts (–)-**32** and (+)-**33** (*Figure 3.15*).

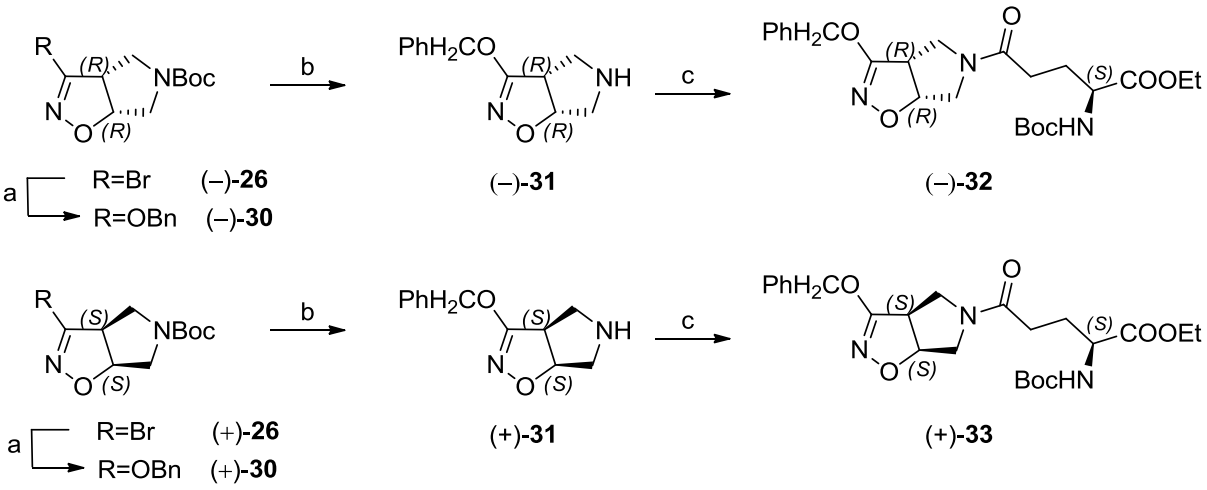


***Figure 3.15.*** a) BnOH, NaH, dry THF; b) 30% TFA, $CH_2Cl_2$ c) (+)-**13**, HOBt, HBTU, DIPEA; $CH_2Cl_2$

Once I have obtained the two diastereoisomers (–)-**32** and (+)-**33**, I evaluated the feasibility of performing an HPLC separation of the two diastereoisomer at this level. A good separation was obtained when I tried as stationary phase the chiral phase mentioned above (tris-(3,5-dimethyl-phenyl)carbamoyl amylose). The optimised chromatographic conditions ($\alpha$ = 1.3; Rs = 2.0; see chapter 6.3) were suitable to separate the two diastereoisomers also on a preparative scale (injection volume: 2 ml, concentration: 22 mg/ml). This finding allowed me to make the overall synthetic pathway more convenient, working on the racemic starting material (±)-**26** and separating the two enantiopure diastereoisomers (–)-**32** and (+)-**33** at this level. (*Figure 3.16*).

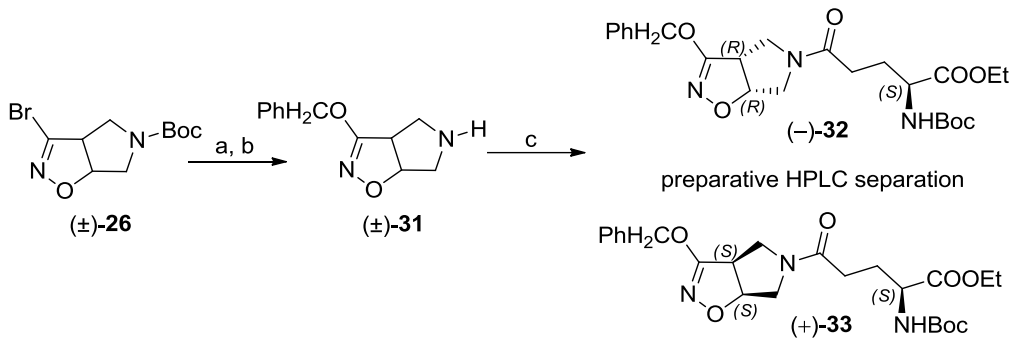


***Figure 3.16.*** a) BnOH, NaH, dry THF; b) 30% TFA, $CH_2Cl_2$ c) (+)-**13**, HOBt, HBTU, DIPEA; $CH_2Cl_2$

Compounds (–)-**32** and (+)-**33** were hydrolyzed at the amino acidic ester with 1N NaOH and then submitted to catalytic hydrogenation with 5% Pd/C to remove the O-benzyl group to give the diacidic intermediates (–)-**34** and (+)-**35**. Finally, treatment with a 30% trifluoroacetic acid solution in $CH_2Cl_2$ gave the final amino acids (–)-**3a** and (+)-**3b**, respectively (*Figure 3.17*).

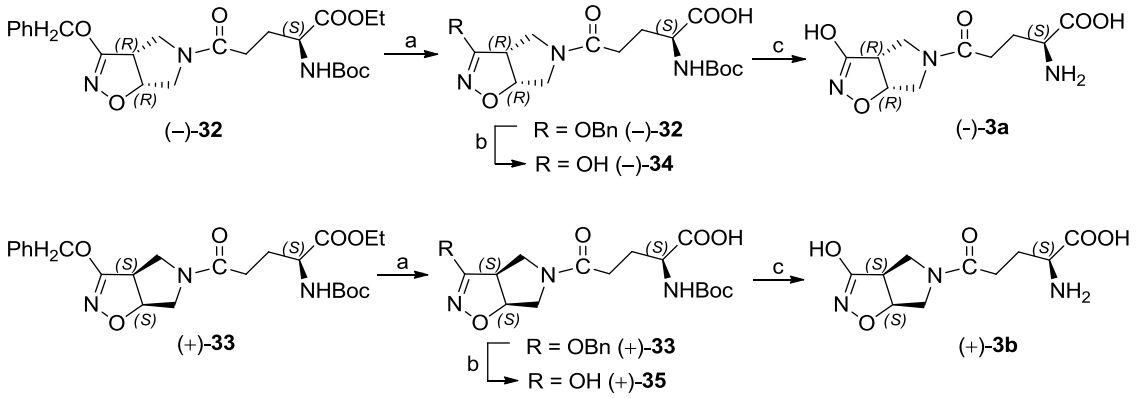


***Figure 3.17.*** a) 1N NaOH, EtOH b) $H_2$, 5% Pd/C, MeOH c) 30% TFA, $CH_2Cl_2$

Amino acids (–)-**4a** and (+)-**4b** were obtained following the same synthetic pathway. The synthesis of compounds (±)-**36** was carried out by exploiting the 1,3-dipolar cycloaddition reaction of the dipolarophile **25** with ethoxycarbonyl formonitrile oxide, generated *in situ* by treatment of ethyl 2-chloro-2-(hydroxyimino)acetate with a base (*Figure 3.18*). Also in this case the reaction was carried

out in a heterogeneous phase, using $NaHCO_3$ as base and EtOAc as solvent.

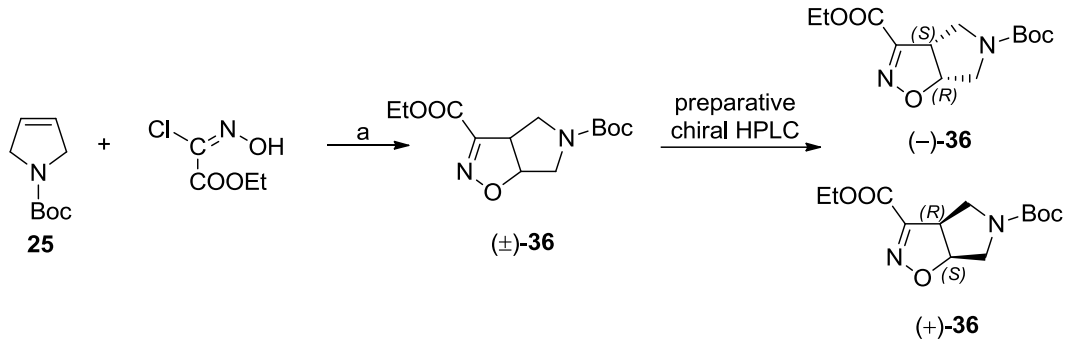


***Figure 3.18***. a) $NaHCO_3$, EtOAc

As reported for racemate (±)-**26**, in order to resolve the racemic mixture, racemate (±)-**36** was analysed by chiral HPLC. In this case, an excellent enantiomeric separation was obtained using the tris-(2-dimethyl-5-chloro-phenyl)carbamoyl amylose as chiral stationary phase and using 4/1 n-hexane/iPrOH as eluent mixture at a flow rate of 1mL/min. (α= 1.9; Rs = 3.9; see chapter 6.3). Derivative (±)-**36** was then subjected to semipreparative HPLC (injection volume: 2 ml, concentration: 20 mg/ml), and substantial amounts of the two enantiomers (–)-**36** and (+)-**36** were collected with high enantiomeric excess (e.e. >99%). Since compounds (–)-**36** and (+)-**36** are not solid and do not contain any heavy atom capable of giving the anomalous scattering necessary for the assignment of the absolute configuration, I tentatively hypothesized the absolute configuration of (–)-**36** and (+)-**36** by comparing their optical rotations with those of their strictly related analogues (–)-(*R*,*R*)-**26** and (+)-(*S*,*S*)-**26** (*Figure 3.19*).

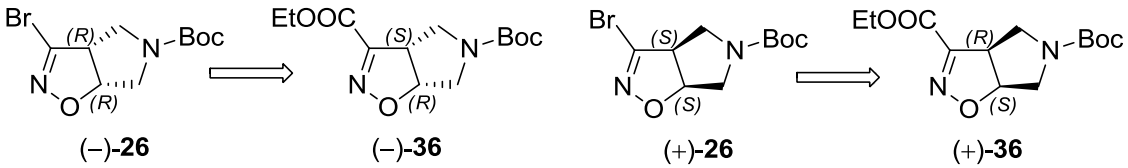


***Figure 3.19***. Initial hypothesis on the absolute configuration of (–)-**36** and (+)-**36**

On both the enantiomers the *N*-tert-butyl carbamate protecting group was removed by treatment with 30% trifluoroacetic acid solution in dichloromethane to give the free amines (–)-**37** and (+)-**37** that were used for the coupling reaction with the protected-L-Glu derivative (+)-**13** (*Figure 3.20*). The reaction was performed under the already optimised condition described above to give the desired diastereoisomers (–)-**38** and (+)-**39** (*Figure 3.20*).

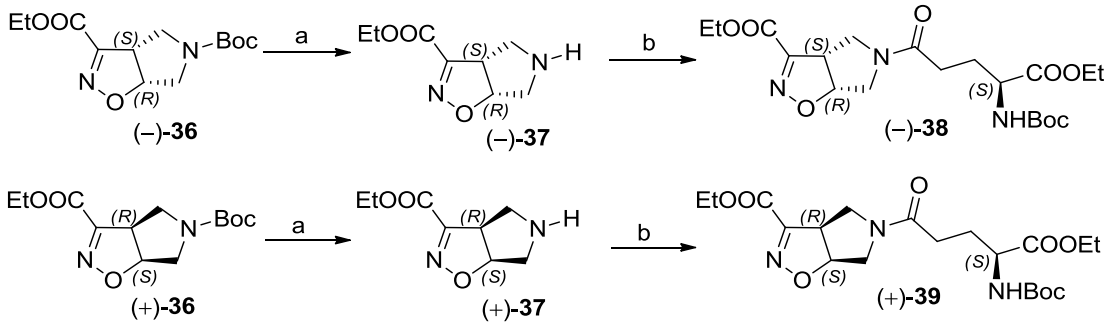


***Figure 3.20.*** a) 30% TFA, $CH_2Cl_2$; b) (+)-**13**, HOBt, HBTU, DIPEA; $CH_2Cl_2$

As before, I envisaged the possibility of separating the diasteroisomers (–)-**38** and (+)-**39** at this level by HPLC. An excellent separation was obtained when I used as stationary phase the tris-(3,5-dimethyl-phenyl)carbamoyl amylose chiral stationary phase. The optimised chromatographic conditions (α= 1.9; Rs = 3.0; see chapter 6.3) were suitable to separate the two diastereoisomers also at a preparative scale (injection volume: 2 ml, concentration: 20 mg/ml). Again, the all synthetic pathway can be optimized by working on racemic (±)-**36**, and then separating the two diastereoisomers (–)-**38** and (+)-**39** by preparative HPLC (*Figure 3.21*).

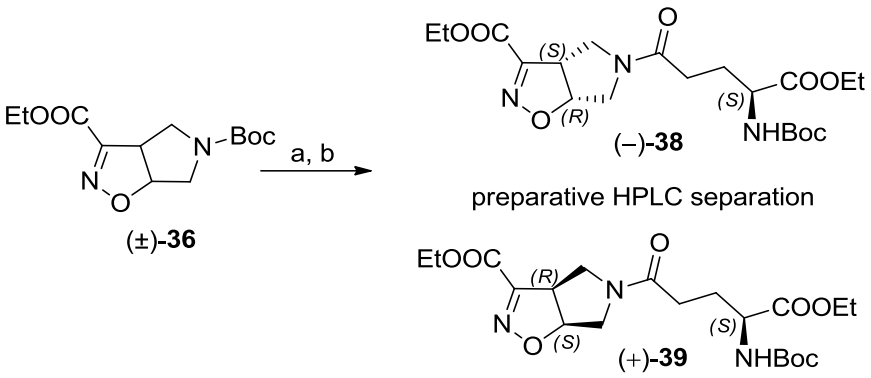


***Figure 3.21.*** a) 30% TFA in $CH_2Cl_2$ b) (+)-**13**, HOBt, HBTU, DIPEA, $CH_2Cl_2$

Compounds (–)-**38** and (+)-**39** were submitted to hydrolysis reaction at the two ester functions with 1N NaOH aqueous solution to give the dicarboxylic intermediates. Finally, treatment with a 30% trifluoroacetic acid solution in dichloromethane gave the final amino acids (–)-**4a** and (+)-**4b**, respectively (*Figure 3.22*).

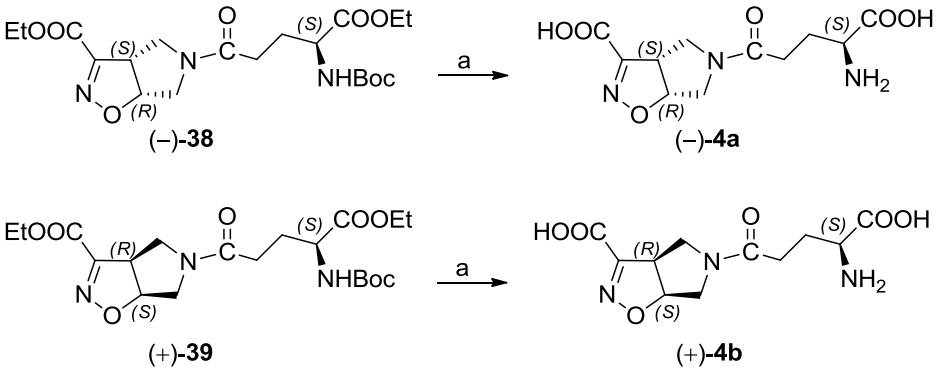


***Figure 3.22.*** a) 1N NaOH, EtOH, 30% TFA in $CH_2Cl_2$

The final derivatives (–)-**4a** and (+)-**4b** have been obtained as white crystals and therefore I tried to secure unequivocally their absolute configurations by X-ray analysis. I focused my efforts on compound (+)-**4b**. Despite the lack of anomalous scatterers in the unit cell, in this case, being the absolute configuration at the α amino acidic carbon known to be *S*, it was sufficient to determine the relative configuration of the three stereogenic centers, to unequivocally assign the absolute configuration (2*S*, 7*S*, 8*R*) to the enantiomer (+)-**4b** (see *Figure 3.23* for numbering) and consequently the absolute configuration (2*S*, 7*R*, 8*S*) to the enantiomer (–)-**4b.** This was in accordance with our initial hypothesis based on a comparison between the optical rotation of

these compounds and those of related derivatives.

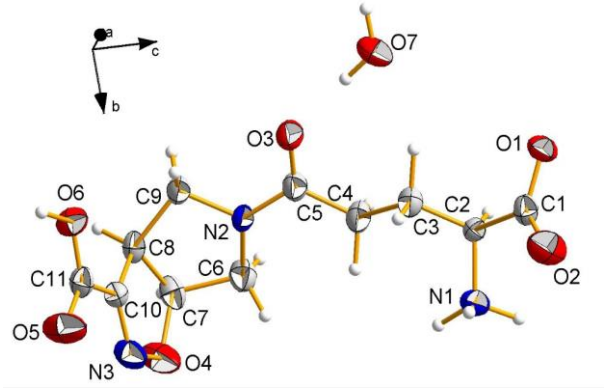


***Figure 3.23.*** Asymmetric unit of (+)-**4b**, with the atom numbering figure.

## 3.2 PHARMACOLOGY

All new amino acids were submitted to preliminar binding assays at native iGluRs and at recombinant homomeric GluK1-3 receptors. Binding assays at native iGluRs were performed using rat brain synaptic membranes from male Sprague–Dawley rats. Affinities for NMDA, AMPA, and KA receptors were determined using 2 nM [3H]CGP39653, 5 nM [3H]AMPA, and 5 nM [3H]KA.[105] Homomeric GluK1-3 receptors were expressed by infecting *Spodoptera frugiperda* (*Sf9*) insect cells with recombinant baculovirus carrying cloned rat GluK1-3.[106] Affinities were determined using [3H]KA as radioligand at a concentration of 10 nM in GluK1 experiments and 5 nM in GluK2-3 experiments. The experiments were performed at the Department of Drug Design and Pharmacology (University of Copenhagen).

## 3.2.1 Pharmacological assays on derivatives **1a-f** and **2b-f**:

| Compound | Rat Brain | | | Recombinant iGluR | | |
|---|---|---|---|---|---|---|
| | AMPA-R | KA-R | NMDA-R | GluK1 | GluK2 | GluK3 |
| | $K_i$ (μM) | $K_i$ (μM) | $K_i$ (μM) | $K_i$ (μM) | $K_i$ (μM) | $K_i$ (μM) |
| **Gly-γ-(*S*)Glu (1a)** | > 100 | 4.1 ± 0.5 | 5.4 ± 0.07 | 2.00± 0.85 | > 100 | > 100 |
| **(*S*)Glu-γ-(*S*)Glu (1b)** | 8.45 ± 1.22 | 0.738 ± 0.16 | 0.92 ±0.03 | 4.77 ± 1.41 | 11.7 ± 1.3 | 13.3 ± 1.5 |
| **(*R*)Glu-γ-(*S*)Glu (2b)** | > 100 | 24.0 ± 1.8 | 9.6 ± 0.08 | 29.4 ± 9.1 | 17.7 ± 1.3 | 20.0 ± 3.0 |
| **(*S*)Phe-γ-(*S*)Glu (1c)** | > 100 | 10.1 ± 0.7 | 40 ± 0.10 | 33.8 ± 13.9 | > 100 | > 100 |
| **(*R*)Phe-γ-(*S*)Glu (2c)** | > 100 | > 100 | > 100 | 8.35 ± 1.41 | > 100 | > 100 |
| **(*S*)Leu-γ-(*S*)Glu (1d)** | > 100 | 15.5 ± 0.9 | 44 ± 0.11 | > 100 | > 100 | > 100 |
| **(*R*)Leu-γ-(*S*)Glu (2d)** | > 100 | > 100 | > 100 | > 100 | > 100 | > 100 |
| **(*S*)Ser-γ-(*S*)Glu (1e)** | > 100 | 4.0 ± 0.4 | 5.8 ± 0.10 | 3.83 ± 1.08 | 48.3 ± 2.6 | > 100 |
| **(*R*)Ser-γ-(*S*)Glu (2e)** | > 100 | 43 ± 7 | 21 ± 0.10 | 36.02 ± 5.60 | > 100 | > 100 |
| **(*S*)Lys-γ-(*S*)Glu (1f)** | > 100 | 9.8 ± 3.4 | 22 ± 0.14 | **0.464 ± 0.094** | > 100 | > 100 |
| **(*R*)Lys-γ-(*S*)Glu (2f)** | > 100 | > 100 | > 100 | > 100 | > 100 | > 100 |

***Table 1.*** $K_i$ and $n_H$ values determined for the tested compounds. Data are given as mean [mean ± SEM] of three independent experiments each conducted in triplicate.

The binding data at native iGluRs (*Table 1*, left part) show that several compounds within the series revealed to have a good affinity ($K_i \leq 10$ μM) for native KARs. These are **1a** ($K_i$ = 4.1 ± 0.5 μM), **1b** ($K_i$ = 0.738 ± 0.16 μM), **1c** ($K_i$ = 10.1 ± 0.7 μM), **1e** ($K_i$ = 4.0 ± 0.4 μM) and **1f** ($K_i$ = 9.8 ± 3.4 μM). Unfortunately, some of them lack KAR selectivity since they show affinity also towards NMDA receptors (*Figure 3.24*). Indeed, the best hit **1b** and the compounds **1a** and **1e** demonstrated high

affinity for NMDARs ($K_i$ = 0.92 ± 0.03, 5.4 ± 0.07 and 5.8 ± 0.10 µM, respectively). This result was quite unexpected since the homology of the primary structure between NMDA and kainate receptors is only 20% and, moreover, NMDA receptors usually show a preference for ligands having the *R* configuration at the α-amino acidic centre, opposite to that of our ligands.

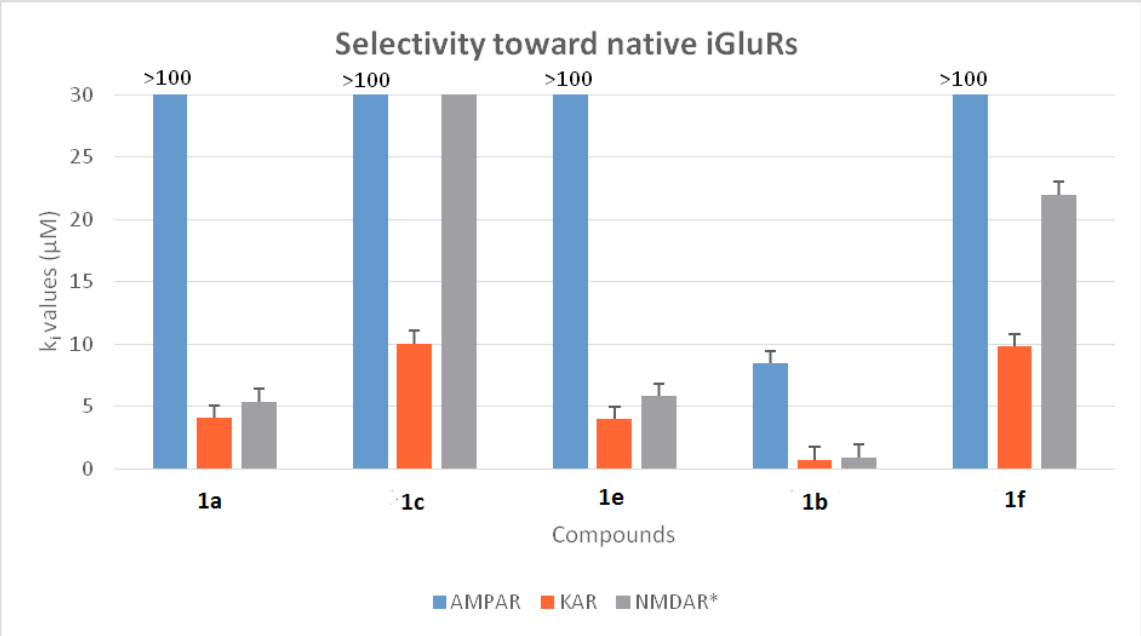


***Figure 3.24.*** $K_i$ values for native rat brain iGluRs. Data are given as mean [mean ± SEM] of three independent experiments each conducted in triplicate.

All derivatives were also tested at recombinant GluK1-3 (*Table 1*, right part) and some compounds (**1a**, **1b, 2c**, **1e**, **1f**) revealed to have good affinities towards the GluK1 subunit. In addition, these compounds also showed a good selectivity for the GluK1 subtype compared to GluK2,3 (*Figure 3.25*).

Among these derivatives, the most interesting appears to be **1f** ((*S*)Lys-γ-(*S*)Glu), which shows a submicromolar affinity ( $K_i$ = 0.464 µM) for GluK1 receptors and a complete selectivity over GluK2 and GluK3 subtypes. The competitive binding curve is shown below (dots are a mean of triplicates).

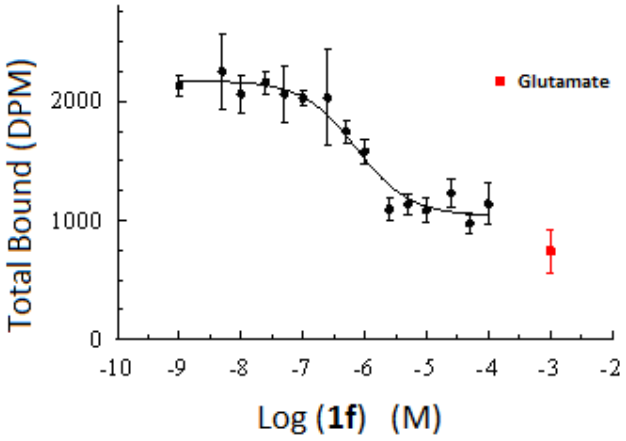


***Graph 1.*** Competition binding curve for **1f** ((S)Lys-γ-(S)Glu) at recombinant homomeric GluK1 receptor

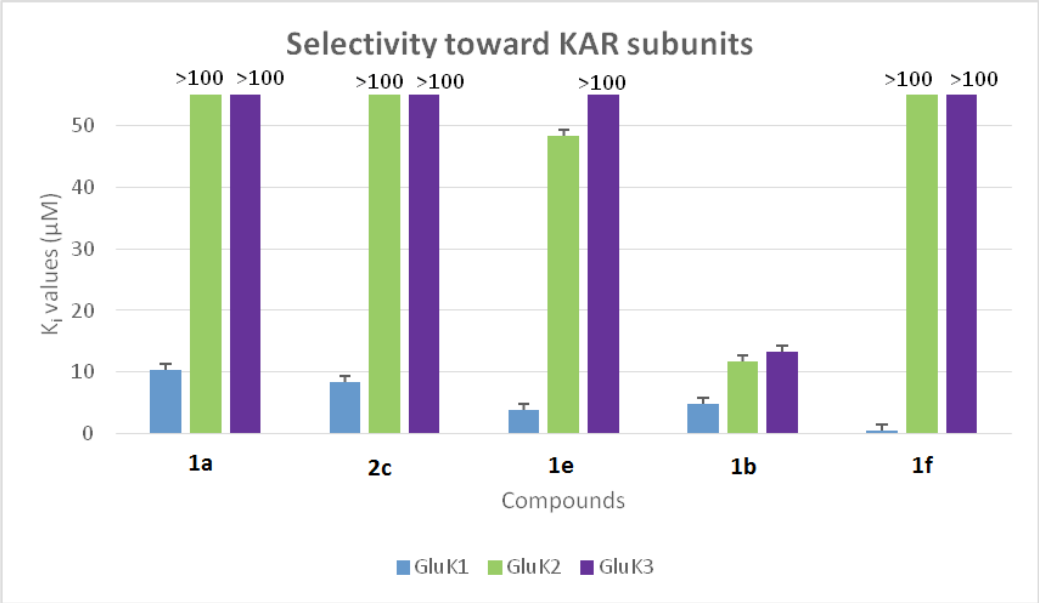


***Figure 3.25.*** $K_i$ values for recombinant homomeric KARs. Data are given as mean [mean ± SEM] of three independent experiments each conducted in triplicate.

Since it is known that the molecular complication of the aspartate/glutamate skeleton may generate molecules that act as blockers of the EAATs, we have also tested our new derivatives as potential inhibitors of glutamate transporters EAAT1-3. In detail, the inhibition of the compounds at cloned human EAAT1-3 stably expressed in HEK293 cells was determined in a [3H]-D-Asp uptake assay performed as previously described[108] using L-Glu and D,L-TBOA as reference ligands. Only **1e** shows a weak activity at all the three transporters, while the other derivatives proved to be inactive up to 300 or 1000 mM concentrations.

## 3.2.2 Pharmacological assays on derivatives **3a,b** and **4a,b**

| Compound | Rat Brain | | | | | | Recombinant iGluR | | |
|---|---|---|---|---|---|---|---|---|---|
| | AMPA-R | | KA-R | | NMDA-R | | GluK1 | GluK2 | GluK3 |
| | $K_i$ (μM) | $n_H$ | $K_i$ (μM) | $n_H$ | $K_i$ (μM) | $n_H$ | $K_i$ (μM) | $K_i$ (μM) | $K_i$ (μM) |
| (−)-**3a** | 43 | 4.37±0,01 | 37 | 4.43±0,05 | 25 | 4.63±0,08 | n.d. | n.d. | n.d. |
| (+)-**3b** | 48 | 4.36±0,12 | 59 | 4.23±0,01 | 41 | 4.41±0,08 | n.d. | n.d. | n.d. |
| (−)-**4a** | 46 | 4.34±0,02 | 66 | 4.20±0,11 | 24 | 4.64±0,10 | n.d. | n.d. | n.d. |
| (+)-**4b** | 67 | 4.18±0,03 | 56 | 4.25±0,03 | 28 | 4.56±0,07 | n.d. | n.d. | n.d. |

***Table 2.*** $K_i$ and $n_H$ values determined for the tested compounds. Data are given as mean [mean ± SEM] of three independent experiments each conducted in triplicate

Compounds **3a,b** and **4a,b** were assayed at native iGluRs as described in paragraph 3.2.1.

As reported in *Table 2*, the compounds showed affinity in the mid-micromolar range for all types of native iGluRs. Binding experiments on GluK1-3 subtypes were not carried out, due to the modest activity shown at native KARs.

## 3.3 DISCUSSION AND CONCLUSION

The Glu backbone has been used to design and synthesize new potential KAR antagonists characterized by an increased length of the amino acidic chain and an increased molecular complexity. Thus, the first series of γ-glutamyl-dipeptides, obtained by coupling the γ-carboxylate of L-Glu with a series of differently functionalized amino acids, was generated.

These derivatives are easy-to-synthesize suitable tools for rapidly probing the stereo-electronic properties of the KA receptor binding pocket, in the search of new selective KA receptor

antagonists.

Interestingly, the most promising compound identified in the present study is compound **1f**, characterized by the presence of a ionizable amino group on the side chain (derived from Lys), which may be responsible for additional hydrogen bonding/ionic interaction with the binding pocket that can give rise to an increased affinity and selectivity for the GluK1 receptor subtype, compared to the other compounds of the series.

Crystallographic studies on **1f** are currently ongoing for the obtainment of a co-crystal structure between **1f** and the GluK1 ligand binding domain to gain new insights into the molecular mechanism of GluK1 receptor ligand binding and pave the way to the development of highly potent and selective GluK1 receptor antagonists. Electrophysiological experiments should also be carried out to confirm the antagonist profile of **1f** and related analogues. However, based on the increased length of the amino acidic chain, an antagonist profile is reasonably expected. Moreover, the co-crystal structure, once obtained, will also give a precise indication on the degree of closure of the LBD, which is associated to agonist/partial agonist/antagonist profile of the ligand under study.

Concerning the series of the isoxazoline-containing β and γ dipeptides, unfortunately any ligand showed a worth noting affinity or selectivity for a specific iGluR receptor.

We can speculate that the conformational constraint imposed by the bicyclic scaffold did not favour the correct orientation of the pharmacophoric groups for a fruitful interaction with the D1 and D2 lobes of iGluRs. Alternatively, the distance between the α-amino acidic group and the distal carboxylate may not be optimal for the interaction and could be tuned to maximize the interaction with the receptor binding pocket; for instance the Glu residue could be replaced with an Asp residue: this type of study is among the already planned future developments of the present work.

# CHAPTER 4. L-TRICHOLOMIC ACID HOMOLOGUES

## 4.1 CHEMISTRY

### 4.1.1 Synthesis of L-Tricholomic acid analogues with an isoxazoline ring

The model compound L-Tricholomic acid was modified at the 3-position of the isoxazoline ring, through the introduction of a phenyl ring, functionalized in the *ortho*, *meta* or *para* position with a carboxylic acid, realizing both an increase of the molecular complexity and an increase of the distance between the distal and the proximal carboxylate (*Figure 4.1*).

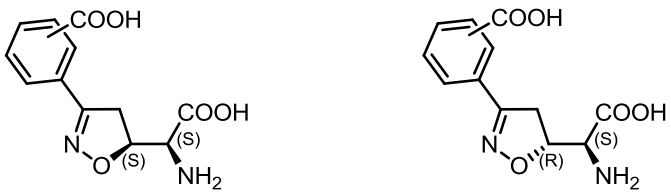


(α*S*,5*S*)-**5a:** *o*-COOH
(α*S*,5*S*)-**5b:** *m*-COOH
(α*S*,5*S*)-**5c:** *p*-COOH

(α*S*,5*R*)-**6a:** *o*-COOH
(α*S*,5*R*)-**6b:** *m*-COOH
(α*S*,5*R*)-**6c:** *p*-COOH

***Figure 4.1.*** Target compounds

The key step for the synthesis of the target compounds is represented by the 1,3-dipolar cycloaddition of nitrile oxide, generated *in situ* by the treatment of its stable chlorooxime precursor with a base, to (*S*)-3-(*tert*-butoxycarbonyl)-2,2-dimethyl-4-vinyloxazolidine **40** (*Figure 4.2*). Alkene **40** was synthesized starting from D-Serine following a reported literature procedure[109].

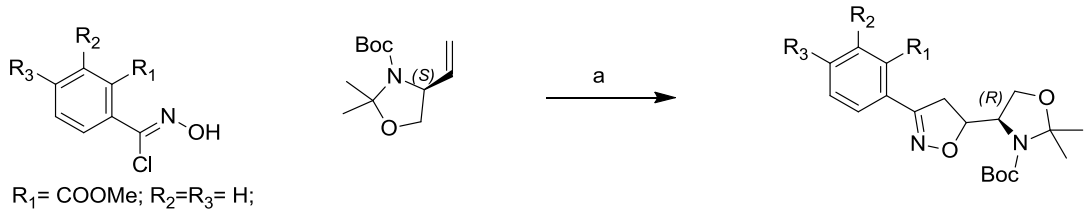


**41** $R_1$= COOMe; $R_2$=$R_3$= H;
**42** $R_2$= COOMe; $R_1$=$R_3$= H;
**43** $R_3$= COOMe; $R_1$=$R_2$= H;

**40**

**44a-c**

***Figure 4.2.*** a) $NaHCO_3$, EtOAc

Chlorooximes **41**, **42** and **43** were prepared starting from aldehydes **45** ,**46** and **47** respectively (*Figure 4.3*).

Condensation of aldehydes with hydroxylamine in a 1:1 mixture of $H_2O$/methanol gave the desired aldooximes **48**,**49** and **50**. Aldooximes **48**,**49** and **50** were then reacted with *N*-chlorosuccinimide in the presence of pyridine to give the corresponding chlorooximes **41**, **42** and **43** respectively, in high yields (*Figure 4.3*).

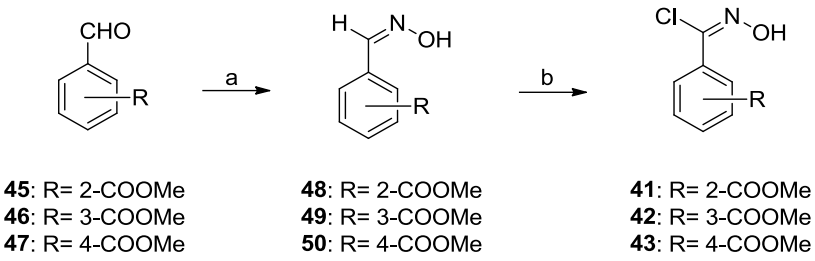


**45**: R= 2-COOMe
**46**: R= 3-COOMe
**47**: R= 4-COOMe

**48**: R= 2-COOMe
**49**: R= 3-COOMe
**50**: R= 4-COOMe

**41**: R= 2-COOMe
**42**: R= 3-COOMe
**43**: R= 4-COOMe

***Figure 4.3.*** a) $NH_2OH$*HCl, $Na_2CO_3$, $H_2O$/MeOH 1:1 b) NCS, pyridine, $CHCl_3$

Whereas methyl 3-formylbenzoate **46** was commercially available, the formyl esters **45** and **47** were synthesized starting from the corresponding carboxylic acid derivatives (*Figure 4.4*).

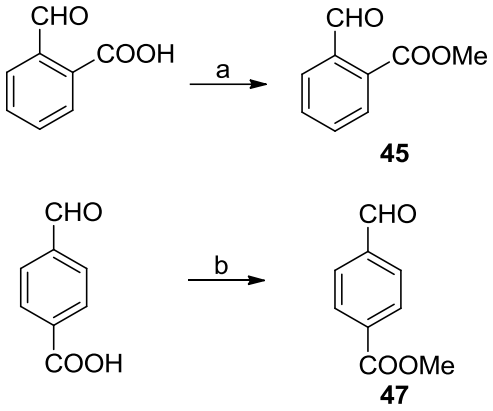


***Figure 4.4.*** a) $K_2CO_3$, $CH_3I$, DMF b) $CH_3COCl$, dry MeOH

Compound **45** was prepared by means of nucleophilic substitution of the carboxylic acid derivative with $CH_3I$, using $K_2CO_3$ as a base and DMF as solvent. The batch reaction was performed at 155°C for 5 hours and the final product was obtained with low yield. Satisfactory results were reached

performing the reaction under microwave irradiation at 100 °C in only 2 hours. The temperature must be kept below 110°C because DMF, at higher temperature, under microwave irradiation, starts to decompose. On the other hand, derivative **47** was synthesized using another synthetic strategy. Standard esterification condition of 4-formylbenzoic acid with $SOCl_2$ and MeOH produced the methyl 4-(dimethoxymethyl)benzoate as the main product. Switching from $SOCl_2$ to acetyl chloride as condensing agent, I was able to obtain methyl-4-formylbenzoate **47** in good yield.

After the cycloaddition reaction, the acetonide function was removed following the procedure reported by Dondoni[110]: treatment of **44a-c** with a 1:5 solution $H_2O$/AcOH led to the desired intermediates (α*R*, 5*S*)-**51a-c** and (α*R*, 5*R*)-**52a-c**. Only at this stage, it was possible to separate the two diasteroisomers by silica gel column chromatography (*Figure 4.5*).

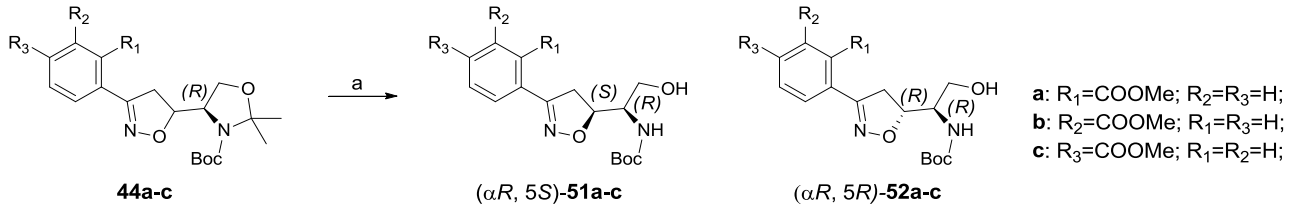


***Figure 4.5.*** a) 1:5 sol. $H_2O$/AcOH

The isolated diasteroisomers were oxidized at the hydroxyl function with PDC in DMF and in turn converted into the final amino acids (α*S*,5*S*)-**5a-c** and (α*S*,5*R*)-**6a-c** by means of standard deprotection reactions: methyl esters were hydrolyzed with 1N NaOH in MeOH whereas the cleavage of the Boc group was performed with a 30% solution of trifluoroacetic acid in $CH_2Cl_2$ (*Figure 4.6*).

The relative configuration for derivatives **5a**/**6a**, **5b**/**6b**, and **5c**/**6c** was assigned by comparing their $^1$H NMR spectroscopic signals with the signals of the model compound L-Tricholomic acid.

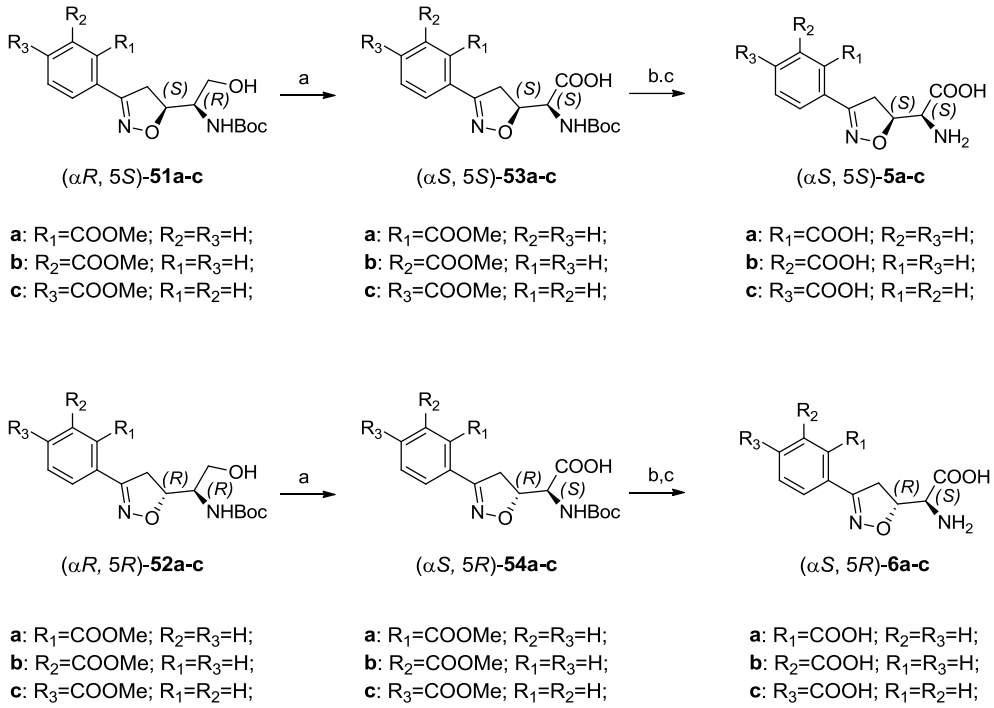


***Figure 4.6.*** a) PDC, DMF b) 1N NaOH, MeOH c) 30% TFA in $CH_2Cl_2$

## 4.1.2 Synthesis of L-Tricholomic acid analogues with a pyrazoline ring

This series of compounds, as new analogues of Tricholomic acid, was characterized by the presence of a $\Delta^2$-pyrazoline nucleus. The heterocyclic scaffold was exploited in order to further increase the molecular complexity of the model compound. In fact, the pyrazoline ring could be variously decorated on the $N^1$ position, introducing further substituents to assure a better interaction with the binding pocket. In particular, the derivatives that were synthesized are shown in *Figure 4.7*.

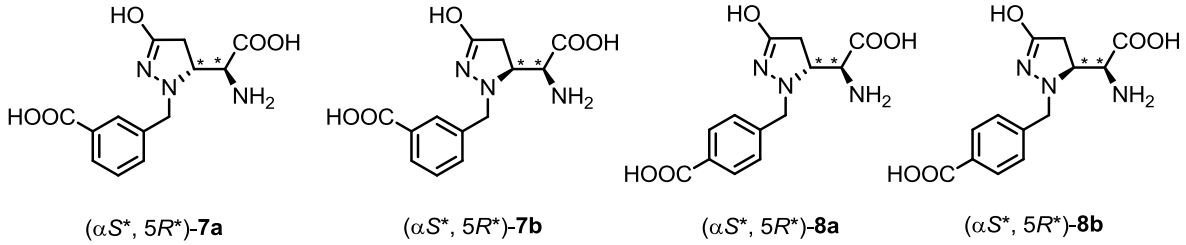


***Figure 4.7.*** Pyrazoline analogues of L-Tricholomic acid

The 3-hydroxy-pyrazoline could be synthesized trough a condensation/intramolecular cyclization

between hydrazine and the α,β-unsatured ester (±)-**55**, in turn obtained starting from D,L-Serine[111] (*Figure 4.8*). The key intermediate (±)-**56** was obtained as a mixture of two racemic diasteroisomers with relative configuration (α*S**,5*S**) and (α*S**,5*R**), inseparable at this point.

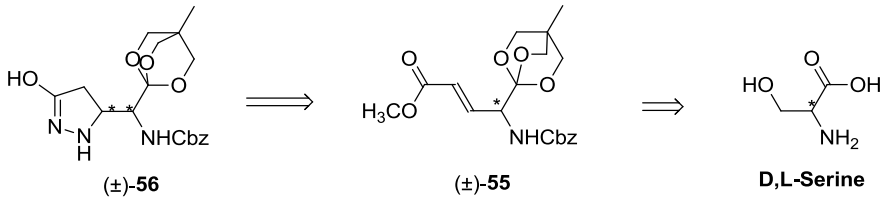


***Figure 4.8.*** Retrosynthesis of (±)-**56**

$N^1$-arylmethyl derivative (±)-**57a** was synthesized by treating (±)-**56** with methyl 3-(bromomethyl)benzoate in the presence of $K_2CO_3$ in THF and heating at 85 °C under microwave irradiation. The same reaction conditions were used to afford, starting from (±)-**56** and methyl 4-(bromomethyl)benzoate, compound (±)-**57b** (*Figure 4.9*).

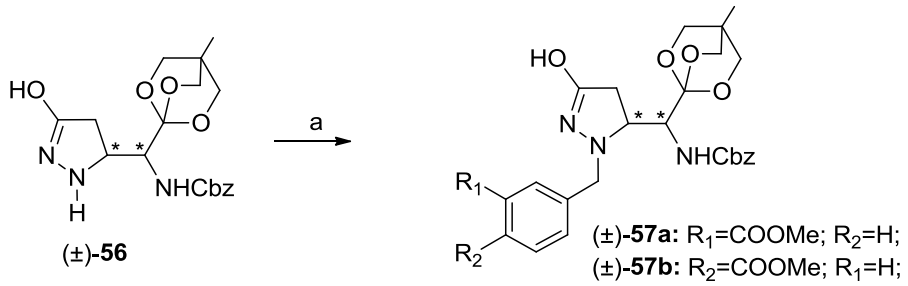


***Figure 4.9.*** a) $ArCH_2Br$, $K_2CO_3$, NaI, $CH_3CN$, 85°C

The next step involved the trans-esterification reaction of the proximal carboxylic acid protecting group (OBO ester) into the corresponding methyl ester trough a two-step reaction. In a first step, the treatment of OBO ester of (±)-**57a** and of (±)-**57b** with pyridinium *p*-toluene sulfonate (PPTS) in a solution of methanol and water led to intermediates (±)-**58a** and (±)-**58b** respectively. Subsequently, the transesterification occurred in methanol in the presence of potassium carbonate and afforded the methyl esters (α*S**,5*R**)-**59a,b**/(α*S**,5*R**)-**60a,b**. At this step, the two diasteroisomers could be easily separated by silica gel column chromatography (*Figure 4.10*).

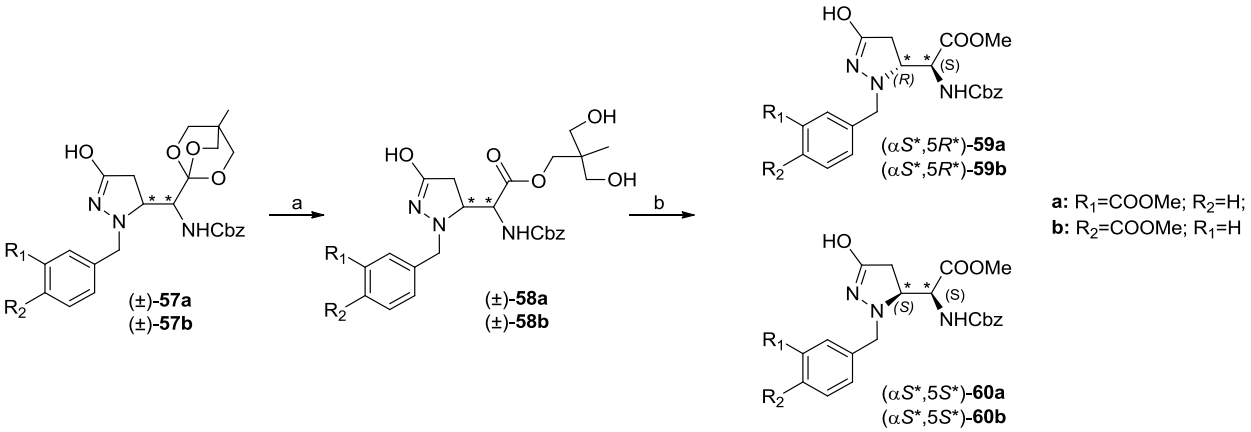


***Figure 4.10.*** a) PPTS, MeOH, $H_2O$ b) $K_2CO_3$, MeOH

The assignment of the relative stereochemistry of the two diasteroisomers was possible only after comparison of the $^1$H-NMR spectra of each diasteroisomer with that of (α*S**,5*R**) and (α*S**,5*R**)-N$^1$-ethyl derivative, previously synthesized by Prof. Conti's research group,[112] whose relative configuration was unambiguously assigned by X-ray analysis (*Figure 4.11*).

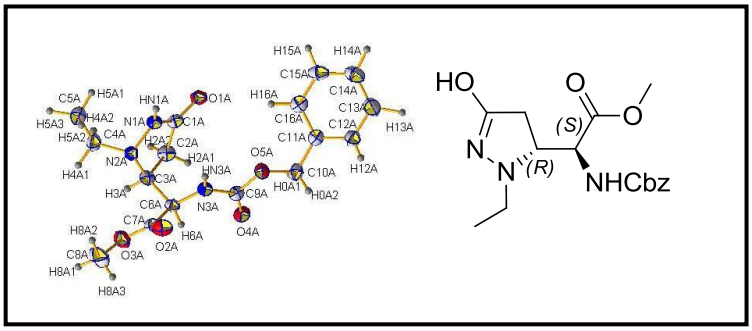


***Figure 4.11.*** X-ray christallographic analysis for (α*S**, 5*R**)-N$^1$-ethyl derivative

The next reactions were carried out on the isolated single diasteroisomers and included the deprotection at the carboxylic and amine function. Final amino acids (α*S**,5*S**)-**7a,b** and (α*S**,5*S**)-**8a,b** were obtained as HBr salts after alkaline hydrolysis of methyl esters followed by cleavage of the Cbz protecting group with hydrobromic acid in a solution of acetic acid (*Figure 4.12*).

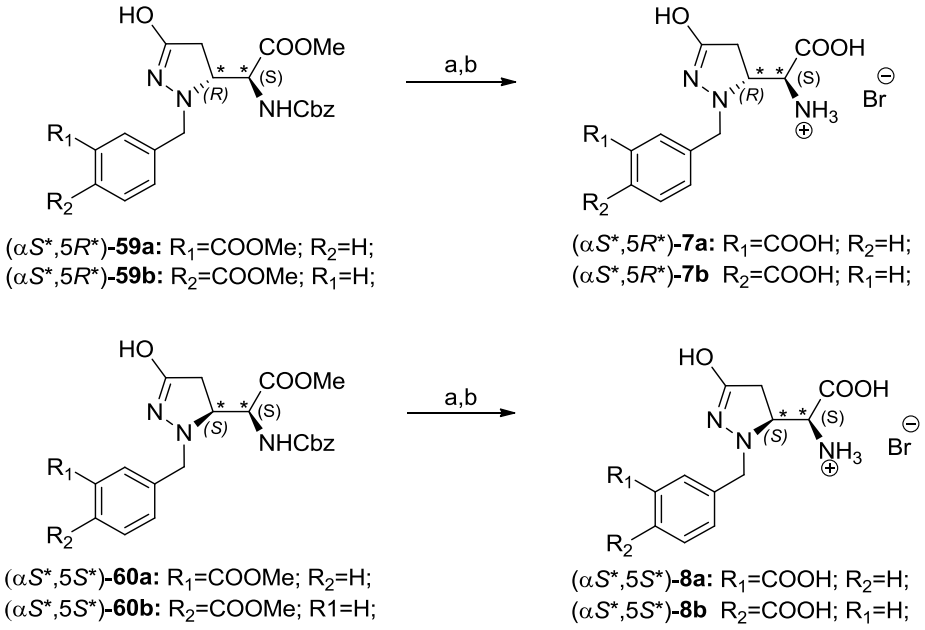


(α*S**,5*R**)-**59a:** $R_1$=COOMe; $R_2$=H;
(α*S**,5*R**)-**59b:** $R_2$=COOMe; $R_1$=H;

(α*S**,5*R**)-**7a:** $R_1$=COOH; $R_2$=H;
(α*S**,5*R**)-**7b** $R_2$=COOH; $R_1$=H;

(α*S**,5*S**)-**60a:** $R_1$=COOMe; $R_2$=H;
(α*S**,5*S**)-**60b:** $R_2$=COOMe; R1=H;

(α*S**,5*S**)-**8a:** $R_1$=COOH; $R_2$=H;
(α*S**,5*S**)-**8b** $R_2$=COOH; $R_1$=H;

***Figure 4.12***. a) Dioxane/NaOH 0.5N b) 33% HBr in AcOH

## 4.2 PHARMACOLOGY

All derivatives were submitted to binding experiments that were carried out on rat brain synaptic membranes of cortex expressing native iGluRs as described in paragraph 3.2.

### 4.2.1 Pharmacological assays on derivatives **5a-c**/**6a-c** and **7a-b**/**8a-b**

| **Compound** | **Rat Brain** | | |
|---|---|---|---|
| | **AMPA-R** $K_i$ (μM) | **KA-R** $K_i$ (μM) | **NMDA-R** $K_i$ (μM) |
| (α*S*, 5*S*)-**5a** | > 100 | > 100 | > 100 |
| (α*S*, 5*R*)-**6a** | > 100 | > 100 | > 100 |
| (α*S*, 5*S*)-**5b** | > 100 | > 100 | > 100 |
| (α*S*, 5*R*)-**6b** | > 100 | > 100 | > 100 |
| (α*S*, 5*S*)-**5c** | > 100 | > 100 | > 100 |
| (α*S*, 5*R*)-**6c** | > 100 | > 100 | > 100 |
| (α*S**, 5*R**)-**7a** | 83 [4.08±0.02] | 22 [4.67±0.09] | > 100 |
| (α*S**, 5*S**)-**7b** | > 100 | > 100 | > 100 |
| (α*S**, 5*R**)-**8a** | > 100 | > 100 | > 100 |
| (α*S**, 5*S**)-**8b** | > 100 | > 100 | > 100 |
| **L-*erythro*-Tricholomic acid** | 0.95 [6.02±0.01] | 0.29 [6.55±0.06] | 41 [4.40±0.07] |

***Table 3.*** Data are given as mean [$pK_i$±SEM] of at least three independent experiments

Binding assays showed for all compounds a general decrease of affinity, in particular if compared to L-*erythro* Tricholomic acid. None of the final amino acid **5a-c** and **6a-c** revealed affinity for AMPA or KA receptors at concentration up to 100 μM.

Replacing the isoxazoline ring with the pyrazoline nucleus didn't improve the binding affinity: among derivatives **7a,b** and **8a,b** only (α*S**, 5*R**)-**7a** is able to interact with AMPA or KA receptors with affinities in the mid-micromolar range. Notably, in this case the binding preference depends on the relative stereochemistry since (α*S**, 5*R**)-**7a** is a non selective AMPA/KA ligand whereas its diasteroisomer (α*S**, 5*S**)-**8a** is devoid of any affinity for iGluRs.

As discussed in paragraph 3.3.1, also derivatives **7a-b** and **8a-b** were tested as potential inhibitors of glutamate transporters EAAT1-3 but, unfortunately, turn out to be inactive up to 300 or 1000 mM concentrations.

## 4.3 DISCUSSION AND CONCLUSION

In the present project, I have synthesized higher homologues of the natural compound L-Tricholomic acid, as new pharmacological tools to investigate the KARs binding domain, in the attempt to identify potential selective antagonists. The rationale was based on the use of classical medicinal chemistry strategies, widely applied in the design of glutamatergic ligands.

For the final amino acids **5a-c** and **6a-c**, the synthesis entailed the use of the 1,3-dipolar cycloaddition to build the 3-hydroxy isoxazoline scaffold, which was decorated at the 3-position a sterically hindered phenyl ring possessing the distal acidic group in different positions. Unfortunately, pharmacologically investigation at native iGluRs did not highlight any ligand endowed with a worth noting affinity or selectivity for a specific receptor. We can speculate that the distance between the α-amino acidic group and the distal carboxylate may not be optimal for the interaction with the residues of the binding cavity.

Also in the series of derivatives (α*S**, 5*S**)-**7a/8a** and (α*S**, 5*R**)-**7b/8b** we do not observe the expected increase of potency associated to an increased molecular complexity. It can be hypothesized that the lack of binding affinity could be due to steric clashes between the $N^1$-substituent and the receptor residues.

# CHAPTER 5. CIP-AS ANALOGUES

## 5.1 CHEMISTRY

The natural compound Willardine is an AMPA/KA receptor partial agonist; the presence of a further acidic function linked through an aromatic/heteroaromatic spacer to the $N^3$ position of the ring has been reported to switch the profile from agonist to antagonist (e.g. compounds UBP 302, UBP 310)[114] . By applying a similar strategy, I have modified the structure of **CIP-AS**, a potent non-selective AMPA/KA agonist[104]. In detail, I have used the isoxazolinyl-proline bicyclic scaffold present in the model agonist compound CIP-AS to design higher homologues containing a benzene or a thiophene aromatic ring as a spacer to increase the distance between the $\alpha$-amino acidic function and the distal carboxylate (*Figure 5.1*). To connect the two moieties an amide bond was chosen due to the ease of synthesis and the superior stability compared to an ester group.

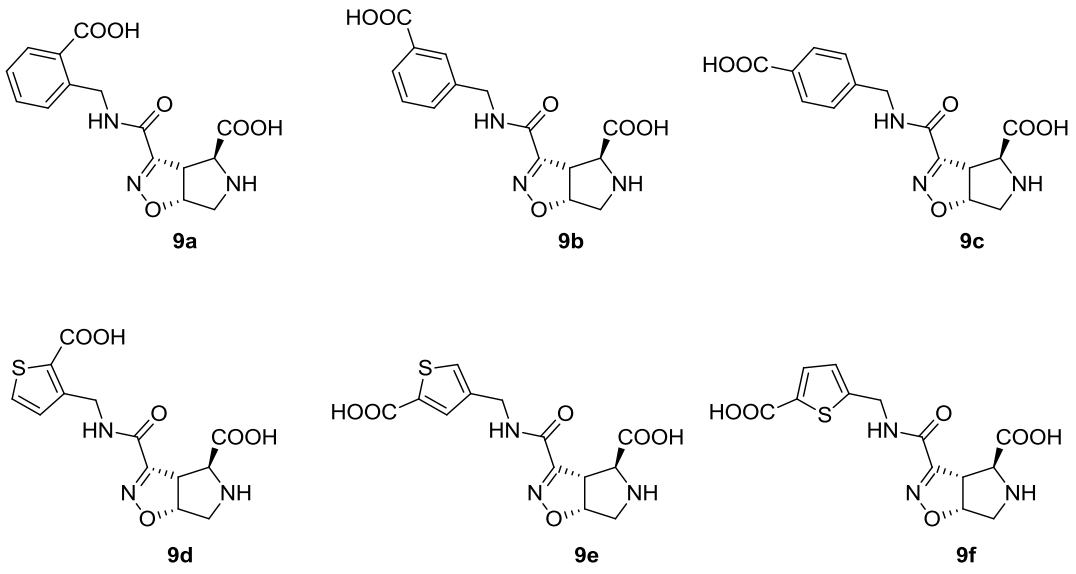


***Figure 5.1.*** CIP-AS analogues

The key intermediate for the preparation of all the new derivatives is enantiomerically pure compound **61**, obtained following a previously reported procedure[114], which used *trans*-4-

hydroxy-L-proline as a source of chirality.

The 1,3 dipolar cycloaddition reaction between **61** and the nitrile oxide generated *in situ* from ethyl 2-chloro-2-(hydroxyimino)acetate by treatment with a base, gave a mixture of three diasteroisomers **62, 63** and **64** in proportion 40: 46: 14 and a 56% yield. (*Figure 5.2*). Since it was not possible to separate the three cycloadducts **62**, **63**, and **64** by silica gel column chromatography, the separation was performed by preparative HPLC. An excellent separation (see chapter 6.3) was obtained with the amylose tris-(5-chloro-2-methyl-phenyl-carbamate) stationary phase (injection volume: 2ml, concentration: 100mg/ml), allowing us to collect the desired amount of each stereoisomer[115].

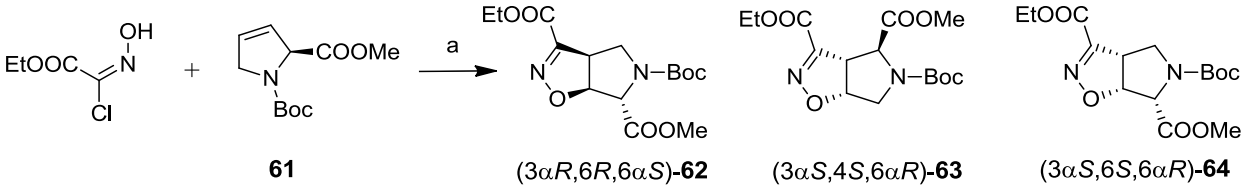


**61** (3α*R*,6*R*,6α*S*)-**62** (3α*S*,4*S*,6α*R*)-**63** (3α*S*,6*S*,6α*R*)-**64**

***Figure 5.2.*** a) $NaHCO_3$, AcOEt, Δ b) Preparative chiral HPLC

The distal ethyl ester of **63** was linked to the electron withdrawing isoxazoline ring and therefore resulted much more activated to hydrolysis in comparison to the methyl ester. Consequently, it was selectively hydrolysed in mild basic conditions using 1 eq. of 5% aqueous $K_2CO_3$ solution in methanol, to obtain the distal carboxylic acid of **65** (*Figure 5.3*).

Intermediate **65** was then coupled to aromatic amines **66a-f** (*Figure 5.4*), using HOBT, HBTU as coupling agents and DIPEA as base, affording the corresponding amides **67a-f** (*Figure 5.3*).

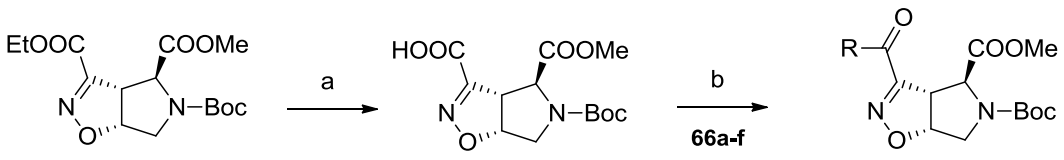


**63** **65** **67a-f**

***Figure 5.3.*** a) 5% aq. $K_2CO_3$, MeOH; b) HOBT, HBTU, DIPEA, $CH_2Cl_2$; c) 1N NaOH, MeOH d) 30% TFA in $CH_2Cl_2$

Below are reported the structures of the aromatic spacers **66a-f** used for the synthesis of the

designed ligands (*Figure 5.4*). They are characterized by an ester function, which will generate the distal carboxylic group necessary for the interaction with the receptor.

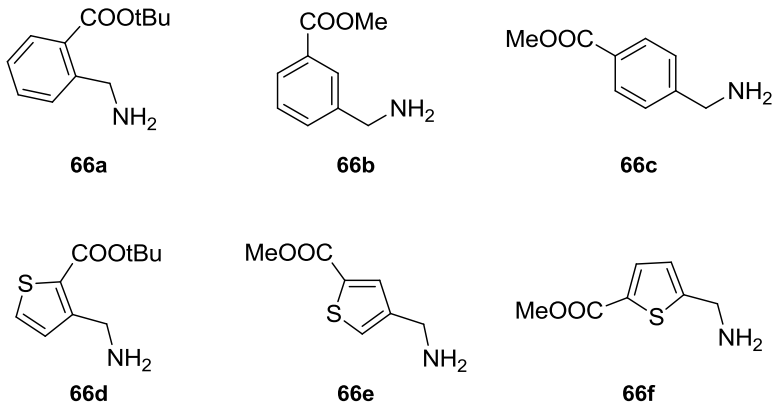


***Figure 5.4.*** Aromatic spacers

A part for amine **66b**, which is commercially available, and for amine **66c,** whose synthesis started from the commercially available methyl 4-(bromomethyl)benzoate, the other amines were prepared following the synthetic pathway reported in *Figure 5.5*.

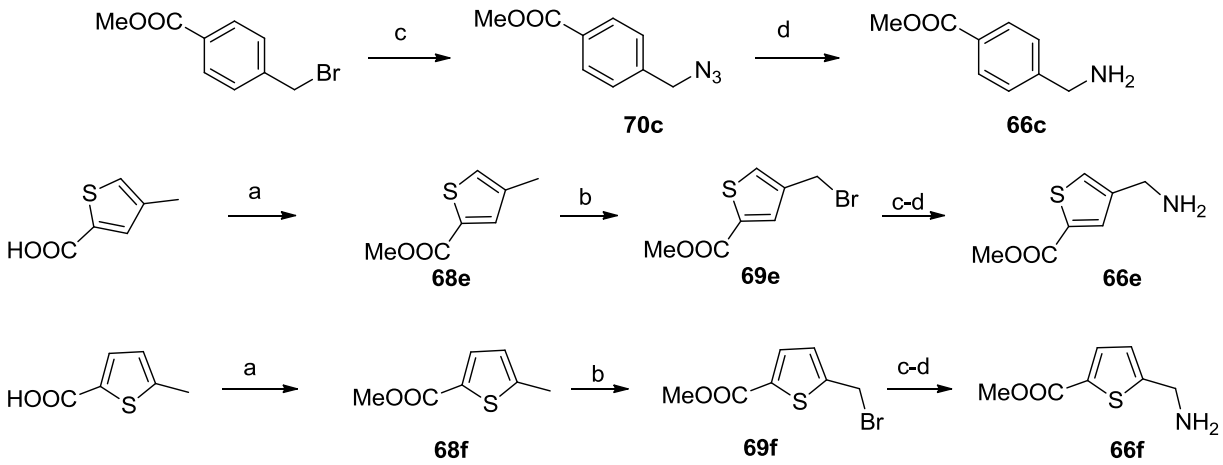


***Figure 5.5.*** a) conc. $H_2SO_4$, dry MeOH, Δ b) NBS, AIBN, $CCl_4$, Δ c) $NaN_3$, DMF, Δ d) $H_2$, 5%Pd/C, THF

Fisher esterification of the carboxylic group followed by radicalic bromination with *N*-bromosuccinimide (NBS) and a catalytic amount of α,α-azoisobutyronitrile (AIBN) as radical initiator, afforded in good yield the bromo-substituted derivatives **69e,f**.

Subsequently, nucleophilic substitution reaction of **69c,e** and **f** with $NaN_3$ gave intermediates **70c,e**

and **f** which were hydrogenated to the final amines **66c,e** and **f** using 5% Pd/C (*Figure 5.5)*.

For the synthesis of the *orto*-substituted amines **66a** and **66d**, which were susceptible to lactamization during the hydrogenation reaction, it was necessary to protect the acidic group as *tert*-butyl ester that is less reactive to the nucleophilic attack.

Consequently, the carboxylic acid was treated with *tert*-butyl 2,2,2-trichloroacetimidate in presence of a Lewis acid to form the *tert*-butyl ester **71a** and **71d**. The synthesized intermediates were finally submitted to the previously described synthetic steps to obtain the aromatic spacers **66a** and **66d** (*Figure 5.6*).

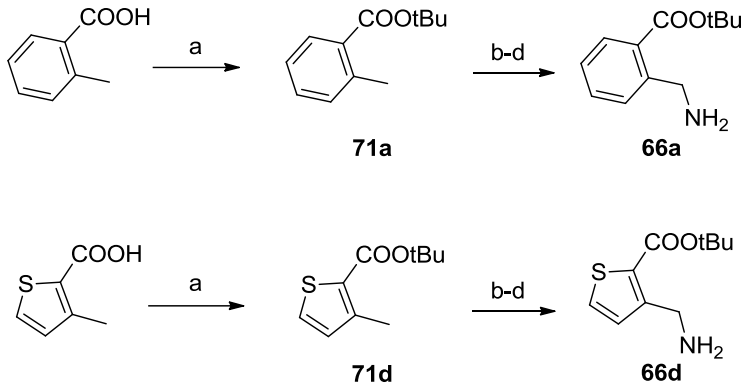


***Figure 5.6.*** a) *tert*-butyl 2,2,2-trichloroacetimidate, $BF_3$*2($Et_2O$), dry $CH_2Cl_2$ , dry THF c) NBS, AIBN, $CCl_4$, Δ d) $NaN_3$, DMF e) $H_2$, 5% Pd/C, THF

All amines **66a-f** were coupled with the bicyclic intermediate **65**. The coupling reaction was performed using HOBt and HBTU as coupling reagents and DIPEA as base, in $CH_2Cl_2$. The reaction took place in 24 hours affording the desired products **72a-f** (*Figure 5.7*).

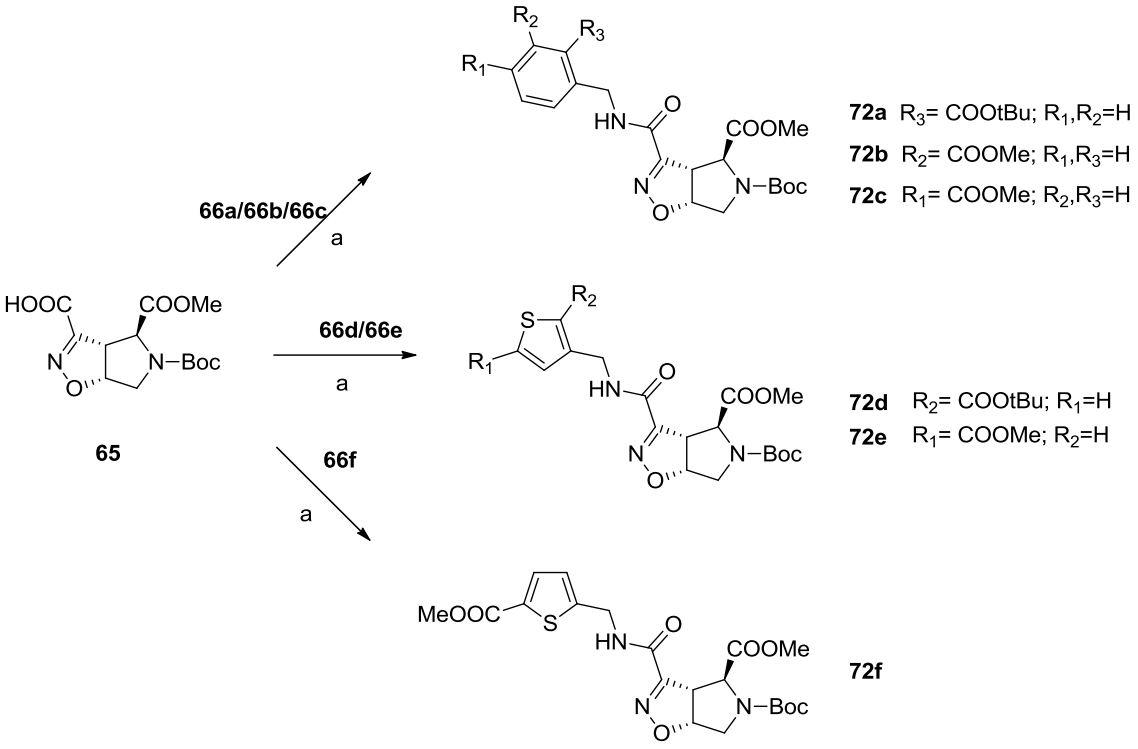


***Figure 5.7.*** a) HOBt hydrate, HBTU, DIPEA, $CH_2Cl_2$

Finally, derivatives **72a-f** were converted into the desired amino acids **9a-f** using standard deprotection conditions (i.e. 1 N NaOH aq., MeOH and 30% TFA in $CH_2Cl_2$). Worth nothing, the same acidic conditions were able to hydrolyse also the *tert*-butyl esters for compounds **72a** and **72d** (*Figure 5.8*).

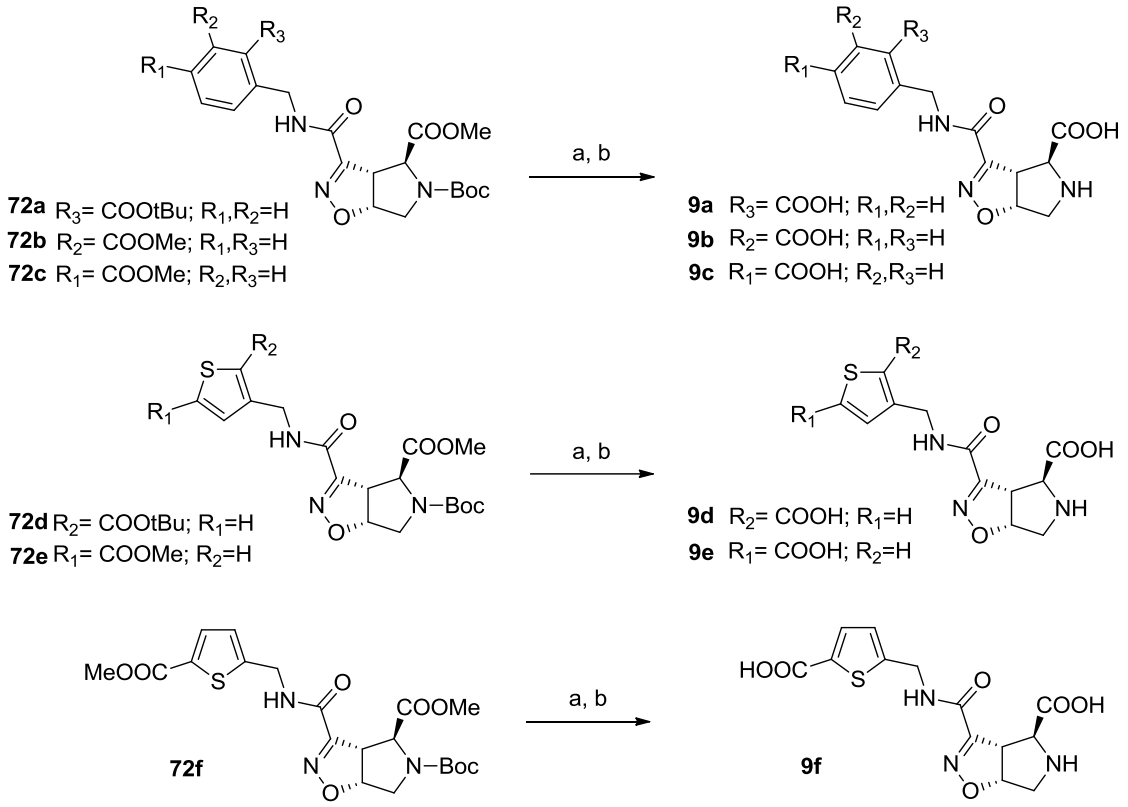


***Figure 5.8.*** a) 1 N NaOH, MeOH b) 30% TFA in $CH_2Cl_2$

## 5.2 PHARMACOLOGY

All new compounds were submitted to binding experiments that were carried out on rat brain synaptic membranes of cortex expressing native iGluRs as described in paragraph 3.2. *Table 4* reports the comparison between the binding affinity of the model compounds **CIP-AS**, **UBP 302** and **UBP 310** and the related new amino acids **9a-f**.

### 5.2.1 Pharmacological assays on derivatives **9a-f**

| Compound | Rat Brain | | | Recombinant iGluR | | |
|---|---|---|---|---|---|---|
| | **AMPA-R** | **KA-R** | **NMDA-R** | **GluK1** | **GluK2** | **GluK3** |
| | $K_i$ (μM) | $K_i$ (μM) | $K_i$ (μM) | $K_i$ (μM) | $K_i$ (μM) | $K_i$ (μM) |
| **9a** | **5.2** | **2.0** | > 100 | **7.17** [1.16 ± 0.05] | **2.62** [0.92 ± 0.08] | **0.206** [0.89 ± 0.04] |
| **9b** | >100 | 55.0 | >100 | n.d | n.d | n.d |
| **9c** | >100 | >100 | 84.0 | n.d | n.d | n.d |
| **9d** | **11** | **5.0** | > 100 | **8.09** [1.05 ± 0.08] | **3.09** [0.86 ± 0.01] | **0.117** [0.92 ± 0.06] |
| **9e** | >100 | 48.0 | 39.0 | n.d | n.d | n.d |
| **9f** | 83.0 | 20.0 | 73.0 | n.d | n.d | n.d |
| **UBP 302** | >100 | 0.402 | >100 | 3.9 | >100 | 4.0 |
| **UBP 310** | 83.0 | 0.018 | >100 | 0.010 | >100 | 0.023 |
| **CIP-AS** | 0.54 | 0.23 | >100 | n.d | n.d | n.d |

***Table 4.*** $K_i$ and $n_H$ values determined for the tested compounds. Data are given as mean of three independent experiments each conducted in triplicate

The binding data at native iGluRs clearly show that derivatives **9a** and **9d** displayed a micromolar affinity for both AMPA and KA receptors (in the range 2-10 μM), with a preference for KARs. This is not surprisingly since compounds **9a** and **9d** are the more closely related to model compounds

**UBP 302** and **UBP 310** and are characterized by an aromatic ring, phenyl or thiophene respectively, bearing a carboxylic group in position 2.

On the other hand, the affinity of the other four derivatives was lower or negligible showing that the position of the distal carboxylate is crucial for maintaining the binding affinity. In the future modeling studies can confirm that the shift of the carboxyl group in the *meta* and *para* position of the phenyl ring lead to unfavorable interaction between the distal carboxylate and Thr residue in lobe D2.

Derivatives **9a-f** were also tested as potential EAATs blockers as described in paragraph 3.3.1 but they turn out to be inactive.

Radioligand displacement studies were performed also at recombinant rat homomeric GluK1-3.

Very interestingly, binding assay displayed for both **9a** and **9d** a submicromolar affinity at homomeric GluK3 receptors ($K_i$= 0.206 µM and 0.117 µM respectively)**,** in contrast to **UBP 302** and **UBP 310** that were GluK1 receptor ligands. Notably, compound **9a** dispayed a 10-fold selectivity for GluK3 *versus* GluK2 and a 35-fold selectivity for GluK3 *versus* GluK1. Even more interestingly, compound **9d** showed a 26-fold selectivity for GluK3 *versus* GluK2 and a 70-fold selectivity for GluK3 *versus* GluK1, being, to the best of my knowledge, the most selective GluK3 ligand yet ever discovered (*Figure 5.9*).

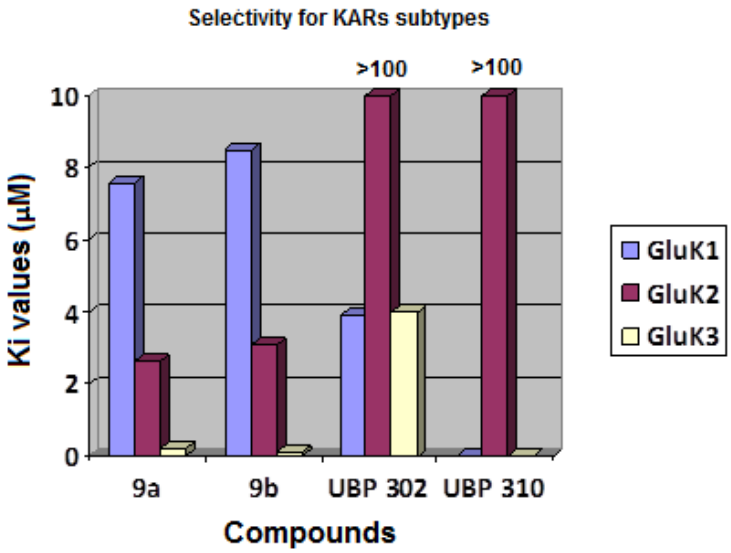


***Figure 5.9.*** $K_i$ values for recombinant homomeric KARs. Data are given as mean of three independent experiments each conducted in triplicate.

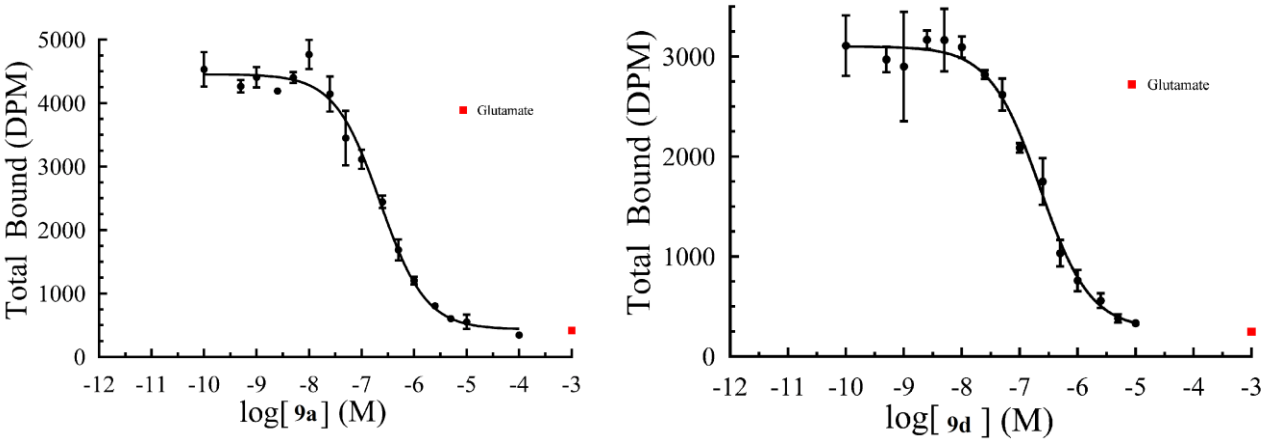


***Graph 2.*** Competition binding curve for **9a** and **9d** at recombinant homomeric GluK3 receptor

## 5.3 DISCUSSION AND CONCLUSION

The most promising compounds identified in the present study, **9a** and **9d**, are characterized by the bicyclic scaffold of **CIP-AS** linked to an aromatic/heteroaromatic moiety bearing a carboxylic function in position 2, as in **UBP 302** and **310**.

Worth noting, they display a submicromolar affinity for GluK3 receptor and a highly remarkable selectivity for this receptor subtype. In particular, compound **9d** is the most selective GluK3 ligand yet ever discovered, displaying a 26-fold selectivity for GluK3 *versus* GluK2 and a 70-fold selectivity for GluK3 *versus* GluK1. Although, on the basis of the amino acidic chain length, it is reasonable to foresee an antagonist profile of these ligands, this has to be confirmed by functional electrophysiological studies, which have been planned and will be performed in the new future.

These results highlight that amino acid chain homologation coupled to the insertion of proper substituents able to establish additional interaction with the binding pocket is the winning strategy to design selective KAR antagonists.

To date pharmacological studies on specific KA receptor subtypes have been greatly hampered by the lack of selective agonists and antagonists and especially selective GluK3 receptor antagonists are needed.

Consequently, the newly identified ligands, and in particular compound **9d**, are valuable tools for characterizing the molecular determinants of subunit-selective binding. Moreover, they could represent ideal pharmacological tools for investigating tha patho-physiological role played by the

least characterized GluK3 subtype.

At present, the group of Prof. Jette Kastrup at the University of Copenhagen is undertaking efforts to obtain a co-crystal structure of ligands **9a** or **9d** with the GluK3 LBD. These results will further help the rational design of highly potent and selective GluK3 receptor antagonists.

# CHAPTER 6. EXPERIMENTAL SECTION

## 6.1 MATERIALS AND METHODS

All reagents were purchased from Sigma. $^{1}H$ NMR and $^{13}C$ NMR spectra were recorded with a Varian Mercury 300 (300 MHz) spectrometer. Chemical shifts ($\delta$) are expressed in ppm, and coupling constants ($J$) are expressed in Hz. TLC analyses were performed on commercial silica gel 60 $F_{254}$ aluminum sheets; spots were further evidenced by spraying with a dilute alkaline potassium permanganate solution or ninhydrin. Flash chromatography were performed on Buchi Pump Manager C-615 and C-601. Chiral HPLC analyses were performed with a Jasco PU-980 pump equipped with a UV–vis detector Jasco UV-975 (wavelength: 220 nm) and a Kromasyl 5-amycoat (4.6 × 250 mm, 5 µm) or a Phenomenex Lux Amylose-2 column (4.6 × 150 mm, 5 µm). Preparative HPLC was performed with a 1525 Extended Flow Binary HPLC Pump, equipped with a Waters 2489 UV-vis detector and a Kromasyl 5-amycoat (21.2 × 250 mm, 5 µm) or a Phenomenex Lux Amylose-2 column (21.2 × 250 mm) at a flow rate of 15 mL/min. Rotary power determinations were carried out with a Jasco P-1010 spectropolarimeter coupled with a Haake N3-B thermostat. Melting points were determined on a model B 540 Büchi apparatus and are uncorrected.

## 6.2 SYNTHETIC PROCEDURES

Synthesis of (+)-**10**

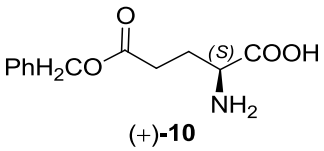


(+)**-10**

(*S*)-Glutamic acid (5.0 g, 34.0 mmol) was suspended in 50 ml of benzylic alcohol. Concentrated HCl (6 ml) was added and the resulting mixture was stirred at 70 °C for 2 hours. The water formed in the reaction was evaporated under reduced pressure. After that, concentrated HCl (1.5 ml) was added and the mixture was evaporated again. Subsequently, a saturated solution of $NaHCO_3$ was added until the solution reached a pH of 6. EtOH was added to allow the precipitation of the ester and the solid was then filtered *in vacuo* and washed with EtOH. Then, $Et_2O$ (50 ml) was added to dry the product and compound (+)-**10** (4.0 g, 16.86 mmol) was obtained.

**Yield:** 50%

**Solid state:** white powder

Synthesis of (+)-**11**

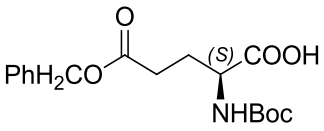


(+)-**11**

Derivative (+)-**10** (4 g, 16.86 mmol) was dissolved in $H_2O$ (40 ml) and $NaHCO_3$ (2.83 g, 3.37 mmol) was added. The solution was cooled down to 0 °C and a solution of $(Boc)_2O$ (4.78 g, 21.92 mmol) in THF (40 ml) was added dropwise. The reaction was stirred at room temperature overnight. Subsequently, the THF was evaporated and the unreacted $(Boc)_2O$ was washed out with ethyl ether (2 x 50 mL). The aqueous layer was made acidic with 2N HCl and extracted with EtOAc (2 x 50 mL). The organic layer was separated and dried over anhydrous $Na_2SO_4$. After evaporation of the solvent, the acidic intermediate (+)-**11** (3.9 g, 11.6 mmol) was obtained as a yellow oil.

**Yield**: 69%

**Solid state**: Yellow oil

**$R_f$** ($CH_2Cl_2$/MeOH 9:1 + 1% AcOH): 0.70

Synthesis of (+)-**12**

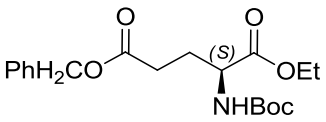


(+)-**12**

To a solution of compound (+)-**11** (3.9 g, 11.6 mmol) in $CH_2Cl_2$ (12.6 ml), EtOH (2.18 ml, 37.5 mmol), DCC (2.7 g, 13.3 mmol) and DMAP (0.425 g, 3.48 mmol) were added. The reaction was stirred at r.t. overnight until completion. The mixture was filtered *in vacuo* using a celite pad in order to eliminate the solid dicyclohexylurea. The solvent was evaporated under reduced pressure. The crude material was purified by column chromatography on silica gel (Cyclohexane/EtOAc 9:1) to give (+)-**12** (3.47 g, 9.50 mmol).

**Yield**: 83%

**Solid state**: Yellow oil

**$R_f$** (cycloexane/EtOAc 8:2): 0.4

**m.p**: 64-66 °C

**$[\alpha]^{D}_{20}$**: (+) 13.2 (c: 1.05 in $CHCl_3$)

**$^1$H-NMR** (300 MHz, $CDCl_3$): 1.25 (t, *J* = 7.2, 3H); 1.45 (s, 9H); 1.95 (dddd, *J* = 6.3, 8.5, 14.6, 14.6, 1H); 2.15-2.26 (m, 1H); 2.35-2.56 (m, 2H); 4.20 (q, *J* = 7.2, 2H); 4.25-4.35 (m, 1H); 5.10 (s, 2H); 7.30-7.40 (m, 5H).

Synthesis of (+)-**13**

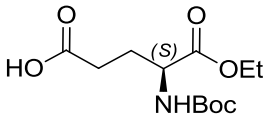


(+)-**13**

Compound (+)-**12** (3.47 g, 9.50 mmol) was dissolved in 30 ml of EtOH and 10% w/w of 5% Pd on active carbon (347 mg) was added. The mixture was stirred at room temperature for 2.5 hours under a $H_2$ atmosphere and the reaction was followed by TLC (cyclohexane/EtOAc 8:2). The mixture was filtered *in vacuo* on a celite pad to eliminate the catalyst. After evaporation of the solvent, the product was dissolved in EtOAc (50 mL) and extracted with 5% $NaHCO_3$ (3 x 40 ml). The extraction was monitored by TLC ($CH_2Cl_2$/MeOH 9:1 + 1% AcOH). The solution was made acidic with 2N HCl and the product was extracted with EtOAc (3 x 70 mL). The organic phase was dried over anhydrous $Na_2SO_4$ and, after evaporation of the solvent, the monoacidic derivate (+)-**13** (2.19 g, 7.95 mmol) was obtained.

**Yield**: 84%

**Solid state**: Yellow oil

**$R_f$** ($CH_2Cl_2$/MeOH 9:1 + 1% AcOH): 0.82

**$[\alpha]^{D}_{20}$**: (+) 9.8 (c: 0.75 in $CHCl_3$)

**$^{1}$H-NMR** (300 MHz, $CDCl_3$): 1.25 (t, *J* = 7.2, 3H); 1.45 (s, 9H); 1.85-2.00 (m, 1H); 2.10-2.25 (m, 1H); 2.35- 2.55 (m, 2H); 4.20 (q, *J* = 7.2, 2H); 4.25-4.35 (m, 1H); 5.20 (bd., *J* = 7.3, 1H).

**$^{13}$C-NMR** (75 MHz, $CDCl_3$): 14.34, 27.84, 28.47, 30.29, 53.06, 61.83, 80.33, 155.77, 172.49, 178.03.

General procedure for the esterification of amino acids

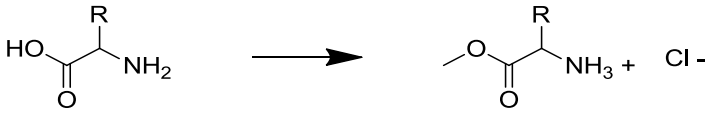


2.00 mmol of free amino acid were dissolved in MeOH (3.6 ml) and the solution was cooled down to −10 °C (bath of ice and salt). $SOCl_2$ (200 µl, 2.8 mmol) was added carefully. When the reaction mixture became limpid the ice-bath was removed and the solution was stirred at r.t for 24 hours. After that, the solvent was evaporated under reduced pressure and the product was precipitated with $Et_2O$. The mixture was filtrated under vacuum to give the solid ester as a hydrochloride salt.

**Yield**: quantitative

Synthesis of lysine methylester Nω-Boc

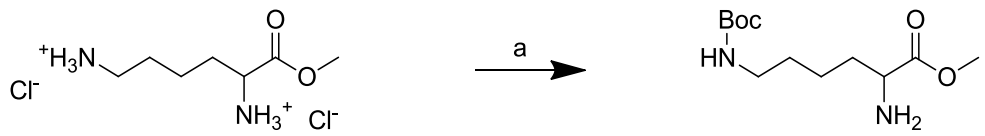


lysine methylester * 2HCl

lysine methylester N-Boc

To a solution of lysine methylester * HCl (1 g, 6.84 mmol) in MeOH (11.6 ml) was added TEA (2.64 ml, 18.96 mmol). After cooling the reaction mixture to − 10 °C, a solution of $(Boc)_2O$ (1.52 g, 6.95 mmol) in $CH_2Cl_2$ (7.75 ml) was added dropwise. The mixture was stirred at r.t. overnight and the disappearance of the starting material was monitored by TLC ($CH_2Cl_2$/MeOH 9:1). The crude material obtained was purified by column chromatography on silica gel ($CH_2Cl_2$/MeOH 9.5:0.5) to give the desired product as yellow oil.

**Yield**: 80%

Synthesis of OTr-serine methylester

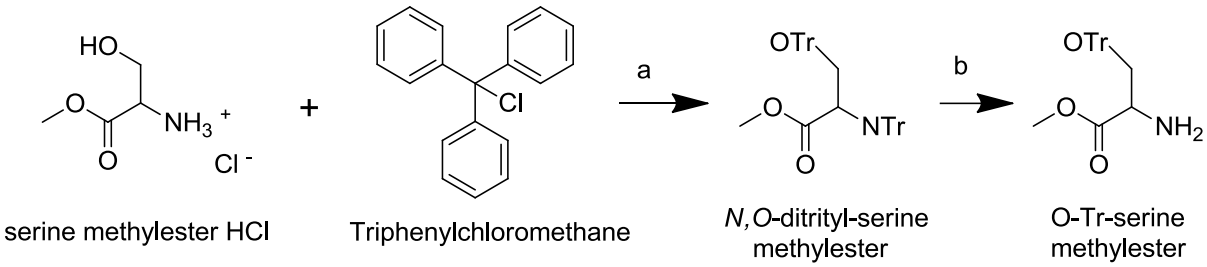


1) Serine methylester * HCl (2 g, 12.9 mmol) was suspended in $CHCl_3$ (25.6 ml). The suspension was cooled to 0 °C and TEA (6.25 ml, 45 mmol) and triphenylchloromethane (7.19 g, 25.8 mmol) were slowly added. After the exothermic phase, the reaction was stirred at r.t. for 17 hours. The reaction mixture was washed with $H_2O$ (3 x 20 ml). The organic phase was dried with $Na_2SO_4$, filtered and concentrated in vacuo. The residue was taken up twice with EtOH and the solvent was evaporated under reduced pressure. The intermediate *N,O*-ditrityl-serine methylester (7.79 g, 12.9 mmol) was obtained as yellow oil.

**Yield**: quantitative

2) *N,O*-ditrityl-serine methylester (7.79 g, 12.9 mmol) was dissolved in $CH_2Cl_2$ (200 ml) and the solution was cooled to 0 °C. A 1% v/v solution of TFA (2 ml) was added and the reaction was stirred at room temperature for 3 minutes. The solvent was evaporated until the volume reached the half of the original one. The reaction mixture was washed twice with 5% $NaHCO_3$ (2 x 50 ml) and once with $H_2O$ (50 ml). The reaction was monitored by TLC (cyclohexane/EtOAc 1/1). The organic phase was dried over anhydrous $Na_2SO_4$ and the crude material was purified by column chromatography on silica gel (cyclohexane/EtOAc 1/1). O-Tr-serine methylester was obtained as a yellowish oil.

**Yield**: 64%

General batch procedure of coupling

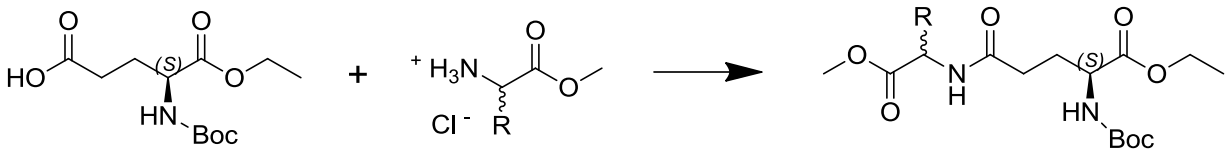

(+)-**13**

Compound (+)-**13** (250 mg, 0.91 mmol) was dissolved in THF (7 ml). HOBt (145 mg, 1.09 mmol), HBTU (413 mg, 1.09 mmol), DIPEA (634 µl, 3.64 mmol) and the methylester amino acid hydrochloride (1.82 mmol) were added. The mixture was stirred at r.t. overnight and the disappearance of the starting material was monitored by TLC.

After evaporation of THF, the reaction mixture was taken up with EtOAc (10 ml) and sequentially washed with 1 N HCl (10 ml), 5% $NaHCO_3$ (10 ml) and distilled $H_2O$ (10 ml).

The organic phase was dried over anhydrous $Na_2SO_4$ and the solvent was evaporated under low pressure. The crude material was purified by column chromatography on silica gel.

Procedure of Coupling in a continuous *flow reactor*

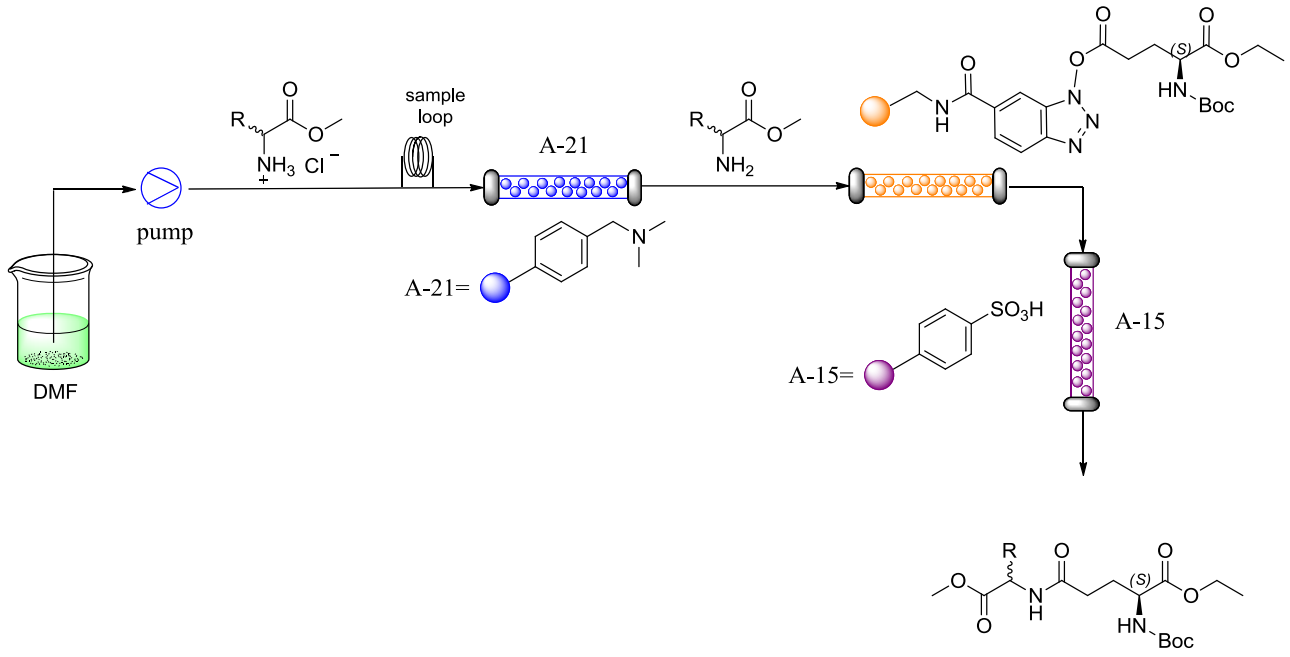


1.00 g of PS-HOBt was packed (loading 1.0 mmol/g) into a glass column (Ø: 6,6 mm; h: 100 mm) and DMF was fluxed for 15 minutes (flow rate: 150 µl/min).

PyBroP (979 mg, 2.1 mmol) and DIPEA (523µl; 3.0 mmol) were added to a 0.1 M solution of (+)-**13** (2.00 mmol in 20.0 ml of DMF) and the resulting solution was fluxed for 1 hour into the flow reactor.

1.00 g of Amberlyst A-21 was packed into a glass column (Ø: 10.0 mm; h: 100) and DMF was fluxed for 10 minutes (flow rate: 150 µl/min). 500 mg of Amberlyst A-15 were packed into a third glass column (Ø: 6,6 mm; h: 100 mm) and and DMF was fluxed for 10 minutes (flow rate: 150 µl/min).

The column containing A-21 was connected with the column packed with PS-HOBt (which is linked to the carboxylic acid) and with the column containing A-15.

A 0.2 M solution of the amino acid methyl ester hydrochloride (1.0 mmol in 5 ml of DMF) was injected *via loop* into the reactor. The flow rate was set in order to obtain a residence time of 10 minutes.

Synthesis of **14**

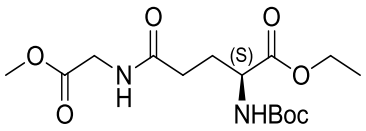


14

Dipeptide **14** was synthesized following the general coupling procedure reported at page 96.

The crude material was purified by column chromatography on silica gel in the first attempt with cyclohexane/EtOAc 7/3. Compound **14** (210 mg, 0.6 mmol) was obtained as a purple oil.

**Yield** : 70%

**Solide state**: purple oil

**R**$_f$ (cyclohexane/EtOAc 1/1): 0.41

**[$\alpha$]$_D^{20}$**: (+)11.3 (c: 1.02 in $CHCl_3$)

**$^1$H-NMR** (300 MHz, $CDCl_3$): 1.25 (t, *J* = 7.0, 3H); 1.45 (s, 9H); 1.80-2.00 (m, 1H); 2.10-2.25 (m, 1H); 2.30- 2.38 (m, 2H); 3.75 (s, 3H); 4.05 (dd, *J* = 5.5, 9.4, 2H); 4.20 (q, *J* = 7.0, 2H); 4.25-4.40 (m, 1H); 5.35 (bd., *J* = 7.1, 1H); 6.70 (bd., *J* = 5.5, 1H).

**$^{13}$C-NMR** (75 MHz, $CDCl_3$): 14.37, 28.50, 29.39, 32.46, 41.51, 52.57, 53.11, 61.81, 80.33, 156.17, 170.68, 172.52, 172.60.

Synthesis of **15**

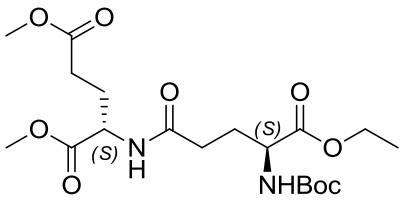

**15**

Dipeptide **15** was synthesized following the general coupling procedure reported at page 96.
The crude material was purified by column chromatography on silica gel using cyclohexane/EtOAc 1/1 and then was precipitated with diisopropyl ether and filtered on hirsh.

**Yield**: 63%

Crystallized from diisopropyl ether as white crystals

**$R_f$** (cyclohexane/EtOAc 4/6): 0.37

**$[\alpha]_D^{20}$**: (+) 21.0 (c: 0.95 in $CHCl_3$)

**M.p.**: 95-97 °C

**$^1$H-NMR** (300 MHz, $CDCl_3$): 1.25 (t, *J* = 7.1, 3H); 1.45 (s, 9H); 1.90-2.10 (m, 2H); 2.15-2.25 (m, 2H); 2.30-2.40 (m, 2H); 2.40-2.50 (m, 2H); 3.65 (s, 3H); 3.75 (s, 3H); 4.20 (q, *J* = 7.1, 2H); 4.20-4.30 (m, 1H); 4.60 (ddd, *J* = 5.0, 7.6, 7.6, 1H); 5.25 (bd., *J* = 7.6, 1H); 6.60 (bd., *J* = 7.6, 1H).

Synthesis of **16**

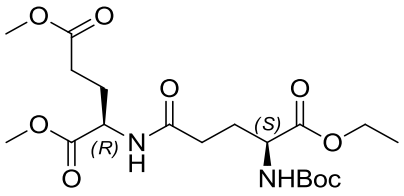


**16**

Dipeptide **16** was synthesized following the general coupling procedure reported at page 96.
The crude material was purified by column chromatography on silica gel using cyclohexane/EtOAc 7/3 and then 6/4.

**Yield**: 73%

**R**$_f$ (cyclohexane/EtOAc 1/1): 0.19

**[$\alpha$]$_D^{20}$**: (–) 6.9 (c: 0.45 in $CHCl_3$)

**M.p.**: 75-77 °C

**$^1$H-NMR** (300 MHz, $CDCl_3$): 1.25 (t, *J* = 7.0, 3H); 1.45 (s, 9H); 1.85-2.00 (m, 1H); 2.00-2.10 (m, 1H); 2.15-2.25 (m, 2H); 2.30-2.40 (m, 2H); 2.40-2.50 (m, 2H); 3.65 (s, 3H); 3.75 (s, 3H); 4.20 (q, *J* = 7.0, 2H); 4.35-4.30-4.45 (m, 1H); 4.60 (ddd, *J* = 5.0, 7.6, 7.6, 1H); 5.305 (bd., *J* = 7.6, 1H); 6.75 (bd., *J* = 7.6, 1H).

Synthesis of **17**

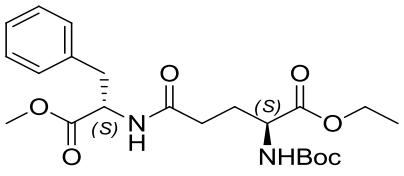


**17**

Dipeptide **17** was synthesized following the general coupling procedure reported at page 96.

The crude material was purified by column chromatography on silica gel using cyclohexane/EtOAc 7/3.

**Yield** = 76%

**Solid state** = yellow oil

**R**$_f$ (cyclohexane/EtOAc 6/4): 0.3

**[$\alpha$]$_D^{20}$**: (+)37.0 (c: 1.00 in $CHCl_3$)

**$^1$H-NMR** (300 MHz, $CDCl_3$): 1.25 (t, *J* = 7.0, 3H); 1.45 (s, 9H); 1.85-2.00 (m, 1H); 2.10-2.20 (m, 1H); 2.20-2.30 (m, 2H); 3.10 (dd, *J* = 6.8, 14.1, 1H); 3.15 (dd, *J* = 5.4, 14.1, 1H); 3.75 (s, 3H); 4.20 (q, *J* = 7.0, 2H); 4.80-4.90 (m, 1H); 5.20 (bd., *J* = 6.9, 1H); 6.35 (bd., *J* = 5.8, 1H); 7.10-7.15 (m, 2H); 7.20-7.30 (m, 3H).

**$^{13}$C-NMR** (75 MHz, $CDCl_3$): 14.39, 28.53, 29.68, 32.64, 37.96, 52.56, 53.07, 53.81, 61.82, 80.40, 127.31, 128.79, 129.46, 136.33, 156.17, 172.08, 172.37, 172.51

Synthesis of **18**

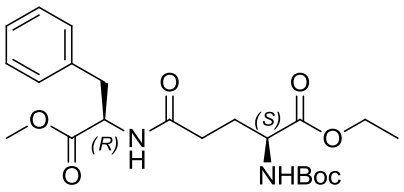


**18**

Dipeptide **18** was synthesized following the general coupling procedure reported at page 96.

The crude material was purified by column chromatography on silica gel using cyclohexane/EtOAc 7/3.

**Yield** = 38%

**Solid state**= yellow oil

**R**$_f$ (cyclohexane/EtOAc 6/4): 0.22

**[$\alpha$]$_D^{20}$**: (–)19.7 (c: 1.05 in $CHCl_3$)

**$^1$H-NMR** (300 MHz, $CDCl_3$): 1.25 (t, *J* = 7.0, 3H); 1.45 (s, 9H); 1.80-1.90 (m, 1H); 2.10-2.30 (m, 3H); 3.06 (dd, *J* = 6.8, 14.1, 1H); 3.17 (dd, *J* = 5.4, 14.1, 1H); 3.75 (s, 3H); 4.20 (q, *J* = 7.0, 2H); 4.35-4.45 (m, 1H); 4.80-4.90 (m, 1H); 5.30 (bd., *J* = 6.8, 1H); 6.75 (bd., *J* = 5.9, 1H); 7.10-7.20 (m, 2H); 7.20-7.30 (m, 3H).

**$^{13}$C-NMR** (75 MHz, $CDCl_3$): 14.39, 28.53, 29.68, 32.64, 37.96, 52.56, 53.07, 53.81, 61.82, 80.40, 127.31, 128.79, 129.46, 136.33, 156.17, 172.08, 172.37, 172.51.

Synthesis of **19**

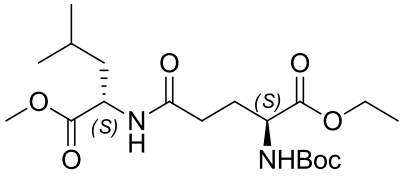

**19**

Dipeptide **19** was synthesized following the general coupling procedure reported at page 96.

The crude material was purified by column chromatography on silica gel using cyclohexane/EtOAc 6/4.

**Yield**: 82%

**Solid state**: yellow oil

**$R_f$** (cyclohexane/EtOAc 6/4): 0.30

**$[\alpha]_D^{20}$**: (+) 5.3 (c: 1.10 in $CHCl_3$)

**$^1$H-NMR** (300 MHz, $CDCl_3$): 0.94 (d, *J* = 6.3, 6H); 1.25 (t, *J* = 7.1, 3H); 1.45 (s, 9H); 1.50-1.70 (m, 3H); 1.80-1.90 (m, 1H); 2.10-2.25 (m, 1H); 2.28-2.36 (m, 2H); 3.75 (s, 3H); 4.20 (q, *J* = 7.1, 2H); 4.20-4.30 (m, 1H); 4.55-4.65 (m, 1H); 5.25 (bd., *J* = 7.7, 1H); 6.35 (bd., *J* = 6.6, 1H).

**$^{13}$C-NMR** (75 MHz, $CDCl_3$): 14.39, 22.12, 23.04, 25.09, 28.52, 29.32, 32.64, 41.70, 51.04, 52.52, 53.15, 61.81, 80.34, 156.05, 171.95, 172.51, 173.78.

Synthesis of **20**

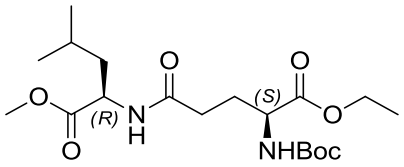


**20**

Dipeptide **20** was synthesized following the general coupling procedure reported at page 96.
The crude material was purified by column chromatography on silica gel using cyclohexane/EtOAc 6/4.

**Yield**: 68%

**Solid state**: yellow oil

**R**$_f$ (cyclohexane/EtOAc 6/4): 0.20

**[$\alpha$]$_D^{20}$**: (+) 13.1 (c: 1.55 in $CHCl_3$)

**$^1$H-NMR** (300 MHz, $CDCl_3$): 0.94 (d, *J* = 6.0, 6H); 1.25 (t, *J* = 7.0, 3H); 1.45 (s, 9H); 1.50-1.70 (m, 3H); 1.80-1.90 (m, 1H); 2.10-2.25 (m, 1H); 2.28-2.36 (m, 2H); 3.75 (s, 3H); 4.20 (q, *J* = 7.0, 2H); 4.35-4.45 (m, 1H); 4.50-4.60 (m, 1H); 5.32 (bd., *J* = 7.1, 1H); 6.90 (bd., *J* = 6.8, 1H).

**$^{13}$C-NMR** (75 MHz, $CDCl_3$): 14.39, 22.05, 23.07, 25.12, 28.52, 29.88, 32.71, 41.39, 51.26, 52.46, 53.08, 61.83, 80.45, 156.31, 172.27, 172.57, 173.79.

Synthesis of **21**

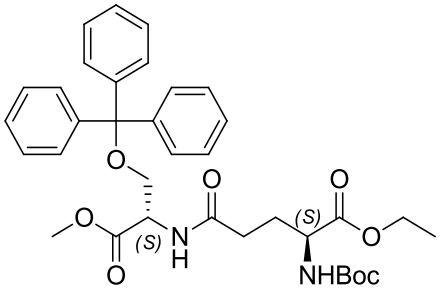


**21**

Dipeptide **21** was synthesized following the general coupling procedure reported at page 96.

The crude material was purified by column chromatography on silica gel using cyclohexane/EtOAc 7/3.

**Yield**: 69%

**Solid state**: yellow/white oil

**R**$_f$ (cyclohexane/EtOAc 7/3): 0.21

**[α]**$_D^{20}$: (–) 20.6 (c: 1.00 in $CHCl_3$)

**$^1$H-NMR** (300 MHz, $CDCl_3$): 1.25 (t, *J* = 7.0, 3H); 1.45 (s, 9H); 1.85-2.00 (m, 1H); 2.10-2.20 (m, 1H); 2.30 (m, 2H); 3.35 (dd, *J* = 3.3, 9.4, 1H); 3.60 (dd, *J* = 3.3, 9.4, 1H); 3.75 (s, 3H); 4.15 (q, *J* = 7.0, 2H); 4.20-4.30 (m, 1H); 4.70 (ddd, *J* = 3.3, 3.3, 8.0, 1H); 5.24 (bd., *J* = 8.0, 1H); 6.55 (bd., *J* = 8.3, 1H); 7.20-7.40 (m, 15H).

**$^{13}$C-NMR** (75 MHz, $CDCl_3$): 14.42, 28.53, 28.91, 32.55, 52.65, 52.86, 60.61, 61.72, 63.82, 80.68, 86.85, 127.46, 128.13, 128.74, 143.59, 155.85, 171.19, 171.80, 172.46.

Synthesis of **22**

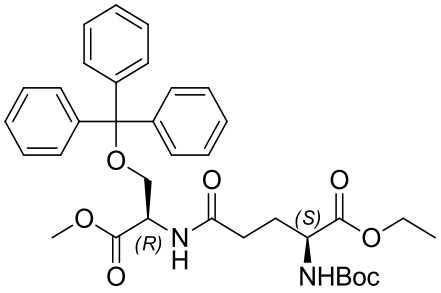


**22**

Dipeptide **22** was synthesized following the general coupling procedure reported at page 96.

The crude material was purified by column chromatography on silica gel using cyclohexane/EtOAc 7/3.

**Yield**: 57%

**Solid state**: yellow oil

**R**$_f$ (cyclohexane/EtOAc 1/1): 0.63

**[$\alpha$]$_D^{20}$**: (–) 1.3 (c: 0.95 in $CHCl_3$)

**$^1$H-NMR** (300 MHz, $CDCl_3$): 1.25 (t, *J* = 7.0, 3H); 1.45 (s, 9H); 1.80-2.00 (m, 1H); 2.10-2.40 (m, 3H); 3.35 (dd, *J* = 3.2, 9.4, 1H); 3.60 (dd, *J* = 3.2, 9.4, 1H); 3.75 (s, 3H); 4.20 (q, *J* = 7.0, 2H); 4.35-4.45 (m, 1H); 4.72 (ddd, *J* = 3.2, 3.2, 7.9, 1H); 5.35 (bd., *J* = 7.9, 1H); 6.86 (bd., *J* = 7.9, 1H); 7.20-7.40 (m, 15H).

**$^{13}$C-NMR** (75 MHz, $CDCl_3$): 14.38, 28.54, 28.98, 32.55, 52.93, 53.10, 59.64, 61.81, 63.11, 80.64, 86.86, 127.46, 128.14, 128.86, 143.61, 156.11, 171.19, 171.23, 172.52

Synthesis of **23**

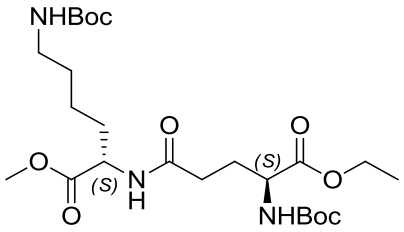


**23**

Dipeptide **23** was synthesized following the general coupling procedure reported at page 96.

The crude material was purified by column chromatography on silica gel using cyclohexane/EtOAc 6/4.

**Yield**: 37%

**Solid state**: yellow oil

**R**$_f$ (cyclohexane/EtOAc 1/1): 0.33

**[$\alpha$]$_D^{20}$**: (+) 8.0 (c: 0.35 in $CHCl_3$)

**$^1$H-NMR** (300 MHz, $CDCl_3$): 1.25 (t, *J* = 7.0, 3H); 1.45 (s, 18H); 1.30-1.50 (m, 1H); 1.65-1.95 (m, 6H); 2.10-2.25 (m, 1H); 2.30-2.40 (m, 2H); 3.05-3.15 (m, 2H); 3.75 (s, 3H); 4.20 (q, *J* = 7.0, 2H); 4.20-4.30 (m, 1H); 4.55 (ddd, *J* = 5.0, 7.7, 7.7, 1H); 4.65 (bs., 1 H); 5.25 (bd., *J* = 7.7, 1H); 6.50 (bd., *J* = 7.7, 1H).

**$^{13}$C-NMR** (75 MHz, $CDCl_3$): 14.38, 22.74, 28.52, 28.63, 29.55, 29.81, 31.87, 32.61, 40.30, 52.40, 52.54, 53.06, 61.80, 79.33, 80.36, 156.19, 156.34, 172.30, 172.55, 173.14.

Synthesis of **24**

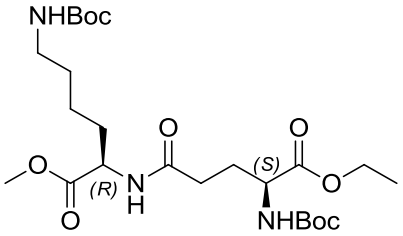


**24**

Dipeptide **24** was synthesized following the general coupling procedure reported at page 96.
The crude material was purified by column chromatography on silica gel using cyclohexane/EtOAc 6/4 and then 4/6.

**Yield**: 87%

**$R_f$** (cyclohexane/EtOAc 1/1): 0.40

**M.p.**: 75°C

**$[\alpha]_D^{20}$**: (+) 5.0 (c: 0.25 in $CHCl_3$)

**$^1$H-NMR** (300 MHz, $CDCl_3$): 1.25 (t, *J* = 7.1, 3H); 1.45 (s, 18H); 1.35-1.50 (m, 1H); 1.65-1.95 (m, 6H); 2.10-2.25 (m, 1H); 2.30-2.40 (m, 2H); 3.05-3.15 (m, 2H); 3.75 (s, 3H); 4.20 (q, *J* = 7.1, 2H); 4.35-4.45 (m, 1H); 4.55 (ddd, *J* = 5.0, 7.4, 7.4, 1H); 4.65 (bs., 1 H); 5.30 (bd., *J* = 6.6, 1H); 6.90 (bd., *J* = 6.6, 1H).

**$^{13}$C-NMR** (75 MHz, $CDCl_3$): 14.38, 22.74, 28.52, 28.63, 29.55, 29.81, 31.87, 32.61, 40.30, 52.40, 52.54, 53.06, 61.80, 79.33, 80.36, 156.19, 156.34, 172.30, 172.55, 173.14.

General procedure for deprotection

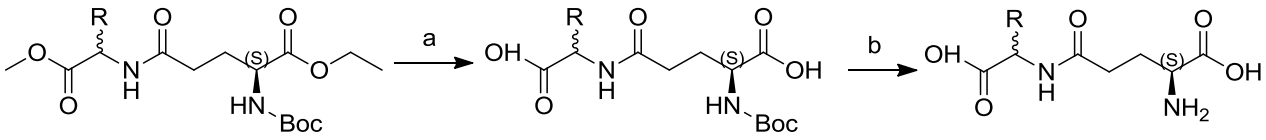


1) The protected dipeptide (1mmol) was dissolved in MeOH (3 ml) and 1N NaOH (3 ml, 3.0 mmol) was added.The mixture was stirred at room temperature for 3 hours and the disappearance of the starting material was monitored by TLC ($CH_2Cl_2$/MeOH 9:1 + 1% AcOH). After evaporation of MeOH, the reaction mixture was taken up with distilled $H_2O$ (5 ml) and washed with $CH_2Cl_2$ (2 x 5 ml). After that, the mixture was made acidic with 2N aqueous HCl until a pH = 2 was reached and then extracted with EtOAc (3 x 5 ml). The organic phase was dried over anhydrous $Na_2SO_4$ and, after evaporation of the solvent, the diacidic intermediate was obtained as a white solid.

2) The diacidic intermediate (1 mmol) was treated with a 30% solution of TFA in $CH_2Cl_2$ (2.5 ml) at 0 °C. The solution was stirred at room temperature for 2 hours and the reaction was followed by TLC ($CH_2Cl_2$/MeOH 9:1 + 1% AcOH). The volatiles were removed under reduced pressure. The obtained solid was dissolved in water (1 ml) and lyophilized to give the deprotected dipeptide as a white powder.

Synthesis of **1a**

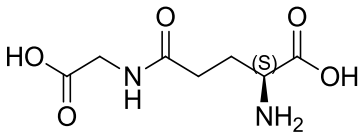


Gly-γ-(*S*)Glu

The final dipeptide Gly-γ-(*S*)Glu was obtained following the general procedure of deprotection reported at page 108.

**Yield**: 31%

**$R_f$** (*n*-butanol/$H_2O$/AcOH 4:2:1): 0.18

**M.p.**: dec. T > 159 °C

**$[\alpha]_D^{20}$**: (+) 5.0 (c: 0.30 in $H_2O$)

**$^1$H-NMR** (300 MHz, $D_2O$): 2.00-2.08 (m, 2H); 2.35 (ddd, *J* = 1.4, 8.5, 8.5, 2H); 3.70 (dd, *J* = 6.3, 6.3, 1H); 3.80 (s, 2H).

**$^{13}$C-NMR** (75 MHz, $D_2O$): 26.11, 31.21, 41.50, 53.63, 173.30, 173.97, 175.16.

**$[M+H]^+$**: 205.0

Synthesis of **1b**

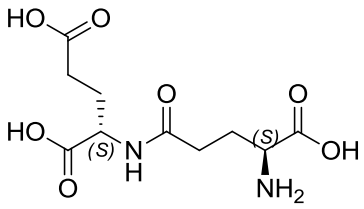

(*S*)Glu-γ-(*S*)Glu

The final dipeptide (*S*)Glu-γ-(*S*)Glu was obtained following the general procedure of deprotection reported at page 108.

**Yield**: 59%

**R**$_f$ (*n*-butanol/$H_2O$/AcOH 4:2:1): 0.29

**[α]**$_D^{20}$: (–) 2.5 (c: 0.40 in $H_2O$)

**M.p.**: 91-93°C

**$^1$H-NMR** (300 MHz, $D_2O$): 1.80-1.95 (m, 1H); 2.00-2.15 (m, 3H); 2.30-2.45 (m, 4H); 3.80 (dd, *J* = 6.3, 6.3, 1H); 4.25 (dd, *J* = 5.0, 9.1, 1H).

**$^{13}$C-NMR** (75 MHz, $D_2O$): 25.91, 26.03, 30.26, 31.25, 52.47, 53.47, 173.10, 174.70, 175.50, 177.30.

**[M+H]$^+$**: 277.0

Synthesis of **2b**

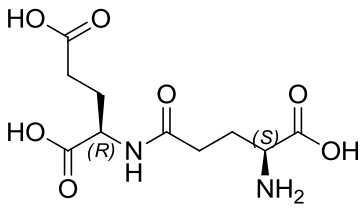

(*R*)Glu-γ-(*S*)Glu

The final dipeptide (*R*)Glu-γ-(*S*)Glu was obtained following the general procedure of deprotection reported at page 108.

**Yield**: 44%

**R**$_f$ (*n*-butanol/$H_2O$/AcOH 4:2:1): 0.29

**[α]**$_D^{20}$: (+) 13.2 (c: 0.25 in $H_2O$)

**M.p.**: 103-105°C

**$^1$H-NMR** (300 MHz, $D_2O$): 1.80-1.95 (m, 1H); 2.00-2.10 (m, 3H); 2.30-2.40 (m, 4H); 3.80 (dd, *J* = 6.3, 6.3, 1H); 4.25 (dd, *J* = 5.0, 9.1, 1H).

**$^{13}$C-NMR** (75 MHz, $D_2O$): 25.91, 25.98, 30.24, 31.03, 52.37, 53.28, 172.87, 174.63, 175.47, 177.32.

**[M+H]$^+$**: 277.0

Synthesis **1c**

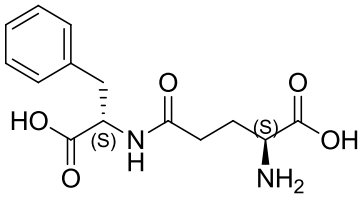


(*S*)Phe-γ-(*S*)Glu

The final dipeptide (*S*)Phe-γ-(*S*)Glu was obtained following the general procedure of deprotection reported at page 108.

**Yield**: 80%

**R**$_f$ (*n*-butanol/$H_2O$/AcOH 4:2:1): 0.49

**[α]**$_D^{20}$: (+) 18.2 (c: 0.25 in $H_2O$)

**M.p.**: dec. T > 186 °C

**$^1$H-NMR** (300 MHz, $D_2O$): 1.80-1.90 (m, 2H); 2.25 (m, 2H); 2.85 (dd, *J* = 9.3, 14.0, 1H); 3.10 (dd, *J* = 5.3, 14.0, 1H); 3.60 (dd, *J* = 6.5, 6.5, 1H); 4.55 (dd, *J* = 5.3, 9.3 1H); 7.10-7.30 (m, 5H).

**$^{13}$C-NMR** (75 MHz, $D_2O$): 26.08, 31.26, 36.83, 53.17, 54.33, 127.27, 128.85, 129.34, 136.80, 172.68, 174.22, 175.28.

**[M+H]$^+$**: 295.0

Synthesis of **2c**

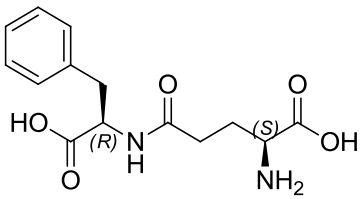


(*R*)Phe-γ-(*S*)Glu

The final dipeptide (*R*)Phe-γ-(*S*)Glu was obtained following the general procedure of deprotection reported at page 108.

**Yield**: 89%

**R**$_f$ ($CH_2Cl_2$/MeOH 9:1 + 1% AcOH): 0.62

**[$\alpha$]$_D^{20}$**: (+) 3.7 (c: 0.30 in $H_2O$)

**M.p.**: 150 °C

**$^1$H-NMR** (300 MHz, $D_2O$): 1.80-2.00 (m, 2H); 2.28 (ddd, *J* = 3.0, 8.2, 8.2, 2H); 2.82 (dd, *J* = 9.7, 14.1, 1H); 3.12 (dd, *J* = 5.3, 14.1, 1H); 3.60 (dd, *J* = 3.0, 6.5, 1H); 4.55 (dd, *J* = 5.3, 9.7, 1H); 7.10-7.25 (m, 5H).

**$^{13}$C-NMR** (75 MHz, $D_2O$): 25.70, 30.36, 36.83, 52.16, 54.03, 127.24, 128.83, 129.38, 136.81, 171.75, 174.02, 175.10.

**[M+H]$^+$**: 295.0

Synthesis of **1d**

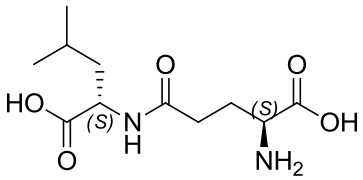


(*S*)Leu-γ-(*S*)Glu

The final dipeptide (*S*)Leu-γ-(*S*)Glu was obtained following the general procedure of deprotection reported at page 108.

**Yield**: 100%

**R**$_f$ (*n*-butanol/$H_2O$/AcOH 4:2:1): 0.56

**[α]**$_D^{20}$: (–) 15.0 (c: 0.25 in $H_2O$)

**M.p.**: 136-138 °C

**$^1$H-NMR** (300 MHz, $D_2O$): 0.70 (d, *J* = 5.8, 3H); 0.80 (d, *J* = 5.8, 3H); 1.45-1.55 (m, 3H); 1.95-2.05 (m, 2H); 2.30-2.40 (m, 2H); 3.72 (dd, *J* = 6.2, 6.2, 1H); 4.20 (dd, *J* = 6.4, 6.4, 1H).

**$^{13}$C-NMR** (75 MHz, $D_2O$): 20.74, 22.30, 24.60, 26.18, 31.27, 39.46, 51.85, 53.50, 173.05, 174.74, 177.00.

**[M+H]$^+$**: 261.0

Synthesis of **2d**

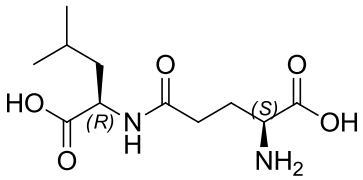


(*R*)Leu-γ-(*S*)Glu

The final dipeptide (*R*)Leu-γ-(*S*)Glu was obtained following the general procedure of deprotection reported at page 108.

**Yield**: 86%

**$R_f$** (*n*-butanol/$H_2O$/AcOH 4:2:1): 0.56

**$[\alpha]_D^{20}$**: (+) 35.0 (c: 0.25 in $H_2O$)

**M.p.**: 100-102°C

**$^1$H-NMR** (300 MHz, $D_2O$): 0.70 (d, *J* = 6.2, 3H); 0.80 (d, *J* = 6.2, 3H); 1.45-1.55 (m, 3H); 1.95-2.10 (m, 2H); 2.35 (ddd, *J* = 1.8, 8.8, 8.8, 2H); 3.80 (dd, *J* = 6.4, 6.4, 1H); 4.22 (dd, *J* = 7.0, 7.0, 1H).

**$^{13}$C-NMR** (75 MHz, $D_2O$): 20.63, 22.27, 24.54, 25.93, 30.90, 39.39, 51.67, 52.99, 172.51, 174.54, 176.88.

**$[M+H]^+$**: 261

Synthesis of **1e**

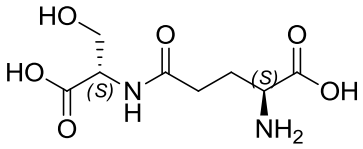


(*S*)Ser-γ-(*S*)Glu

The final dipeptide (*S*)Ser-γ-(*S*)Glu was obtained following the general procedure of deprotection reported at page 108.

**Yield**: 40%

**$R_f$** (*n*-butanol/$H_2O$/AcOH 4:2:1): 0.24

**M.p.**: dec. T > 164°C

**$[\alpha]_D^{20}$**: (+) 11.6 (c: 0.35 in $H_2O$)

**$^1$H-NMR** (300 MHz, $D_2O$): 2.00-2.10 (m, 2H); 2.40 (ddd, *J* = 3.5, 6.2, 6.2, 2H); 3.70-3.85 (m, 3H); 4.38 (dd, *J* = 4.1, 4.1, 1H).

**$^{13}$C-NMR** (75 MHz, $D_2O$): 26.47, 31.91, 54.49, 57.34, 62.14, 174.26, 174.60, 176.37.

**$[M+H]^+$**: 235.0

Synthesis of **2e**

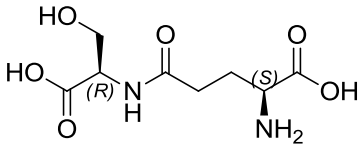


(*R*)Ser-γ-(*S*)Glu

The final dipeptide (*R*)Ser-γ-(*S*)Glu was obtained following the general procedure of deprotection reported at page 108.

**Yield**: 40%

**$R_f$** (*n*-butanol/$H_2O$/AcOH 4:2:1): 0.26

**M.p.**: dec. T > 156°C

**$[\alpha]_D^{20}$**: (+) 12.3 (c: 0.40 in $H_2O$)

**$^1$H-NMR** (300 MHz, $D_2O$): 2.00-2.10 (m, 2H); 2.40 (ddd, *J* = 3.5, 6.2, 6.2, 2H); 3.70-3.85 (m, 3H); 4.38 (dd, *J* = 4.1, 4.1, 1H).

**$^{13}$C-NMR** (75 MHz, $D_2O$): 25.93, 31.05, 53.24, 55.14, 61.19, 172.87, 173.83, 174.65.

**$[M+H]^+$**: 235.0

Synthesis of **1f**

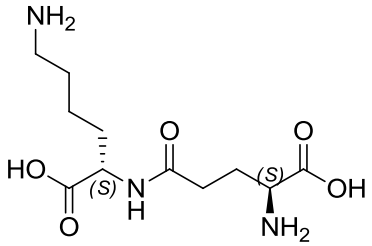


(*S*)Lys-γ-(*S*)Glu

The final dipeptide (*S*)Lys-γ-(*S*)Glu was obtained following the general procedure of deprotection reported at page 108.

In this case the distal amino group was obtaoined as a trifluoroacetic acid salt, therefore, to obtain the corresponding free amine, the product was submitted to ion exchange chromatography. The residue was dissolved in a few drops of bidistilled water and purified on a column packed with Amberlite IR120. The resin was washed with bidistilled $H_2O$ until the pH was neutral and then the product was released from the resin with acqueous 1N $NH_3$.The fractions containing the amino acid (detected with ninhydrine on a TLC plate) were collected and liophilized to give the desired product.

**Yield:** 79%

**$R_f$** (*n*-butanol/$H_2O$/AcOH 4:2:1): 0.14

**$[\alpha]_D^{20}$**: (-) 9.0 (c: 0.20 in $H_2O$)

**M.p.**: dec. T > 215°C

**$^1$H-NMR** (300 MHz, $D_2O$): 1.25-1.35 (m, 2H); 1.50-1.60 (m, 3H); 1.60-1.70 (m, 1H); 1.95-2.05 (m, 2H); 2.30-2.40 (m, 2H); 2.86 (ddd, *J* = 7.6, 7.6, 7.6, 2H); 3.62 (dd, *J* = 6.5, 6.5, 1H); 4.00 (dd, *J* = 5.3, 8.5, 1H).

**$^{13}$C-NMR** (75 MHz, $D_2O$): 22.32, 26.46, 26.53, 31.02, 31.94, 39.38, 54.44, 55.22, 174.24, 174.38, 179.25.

**$[M+H]^+$**: 276.0

Synthesis of **2f**

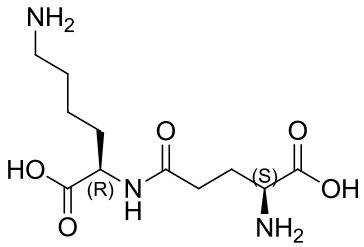


(*R*)Lys-γ-(*S*)Glu

The final dipeptide (*R*)Lys-γ-(*S*)Glu was obtained following the general procedure of deprotection reported at page 108.

In this case the distal amino group was obtaoined as a trifluoroacetic acid salt, therefore, to obtain the corresponding free amine, the product was submitted to ion exchange chromatography. The residue was dissolved in a few drops of bidistilled water and purified on a column packed with Amberlite IR120. The resin was washed with bidistilled $H_2O$ until the pH was neutral and then the product was released from the resin with acqueous 1N $NH_3$.The fraction containing the amino acid (detected with ninhydrine on a TLC plate) were collected and liophilized to give the desired product.

**Yield**: 65%

**$R_f$** (*n*-butanol/$H_2O$/AcOH 4:2:1): 0.14

**$[\alpha]_D^{20}$**: (+) 6.0 (c: 0.35 in $H_2O$)

**M.p.**: dec. T > 205°C

**$^1$H-NMR** (300 MHz, $D_2O$): 1.20-1.40 (m, 2H); 1.50-1.60 (m, 2H); 1.60-1.75 (m, 2H); 1.95-2.05 (m, 2H); 2.25-2.35 (m, 2H); 2.86 (ddd, *J* = 7.3, 7.3, 7.3, 2H); 3.66 (dd, *J* =5.9, 5.9, 1H); 4.02 (dd, *J* = 5.0, 8.2, 1H).

**$^{13}$C-NMR** (75 MHz, $D_2O$): 22.34, 26.41, 26.48, 31.03, 31.25, 39.40, 54.26, 55.19, 174.22, 174.90, 179.25.

**$[M+H]^+$**: 276.0

Synthesis of 2,2-dibromo-formaldoxime

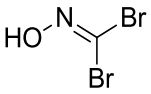


To a solution of glyoxylic acid monohydrate (25.0 g; 0.34 mol) dissolved in distilled $H_2O$ (200 ml), $NH_2OH$*HCl (23.5 g; 0.34 mol) and $NaHCO_3$ (58.8 g; 0.70 mol) were added portionwise under stirring. The solution was left at r.t for 24 hours.

$Br_2$ solution (24.1 mL; 48 mmol) in $CH_2Cl_2$ (125 mL) was added dropwise at 0°C. The reaction was stirred for 3 h at r.t. then the organic phase was separated and the water phase extracted with $CH_2Cl_2$.

The combined organic layers were dried over $Na_2SO_4$, filtered and concentrated *in vacuo*.

2,2-dibromo-formaldoxime (17.8 g; 8.77 mmol) was crystallized from cold $Et_2O$ as white-green crystals.

**Yield:** 25%

**Solid state:** white-green crystals

Synthesis of (–)-**26** and (+)-**26**

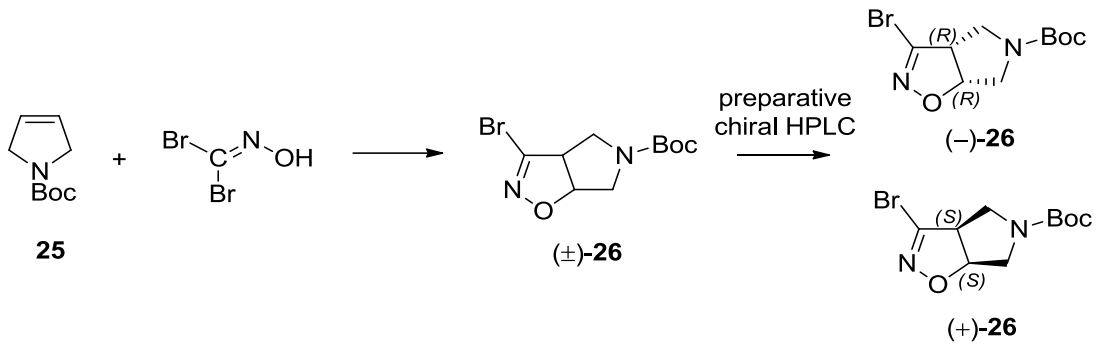


To a solution of **25** (1 g, 5.9 mmol) in EtOAc (20 mL), 2,2-dibromo-formaldoxime (2.4 g; 11.8 mmol) and solid $NaHCO_3$ (5 g; 5.9 mmol) were added. The mixture was vigorously stirred for 3 days. The progress of the reaction was monitored by TLC (Cyclohexane/AcOEt 7:3). Distilled $H_2O$ (10 mL) was added to the reaction mixture, and the organic layer was separated. The aqueous phase was further extracted with EtOAc and the combined organic layers were dried over anhydrous $Na_2SO_4$. The crude material, obtained after evaporation of the solvent, was purified by flash chromatography (Cyclohexane/AcOEt 7:3) and recrystallized from iPrOH to give (±)-**26** (1.7 g, 5.9 mmol). Enantiomeric separation was obtained using a Kromasyl 5-amycoat (21.2 × 250 mm, 5 ìm) and 9/1 n-hexane/iPrOH as eluent mixture at a flow rate of 15 mL/min.

**Yield**: quantitative

**Solid state**: Colourless prism

**$R_f$** (Cyclohexane/EtOAc 7:3): 0.35

**$^1$H-NMR** (300 MHz, $CDCl_3$): 1.43 (s, 9 H), 3.40 (dd, *J*= 8.0, 12.1 , 1H), 3.51 (dd, *J*= 5.8, 13.1, 1 H), 3.80–4.10 (m, 3 H), 5.24 (ddd, *J* = 1.8, 5.8, 9.1, 1 H).

**$^{13}$C NMR** (75 MHz,$CDCl_3$): 28.54, 48.57, 53.96, 57.43, 80.79, 85.01, 139.58, 154.23

**$[M+H]^+$**: 291.14

(−)-**26** = **[α]$^{D}_{20}$** : ( −)100.0 (c: 0.60 in $CHCl_3$)

(+)-**26**= **[α]$^{D}_{20}$** : (+) 101.0 (c: 0.64 in $CHCl_3$)

Synthesis of (–)-**30**

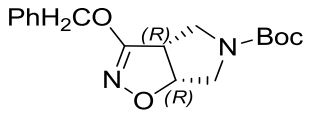


(–)-**30**

To a solution of benzyl alcohol (1.46 mL) in dry THF (50 mL) was added in small portions NaH (60% dispersion in oil, (280 mg; 7.00 mmol), and the mixture was stirred at r.t. under a nitrogen atmosphere for 30 min.

A solution of (–)-**26** (678 mg; 2.33 mmol) in dry THF (3.7 mL) was then added and the mixture was refluxed at 65°C for 3 hours. The progress of the reaction was monitored by TLC (cyclohexane/EtOAc 8:2). The reaction was quenched with 2N HCl and, after evaporation of the solvent, the aqueous layer was extracted with $Et_2O$.

The organic phase was dried over $Na_2SO_4$ and concentrated *in vacuo*.

The residue was then purified by flash chromatography (Cyclohexane/EtOAc 9:1) and recrystallized from $Et_2O$ to give (–)-**30** (697mg; 2.19 mmol).

**Yield**: 94%

**Solid state**: White solid

**$R_f$** (cyclohexane/EtOAc 8:2): 0.28

**M.p**: 152-153°C

**$[\alpha]^D_{20}$** = (–) 90.1 (c : 0.85 in $CHCl_3$)

**$^1$H-NMR** (300 MHz, $CDCl_3$): 1.45 (s, 9H); 3.41 (dd, *J*= 8.3, 11.8, 1H); 3.48-3.62 (m, 1H); 3.75 (d.t, *J*= 2.2, 8.3, 1H); 3.83 (d.d, *J*= 1.9, 13.8, 1H); 3.88 (m, 2H); 5.14 (s, 2H); 5.21 (d.d.d *J*= 1.9, 6.1, 8.3, 1H); 7.40 (s, 5H)

**$[M+H]^+$**: 319.2

Synthesis of (–)-**31**

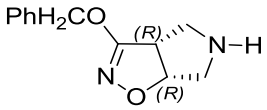


(–)-**31**

A solution of (–)-**30** (697mg; 2.19 mmol) in $CH_2Cl_2$ (7.40 mL; 3.19 mmol) was cooled to 0°C and TFA (2.49 mL; 21.9 mmol) was added.

The resulting mixture was stirred for 1.5 hours at r.t., and the progress of reaction followed by TLC (cyclohexane/EtOAc 8:2).

After evaporation of the solvent, the crude was diluted in EtOAc and washed with a 5% aqueous solution of $NaHCO_3$.The organic layer was dried over anhydrous $Na_2SO_4$.

The crude material, obtained after evaporation of the solvent, was purified by flash chromatography (EtOAc/MeOH 9:1) to give the free amine (–)-**31** (348 mg; 1.59 mmol).

**Yield**: 74%

**Solid state**: Brown Oil

**$R_f$** ($CH_2Cl_2$/MeOH 9:1)**:** 0.22

**$^1$H-NMR** (300 MHz, $CDCl_3$)**:** 2.32 (s, 1H); 2.56 (d.d, *J*= 3.9, 13.8, 1H); 2.58 (d.d, *J*= 7.4, 12.7, 1H); 3.38 (d, *J*= 12.4); 3.42 (d, *J*= 12.7); 3.65 (d.d, *J*=7.7, 7.7, 2H); 5.10 (d, *J*= 11.6, 1H); 5.18 (d, *J*=11.6, 1H); 7.3-7.4 (m, 5H)

Syntesis of (–)-**32**

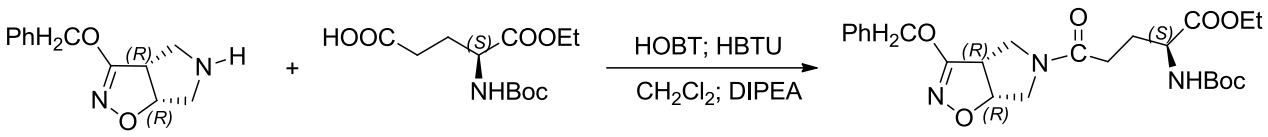


(–)-**31** (+)-**13** (–)-**32**

Compound (+)-**13** (220 mg; 0.80 mmol) was dissolved in $CH_2Cl_2$ (2.0 ml).

HOBt hydrate (216 mg; 1.6 mmol), HBTU (214 mg; 1.6 mmol), DIPEA (238 µl; 1.6 mmol) and a solution of (–)-**31** (160 mg; 0.80 mmol) in $CH_2Cl_2$ (0.5 ml) were added to the flask. Then the reaction was stirred at r.t. for 24 hours.

The progress of the reaction was followed by TLC (Cyclohexane/EtOAc 3:7).

After removal of the solvent, the residue was diluted with EtOAc and the organic phase washed with distilled $H_2O$, dried over $Na_2SO_4$ and concentrated *in vacuo*.

The crude material was purified by flash chromatography (Cyclohexane/EtOAc 3:7) to give 266 mg (0.56 mmol) of (–)-**32**.

**Yield**: 70%

**Solid state**: brown oil

**$R_f$** (Cyclohexane/EtOAc 9:1): 0.3

**M.p**: 137.7-139°C

**$[\alpha]^{20}_D$**: (–) 61.70 (c: 0.5 in $CHCl_3$)

**$^1$H-NMR** (300 MHz, $CDCl_3$): 1.18-1.34 (m, 3H); 1.40-1.52 (m, 9H); 1.84-2.10 (m, 3H); 2.1-2.55 (m, 3H); 3.40-3.73 (m, 2H); 3.74-4.07 (m, 2H); 4.13-4.33 (m, 2H); 3.9-4.1 (m, 3H); 5.10 (d, *J*= 8.5 1H); 5.14 (d, *J*= 8.5 1H); 5.22-5.34 (m, 1H); 7.34-7.42 (m, 5H)

**$^{13}$C-NMR** (75 MHz, $CDCl_3$): 14.39; 27.71; 28.54; 31.01; 47.92; 48.54; 50.10; 53.87; 61.68; 72.84; 80.10; 84.85; 128.62; 128.90; 129.08; 135.30; 155.80; 166.92; 170.93; 172.55

**$[M+H]^+$** : 476.3

Synthesis of (–)-**34**

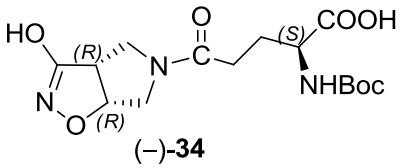


(–)-**34**

1) Derivative (–)-**32** (190 mg; 0.40 mmol) was dissolved in EtOH (1.2 mL) and treated with 1N aqueous NaOH (0.57 mL; 0.57 mmol).The mixture was stirred at r.t. for 1 hour and the disappearance of the starting material was monitored by TLC (Cyclohexane/EtOAc 3:7).

After evaporation of EtOH, the aqueous layer was washed with $Et_2O$, made acidic with 2N aqueous HCl and extracted with EtOAc (3x10 mL). The organic phase was dried over $Na_2SO_4$ and concentrated *in vacuo* to give the acidic intermediate (170 mg, 0.38 mmol).

**Yield**: 95%

**Solid state**: Yellow oil

**R**$_f$ ($CH_2Cl_2$/MeOH 9:1): 0.5

2) the acidic intermediate (170 mg, 0.38 mmol) was dissolved in MeOH (3 ml) and 10% w/w of 5% Pd/C (8 mg) was added. The mixture was stirred at r.t. for 30 minutes under $H_2$ atmosphere and the reaction was followed by TLC ($CH_2Cl_2$/MeOH 9:1 + 1% AcOH).

The mixture was filtered *in vacuo* on a celite pad to eliminate the catalyst to obtain, after removal of the solvent, (–)-**34** (121 mg; 0.34 mmol) was obtained.

**Yield**: 89%

**Solid state**: Yellow oil

**R**$_f$ ($CH_2Cl_2$/MeOH 9:1 + 1% AcOH): 0.25

Synthesis of (–)-**3a**

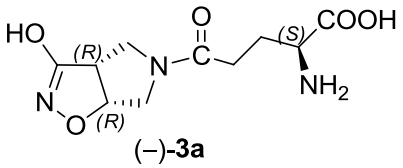


(–)-**3a**

Intermediate (–)-**34** (121 mg; 0.34 mmol) was treated with a 30% trifluoroacetic acid (246 µL; 3.4 mmol) solution in $CH_2Cl_2$ at 0°C. The solution was stirred at r.t. for 3 hours and the reaction was followed by TLC ($CH_2Cl_2$/MeOH 9:1 + 1% AcOH).

The volatiles were removed under reduced pressure and the solid residue was taken up with MeOH, filtered, washed with $Et_2O$ and dried to give (–)-**3a** (82 mg; 0.32 mmol).

**Yield**: 94%

**Solid state:** white solid

**$R_f$** (*n*-butanol/$H_2O$/AcOH 4:2:1): 0.11

**M.p:** dec. T > 60°C

**$[\alpha]^{20}_D$** : (–) 13.97 (c: 0.12 in $H_2O$)

**$^1$H-NMR** (300 MHz, $D_2O$): 2.02-2.14 (m, 2H); 2.38-2.62 (m, 2H) 3.44-3.94 (m, 5H); 5.26-5.38 (m, 1H)

**$^{13}$C-NMR** (75 MHz, $D_2O$): 25.20; 29.95; 46.18; 47.51; 51.88; 52.94; 82.99; 161.80; 172.59; 172.96

**$[M+H]^+$**: 258.1

Synthesis of (+)-**30**

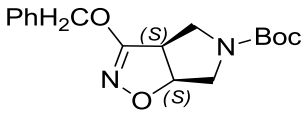


(+)-**30**

Compound (+)-**30** was synthesized following the procedure reported for (–)-**30** starting from (+)-**26** (678 mg; 2.33 mmol).

**Yield**: 94%

**Solid state**: White solid

***R<sub>f</sub>*** (Cyclohexane/EtOAc 8:2): 0.28

**M.p:** 152-153°C

**$[\alpha]^{D}_{20}$** : (+) 90.1 (c : 0.85 in $CHCl_3$)

**$^1$H-NMR** (300 MHz, $CDCl_3$): 1.45 (s, 9H); 3.41 (dd, *J*= 8.3, 11.8, 1H); 3.48-3.62 (m, 1H); 3.75 (d.t, *J*= 2.2, 8.3, 1H); 3.83 (d.d, *J*= 1.9, 13.8, 1H); 3.88 (m, 2H); 5.14 (s, 2H); 5.21 (d.d.d, *J*= 1.9, 6.1, 8.3, 1H); 7.40 (s, 5H)

**$[M+H]^+$:** 319.2

Synthesis of (+)-**31**

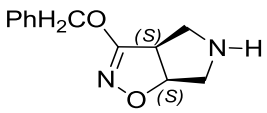


**(+)-31**

Compound (+)-**31** was synthesized following the procedure reported for (−)-**31** starting from (+)-**30** (478 mg; 2.19 mmol).

**Yield**: 74%

**Solid state**: Brown Oil

***R<sub>f</sub>*** ($CH_2Cl_2$/MeOH 9:1): 0.22

**$^1$H-NMR** (300 MHz, $CDCl_3$): 2.32 (s, 1H); 2.56 (d.d, *J*= 3.9, 13.8, 1H); 2.58 (d.d, *J*= 7.4, 12.7, 1H); 3.38 (d, *J*= 12.4, 1H); 3.42 (d, *J*= 12.7, 1H); 3.65 (d.d, *J*=7.7, 7.7, 2H); 5.10 (d, *J*= 11.6, 1H); 5.18 (d, *J*=11.6, 1H); 7.3-7.4 (m, 5H)

Synthesis of (+)-**33**

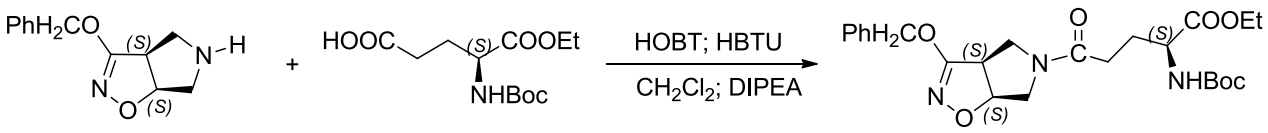


(+)-**31** (+)-**13** (+)-**33**

Compound (+)-**33** was synthesized following the procedure reported for (–)-**32** starting from (+)-**31** (354 mg; 1.62 mmol).

**Yield**: 70%

**Solid state**: White Solid

**R**$_f$ (cyclohexane/EtOAc 9:1): 0.3

**M.p**: 45-47°C

**[α]$^{20}_D$** : (+)83.73 (c: 0.55 in $CHCl_3$)

**$^1$H-NMR** (300 MHz, $CDCl_3$): 1.20-1.32 (m, 3H); 1.41-1.50 (m, 9H); 1.81-2.09 (m, 1H); 2.10-2.42 (m, 3H); 3.40-3.55 (m, 2H); 3.56-4.11 (m, 1H); 4.12-4.35 (m, 3H); 5.09 (d, *J*= 11.8, 1H); 5.14 (d, *J*=11.8 1H), 5.20-5.34 (m, 1H); 7.32-7.42 (m, 5H)

**$^{13}$C-NMR** (75 MHz, $CDCl_3$): 14.41; 27.77; 28.54; 30.78; 47.93; 48.57; 50.10; 53.79; 61.70; 72.82; 80.16; 84.89; 128.60; 128.91; 129.09; 135.30; 155.83; 166.97; 170.85; 172.63

**[M+H]$^+$**: 476.3

Synthesis of (+)-**35**

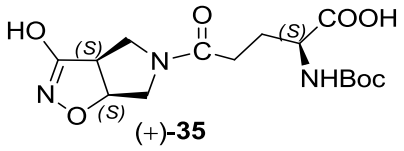


(+)-**35**

1) Derivative (+)-**33** (90 mg; 0.19 mmol) was dissolved in 1:1 mixture EtOH/Dioxane (2.4 mL) and treated with 1N aqueous NaOH (1.14 mL; 1.14 mmol).The mixture was stirred at r.t. for 1.5 hours and the disappearance of the starting material was monitored by TLC (cyclohexane/EtOAc 3:7).

After evaporation of the solvent, the aqueous layer was washed with $Et_2O$, made acidic with 2N aqueous HCl and extracted with EtOAc (3x10 mL). The organic phase was dried over anhydrous $Na_2SO_4$ and concentrated to the acidic intermediate (75 mg; 0.17 mmol).

**Yield**: 90%

**Solid state**: white foam

**$R_f$** ($CH_2Cl_2$/MeOH 9:1): 0.51

2) The acidic intermediate (75 mg; 0.17 mmol) was dissolved in EtOH (3 ml) and 10% w/w of 5% Pd/C (8 mg) was added. The mixture was stirred at r.t. for 30 minutes under $H_2$ atmosphere and the reaction was followed by TLC ($CH_2Cl_2$/MeOH 9:1 + 1% AcOH).

The mixture was filtered *in vacuo* on a celite pad to eliminate the catalyst to obtain, after removal of the solvent, (+)-**35** (60 mg; 0.17 mmol) was obtained.

**Yield**: quantitative

**Solid state**: White foam

**$R_f$** ($CH_2Cl_2$/MeOH 9:1 + 1% AcOH): 0.51

Synthesis of (+)-**3b**

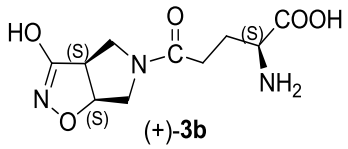

(+)-**3b**

Intermediate (+)-**35** (60 mg; 0.17 mmol) was treated with a 30% trifluoroacetic acid (123 µL; 1.6 mmol) solution in $CH_2Cl_2$at 0°C. The solution was stirred at r.t. for 3 hours and the reaction was followed by TLC ($CH_2Cl_2$/MeOH 9:1 + 1% AcOH).

The volatiles were removed under reduced pressure and the solid residue was taken up with MeOH, filtered, washed with $Et_2O$ and dried to give (+)-**3b** (42 mg, 0.16 mmol).

**Yield**: 94%

**Solid state**: White Solid

**$R_f$** (*n*-butanol/$H_2O$/AcOH 4:2:1): 0.11

**$[\alpha]^{20}_D$**: **(**+) 51.9 (c : 0.14 in $H_2O$)

**M.p**: dec. T > 60°C

**$^1$H-NMR** (300 MHz, $D_2O$): 2.00-2.20 (m, 2H); 2.40-2.52 (m, 2H); 3.40-3.58 (m, 5H); 5.20-5.40 (m, 1H)

**$^{13}$C-NMR** (75 MHz, $D_2O$): 25.20; 29.95; 46.18; 47.37; 51.47; 53.15; 82.35; 163.80; 172.59; 172.96

**$[M+H]^+$** : 258.1

Synthesis of ethyl 2-chloro-2-(hydroxyimino) acetate

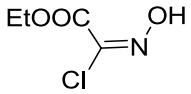


To a solution of glycine ethylester*HCl (69.7 g; 499.4 mmol) in distilled $H_2O$ (95 ml) at −10° C, was added 37% HCl (41 ml; 499.4 mmol). Then, a solution of $NaNO_2$ (34.5 g; 499.4 mmol) in distilled $H_2O$ (50 ml) was added dropwise and the reaction was stirred at −10°C for 5 minutes. Brown fumes were formed and the reaction mixture became light green.

Another portion of 37%*HCl (41 ml; 499.4 mmol) and of the solution of $NaNO_2$ (34.5 g; 499.4 mmol) in distilled $H_2O$ (50 ml) were added at −10 °C, the reaction was stirred −10°C for 10 minutes and at r.t. for 50 minutes. The aqueous phase was extracted with $CH_2Cl_2$, dried over $Na_2SO_4$, and concentrated *in vacuo*. The final product was precipitated from cold $Et_2O$ to give ethyl 2-chloro-2-(hydroxyimino) acetate (18.6 g 122.7 mmol).

**Yield:** 25%

**Solid state:** white solid

**$^1$H-NMR** (300 MHz, $CDCl_3$): 1.34 (s, 9H); 4.36 (q, *J*=7.2, 2H); 9.40 (bs, 1H)

Synthesis of (–)-**36** and (+)-**36**

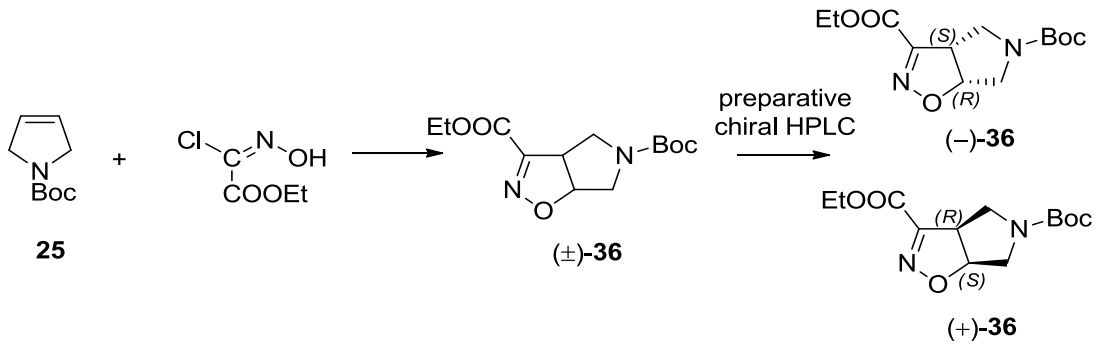


To a solution of **25** (1.0 g, 5.9 mmol) in EtOAc (20 mL) was added ethyl 2-chloro-2-(hydroxyimino)acetate (1.79 g; 11.8 mmol) and solid $NaHCO_3$ (2.0 g; 23.81 mmol). The mixture was vigorously stirred for 5 days. The progress of the reaction was monitored by TLC (cyclohexane/EtOAc 8:2).

Distilled $H_2O$ (10 mL) was added to the reaction mixture, and the organic layer was separated.

The aqueous phase was further extracted with EtOAc, and the combined organic layers were dried over anhydrous $Na_2SO_4$. The crude material, obtained after evaporation of the solvent, was purified by flash chromatography (Cyclohexane/EtOAc 9:1 to 1:1) to give compound (±)-**36** (800 mg; 2.81 mmol). Enantiomeric separation was obtained using a Lux 2-amycoat (21.2 × 250 mm, 5 ìm) and 7/3 n-hexane/iPrOH as eluent mixture at a flow rate of 15 mL/min.

**Yield**: 48%

**Solid state**: Yellow Oil

**$R_f$** (cyclohexane/EtOAc 8:2): 0.17

**$^1$H-NMR** (300 MHz, $CDCl_3$): 1.35 (t, *J*= 7.2, 3 H), 1.42 (s, 9 H), 3.41–3.54 (m, 2 H), 3.79–4.08 (m, 1 H), 3.80–4.10 (m, 2 H), 4.35 (q, *J*= 7.2, 2 H), 5.32 (dd, *J*= 5.4, 9.6, 1 H).

**$[M+H]^+$**: 285.0

(–)-**36**= **$[\alpha]^D_{20}$** : (–) 172.4 (c: 0.76 in $CHCl_3$)

(+)-**36= [α]$^{D}_{20}$** : (+)173.0 (c: 0.74 in $CHCl_3$)

Synthesis (–)-**37**

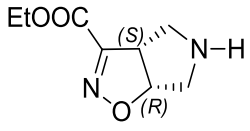


(–)-**37**

A solution of (–)-**36** (500 mg; 1.75 mmol) in $CH_2Cl_2$ (4.1 mL) was cooled to 0°C and TFA (1.35 mL; 17.5 mmol) was added.

The resulting mixture was stirred for 1.5 hours at r.t. and the progress of the reaction followed by TLC (cyclohexane/EtOAc 8:2).

After evaporation of the solvent, the crude was diluted in EtOAc and washed with a 5% aqueous solution of $NaHCO_3$. The organic layer was dried over anhydrous $Na_2SO_4$.

The crude material, obtained after evaporation of the solvent, was purified by flash chromatography on silica gel (EtOAc/MeOH 9:1) to give (–)-**37** (168 mg; 0.91 mmol).

**Yield**: 52%

**Solid state**: Yellow oil

**$R_f$** (EtOAc/MeOH 9:1): 0.2

**$^1$H-NMR** (300 MHz, $CDCl_3$): 1.37 (t, *J*= 7.2, 3H); 1.70 (s, 1H); 2.84 (d.d, *J*= 3.0*;* 13.8; 1H); 2.98 (d.d, *J*= 7.4; 12.9; 1H); 3.38 (d, *J*= 12.9; 1H); 3.48 (d, *J*= 13.8; 1H); 3.98 (d.d, $J_1$= 8.3; 8.3, 1H); 4.36 (d.q, *J*= 1.1, 7.2; 2H); 5.38 (d.d, *J*= 3.0; 8.3; 1H)

Synthesis of (-)-**38**

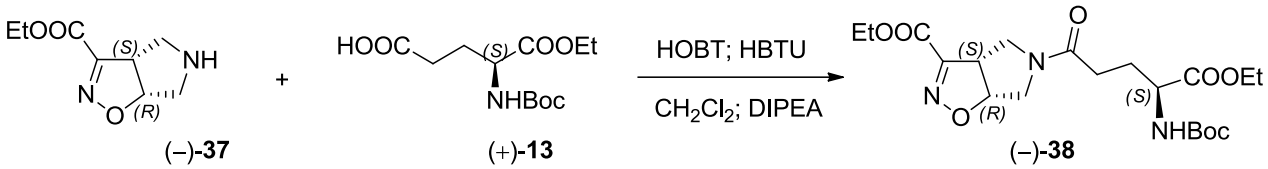


Compound (+)-**13** (168 mg; 0.91 mmol) was dissolved in $CH_2Cl_2$ (2.5 ml).

HOBt hydrate (246 mg; 1.82mmol), HBTU (242 mg; 1.82 mmol), DIPEA (317 ìL; 1.82 mmol) and a solution of (–)-**37** (168 mg; 0.91 mmol) in $CH_2Cl_2$ (0.5 mL) were added to the flask.

Then the reaction was stirred at r.t. for 24 hours. The progress of the reaction was followed by TLC (Cyclohexane/EtOAc 3:7).

After removal of the solvent, the residue was diluted with EtOAc and the organic phase washed with distilled $H_2O$, dried over $Na_2SO_4$ and concentrated *in vacuo*.

The crude material was purified by flash chromatography (Cyclohexane/EtOAc 3:7) to give 261 mg (0.59 mmol) of (–)-**38**.

**Yield**: 65%

**Solid state**: Pale yellow oil

**$R_f$** (Cyclohexane/EtOAc 3:7): 0.3

**$[\alpha]^{20}_D$** : (–) 131.91 (c: 0.1 in $CHCl_3$)

**$^1$H-NMR** (300 MHz, $CD_3OD$)**:** 1.24-1.30 (t, *J*= 7.15, 3H); 1.30-1.38 (m, 3H); 1.43 (s, 9H); 1.78-1.96 (m, 1H); 2.0-2.16 (m, 1H); 2.3-2.56 (m, 2H); 3.44-3.62 (m, 1H); 3.68-3.80 (m, 1H) 3.84-4.40 (m, 1H); 4.02-4.24 (m, 5H); 4.26-4.38 (m, 2H); 5.37-5.50 (m, 1H)

**$^{13}$C-NMR** (75 MHz, $CD_3OD$): 13.22; 13.38; 26.514; 27.57; 49.69; 49.82; 51.31; 52.56; 53.53; 61.14; 62.04; 79.46; 87.48; 152.80; 156.89; 160.31; 171.93; 172.79

**$[M+H]^+$** : 442.4

Synthesis of (–)-**4a**

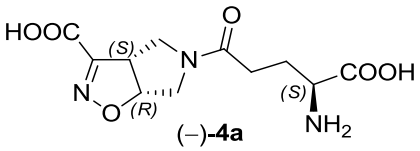


(–)-**4a**

1) Derivative (–)-**38** (136 mg; 0.31 mmol) was dissolved in EtOH (1.0 mL) and treated with 0.5N aqueous NaOH (1.00 mL; 0.47 mmol). The mixture was stirred at r.t. for 1.5 hours and the disappearance of the starting material was monitored by TLC (Cyclohexane/EtOAc 2:8). After evaporation of the solvent, the aqueous layer was washed with $Et_2O$, made acidic with 2N aqueous HCl and extracted with EtOAc (3x10 mL). The organic phase was dried over anhydrous $Na_2SO_4$ and concentrated to give the diacidic intermediate (119 mg; 0.31 mmol).

**Yield**: quantitative

**Solid state**: White foam

**$R_f$** ($CH_2Cl_2$/MeOH 7:3): 0.2

2) The diacidic Intermediate (119 mg; 0.31 mmol) was treated with a 30% trifluoroacetic acid (488 µL; 3.20 mmol) solution in $CH_2Cl_2$ at 0°C. The solution was stirred at r.t. for 3 hours.
The volatiles were removed under reduced pressure and the solid residue was taken up with MeOH, filtered, washed with $Et_2O$ and dried to give (–)-**4a** (78 mg; 0.27 mmol).

**Yield**: 88%

**Solid state**: White solid

**$R_f$** (*n*-butanol/$H_2O$/AcOH 4:2:1): 0.1

**$[\alpha]^{20}_D$**: (–) 100.8 (c : 0.1 in $H_2O$)

**M.p:** dec. T > 80°C

**$^{1}$H-NMR** (300 MHz, $D_2O$): 1.94-2.12 (m, 2H); 2.34-2.60 (m, 2H); 3.36-3.52 (m, 1H); 3.60-3.74 (m, 1H); 3.78-4.0 (m, 3H); 4.04-4.20 (m, 1H); 5.30-5.46 (m, 1H)

**$^{13}$C-NMR** (75 MHz, $D_2O$): 25.25; 30.03; 49.40; 50.91; 53.35; 87.05; 156.20; 164.04; 172.41; 172.69

**$[M+H]^+$**: 286.0

Synthesis of (+)-**37**

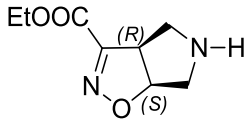


(+)-**37**

Compound (+)-**37** was synthesized following the procedure reported for (–)-**37** starting from (+)-**36** (805 mg, 2.83 mmol).

**Yield**: 52%

**Solid state**: Yellow oil

**$R_f$** (EtOAc/MeOH 9:1): 0.2

**$^1$H-NMR** (300 MHz, $CDCl_3$): 1.37 (t, *J*= 7.2, 3H); 1.70 (s, 1H); 2.84 (d.d, *J*= 3.0*;* 13.8; 1H); 2.98 (d.d, *J*= 7.4; 12.9; 1H); 3.38 (d, *J*= 12.9; 1H); 3.48 (d, *J*= 13.8; 1H); 3.98 (d.d, *J*= 8.3; 8.3; 1H); 4.36 (d.q, *J*= 1.1, 7.2; 2H); 5.38 (d.d, *J*= 3.0; 8.3; 1H)

Synthesis of (+)-**39**

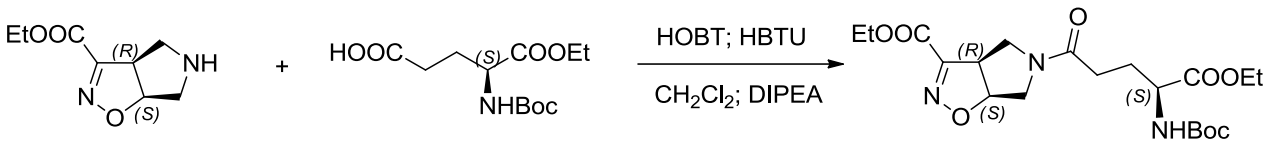


(+)-**37** (+)-**13** (+)-**39**

Compound (+)-**39** was synthesized following the procedure reported for (–)-**38**starting from (+)-**37** (271 mg, 1.47 mmol).

**Yield**: 60%

**Solid State**: Pale Yellow oil

**$R_f$**(Cyclohexane/EtOAc 3:7): 0.3

**$[\alpha]^{20}_D$** :(+) 120.46 (c: 0.1 in $CHCl_3$)

**$^1$H-NMR** (300 MHz, $CD_3OD$): 1.26-1.3 (t, *J*=7.2, 3H); 1.30-1.38 (m, 3H); 1.42 (s, 9H); 1.80-1.96 (m, 1H ); 2.0-2.18 (m, 1H); 2.30-2.54 (m, 2H ); 3.42-3.62 (m, 1H ); 3.68-3.80 (m, 1H ); 3.84-4.26 (m, 6H); 4.26-4.40 (m, 2H) 5.38-3.50 (m, 1H); 6.90-7.40 (m, 1H)

**$^{13}$C-NMR** (75 MHz, $CD_3OD$): 13.19; 13.34; 26.53; 27.53; 49.71; 49.83; 51.28; 52.51; 53.57; 61.141; 62.03; 79.46; 86.48; 152.81; 156.94; 160.30; 171.97; 172.81

**$[M+H]^+$** : 442.4

Synthesis of (+)-**4b**

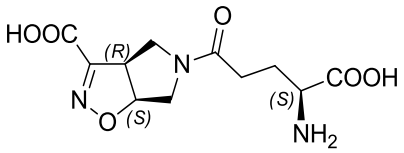


(+)-**4b**

1) Derivative (+)-**39** (65 mg; 0.15 mmol) was dissolved in EtOH (1.0 mL) and treated with 0.5N aqueous NaOH (1.00 mL; 0.47 mmol).

The mixture was stirred at r.t. for 1.5 hours and the disappearance of the starting material was monitored by TLC (Cyclohexane/EtOAc 2:8).

After evaporation of the solvent, the aqueous layer was washed with $Et_2O$, made acidic with 2N aqueous HCl and extracted with EtOAc (3x10 mL).

The organic phase was dried over anhydrous $Na_2SO_4$ and concentrated to give the diacidic intermediate (58 mg, 0.15 mmol).

**Yield**: quantitative

**Solid state**: White foam

**$R_f$** ($CH_2Cl_2$/MeOH 7:3): 0.17

2) The diacidic intermediate (58 mg; 0.15 mmol) was treated with a 30% trifluoroacetic acid (244 µL; 1.60 mmol) solution in $CH_2Cl_2$ at 0°C. The solution was stirred at r.t.for 3 hours.

The volatiles were removed *in vacuo* and the solid residue was taken up with MeOH, filtered, washed with $Et_2O$ and dried to give (+)-**4b** (35 mg; 0.15 mmol).

**Yield**: 82%

**Solid state**: White solid

**$R_f$** (*n*-butanol/$H_2O$/AcOH 4:2:1): 0.1

**M.p**: dec. T > 80°C

**$[\alpha]^{20}_D$** : **(**+) 125.7 (c: 0.1 in $H_2O$)

**$^1$H-NMR** (300 MHz, $D_2O$): 1.94 2.12 (m, 2H); 2.34-2.62 (m, 2H); 3.37-3.52 (m, 1H); 3.62-3.74 (m, 1H); 3.78-4.00 (m, 3H); 4.04-4.20 (m, 1H); 5.28-5.44 (m, 1H)

**$^{13}$C-NMR** (75 MHz, $D_2O$)**:** 25.25; 30.03; 49.40; 50.91; 53.35; 87.05; 156.20; 164.04; 172.41; 172.69

**$[M+H]^+$**: 286.0

Synthesis of **45**

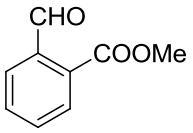


**45**

To a solution of 2-formylbenzoic acid (1.0 g, 6.67 mmol) in dry DMF (6.2 ml), $K_2CO_3$ (1.70 g, 12.30 mmol) and $CH_3I$ (0.8 ml, 12.40 mmol) were added. The esterification was performed as a microwave-assisted reaction (Settings: 100°C, 15 bar, 200W, 2 hours). The reaction was followed by TLC ($CH_2Cl_2$/MeOH 9:1 + 1% AcOH). The resulting mixture was diluted with $CH_2Cl_2$ and then washed with distilled $H_2O$, 1N HCl and brine. The organic phase was dried with $Na_2SO_4$, filtered and concentrated in vacuo. The crude material obtained after evaporation of the solvent was purified by column chromatography on silica gel (Cyclohexane/EtOAc 9:1) to give the title compound **45** (720 mg, 4.39 mmol) as a yellowish oil.

**Yield**: 66%

**Solid state**: yellowish oil

$\mathbf{R}_f$ (cyclohexane/EtOAc 9:1): 0.38

$^{1}$**H-NMR** (300 MHz, $CDCl_3$): 3.95 (s, 3H); 7.62-7.65 (m, 2H); 7.90-7.97 (m, 2H); 10.59 (s, 1H).

$^{13}$**C-NMR** (75 MHz, $CDCl_3$): 52.9; 128.5; 130.5; 132.5; 133.1; 134.5; 137.1; 166.9; 192.3

Synthesis of **47**

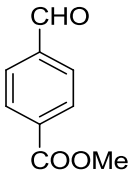


**47**

A solution of 4-formylbenzoic acid (1.0 g, 6.66 mmol) in dry MeOH (20 ml) was cooled to 0°C. $CH_3COCl$ (2.4 ml, 33.33 mmol) was slowly added in nitrogen atmosphere. The resulting mixture was stirred at r.t. for 24 hours and the reaction was followed by TLC ($CH_2Cl_2$/MeOH 9:1 + 1% AcOH). MeOH was evaporated and the mixture was diluted with EtOAc and then washed with 1N NaOH and brine. The organic phase was dried with $Na_2SO_4$, filtered and concentrated *in vacuo* to give the title compound **47** (960 mg, 5.92 mmol) as a yellowish solid, which was used in the next step without further purification.

**Yield**: 88%

**Solid state**: yellow solid

**$R_f$** (cyclohexane/EtOAc 8:2): 0.45

**$^1$H-NMR** (300 MHz, $CDCl_3$): 3.95 (s, 3H); 7.90 (d, *J* = 8.4, 2H); 8.07 (d, *J* = 8.4, 2H); 10.10 (s, 1H).

**$^{13}$C-NMR** (75 MHz, $CDCl_3$): 52.78; 129.71; 130.38; 135.26; 139.34; 166.24; 191.86.

Synthesis of **48**

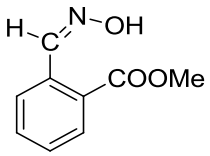


**48**

To a suspension of **45** (720 mg, 4.39 mmol) and hydroxylamine hydrochloride (317 mg, 4.57 mmol) in a 1:1 mixture of $H_2O$/methanol (40 mL), an aqueous solution of $Na_2CO_3$ (256 mg, 2.41 mmol, 12 mL) was slowly added. The resulting mixture was stirred at r.t. for 3 hours and methanol was evaporated. The aqueous phase was extracted with $Et_2O$ (3 x 10 mL). The combined organic phases were washed with brine, dried over $Na_2SO_4$, filtered and concentrated in vacuo to give the title compound **48** (750 mg, 4.19 mmol) as a white solid, which was used in the next step without further purification.

**Yield**: 95%

**Solid state**: white solid

**$R_f$** (cyclohexane/EtOAc 8:2): 0.35

**$^1$H-NMR** (300 MHz, $CDCl_3$): 3.95 (s, 3H); 7.50 (m, 2H); 7.85 (d, *J* = 7.6, 1H); 8.00 (d, *J* = 7.6, 1H); 8.95 (s, 1H).

**$^{13}$C-NMR**(75 MHz, $CDCl_3$): 52.70; 127.73; 129.44; 129.76; 130.96; 132.64; 133.13; 150.13; 167.30.

Synthesis of **49**

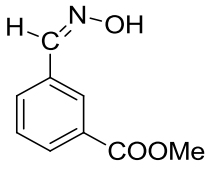


**49**

To a suspension of metyl 3-formylbenzoate **46** (1.0 g, 6.12 mmol) and hydroxylamine hydrochloride (441 mg, 6.36 mmol) in a 1:1 mixture of $H_2O$/methanol (55 mL), an aqueous solution of $Na_2CO_3$ (369 mg, 3.51 mmol, 20 mL) was slowly added. The resulting mixture was stirred at room temperature for 3 hours and methanol was evaporated. The aqueous phase was extracted with $Et_2O$ (3 x 10 mL). The combined organic phases were washed with brine, dried over $Na_2SO_4$, filtered and concentrated in vacuo to give the title compounds **49** (1.10 g, 6.12 mmol) as a white solid, which were used in the next step without further purification.

**Yield**: quantitative

**Solid state**: white solid

**$R_f$** (cycloexane/EtOAc 7:3): 0.47

**$^1$H-NMR** (300 MHz, $CDCl_3$): 3.95 (s, 3H); 7.50 (t, *J* = 7.7, 1H); 7.80 (d, *J* = 7.7, 1H); 8.05 (d, *J* = 7.7, 1H); 8.20 (d, *J* = 5.2, 1H); 8.60 (s, 1H).

**$^{13}$C-NMR** (75 MHz, $CDCl_3$): 52.62; 128.69; 129.16; 130.98; 131.06; 131.18; 132.68; 149.62; 166.88.

Synthesis of **50**

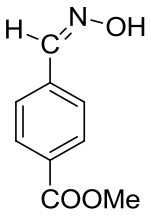


**50**

To a suspension of **47** (825 mg, 5.03 mmol) and hydroxylamine hydrochloride (338 mg, 5.23 mmol) in a 1:1 mixture of $H_2O$/methanol (45 mL), an aqueous solution of $Na_2CO_3$ (293 mg, 2.76 mmol, 15 mL) was slowly added. The resulting mixture was stirred at r.t for 3 hours and methanol was evaporated. The aqueous phase was extracted with $Et_2O$ (3 x 10 mL). The combined organic phases were washed with brine, dried over $Na_2SO_4$, filtered and concentrated in vacuo to give the title compound **50** (800 mg, 4.47 mmol) as a white solid, which was used in the next step without further purification.

**Yield**: 89%

**Solid state**: white solid

**$R_f$** (cycloexane/EtOAc 7:3): 0.50

**$^1$H-NMR** (300 MHz, $CDCl_3$): 3.95 (s, 3H); 7.65 (d, *J* = 8.2, 2H); 8.07 (d, *J* = 8.5, 2H); 8.20 (s, 1H).

**$^{13}$C-NMR** (75 MHz, $CDCl_3$): 52.53; 127.13; 130.22; 131.14; 136.51; 149.77; 166.81.

Synthesis of **41**

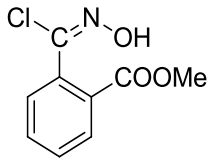


**41**

To a solution of the proper aldoxime **48** (750 mg, 4.19 mmol) in $CHCl_3$ (6 mL), pyridine (34 µL, 0.42 mmol) was added. The reaction mixture was heated at 40°C and *N*-Chlorosuccinimide (615 mg, 4.60 mmol) was added portionwise. After the reaction was complete (4 hours on reflux, monitored by TLC), the mixture was diluted with $CH_2Cl_2$ (10 mL) and washed with brine (3 x 10 mL). The organic phase was dried over $Na_2SO_4$, filtered and concentrated in vacuo to give the title compound **41** (890 mg, 4.17 mmol) as a yellowish oil, which was used in the cycloaddition step without further purification.

**Yield**: quantitative

**Solid state**: yellow oil

**R**$_f$ (cycloexane/EtOAc 7:3): 0.60

**$^1$H-NMR** (300 MHz, $CDCl_3$): 3.95 (s, 3H); 7.45-7.60 (m, 3H); 7.85 (dd, *J*= 1.7, 8.0, 1H); 9.20 (s, 1H).

**$^{13}$C-NMR** (75 MHz, $CDCl_3$): 52.95; 130.28; 130.32; 130.44; 130.93; 132.04; 134.01; 138.11; 167.78.

Synthesis of **42**

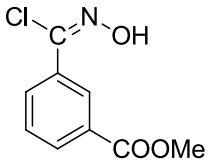


**42**

To a solution of the aldoxime **49** (1.1 g, 6.12 mmol) in $CHCl_3$ (9 mL), pyridine (49 µL, 0.61 mmol) was added. The reaction mixture was heated at 40°C and *N*-Chlorosuccinimide (896 mg, 6.71 mmol) was added portionwise. After the reaction was complete (3 hours on reflux, monitored by TLC), the mixture was diluted with $CH_2Cl_2$ (10 mL) and washed with brine (3 x 10 mL). The organic phase was dried over $Na_2SO_4$, filtered and concentrated in vacuo to give the title compound **42** (1.2 g, 5.61 mmol) as a white solid, which was used in the cycloaddition step without further purification.

**Yield**: 94%

Crystallized from EtOAc/n-hexane as a white crystals

**R**$_f$ (cycloexane/EtOAc 7:3): 0.64

**M.p.**: 106-108 °C.

**$^1$H-NMR** (300 MHz, $CDCl_3$): 3.95 (s, 3H); 7.48 (ddd, *J*= 0.5, 7.9, 7.9, 1H); 8.05 (ddd, *J*= 1.1, 1.9,7.9, 1H); 8.10 (ddd, *J*= 1.1, 1.6, 7.9, 1H); 8.5 (ddd, *J*= 0.5, 1.9, 1.9, 1H); 9.20 (s, 1H).

**$^{13}$C-NMR** (75 MHz, $CDCl_3$): 52.79; 128.58; 128.93; 130.69; 131.57; 131.78; 133.27; 138.92; 166.94.

Synthesis of **43**

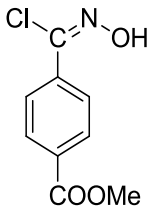


**43**

To a solution of the aldoxime **50** (910 m g, 5.08 mmol) in $CHCl_3$ (7.5 mL), pyridine (41 µL, 0.50 mmol) was added. The reaction mixture was heated at 40°C and *N*-Chlorosuccinimide (746 mg, 5.59 mmol) was added portionwise. After the reaction was complete (3 hours on reflux, monitored by TLC), the mixture was diluted with $CH_2Cl_2$ (10 mL) and washed with brine (3 x 10 mL). The organic phase was dried over $Na_2SO_4$, filtered and concentrated in vacuo to give the title compound **43** (1.0 g, 4.68 mmol) as a white solid, which was used in the cycloaddition step without further purification.

**Yield**: 92%

Crystallized from EtOAc/n-hexane as a white crystals

**$R_f$** (cycloexane/EtOAc 7:3): 0.58

**M.p.**: 138-140 °C.

**$^1$H-NMR** (300 MHz, $CDCl_3$): 3.95 (s, 3H); 7.90 (ddd, *J*= 1.7, 1.9, 8.8, 2H); 8.07 (ddd, *J*= 1.9 1.9, 8.8, 2H); 8.80 (s, 1H).

**$^{13}$C-NMR** (75 MHz, $CDCl_3$): 52.73; 127.39; 129.94; 131.98; 136.80; 139.18; 166.85.

Synthesis of **44a**


**41** **40** **44a**

To a solution of alkene **40** (500 mg, 2.2 mmol) in EtOAc (10 mL) was added **41** (470 mg, 2.2 mmol) and solid $NaHCO_3$ (924 mg, 11.0 mmol). The mixture was vigorously stirred overnight, then other 0.3 equivalents (141.0 mg, 0.7 mmol) of chlorooxime and $NaHCO_3$ (55 mg, 0.7 mmol) were added. $NaHCO_3$ was removed by filtration and the crude material, obtained after evaporation of the solvent, was purified by column chromatography on silica gel (Cyclohexane/EtOAc 85:15) to give **44a** (890 mg, 2.2 mmol) as a mixture of diasteroisomers.

**Yied**: quantitative

**Solid state**: pale yellow oil

$\mathbf{R}_f$ (cyclohexane/EtOAc 8:2): 0.30

Synthesis of (α*R*,5*S*)-**51a** and (α*R*,5*R*)-**52a**

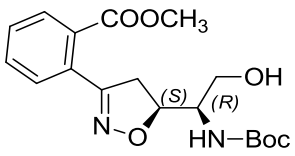


(α*R*, 5*S*)-**51a**

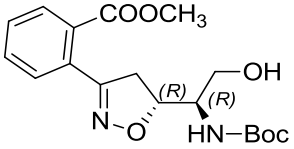


(α*R*, 5*R*)-**52a**

**44a** (890 mg, 2.2 mmol) was treated with a 1/5 mixture of distilled $H_2O$ /AcOH at r.t. After 72 hours the azeotrope $H_2O$ /AcOH was evaporated under reduced pressure and the crude was purified by flash chromatography using cyclohexane/EtOAc (6:4 to 1:1 gradient) as eluent to isolate the diasteroisomers (α*R*, 5*S*)-**51a** and (α*R*, 5*R*)-**52a**.

**Yield**: 65%

(α*R*, 5*S*)-**51a:** (340 mg)

**Solid state**: colourless oil

**R**$_f$ (cyclohexane/ EtOAc 7:3): 0.20

**[α]**$^{20}_{D}$: (+) 65.23 (c: 1.0 in $CHCl_3$)

**$^1$H-NMR** (300 MHz, $CDCl_3$): 1.44 (s, 3H); 3.35 (dd, *J*= 7.9, 17.0, 1H); 3.45 (dd, *J*= 10.4, 17.0, 1H); 3.81 (dd, *J*= 4.1, 10.9, 1H); 3.91 (s, 3H); 3.96-4.04 (m, 1H); 4.10 (d, *J*= 7.2, 1H); 4.88-5.0 (m, 1H); 5.33 (d, *J*=6.7, 1H); 7.41-7.48 (m, 1H); 7.51 (ddd, *J*= 1.6, 8.7, 16.2, 1H); 7.58 (dd, *J*= 1.6, 7.6, 1H); 7.92 (dd, *J*= 1.2, 7.6, 1H);

**$^{13}$C-NMR** (75 MHz, $CDCl_3$): 28.57, 41.38, 52.86, 54.73, 62.15, 80.16, 81.34, 129.90, 129.93, 130.40, 130.52, 130.87, 132.40, 156.36, 158.79, 167.52

**[M+H]$^+$**: 365.1

(α*R*, 5*R*)-**52a:** (185 mg)

**Solid state**: colourless oil

**R**$_f$ (cyclohexane/ EtOAc 7:3): 0.10

**[α]**$^{20}_{D}$: (–)78.09 (c: 0.98 in $CHCl_3$)

**$^1$H-NMR** (75 MHz, $CDCl_3$): 1.44 (s, 9H); 3.24 (dd, *J*= 8.3, 16.9, 1H); 3.49 (dd, *J*= 10.7, 16.9, 1H); 3.79 (dd, *J*= 7.2, 12.8, 1H); 3.87 (d, *J*= 4.6, 1H); 3.90 (s, 3H); 4.99-5.09 (m, 1H); 5.18 (d ,*J*=6.7, 1H); 7.42 (dd, *J*= 1.1,7.5, 1H); 7.51 (ddd, *J*= 1.8, 5.0, 12.7, 1H); 7.58 (dd, *J*= 1.8, 7.5, 1H); 7.90 (dd, *J*= 1.8, 7.5, 1H);

**$^{13}$C-NMR** (75 MHz, $CDCl_3$): 28.53, 41.07, 52.78, 54.30, 60.64, 63.99, 80.23, 81.48, 129.69, 129.95, 130.47, 130.57, 130.85, 132.19

**[M+H]$^+$**: 365.1

Synthesis of (α*S*, 5*S*)-**53a**

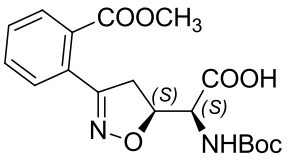


(α*S*, 5*S*)-**53a**

Pyridinium dichromate (5.19 g, 14.0 mmol) was added to a solution of (α*R*, 5*S*)-**51a** (340 mg, 0.93 mmol) in DMF (5.2 ml) and the reaction was stirred for 6 hours at r.t.

The reaction mixture was poured in distilled $H_2O$ and extracted with EtOAc. The organic phase was dried over $Na_2SO_4$ and concentrated in vacuo to give (α*S*, 5*S*)-**53a** (416 mg, 1.1 mmol) as a brow oil.

**Yield**: quantitative

**Solid state**: brown oil

**R**$_f$ ($CH_2Cl_2$/MeOH 9:1 + 1% AcOH): 0.5

Synthesis of **5a**

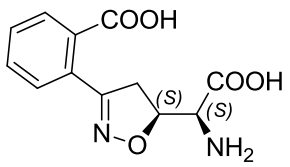


(α*S*, 5*S*)-**5a**

1) Derivative (α*S*, 5*S*)-**53a** (352 mg, 0.93 mmol) was treated with 0.5 N aqueous NaOH (9.3 mL).The mixture was stirred at r.t. for 2 hours and the disappearance of the starting material was monitored by TLC ($CH_2Cl_2$/MeOH 9:1+ 1% AcOH).The reaction mixture was washed with $Et_2O$, made acidic with 1N aqueous HCl and extracted with EtOAc. The organic phase was dried over anhydrous $Na_2SO4$ and after evaporation of the solvent the diacidic derivate (300 mg, 0.82 mmol) was obtained as a white solid.

2) The diacidic derivate (300 mg, 0.82 mmol) was treated with a 30% $CH_2Cl_2$ solution of trifluoroacetc acid (3.7 ml) at 0°C. The solution was stirred at r.t. for 3 hours until completion by TLC ($CH_2Cl_2$/MeOH 9:1 + 1% AcOH).
The volatiles were removed under reduced pressure. The residue was precipitated from MeOH/$Et_2O$ to give (α*S*, 5*S*)-**5a** (87 mg, 0.33 mmol) as a white solid

**Yield**: 64% (yield after two steps)

**Solid state**: white solid

**R**$_f$ (*n*-butanol/$H_2O$/AcOH 4:2:1): 0.44

**M.p.**: dec. T > 140 °C

**$^1$H-NMR** (300 MHz, $D_2O$): 3.41 (dd, *J*= 7.3, 18.1, 1H); 3.57 (dd, *J*= 11.2, 18.1, 1H); 4.09 (d, *J*= 3.7, 1H); 5.22 (ddd, *J*= 3.7, 7.3, 11.2, 1H); 7.38 (d, *J*= 7.4, 1H); 7.44-7.58 (m, 2H); 7.76 (d, *J*= 7.1, 1H);

**$^{13}$C-NMR** (75 MHz, $D_2O$): 39.24, 56.30, 78.84, 127.66, 129.56, 129.79, 130.77, 131.91, 132.15, 160.64,

170.07, 172.24

**[M+H]$^+$**: 265.0

Synthesis of (α*S*,5*R*)-**54a**

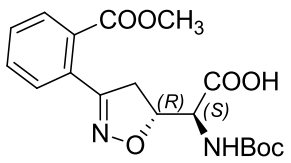


(α*S*, 5*R*)-**54a**

Compound (α*S*, 5*R*)-**54a** was synthesized following the procedure reported for **53a** starting from intermediate (α*R*, 5*R*)-**52a** (185 mg, 0.51 mmol).

**Yield**: quantitative

**Solid state**: brown oil

**R**$_f$ ($CH_2Cl_2$/MeOH 9:1 + 1% AcOH): 0.6

Synthesis of **6a**

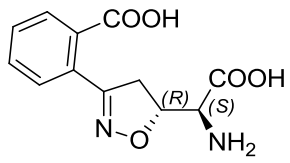


(α*S*, 5*R*)-**6a**

Compound (α*S*, 5*R*)-**6a** was synthesized following the procedure reported for **5a** starting from intermediate (α*S*, 5*R*)-**54a** (193 mg, 0.51 mmol). The final amino acid was precipitated from iPrOH/$Et_2O$.

**Yield**: 73% (yield after two steps)

**Solid state**: white solid

**$R_f$** (*n*-butanol/$H_2O$/AcOH 4:2:1): 0.5

**M.p.**: dec. T > 130 °C

**$^1$H-NMR** (300 MHz, $D_2O$): 3.52 (dd, *J*= 7.0, 18.2,1H); 3.62 (dd, *J*= 10.4, 18.2, 1H); 3.91 (d, *J*=7.3, 1H); 5.07 (ddd, *J*= 7.0, 7.3, 10.4, 1H); 7.39 (d, *J*= 7.1, 1H); 7.45-7.59 (m, 2H); 7.79 (d, *J*= 7.1, 1H);

**$^{13}$C-NMR** (75 MHz, $D_2O$): 41.74, 56.65, 78.74, 127.96, 129.58, 130.08, 130.78, 131.28, 132.44, 160.95, 170.54, 171.65

**[M+H]$^+$**: 265.0

Synthesis of **44b**


**42** **40** **44b**

To a solution of alkene **40** (500 mg, 2.20 mmol) in EtOAc (10 mL) was added **42** (924 mg, 11 mmol) and solid $NaHCO_3$ (916 mg, 11 mmol). The mixture was vigorously stirred overnight, then other 0.3 equivalents (141.0 mg, 0.66 mmol) of chlorooxime and $NaHCO_3$ (55 mg, 0.66 mmol) were added. $NaHCO_3$ was removed by filtration and the crude material,l obtained after evaporation of the solvent was purified by column chromatography on silica gel (Cyclohexane/EtOAc 85:15) to give **44b** (540 mg, 1.34 mmol) as a mixture of diasteroisomers.

**Yied**: 61%

**Solid state**: pale yellow oil

$\mathbf{R}_f$ (cyclohexane/EtOAc 8:2): 0.34

Synthesis of (α*R*,5*S*)-**51b** and (α*R*,5*R*)-**52b**

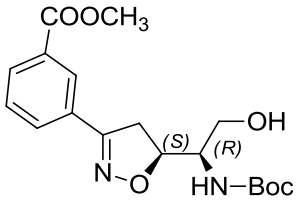


(α*R*, 5*S*)-**51b**

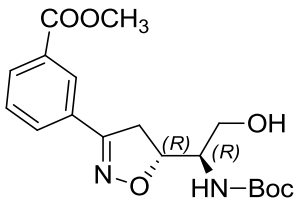


(α*R*, 5*R*)-**52b**

**44b** (1.0 g, 2.47 mmol) was reacted with a 1/5 mixture of distilled $H_2O$ /AcOH at room temperature. After 72 hours the azeotrope $H_2O$ /AcOH was evaporated under reduced pressure and the crude was purified by flash chromatography using cyclohexane/EtOAc (6:4 to 1:1 gradient) as eluent to isolate the diasteroisomers (α*R*, 5*S*)-**51b** and (α*R*, 5*S*)-**52b**.

**Yield**: 69%

(α*R*, 5*S*)-**51b**: (400 mg)

Crystallized from n-hexane/iPrOH as needle crystals

**$R_f$** cyclohexane/ EtOAc 6:4): 0.21 (

**$[\alpha]^{20}_D$**: (+) 105.7 (c: 0.5 in $CHCl_3$)

**M.p.**: 139-142 °C

**$^1$H-NMR** (300 MHz, $CDCl_3$): 1.42 (s, 9H); 3.42 (dd, *J*= 8.0, 17.1, 1H)); 3.48 (dd, *J*= 9.9, 17.1, 1H); 3.76 (d, *J*=8.5, 2H) 3.94 (s, 3H); 3.95-4.3 (m, 1H) 4.9 (ddd, *J*= 8.0, 9.9, 17.1, 1H); 5.18 (d, *J*=6.7, 1H); 7.49 (dd, *J*=7.7,7.7, 1H); 7.93 (d, *J*= 8.0, 1H); 8.18 (d, *J*= 8.0, 1H); 8.24 (s, 1H);

**$^{13}$C-NMR** (75 MHz, $CDCl_3$): 28.54, 38.03, 52.57, 54.61, 61.78, 80.36, 80.94, 128.19, 129.15, 129.85, 130.92, 131.11, 131.44, 156.34, 156.85, 166.66

**$[M+H]^+$**: 365.2

(α*R*, 5*R*)-**52b*:*** (223 mg)

**Solid state**: waxy rosed solid

**R**$_f$ (cyclohexane/ EtOAc 6:4): 0.15

**[α]$^{20}_D$**: (–) 130.1 (c: 0.5 in $CHCl_3$)

**$^1$H-NMR** (300 MHz, $CDCl_3$): ): 1.45 (s, 9H); 3.41 (dd, *J*= 7.9, 17.0, 1H)); 3.48 (dd, *J*= 9.9, 17.0, 1H); 3.77 (d, *J*=8.5, 2H) 3.93 (s, 3H); 3.95-4.03 (m, 1H) 4.89 (ddd, *J*= 7.9, 9.9, 17.0, 1H); 5.17 (d, *J*=6.7, 1H); 7.49 (dd, *J*=8.0,8.0, 1H); 7.93 (d, *J*= 7.9, 1H); 8.09 (d, *J*= 7.9, 1H); 8.24 (s, 1H);

**$^{13}$C-NMR** (75 MHz, $CDCl_3$): 28.37, 37.83, 52.57, 54.68, 63.44, 80.27, 81.16, 128.12, 129.14, 129.75, 130.96, 131.02, 131.46, 156.85, 157.12, 166.57

**[M+H]$^+$**: 365.2

Synthesis of (α*S*,5*S*)-**53b**

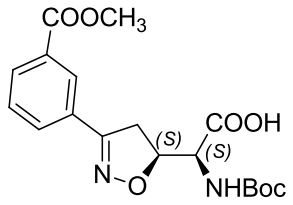


(α*S*, 5*S*)-**53b**

Pyridinium dichromate (4.09 g, 11 mmol) was added to a solution of (α*R*, 5*S*)-**51b** (400 mg, 1.10 mmol) in DMF (4 ml) and the reaction was stirred for 6 hours at r.t.

The reaction mixture was poured in distilled $H_2O$ and extracted with EtOAc. The organic phase was dried over $Na_2SO_4$ and concentrated in vacuo to give (α*S*, 5*S*)-**53b** (416 mg, 1.1 mmol) as a brow oil.

**Yield**: quantitative

**Solid state**: brown oil

**R**$_f$ ($CH_2Cl_2$/MeOH 9:1 + 1% AcOH): 0.53

Synthesis of **5b**

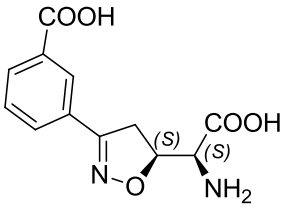


(α*S*, 5*S*)-**5b**

1) Derivative (α*S*, 5*S*)-**53b** (416 mg, 1.1 mmol) was treated with 0.5 N aq. NaOH (11 mL).The mixture was stirred at r.t. for 2 hours until completion by TLC ($CH_2Cl_2$/MeOH 9:1+1% µL AcOH).The reaction mixture was washed with $Et_2O$, made acidic with 1N aqueous HCl and extracted with EtOAc. The organic phase was dried over anhydrous $Na_2SO4$ and after evaporation of the solvent the diacidic derivate (310 mg, 0.85 mmol) was obtained as a white solid.

2) The diacidic derivate (310 mg, 0.85 mmol) was treated with a 30% $CH_2Cl_2$ solution of trifluoroacetc acid (3.9 ml) at 0°C. The solution was stirred at room temperature for 3 hours and thereaction was followed by TLC ($CH_2Cl_2$/MeOH 9:1 + 1% AcOH).
The volatiles were removed under reduced pressure and the residue was precipitated from MeOH/$Et_2O$ to give (α*S*, 5*S*)-**5b** (95 mg, 0.36 mmol) as a white solid.

**Yield**: 60% (yield after two steps)

**Solid state**: rosed solid

**R**$_f$ (*n*-butanol/$H_2O$/AcOH 4:2:1): 0.5

**M.p.**: dec. T > 165 °C

**$^1$H-NMR**: 3.50 (dd, *J*=11.4, 17.3, 1H); 3.51 (dd, *J*= 9.4, 17.6, 1H); 5.12 (ddd, *J*= 3.5, 9.4, 11.4, 1H); 7.51 (dd, *J*= 7.92, 7.92, 1H); 7.85 (d, *J*= 7.9, 1H); 8.0 (d, *J*= 7.9, 1H); 8.38 (s, 1H);

**$^{13}$C-NMR**: 36.01, 56.23, 80.89, 128.03, 129.84, 130.40, 131.28, 131.37, 132.11, 157.39, 167.12, 167.51

**[M+H]$^+$**: 265.0

Synthesis of (α*S*,5*R*)-**54b**

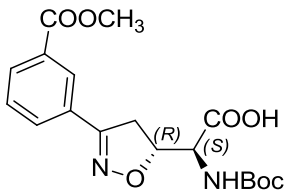


(α*R*, 5*S*)-**54b**

Compound (α*S*, 5*R*)-**54b** was synthesized following the procedure reported for **53b** starting from intermediate (α*R*, 5*R*)-**52b** (223 mg, 1.10 mmol).

**Yield**: quantitative

**Solid state**: brown oil

**R**$_f$ ($CH_2Cl_2$/MeOH 9:1 + 1% AcOH)*:* 0.53

Synthesis of **6b**

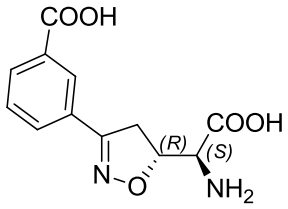


(α*S*, 5*R*)-**6b**

Compound (α*S*, 5*R*)-**6b** was synthesized following the procedure reported for **5b** starting from intermediate (α*S*, 5*R*)-**54b** (230 mg, 0.61 mmol).

**Yield**: 75% (yield after two steps)

**Solid state**: rosed solid

**R**$_f$ (*n*-butanol/$H_2O$/AcOH 4:2:1): 0.5

**M.p.**: dec. T > 155 °C

**$^1$H-NMR** (300 MHz, DMSO): 3.36 (d, *J*= 7.7, 1H); 3.52 (dd, *J*= 6.9, 17.6, 1H); 3.56 (dd, *J*= 6.9, 17.6, 1H); 4.58 (ddd, *J*= 6.9, 7.7, 10.7, 1H); 7.52 (dd, *J*= 7.7, 7.7, 1H); 7.58 (d, *J*= 7.7, 1H); 8.0 (d, *J*= 7.7, 1H);

**$^{13}$CNMR** (75 MHz, DMSO): 38.66, 57.31, 80.78, 127.95, 129.93, 130.17, 131.29, 131.43 132.27, 157.67, 167.48, 167.54

**[M+H]$^+$**: 265.0

Synthesis of **44c**

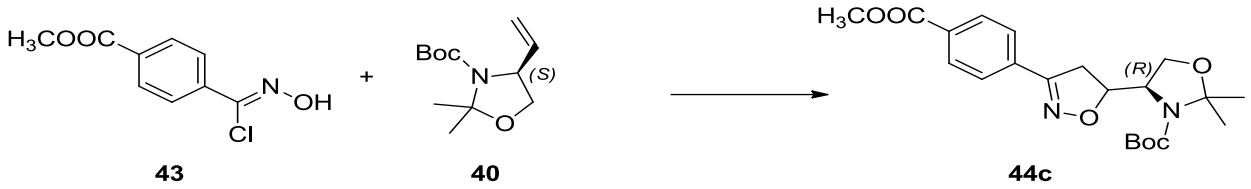


**43** **40** **44c**

To a solution of alkene **40** (500 mg, 2.20 mmol) in EtOAc (10 mL) was added **43** (924 mg, 4.33 mmol) and solid $NaHCO_3$ (916 mg, 10.90 mmol). The mixture was vigorously stirred overnight, then other 0.3 equivalents (141 mg, 0.66 mmol) of chlorooxime and $NaHCO_3$ (55 mg, 0.66 mmol) were added. $NaHCO_3$ was removed by filtration and the crude material, obtained after evaporation of the solvent, was purified by column chromatography on silica gel (Cyclohexane/EtOAc 85:15) to give **44c** (560 mg, 1.38 mmol) as a mixture of diasteroisomers.

**Yied**: 63%

**Solid state**: pale yellow oil

**$R_f$** (cyclohexane/EtOAc 85:15): 0.24

Synthesis of (α*R*,5*S*)-**51c** and (α*R*,5*R*)-**52c**

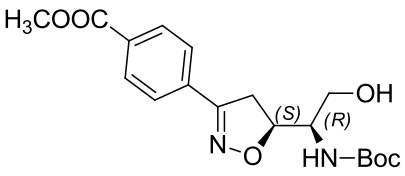


(α*R*, 5*S*)-**51c**

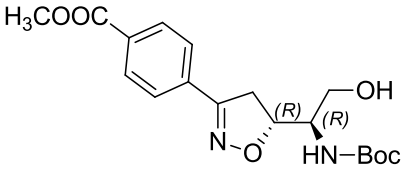


(α*R*, 5*R*)-**52c**

**44c** was treated with a 1/5 mixture of dist. $H_2O$ /AcOH at r.t. After 72 hours the azeotrope $H_2O$/AcOH was evaporated under reduced pressure and the crude was purified by flash chromatography using cyclohexane/EtOAc (6:4 to 1:1 gradient)as eluent to isolate the diasteroisomers (α*R*, 5*S*)-**51c** and (α*R*, 5*R*)-**52c**.

**Yield**: 53%

(α*R*, 5*S*)-**51c:** (200 mg)

Crystallized from n-hexane/iPrOH as needle crystals

**R**$_f$ (cyclohexane/ EtOAc 6:4): 0.23

**[α]**$^{20}_D$: (+) 92.6 (c: 1.02 in $CHCl_3$)

**M.p.**: 154-156 °C

**$^1$H-NMR** (300 MHz, $CDCl_3$): 1.32 (s, 9H); 3.40-3.47 (m, 2H); 3.73-3.83 (m, 2H); 3.94 (s, 3H); 3.95-4.03 (m, 1H); 4.82-1.95 (m, 1H); 5.19 (bs, 1H); 7.72 (d, *J*= 8.3, 2H); 8.07 (d, *J*=8.3, 2H);

**$^{13}$C-NMR** (75 MHz, $CDCl_3$): 28.56, 37.91, 52.56, 54.57, 61.90, 80.43, 81.29, 126.95, 130.19, 131.70, 133.56, 156.28, 156.83, 166.66

**[M+H]$^+$**: 365.1

(α*R*, 5*R*)-**52c:** (140 mg)

**Solid state:** waxy solid

**$R_f$** (cyclohexane/ EtOAc 6:4): 0.15

**$[\alpha]^{20}_D$**: (–) 127.8 (c: 0.96 in $CHCl_3$)

**$^1$H-NMR** (300 MHz, $CDCl_3$): 1.45 (s, 9H); 3.37 (dd, *J*=8.3, 16.8, 1H); 3.46 (dd, *J*= 10.5, 16.8, 1H); 3.78 (dd, *J*= 6.2, 11.0, 1H); 3.86 (dd, *J*= 7.5, 11.0, 1H); 3.93 (s, 3H); 4.98 (bs, 1H); 5.05 (d, *J*=6.7, 1H); 7.72 (d, *J*= 8.4, 2H); 8.07 (d, *J*=8.4, 2H);

**$^{13}$C-NMR** (75 MHz, $CDCl_3$): 28.36, 37.71, 52.59, 54.54, 63.79, 80.37, 81.76, 126.91, 130.19, 131.76, 133.41, 156.81, 157.14, 166.63

**$[M+H]^+$**: 365.1

Synthesis of (α*S*,5*S*)-**53c**

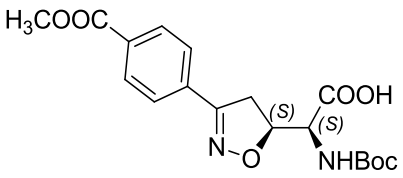


(α*S*, 5*S*)-**53c**

Pyridinium dichromate (3.070 g, 8.25 mmol) was added to a solution of (α*R*, 5*S*)-**51c** (200 mg, 0.55 mmol) in DMF (3.1 ml) and the reaction was stirred for 6 hours at r.t.

The reaction mixture was poured in distilled $H_2O$ and extracted with EtOAc. The organic phase was dried over $Na_2SO_4$ and concentrated in vacuo to give (α*S*, 5*S*)-**53c** (208 mg, 0.55 mmol) as a brow oil.

**Yield**: quantitative

**Solid state**: brown oil

**R**$_f$ ($CH_2Cl_2$/MeOH 9:1 + 1% AcOH): 0.5

Synthesis of **5c**

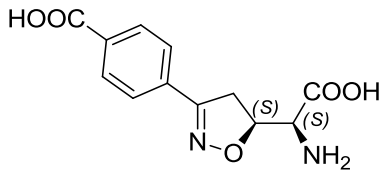


(α*S*, 5*S*)-**5c**

1) Derivative (α*S*, 5*S*)-**53c** (208 mg, 0.55 mmol) was treated with 0.5 Naqueous NaOH (6.6 mL).The mixture was stirred at r.t. for 2 hours until completion by TLC ($CH_2Cl_2$/MeOH 9:1+ 1% AcOH).The reaction mixture was washed with $Et_2O$, made acidic with 1N aqueous HCl and extracted with EtOAc. The organic phase was dried over anhydrous $Na_2SO4$ and after evaporation of the solvent the diacidic derivate (200 mg, 0.55 mmol) was obtained as a white solid.

2) The diacidic derivate (200 mg, 0.55 mmol) was treated with a 30% $CH_2Cl_2$ solution of trifluoroacetc acid (2.5 ml) at 0°C. The solution was stirred at room temperature for 3 hours and thereaction was followed by TLC ($CH_2Cl_2$/MeOH 9:1 + 1% AcOH).
The volatiles were removed under reduced pressure and the residue was precipitated from MeOH/$Et_2O$ to give (α*S*, 5*S*)-**5c** (130 mg, 0.49 mmol) as a white solid.

**Yield**: 82% (yield after two steps)

**Solid state**: white solid

**R**$_f$ (*n*-butanol/ $H_2O$/AcOH 4:2:1): 0.45

**M.p.**: dec. T > 170 °C

$^1$**H-NMR** (300 MHz, DMSO): 3.45 (dd, *J*= 11.4,17.3, 1H); 3.55 (dd, *J*= 9.6, 17.3, 1H); 3.63 (d, *J*= 3.6, 1H); 5.13 (ddd, *J*= 3.6, 9.6, 11.4, 1H); 7.74 (d, *J*= 8.2, 2H); 7.98 (d, *J*= 8.2, 2H);

$^{13}$**C-NMR** (75 MHz, DMSO): 35.75, 56.17, 81.37, 127.44, 130.29, 132.65, 133.97, 157.43, 166.90, 167.53

**[M+H]$^+$**: 265.0

Synthesis of (α*S*,5*R*)-**54c**

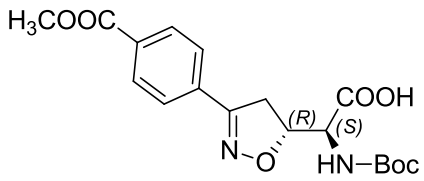


(α*S*, 5*R*)-**54c**

Compound (α*S*, 5*R*)-**54c** was synthesized following the procedure reported for **53c** starting from intermediate (α*R*, 5*R*)-**52c** (140 mg, 0.38 mmol).

**Yield**: quantitative

**Solid state**: brown oil

**R**$_f$ ($CH_2Cl_2$/MeOH 9:1 + 1% AcOH): 0.55

Synthesis of **6c**

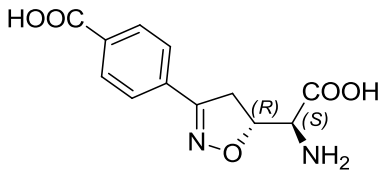


(α*S*, 5*R*)-**6c**

Compound (α*S*, 5*R*)-**6c** was synthesized following the procedure reported for **5c** starting from intermediate (α*S*, 5*R*)-**54c** (144 mg, 0.38 mmol).

**Yield**: 85% (yield after two steps)

**R**$_f$ (*n*-butanol/$H_2O$/AcOH 4:2:1): 0.5

**M.p.**: dec. T > 170 °C

**$^1$H-NMR** (300 MHz, DMSO): 3.35 (d, *J*= 7.8, 1H); 3.58 (dd, *J*= 10.8, 17.7, 1H); 3.75 (dd, *J*= 6.9, 17.7, 1H); 4.89 (ddd, *J*= 6.9, 7.8 10.8, 1H); 7.75 (d, *J*= 8.4, 2H); 7.98 (d, *J*= 8.4, 2H);

**$^{13}$C-NMR** (75 MHz, DMSO): 38.58, 57.35, 81.11, 100.24, 127.44, 130.42, 132.70, 133.72, 157.72, 167.32, 167.48

**[M+H]$^+$**: 265.0

Synthesis of (±)-**56**

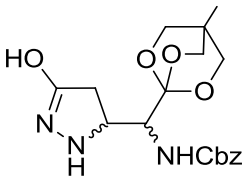


(±)-**56**

To a solution of (±)-**55** (5.18 g, 13.75 mmol) in EtOH (116 ml) was added hydrazine monohydrate (3.33 ml, 68.73mmol). The reaction mixture was stirred at 95 °C under reflux for 3 hours until completion.

The solvent was removed and the crude product was purified by flash chromatography on silica gel ($CH_2Cl_2$/MeOH, 95:5 to 90:10 gradient) to give (±)-**56** as an unseparable mixture of the two diastereoisomers (4.16 g, 11.02 mmol).

**Yield**: 80%

**Solid state**: white foam

**$R_f$** ($CH_2Cl_2$/MeOH 9:1): 0.55

**M.p.**: dec. T > 170 °C

**$[\alpha]^{20}_D$**: (–) 49 (c : 0.12 in $H_2O$);

**$[M+H]^+$**: 378.3

Synthesis of (±)-**57a**

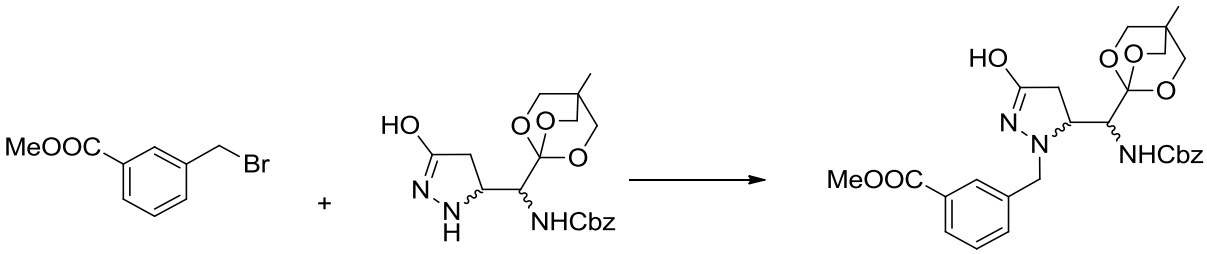


(±)-**56** (±)-**57a**

Under nitrogen atmosphere, (±)-**56** (1.00 g, 2.65 mmol.) was dissolved in acetonitrile (18 mL). NaI (18 mg, 0.12 mmol), $K_2CO_3$ (366 mg, 2.65 mmol) and methyl 3-(bromomethyl)benzoate (607 mg, 2.65 mmol) were added to the solution. The reaction was allowed to stir under nitrogen atmosphere at 80 °C for 3 hours. After cooling to rt. acetonitrile was evaporated, EtOAc (40 mL) was added to the crude product and extracted with $H_2O$ (30 mL), dried over $Na_2SO_4$, filtrated, and evaporated to dryness. The crude was purified by flash chromatography on silica gel(EtOAc/n-hexane, 1:1 to 100 % EtOAc gradient) to give (±)-**57a** as an unseparable mixture of the two diastereoisomers (1.17 g, 2.22 mmol).

**Yield**: 84 %

**Solid state**: white foam

**$R_f$** (EtOAc/cyclohexane 8:2): 0.4

**[M+H]$^+$**: 526.3

Synthesis of (±)-**58a**

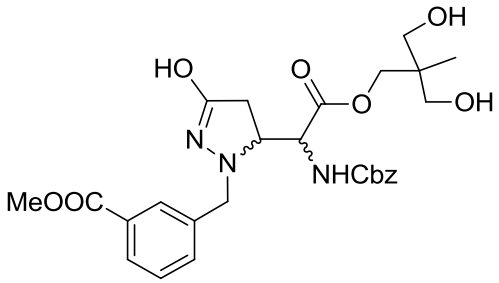


(±)-**58a**

To a solution of (±)-**57a** (1.17 g, 2.22 mmol) in MeOH/$H_2O$ (6:1) (17 mL), a catalytic amount of PPTS (56 mg, 0.22 mmol) was added. The reaction mixture was stirred at rt. for 1 hour until completion.

MeOH was evaporated. The crude was dissolved in EtOAc (30 mL) and washed with $H_2O$ (2 × 20 mL). The organic layer was dried over $Na_2SO_4$, filtered and evaporated to dryness to yield (±)-**58a** (1.18 g, 2.18 mmol).

**Yield**: 98%

**Solid state**: white foam

**$R_f$**(EtOAc): 0.28

Synthesis of (α*S**,5*R**)-**59a** and (α*S**,5*S**)-**60a**

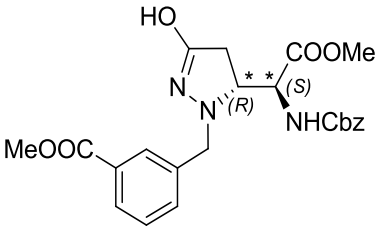


(α*S**,5*R**)-**59a**

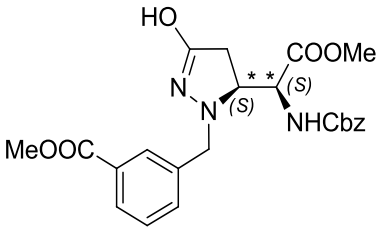


(α*S**,5*S**)-**60a**

To a solution of (±)-**58a** (1.18 g, 2.18 mmol) in MeOH (19 mL) was added $K_2CO_3$ (150 mg, 1.09 mmol). The reaction mixture was allowed to stir at rt. for 3 hours until completion.

The solvent was partially evaporated and the residue was dissolved in EtOAc and washed with 3% $NH_4Cl$. The organic phase was dried over anhydrous $Na_2SO_4$, filtered and concentrated to dryness. Purification via flash chromatography (EtOAc/n-hexane, 1:1 to 100 % EtOAc gradient) allowed the separation of the two diasteroisomers (α*S**,5*R**)-**59a** and (α*S**,5*S**)-**60a**.

**Yield**: 38%

(α*S**, 5*R**)-**59a**: (270 mg)

Crystallized from n-hexane/EtOAc as white prisms.

**R**$_f$ (EtOAc): 0.50

**M.p.**: 155 – 156 °C;

**$^1$H-NMR** (300 MHz, CDCl3): 2.41 (dd, *J*= 2.5,17.6, 1H); 2.88 (dd, *J*= 9.4,17.6,1H); 3.66(s, 3H); 3.84 (d, *J*= 12.7, 1H); 3.91 (s, 3H); 3.93 (d, *J*= 12.7, 1H);4.00-4.07 (m, 1H); 4.50 (dd, *J*= 3.0, 9.6, 1H); 5.06 (d, *J*= 12.4, 1H);5.15 (d, *J*= 12.4, 1H); 5.61 (d, *J*= 9.6, 1H); 7.10 (bs, 1H); 7.30-7.38 (m,5H); 7.39-7.49 (m, 2H); 7.92 (s, 1H); 7.98 (d, *J*= 6.9, 1H);

**$^{13}$C-NMR**(75 MHz, CDCl3): 31.5, 52.6, 53.0, 58.2, 62.7, 64.6, 67.8, 128.3, 128.5, 128.8, 129.2, 129.8, 130.9, 131.0, 134.4, 135.5, 136.1, 157.1, 166.8, 170.4, 173.4

**[M+H]**$^{+}$: 456.2

(α*S**, 5*S**)-**60a**: (270 mg)

Crystallized from n-hexane/EtOAc as white prisms.

**R**$_f$ (EtOAc): 0.40

**M.p.**: 154 – 155 °C;

$^{1}$**H-NMR** (300 MHz, CDCl3): 2.52 (d, *J*= 17.3, 1H); 2.89 (dd, *J*= 9.4, 17.3, 1H); 3.65-3.80 (m, 1H), 3.72 (s, 3H); 3.88 (d, *J*= 12.0, 1H); 3.89 (s, 3H); 3.93 (d,*J*= 12.0, 1H); 4.32 (dd, *J*= 4.4, 8.5, 1H); 4.94 (d, *J*= 12.3, 1H); 5.05 (d, *J*= 12.3, 1H); 5.65 (d, *J*= 8.5, 1H); 7.10 (bs, 1H); 7.28-7.44 (m, 5H);7.48-7.54 (m, 2H);7.94-7.99 (m, 2H);

$^{13}$**C-NMR**(75 MHz, CDCl3): 31.4, 52.5, 53.0, 56.4, 64.0, 64.2, 67.4, 128.4, 128.5, 128.8, 129.2, 129.8, 130.9, 131.0, 134.3, 135.7, 136.2, 155.6, 166.8, 170.2, 173.5;

**[M+H]**$^{+}$: 456.2

Synthesis of **7a**

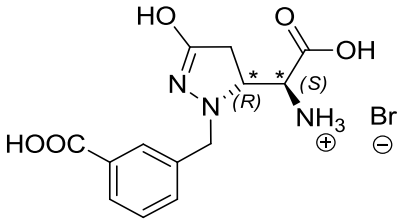


(α*S**, 5*R**)-**7a**

1) (α*S**, 5*R**)-**59a** (270 mg, 0.59 mmol) was dissolved in dioxane (4 mL) and 0.5 N NaOH (4 mL) was added. The reaction was stirred at rt. for 2 hours. After evaporation of dioxane, the aqueous layer was washed with $Et_2O$, made acidic with 2 N aqueous HCl, and extracted with EtOAc. The organic layer was dried over anhydrous $Na_2SO_4$, filtered and evaporated in vacuo to give the carboxylic acid (220 mg, 0.51 mmol) which was used in the next step without further purifications.

**Solid state**: white solid

**R**$_f$ ($CH_2Cl_2$/MeOH 9:1 + 1% AcOH): 0.55

2) The diacidic intermediate(220 mg, 0.51 mmol) was dissolved in HBr (2.0 mL, 33 % in glacial acetic acid) and allowed to stir for 2 hours at rt. The volatiles were removed under vacuum. The final aminoacid (α*S**, 5*R**)-**7a** (116 mg, 0.31 mmol) was obtained as HBr salt by direct crystallization from iPrOH/$Et_2O$.

**Yield**: 73% (yield after two steps)

**Solid state**: white solid

**R**$_f$ (*n*-butanol/$H_2O$/AcOH 4:2:1): 0.3

**M.p.**: dec. T> 165 °C

**$^1$H-NMR** (300 MHz , $D_2O$): 2.42 (dd, *J*= 1.5, 17.9, 1H);2.79 (dd, *J*= 7.6,17.9, 1H); 3.80 (s, 1H); 3.82 (dd, *J*=1.5, 7.6, 1H); 3.89(d, *J*= 13.2, 1H); 3.97 (d, *J*= 13.2, 1H); 7.39 (t, *J*= 7.6, 1H); 7.71 (d,*J*= 7.6, 1H); 7.84-7.89(m, 2H);

**$^{13}$C-NMR** (75 MHz, $D_2O$): 32.5, 55.2,60.4, 62.1, 129.3, 129.8, 130.2, 131.2, 135.3, 135.4, 170.3, 170.4, 175.4

**[M-H]**$^{-}$: 291.8

Synthesis of **8a**

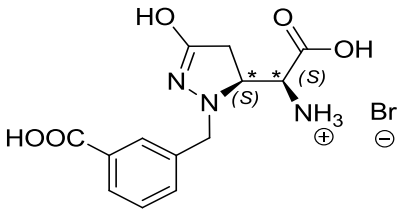


Compound (α*S**, 5*S**)-**8a** was synthesized following the procedure reported for **7a** starting from intermediate **60a** (270 mg, 0.59 mmol).

**Yield**: 78% (yield after two steps)

**Solid state**: white solid

**R**$_f$ (*n*-butanol/$H_2O$/AcOH 4:2:1): 0.3

**M.p.**: dec. T> 183 °C

**$^1$H-NMR** (300 MHz , $D_2O$): 2.40 (dd, *J*= 2.3, 17.9, 1H); 2.65 (dd, *J*= 9.3, 17.9, 1H); 3.82 (d, *J*= 3.8, 1H); 3.88 (d, *J*= 13.2, 1H); 3.90 (ddd, *J*= 2.3, 3.8, 9.3, 1H); 3.98 (d, *J*= 13.2, 1H); 7.40 (t, *J*= 7.9, 1H); 7.53 (d, *J*= 7.9, 1H); 7.85-7.91 (m, 2H); 2.40 (dd, *J*= 2.3, 17.9, 1H); 2.65 (dd, *J*= 9.3, 17.9, 1H); 3.82 (d, *J*= 3.8, 1H); 3.88 (d, *J*= 13.2, 1H); 3.90 (ddd, *J*= 2.3, 3.8, 9.3, 1H); 3.98 (d, *J*= 13.2, 1H); 7.40 (t, *J*= 7.9, 1H); 7.53 (d, *J*= 7.9, 1H); 7.85-7.91 (m, 2H);

**$^{13}$C-NMR** (75 MHz, $D_2O$): 31.6, 55.3, 60.8, 62.4, 129.3, 129.8, 130.3, 131.2, 135.2, 135.4, 169.9, 170.5, 175.7

**[M-H]$^-$**: 291.8

Synthesis of (±)-**57b**

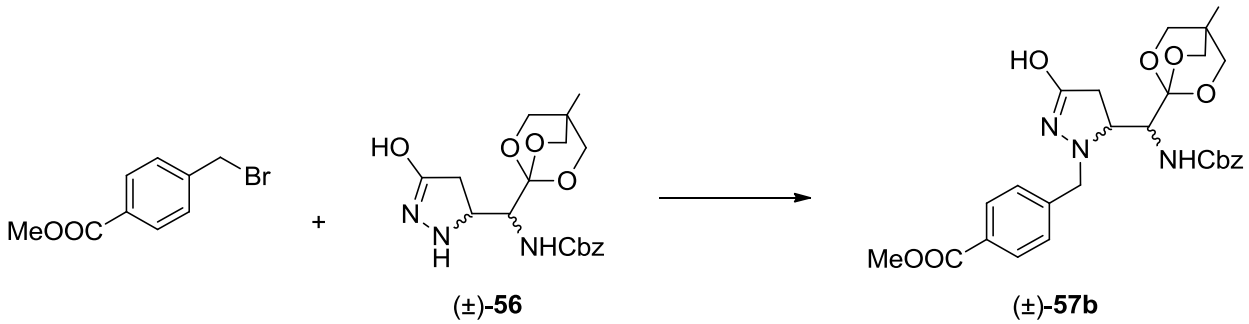


(±)-**56** (±)-**57b**

Under nitrogen atmosphere, (±)-**56** (1.0 g, 2.65 mmol.) was dissolved in acetonitrile (18 mL). NaI (18 mg, 0.12 mmol), $K_2CO_3$ (366 mg, 2.65 mmol) and methyl 3-(bromomethyl)benzoate (607 mg, 2.65 mmol) were added to the solution. The reaction was allowed to stir under nitrogen atmosphere at 80 °C for 3 hours. After cooling to rt. acetonitrile was evaporated, EtOAc (40 mL) was added to the crude product and extracted with $H_2O$ (30 mL), dried over $Na_2SO_4$, filtrated, and evaporated to dryness. The crude was purified by flash chromatography on silica gel (EtOAc/n-hexane, 1:1 to 100 % EtOAc gradient) to give (±)-**57b** as an unseparable mixture of the two diastereoisomers (1.10 g, 2.09 mmol).

**Yield**: 79%

**Solid state**: white foam

**$R_f$** (EtOAc/cyclohexane 8:2): 0.37

**[M+H]$^+$**: 526.3

Synthesis of (±)-**58b**

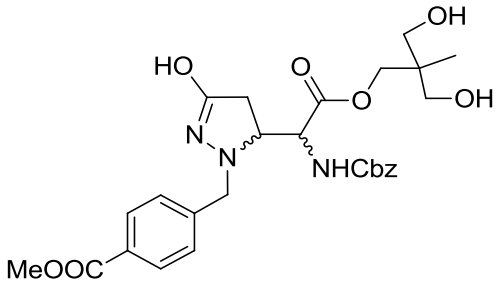


(±)-**58b**

To a solution of (±)-**57b** (1.10 g, 2.09 mmol) in MeOH/$H_2O$ (6:1) (16 mL), a catalytic amount of PPTS (55 mg, 0.21 mmol) was added. The reaction mixture was stirred at rt. for 1 hour until completion.
MeOH was evaporated. The crude was dissolved in EtOAc (30 mL) and washed with $H_2O$ (2 × 20 mL). The organic layer was dried over $Na_2SO_4$, filtered and evaporated to dryness to yield (±)-**58b** (1.09 g, 2.01 mmol).

**Yield**: 96%

**Solid state**: white foam

**$R_f$** (EtOAc): 0.32

Synthesis of (α*S**,5*R**)-**59b** and (α*S**,5*S**)-**60b**

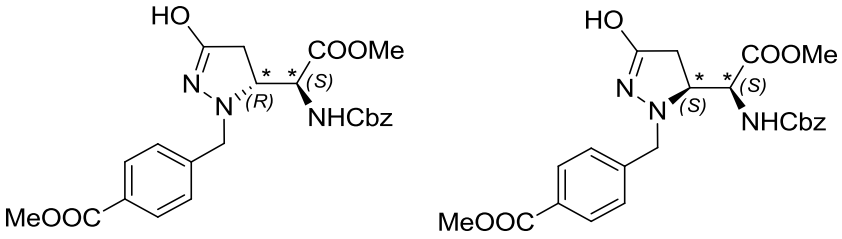


To a solution of (±)-**58b** (1.09 g, 2.01 mmol) in MeOH (17 mL) was added $K_2CO_3$ (138 mg, 1.0 mmol). The reaction mixture was allowed to stir at rt. for 3 hours until completion.

The solvent was partially evaporated and the residue was dissolved in EtOAc and washed with 3% $NH_4Cl$. The organic phase was dried over anhydrous $Na_2SO_4$, filtered and concentrated to dryness. Purification via flash chromatography (EtOAc/n-hexane, 1:1 to 100 % EtOAc gradient) allowed the separation of the two diasteroisomers (α*S**,5*R**)-**59b** and (α*S**,5*S**)-**60b**.

**Yield**: 36%

(α*S**, 5*R**)-**59b**: (244 mg)

Crystallized from n-hexane/EtOAc as white prisms.

**R**$_f$ (EtOAc): 0.6

**M.p.**: 157–159°C

**$^1$H-NMR** (300 MHz, $CDCl_3$): 2.41 (dd, *J*= 2.1, 17.6, 1H); 2.86 (dd, *J*= 9.4,17.6, 1H); 3.66 (s, 3H); 3.85 (d, *J*= 13.0, 1H); 3.92 (s, 3H); 3.94 (d, *J*= 13.0, 1H); 3.98-4.06 (m, 1H); 4.51 (dd, *J*= 3.2, 9.4, 1H); 5.07 (d, *J*= 12.3, 1H); 5.15 (d, *J*= 12.3, 1H); 5.60 (d, *J*= 9.4, 1H); 7.10 (bs, 1H); 7.30-7.39 (m, 7H); 8.05 (d, *J*= 8.2, 2H);

**$^{13}$C-NMR**(75 MHz, $CDCl_3$): 31.5, 52.5, 53.0, 58.2, 62.8, 64.7, 67.8, 128.3, 128.5, 128.8, 129.7, 130.3, 130.4, 136.1, 140.4, 157.1, 166.8, 170.5, 173.5

**[M+H]$^+$**: 456.2

(α*S**, 5*S**)-**60b**: (244 mg)

Crystallized from n-hexane/EtOAc as white prisms.

**$R_f$** (EtOAc): 0.51

**M.p.**: 177–179°C

**$^1$H-NMR** (300 MHz, $CDCl_3$): 2.51 (d, *J*= 17.3, 1H); 2.86 (dd, *J*= 9.1, 17.3, 1H); 3.71 (s, 3H); 3.71-3.80 (m, 1H); 3.88 (d, *J*= 13.0, 1H); 3.90 (s, 3H); 3.94 (d, *J*= 13.0, 1H); 4.30 (dd, *J*= 4.1, 7.9, 1H); 4.92 (d, *J*= 12.1, 1H); 5.07 (d, *J*= 12.1, 1H); 5.68 (d, *J*= 12.0, 1H); 7.12 (bs, 1H); 7.35-7.42 (m, 7H); 8.05 (d, *J*= 8.2, 2H);

**$^{13}$C-NMR**(75 MHz, $CDCl_3$): 31.5, 52.5, 53.0, 56.5, 64.0, 64.3, 67.4, 128.3, 128.5, 128.8, 129.7, 130.2, 130.3, 136.2, 140.5, 155.6, 166.9, 170.2, 173.7

**$[M+H]^+$**: 456.2

Synthesis of **7b**

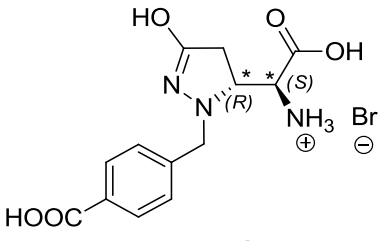


(α*S**,5*R**)-**7b**

1) (α*S**, 5*R**)-**59b** (244 mg, 0.52 mmol) was dissolved in dioxane (3.5 mL) and 0.5 N NaOH (3.5 mL) was added. The reaction was stirred at rt. for 2 hours. After evaporation of dioxane, the aqueous layer was washed with $Et_2O$, made acidic with 2 N aqueous HCl, and extracted with EtOAc. The organic layer was dried over anhydrous $Na_2SO_4$, filtered and evaporated in vacuo to give the carboxylic acid (222 mg, 0.52 mmol) which was used in the next step without further purifications.

**Solid state**: white solid

**R**$_f$ ($CH_2Cl_2$/MeOH 9:1 + 1% AcOH): 0.53

2) The diacidic intermediate(222 mg, 0.52 mmol) was dissolved in HBr (2.0 mL, 33 % in glacial acetic acid) and allowed to stir for 2 hours at r.t. The volatiles were removed under vacuum. The final aminoacid (α*S**,5*R**)-**7b** (127 mg, 0.34 mmol) was obtained as HBr salt by direct crystallization from iPrOH/$Et_2O$.

**Yield**: 66% (yield after two steps)

**Solid state**: white solid

**R**$_f$ (*n*-butanol/$H_2O$/AcOH 4:2:1): 0.3

**M.p.**: dec. T > 237 °C

**$^1$H-NMR** (300 MHz, $D_2O$): 2.42 (dd, *J*= 1.5, 18.2, 1H); 2.79 (dd, *J*= 7.9, 18.2, 1H); 3.78-3.88 (m, 2H); 3.89 (d, *J*= 13.2, 1H); 3.99 (d, *J*= 13.2, 1H); 7.36 (d, *J*= 8.2, 2H); 7.86 (d, *J*= 8.2, 2H);

**$^{13}$C-NMR** (75 MHz, $D_2O$): 32.5, 55.2, 60.5, 62.3, 129.7, 130.1, 130.4, 140.5, 170.3, 170.5, 175.4

**[M-H]**$^-$: 292.1

Synthesis of **8b**

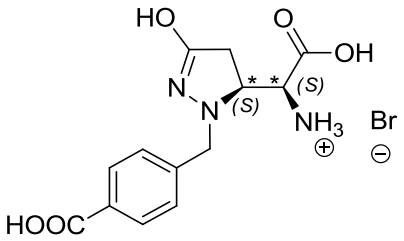


(α*S**,5*S**)-**8b**

Compound (α*S**, 5*S**)-**8b** was synthesized following the procedure reported for **8a** starting from intermediate **60b** (244 mg, 0.52 mmol).

**Yield**: 84% (yield after two steps)

**Solid state**: white solid

**R**$_f$ (*n*-butanol/$H_2O$/AcOH 4:2:1): 0.3

**M.p.**: dec. T > 225°C

**$^1$H-NMR** (300 MHz, $D_2O$): 2.41 (dd, *J*= 1.8, 18.2, 1H); 2.69 (dd, *J*= 8.5, 18.2, 1H); 3.86-4.02 (m, 4H); 7.39 (d, *J*= 8.2, 2H); 7.88 (d, *J*= 8.2, 2H);

**$^{13}$C-NMR** (75 MHz, $D_2O$): 31.7, 55.1, 60.9, 62.5, 129.7, 130.2, 130.3, 140.4, 169.6, 170.4, 175.7;

**[M-H]$^-$**: 291.7

Synthesis of (3α*R*,6*R*,6α*S*)-**62**, (3α*S*,4*S*,6α*R*)-**63** and (3α*S*,6*S*,6α*R*)-**64**

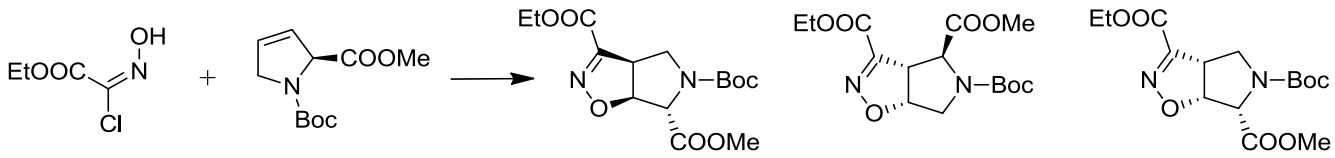


To a solution of **61** (3.46 g; 15.22 mmol) in EtOAc (67 ml) were added ethyl 2-chloro-2-(hydroxyimino) acetate (2.31 g; 15.22 mmol) and $NaHCO_3$ (5.11 g; 60.88 mmol). The reaction was refluxed at 80°C for 3 days.

Other 3 eq of ethyl 2-chloro-2-(hydroxyimino) acetate and 3 eq of $NaHCO_3$ were added and the reaction strirred at 80°C for other 3 days. The progress of the reaction was monitored by TLC (cyclohexane/EtOAc 7:3).

After 6 days distilled $H_2O$ was added and the organic layer separated and dried over $Na_2SO_4$. The crude material, obtained after evaporation of the solvent was purified by flash chromatography (cyclohexane/EtOAc 7:3) to yield the mixture of cycloadducts in a 56% overall yield (2.92 g, 8.53 mmol).

The three diasteroisomers were separated by preparative HPLC (Phenomenex Lux Amylose-2 column (21.2 × 250 mm) and 8/2 n-hexane/iPrOH as eluent at a flow rate of 15 mL/min, see chapter 6.3).

(3α*R*,6*R*,6α*S*)-**62:**

Crystallized from diisopropylether as colourless prisms

**R**$_f$ (cyclohexane/EtOAc 7:3): 0.35

**M.p.**: 78-80°C

**$^1$H-NMR** (300 MHz, $C_7D_8$): 1.00 (t, *J*=7.1, 3H); 1.35 (s, 9H); 3.37 (s, 3H); 3.47 (dddd, *J*=0.8, 2.1, 7.6, 9.5, 4H); 3.63 (dd, *J*=8.0, 11.6, 1H); 3.98 (m, 2H); 4.09 (bd, *J*=11.6, 1H); 4.80 (bs, 1H); 4.88 (bd, *J*=9.5, 1H)

(3α*S*,4*S*,6α*R*)-**63:**

**Solid state**: colourless oil

**R**$_f$ (cyclohexane/EtOAc 7:3): 0.30

**$^1$H-NMR** (300 MHz, $C_7D_8$): 1.02 (t, *J*= 6.9, 3H); 1.35 (s, 9); 3.39 (s, 3H); 3.56 (dd, *J*=6.0, 12.6, 1H); 3.68 ( bd, *J*= 10.0, 1H); 3.84 (dd, *J*=0.7,12.6, 1H); 3.97 (m, 2H); 4.69 (ddd, *J*=0.7, 6.0, 10.0, 1H); 4.90 (bs, 1H)

(3α*S*,6*S*,6α*R*)-**64:**

**Solid state**: colourless oil

**R**$_f$ (cyclohexane/EtOAc 7:3): 0.30

**$^1$H-NMR** (300 MHz, $C_7D_8$):0.98 (t, *J*=69, 3H); 1.37 (s, 9H); 3.46 (s, 3H); 3.48 (ddd, *J*=5.2, 9.0, 10.5, 1H); 3.70 (dd, *J*=9.0, 11.5, 1H); 3.82 (dd, *J*=5.2, 11.5, 1H); 3.95 (m, 2H); 4.48 (d, *J*=8.0, 1H); 4.80 (dd, *J*=8.0, 10.5, 1H)

Synthesis of **65**

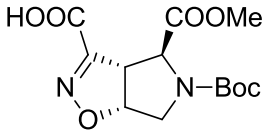


**65**

To a solution of (3α*S*,6*S*,6α*R*)-**63** (852 mg; 2.49 mmol) in MeOH (6.8 ml) a 5% m/m aqueous sol. of $K_2CO_3$ (6.8 ml; 2.49 mmol) was added dropwise. The reaction was monitored by TLC ($CHCl_3$/MeOH 8:2 + 1% AcOH).

After 10 minutes, distilled $H_2O$ was added and the reaction mixture washed with $Et_2O$. The aqueous layer was made acidic with 1N HCl and extracted with EtOAc. The organic phase was dried over $Na_2SO_4$ and the solvent removed *in vacuo*.

The crude of the reaction was purified by flash chromatography (gradient from EtOAc to 8:2 EtOAc/MeOH) to afford **65** (579 mg; 1.84 mmol).

**Yield**: 74%

**Solid state**: white solid

**R**$_f$ ($CHCl_3$/MeOH 8:2 + 1% AcOH): 0.44

Synthesis of **71a**

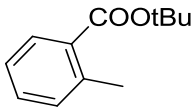


**71a**

A solution of 2-methyl benzoic acid (0.82 ml; 10.15 mmo)l (1.20 g; 8.46 mmol) in dry $CH_2Cl_2$ (59 ml) and dry THF (23.3 ml) was treated with *tert*-butyl 2,2,2-trichloroacetimidate (3.63 ml; 20.3 mmol) and $BF_3*O(C_2H_5)_2$ (180 μl; 1.44 mmol). The reaction was allowed to stir at r.t. for 21 hours under nitrogen atmosphere. The reaction was then concentrated under reduced pressure and redissolved in EtOAc.
The solution was washed with 5% aqueous sol. $NaHCO_3$ and brine. The organic layer was dried over $Na_2SO_4$, filtered and concentrated. The crude product was purified by flash chromatography (cyclohexane/EtOAc 9:1) to give **71a** (140 g; 7.31 mmol).

**Yield**: 72%

**Solid state**: colourless oil

**$R_f$** (Cyclohexane/EtOAc 95:5): 0.68

**$^1$H-NMR** (300 MHz, $CDCl_3$): 1.59 (s, 9H); 2.57 (s, 3H); 7.18–7.24 (m, 2H); 7.33 (t, *J*= 7.0, 1H); 7.83 (d, *J*= 7.3, 1H)

Synthesis of **69a**

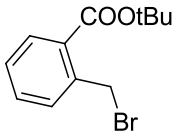


A solution of **71a** (1 g; 5.20 mmol) in $CCl_4$ (3 ml) was treated with *N*-bromo-succinimmide (1.02 g; 5.72 mmol) and AIBN (22 mg; 0.13 mmol). The reaction was refluxed at 85°C and monitored by TLC (cyclohexane/EtOAc 95:5).

After 4 hours, *N*-bromo-succinimmide was removed by filtration and the organic phase was washed with distiled $H_2O$, brine and dried over $Na_2SO_4$. The crude obtained after evaporation of the solvent was purified by flash chromatography (cyclohexane/EtOAc 95:5) to afford **69a** (990mg; 5.16 mmol).

**Yield**: 69%

**Solid state**: yellow oil

**$R_f$** (cyclohexane/EtOAc 95:5): 0.62

**$^1$H-NMR** (300 MHz, $CDCl_3$): 1.62 (s, 9H); 4.93 (s, 2H); 7.29–7.48 (m, 3H); 7.87 (d, *J*= 7.3, 1H)

Synthesis of **70a**

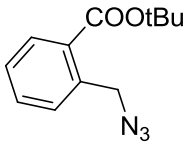


**70a**

$NaN_3$ (112 mg; 1.73 mmol) was added to the solution of **69a** (390 mg; 1.44 mmol) in DMF (1.8 ml). The reaction was stirred at 110 °C until completion (cyclohexane/EtOAc 98:2).

After 3 hours, EtOAc was added to the flask and the organic phase washed with distilled $H_2O$ and dried over $Na_2SO_4$. After evaporation of the solvent *in vacuo*, the crude was purified by flash chromatography (cyclohexane/EtOAc 95:5) to afford **70a** (284 mg; 1.22 mmol).

**Yield**: 85%

**Solid state**: yellow oil

**$R_f$** (cyclohexane/EtOAc 98:2): 0.20

**$^1$H-NMR** (300 MHz, $CDCl_3$): 1.60 (s, 9H); 4.80 (s, 2H); 7.38 (t, *J*= 7.0, 1H); 7.40-7.55 (m, 2H); 7.95 (d, *J*= 7.3, 1H)

**$^{13}$C-NMR** (75 MHz, $CDCl_3$): 28.43 (3C), 53.36, 82.15, 128.27, 129.94, 131.20, 131.23, 132.32, 136.76, 166.37

Synthesis of **66a**

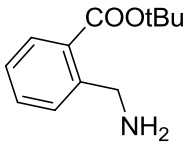


**66a**

To a solution of **70a** (284 mg; 1.22 mmol) in THF (10 ml), a catalytic amount of 5% Pd/C was added. The mixture was stirred at r.t. for 2 hours under a $H_2$ atmosphere and the reaction was followed by TLC ($CHCl_3$/MeOH 95:5).

The mixture was filtered under vacuum on a celite pad to eliminate the catalyst. After evaporation of the solvent, the crude was purified by flash chromatography using $CH_2Cl_2$/MeOH (95:5 to 8:2 gradient) as eluent to afford **66a** (154 mg; 0.74 mmol).

**Yield**: 61%

**Solid state**: yellow oil

**$R_f$** ($CHCl_3$/MeOH 95:5): 0.22

**$^1$H-NMR** (300 MHz, $CDCl_3$): 1.60 (s, 9H); 2.30 (bs, 2H); 4.05 (s, 2H); 7.32 (t, *J*= 7.0, 1H); 7.39-7.52 (m, 2H); 7.82 (d, *J*= 7.3, 1H)

Synthesis of **70b**

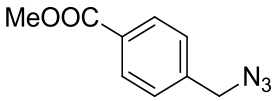


To a solution of 4-bromomethyl-methylbenzoate (400 mg; 1.74 mmol) in DMF (2.2 ml), $NaN_3$ (136 mg; 2.09 mmol) was added. The reaction was monitored by TLC (cyclohexane/EtOAc 95:5) until completion.
After 3 hours EtOAc was added and washed with distilled $H_2O$. The organic layer was dried over $Na_2SO_4$ and the solvent removed under reduced pressure.
The crude was purified by flash chromatography (cyclohexane/EtOAc 98:2) to afford **70b** (304 mg; 1.59 mmol).

**Yield**: 91%

**Solid state**: colourless solid

**$R_f$** (cyclohexane/EtOAc 95:5): 0.34

**$^1$H-NMR** (300 MHz, $CDCl_3$): 3.91 (s, 3H); 4.42 (s, 2H); 4.05 (s, 2H); 7.39(d, *J*= 7.8, 2H); 8.11 (d, *J*= 7.8, 2H)

**$^{13}$C-NMR** (75 MHz, $CDCl_3$): 52.53, 54.59, 128.29, 130.40, 130.41, 140.43, 166.95

Synthesis of **66b**

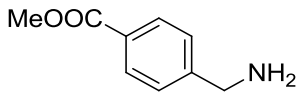


**66b**

To a solution of **70b** (304 mg; 1.59 mmol) in THF (13 ml), a catalytic amount of 5% Pd/C was added. The mixture was stirred at r.t. for 2 hours under a $H_2$ atmosphere and the reaction was followed by TLC ($CH_2Cl_2$/MeOH 9:1).

The mixture was filtered under vacuum on a celite pad to eliminate the catalyst. After evaporation of the solvent, the crude was purified by flash chromatography using $CH_2Cl_2$/MeOH (95:5 to 8:2 gradient) as eluent to afford **66b** (148 mg; 0.90 mmol).

**Yield**: 56%

**Solid state**: yellow oil

**$R_f$** ($CH_2Cl_2$/MeOH 9:1): 0.14

**$^1$H-NMR** (300 MHz, $CDCl_3$): 3.85 (s, 3H); 3.87 (s, 2H); 7.39 (d, *J*= 8.2, 2H); 8.00 (d, *J*= 8.2, 2H)

Synthesis of **71d**

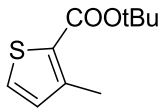


**71d**

A solution of 2-carboxy-3-methylthiophene (1.20 g; 8.46 mmol) in dry $CH_2Cl_2$ (49.2 ml) and dry THF (19.4 ml) was treated with *tert*-butyl 2,2,2-trichloroacetimidate (3.03 ml; 16.92 mmol) and $BF_3*O(C_2H_5)_2$ (150 µl; 1.20 mmol). The reaction was allowed to stir at r.t. for 21 hours under nitrogen atmosphere. The reaction was then concentrated under reduced pressure and redissolved in EtOAc.
The solution was washed with 5% aqueous sol. $NaHCO_3$ and brine. The organic layer was dried over $Na_2SO_4$, filtered and concentrated. The crude product was purified by flash chromatography (cyclohexane/EtOAc 9:1) to give **71d** (1.33 g; 6.72 mmol)

**Yield**: 79%

**Solid state**: yellow oil

**$R_f$** (cyclohexane/EtOAc 9:1): 0.65

**$^1$H-NMR** (300 MHz, $CDCl_3$): 1.58 (s, 9H); 2.52 (s, 3H); 6.88 (d, *J*= 5.3, 1H); 7.33 (d, *J*= 5.3, 1H)

Synthesis of **69d**

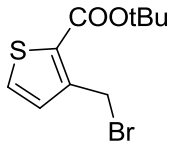


**69d**

A solution of **71d** (1.19 g; 6.02 mmol) in $CCl_4$ (23.8 ml) was treated with *N*-bromo-succinimmide (1.17 g; 6.57 mmol) and AIBN (95 mg; 0.55 mmol). The reaction was refluxed at 85°C and monitored by TLC (cyclohexane/EtOAc 98:2).

After 4 hours the *N*-bromo-succinimmide was removed by filtration and the organic phase was washed with distilled $H_2O$, brine and dried over $Na_2SO_4$. The crude obtained after evaporation of the solvent was purified by flash chromatography (cyclohexane/EtOAc 98:2) to afford **69d** (1.05 g; 4.51 mmol).

**Yield**: 63%

**Solid state**: yellow oil

**$R_f$** (petroleum ether/EtOAc 98:2): 0.61

**$^1$H-NMR** (300 MHz, $CDCl_3$): 1.60 (s, 9H); 4.88 (s, 2H); 7.14 (d, *J*= 5.0, 1H); 7.40 (d, *J*= 5.0, 1H)

Synthesis of **70d**

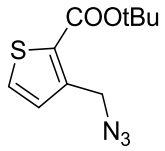


**70d**

$NaN_3$ (293 mg; 4.51 mmol) was added to the solution of **69d** (1.05 g; 3.77 mmol) in DMF (8.71 ml). The reaction was stirred at 110 °C until completion (cyclohexane/EtOAc 98:2).

After 3 hours, the reaction was concentrated under reduced pressure and redissolved in EtOAc. The organic phase washed with distilled $H_2O$ and dried over $Na_2SO_4$.

After evaporation of the solvent *in vacuo*, the crude was purified by flash chromatography (cyclohexane/EtOAc 98:2) to afford **70d** (550 mg; 2.30 mmol).

**Yield**: 61%

**Solid state**: yellow oil

**$R_f$** (cyclohexane/EtOAc 98:2): 0.42

**$^1$H-NMR** (300 MHz, $CDCl_3$): 1.57 (s, 9H); 4.71 (s, 2H); 7.10 (d, *J*= 5.2, 1H); 7.43 (d, *J*= 5.2, 1H)

Synthesis of **66d**

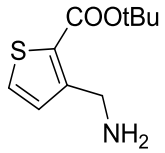


**66d**

To a solution of **70d** (550 mg; 2.30 mmol) in THF (18.8 ml), a catalytic amount of 5% Pd/C was added. The mixture was stirred at r.t. for 2 hours under a $H_2$ atmosphere and the reaction was followed by TLC ($CHCl_3$/MeOH 95:5).

The mixture was filtered under vacuum on a celite pad to eliminate the catalyst. After evaporation of the solvent, the crude was purified by flash chromatography using $CH_2Cl_2$/MeOH (95:5 to 8:2 gradient) as eluent to afford **66d** (324 mg; 1.52 mmol).

**Yield**: 66%

**Solid state**: yellow oil

**$R_f$** ($CHCl_2$/MeOH 95:5): 0.15

**$^1$H-NMR** (300 MHz, $CDCl_3$): 1.56 (s, 9H); 1.82 (s, 2H); 4.05 (s, 2H); 7.05 (d, *J*= 4.9, 1H); 7.36 (d, *J*= 4.9, 1H)

Synthesis of **68e**

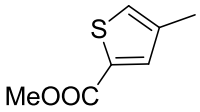


**68e**

A solution of 2-carboxy-4-methylthiophene (1.0 g; 7.03 mmol) in dry MeOH (10.2 ml) was treated with concentrated $H_2SO_4$ (1.02 ml). The reaction was refluxed at 66°C for 24 hours and monitored by TLC (cyclohexane/EtOAc 9:1). After concentration, the mixture was redissolved in $Et_2O$ and washed with 2N NaOH, distilled $H_2O$ and brine.

The organic layer was dried over $Na_2SO_4$, filtered and concentrated *in vacuo* to give **68e** (970 mg; 6.21 mmol)

**Yield**: 88%

**Solid state**: brown oil

**$R_f$** (cyclohexane/EtOAc 9:1): 0.44

**$^1$H-NMR** (300 MHz, $CDCl_3$): 2.27 (s, 3H); 3.86 (s, 3H); 7.12 (d, *J*= 1.5, 1H); 7.60 (d, *J*= 1.5, 1H)

Synthesis of **69e**

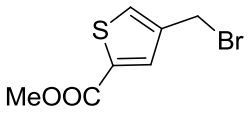


**69e**

A solution of **68e** (970 mg; 6.21 mmol) in $CCl_4$ (24.6 ml) was treated with *N*-bromo-succinimmide (1.22 g; 6.83 mmol) and AIBN (96 mg; 0.58 mmol). The reaction was refluxed at 85°C and monitored by TLC (cyclohexane/EtOAc 98:2).

After 4 hours the *N*-bromo-succinimmide was removed by filtration and the organic phase was washed with distilled $H_2O$, brine and dried over $Na_2SO_4$. The crude obtained after evaporation of the solvent was purified by flash chromatography (cyclohexane/EtOAc 98:2) to afford **69e** (680 mg; 2.89 mmol).

**Yield**: 47%

**Solid state**: brown oil

**$R_f$** (cyclohexane/EtOAc 98:2): 0.20

**$^1$H-NMR** (300 MHz, $CDCl_3$): 3.89 (s, 3H); 4.46 (s, 2H); 7.49 (d, *J*= 1.6, 1H); 7.80 (d, *J*= 1.6, 1H)

Synthesis of **70e**

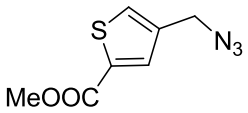


**70e**

$NaN_3$ (226 mg; 3.47 mmol) was added to the solution of **69e** (680 mg; 2.89 mmol) in DMF (6.7 ml). The reaction was stirred at 110 °C until completion (cyclohexane/EtOAc 98:2).

After 3 hours, the reaction was concentrated under reduced pressure and redissolved in EtOAc. The organic phase washed with distilled $H_2O$ and dried over $Na_2SO_4$.

After evaporation of the solvent *in vacuo*, the crude was purified by flash chromatography (cyclohexane/EtOAc 98:2) to afford **70e** (502 mg; 2.55 mmol).

**Yield**: 88%

**Solid state**: yellow oil

**$R_f$** (cyclohexane/EtOAc 98:2): 0.13

**$^1$H-NMR** (300 MHz, $CDCl_3$): 3.90 (s, 3H); 4,35 (s, 2H); 7.45 (d, *J*= 1.6, 1H); 7.75 (d, *J*= 1.6, 1H)

Synthesis of **66e**

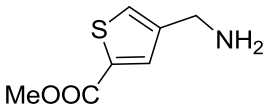


**66e**

To a solution of **70e** (502 mg; 2.55 mmol) in THF (21 ml), a catalytic amount of 5% Pd/C was added. The mixture was stirred at r.t. for 2 hours under a $H_2$ atmosphere and the reaction was followed by TLC ($CHCl_3$/MeOH 9:1).

The mixture was filtered under vacuum on a celite pad to eliminate the catalyst. After evaporation of the solvent, the crude was purified by flash chromatography using $CH_2Cl_2$/MeOH (95:5 to 8:2 gradient) as eluent to afford **66e** (150 mg; 0.88 mmol).

**Yield**: 35%

**Solid state**: yellow oil

**$R_f$** ($CHCl_3$/MeOH 85:15): 0.29

**$^1$H-NMR** (300 MHz, $CDCl_3$): 3.80 (s, 2H); 3.85 (s, 3H); 7.55 (d, *J*= 1.6, 1H); 7.80 (d, *J*= 1.6, 1H)

**[M+H]$^+$**: 172.0

Synthesis of **68f**

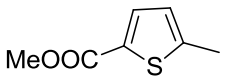


**68f**

A solution of 2-carboxy-5-methylthiophene (1.0 g; 7.03 mmol) in dry MeOH (10.2 ml) was treated with concentrated $H_2SO_4$ (1.02 ml). The reaction was refluxed at 66°C. for 24 hours and monitored by TLC (cyclohexane/EtOAc 9:1). After concentration, the mixture was redissolved in $Et_2O$ and washed with 2N NaOH, distilled $H_2O$ and brine.

The organic layer was dried over $Na_2SO_4$, filtered and concentrated in vacuo to give **68f** (845 mg; 5.41 mmol)

**Yield**: 77%

**Solid state**: yellow oil

**$R_f$** (cyclohexane/EtOAc 9:1): 0.44

**$^1$H-NMR** (300 MHz, $CDCl_3$): 2.51 (s, 3H); 3.85 (s, 3H); 6.75 (d, *J*= 3.7, 1H); 7.61 (d, *J*= 3.7, 1H)

Synthesis of **69f**

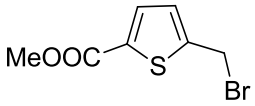


**69f**

A solution of **68f** (845mg; 5.41 mmol) in $CCl_4$ (21.4 ml) was treated with *N*-bromo-succinimmide (1.059 g; 5.95 mmol) and AIBN (84 mg; 0.51 mmol). The reaction was refluxed at 85°C and monitored by TLC (cyclohexane/EtOAc 98:2).

After 4 hours *N*-bromo-succinimmide was removed by filtration and the organic phase was washed with distilled $H_2O$, brine and dried over $Na_2SO_4$. The crude obtained after evaporation of the solvent was purified by flash chromatography (cyclohexane/EtOAc 98:2) to afford **69f** (755 mg; 3.21 mmol).

**Yield**: 59%

**Solid state**: brown oil

**$R_f$** (cyclohexane/EtOAc 98:2): 0.20

**$^1$H-NMR** (300 MHz, $CDCl_3$): 3.90 (s, 3H); 4.70 (s, 2H); 7.10 (d, *J*= 3.7, 1H); 7.65 (d, *J*= 3.7, 1H)

Synthesis of **70f**

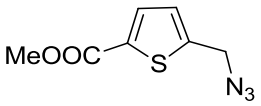


**70f**

$NaN_3$ (251 mg; 3.85 mmol) was added to the solution of **69f** (755 mg; 3.21 mmol) in DMF (7.4 ml). The reaction was stirred at 110 °C until completion (cyclohexane/EtOAc 98:2).

After 3 hours, the reaction was concentrated under reduced pressure and redissolved in EtOAc. The organic phase washed with distilled $H_2O$ and dried over $Na_2SO_4$.

After evaporation of the solvent *in vacuo*, the crude was purified by flash chromatography (cyclohexane/EtOAc 98:2) to afford **70f** (456 mg; 2.31 mmol).

**Yield**: 72%

**Solid state**: yellow oil

**$R_f$** (cyclohexane/EtOAc 98:2): 0.35

**$^1$H-NMR** (300 MHz, $CDCl_3$): 3.90 (s, 3H); 4.50 (s, 2H); 7.02 (d, *J*= 3.7, 1H); 7.70 (d, *J*= 3.7, 1H)

Synthesis of **66f**

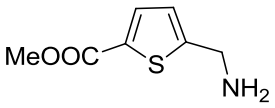


**66f**

To a solution of **70f** (456 mg; 2.31 mmol) in THF (18.8 ml), a catalytic amount of 5% Pd/C was added. The mixture was stirred at r.t. for 2 hours under a $H_2$ atmosphere and the reaction was followed by TLC ($CHCl_3$/MeOH 95:5).

The mixture was filtered under vacuum on a celite pad to eliminate the catalyst. After evaporation of the solvent, the crude was purified by flash chromatography using $CH_2Cl_2$/MeOH (95:5 to 8:2 gradient) to afford **66f** (208 mg; 1.21 mmol).

**Yield**: 53%

**Solid state**: yellow oil

**$R_f$** ($CHCl_3$/MeOH 95:5): 0.22

**$^1$H-NMR** (300 MHz, $CDCl_3$): 3.84 (s, 3H); 4.05 (s, 2H); 6.89 (d, *J*= 3.9, 1H); 7.64 (d, *J*= 3.9, 1H)

Synthesis of **72a**

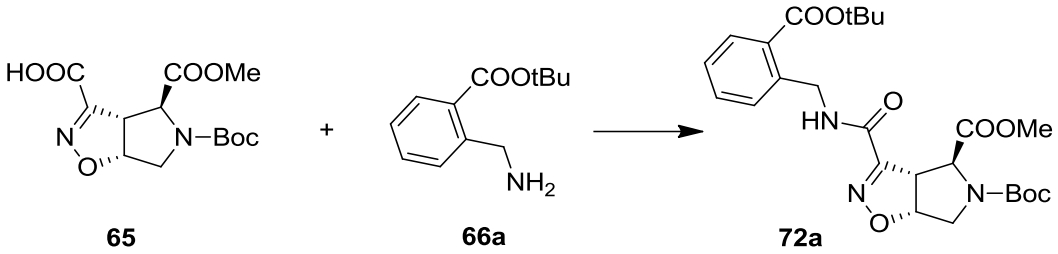


**65** **66a** **72a**

Compound **65** (152 mg; 0.48 mmol) was suspended in $CH_2Cl_2$ (16 ml).

HOBT hydrate (155 mg; 1.15 mmol), HBTU (436 mg; 1.15 mmol), DIPEA (418 µl; 2.40 mmol) and **66a** (110 mg; 0.53 mmol ).

The reaction was stirred at r.t. for 24 hours and was monitored by TLC (cyclohexane/EtOAc 6:4).

The organic phase was washed with distilled $H_2O$, dried over $Na_2SO_4$ and filtered.

After removal of the solvent, the crude was purified by flash chromatography (cyclohexane/EtOAc 6:4) to afford **72a** (140 mg; 0.24 mmol)

**Yield**: 58%

**Solid state**: white foam

**$R_f$** (cyclohexane/EtOAc 6:4): 0.33

**$[\alpha]^{20}_D$**= (–) 91.8 (c: 0.80 in $CHCl_3$)

**$^1$H-NMR** (300 MHz, DMSO/temp:100°C): 1.36 (s, 9H); 1.57 (s, 9H); 3.63 (dd, *J*= 5.0, 12.9, 1H); 3.70 (s, 3H); 3.78 (d, *J*= 12.9, 1H); 4.32 (dd, *J*= 1.2, 9.4, 1H); 4.67 (d, *J*= 1.2, 1H); 4.69 (d, *J*= 6.2, 2H); 5.34 (dd, *J*= 4.1, 9.4, 1H); 7.34 (d, *J*= 7.3, 1H); 7.40 (d, *J*= 8.2, 1H); 7.49 (t, *J*= 7.9, 1H); 7.76 (d, *J*= 7.9, 1H); 8.46 (t, *J*= 6.2, 1H)

**$^{13}$C-NMR** (75 MHz, $CDCl_3$): 28.42 (6C), 42.80, 52.93, 54.93, 55.70, 62.60, 81.29, 82.36, 86.00, 128.16, 131.29 (2C), 131.81, 132.63, 138.66, 152.66, 154.03, 158.50, 166.91, 171.55

**$[M+H_2O]^+$**: 521.3

Synthesis of **9a**

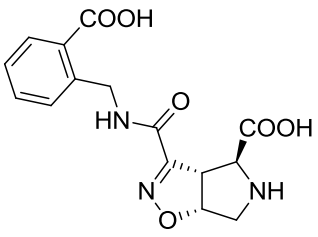


**9a**

1) Derivative **72a** (140 mg, 0.24 mmol) was dissolved in MeOH (0.84 mL) and treated with 1N aqueous NaOH (0.84 mL).The mixture was stirred at room temperature for 3 hours and the disappearance of the starting material was monitored by TLC (cyclohexane/EtOAc 6:4).
After evaporation of MeOH, the aqueous layer was washed with $Et_2O$, made acidic with 2N aqueous HCl and extracted with EtOAc. The organic phase was dried over anhydrous $Na_2SO_4$ and, after evaporation of the solvent, the acidic intermediate (120 mg, 0.24 mmol,) was obtained as a pale yellow solid.

**Yield**: 88%

**Solid state**: pale yellow solid

**R**$_f$ ($CHCl_3$/MeOH 9:1 + 1% AcOH): 0.60

2) The acidic intermediate (120 mg, 0.24 mmol) was treated with a 30% $CH_2Cl_2$ solution of trifluoroacetic acid (820 µL,) at 0°C. The solution was stirred at room temperature for 3 hours and the reaction was followed by TLC ($CH_2Cl_2$/MeOH 9:1 + 1% AcOH).
The volatiles were removed under reduced pressure and the solid residue was taken up with MeOH, filtered, washed with MeOH and $Et_2O$ and dried to give **9a** (50 mg, 0.15 mmol) as a white powder.

**Yield**:63%

**Solid state**: white solid

**$R_f$** (*n*-butanol/$H_2O$ /AcOH 4:2:1): 0.41

**$[\alpha]^{20}_D$**: not determined

**M.p.**: dec. T > 200°C

**$^1$H-NMR** (300 MHz, DMSO): 3.20-3.26 (m, 2H); 4.00 (s, 1H); 4.33 (d, *J*= 9.4, 1H); 4.69 (d, *J*= 4.5, 2H); 5.29-5.37 (m, 1H); 7.32-7.42 (m, 2H); 7.53 (t, *J*= 7.0, 1H); 7.87 (d, *J*= 7.3, 1H); 9.14-9.23 (m, 1H)

**$^{13}$C-NMR** (75 MHz, DMSO): 41.72, 53.69, 56.13, 65.30, 87.66, 127.61, 128.45, 130.34, 131.12, 132.69, 140.37, 154.29, 159.69, 169.20, 171.00

**$[M-H]^-$**: 331.9

Synthesis of **72b**

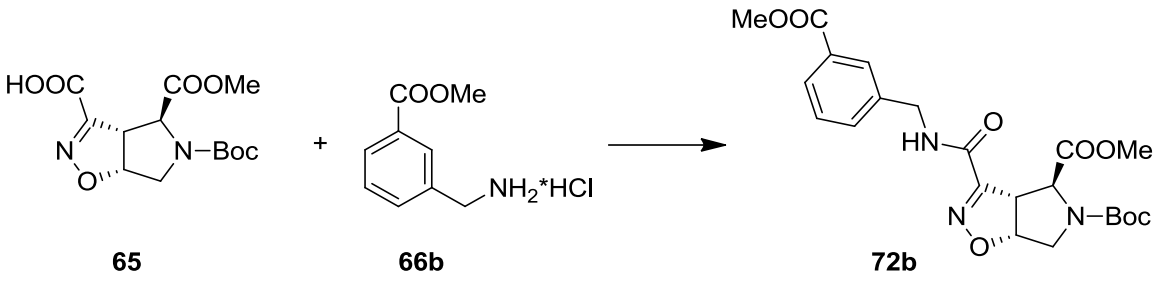


**65** **66b** **72b**

Compound **65** (214 mg; 0.68 mmol) was suspended in $CH_2Cl_2$ (22 ml).

HOBT hydrate (182 mg; 1.34 mmol), HBTU (508 mg; 1.34 mmol), DIPEA (294 µl; 1.68 mmol) and a solution of **66b** (125 mg; 0.62 mmol) in $CH_2Cl_2$ (2.8 ml) and DIPEA (196 µl; 1.12 mmol) were added to the flask.

The reaction was stirred at r.t. for 24 hours and was monitored by TLC (cyclohexane/EtOAc 6:4).

The organic phase was washed with distilled $H_2O$, dried over $Na_2SO_4$ and filtered.

After removal of the solvent, the crude was purified by flash chromatography (cyclohexane/EtOAc 7:3) to afford **72b** (166 mg; 0.36 mmol).

**Yield**: 58%

**Solid state**: white foam

**R**$_f$ (cyclohexane/EtOAc 6:4): 0.24

$[\alpha]^{20}_D$= (–)97.9 (c: 0.90 in $CHCl_3$)

**$^1$H-NMR** (300 MHz, DMSO/temp:100°C): 1.36 (s, 9H); 3.63 (dd, *J*= 5.3, 12.9, 1H); 3.69 (s, 3H); 3.76 (d, *J*= 12.9, 1H); 3.85 (s, 3H); 4.32 (d, *J*= 8.9, 1H); 4.36-4.54 (m, 2H); 4.65 (s, 1H); 5.34 (dd, *J*= 5.3, 8.9, 1H); 7.46 (t, *J*= 7.6, 1H); 7.57 (d, *J*= 7.6, 1H); 7.83 (d, *J*= 7.6, 1H); 7.92 (s, 1H); 8.84-8.94 (m, 1H)

**$^{13}$C-NMR** (75 MHz, $CDCl_3$): 28.43 (3C), 43.38, 52.44, 52.97, 54.09, 55.14, 62.64, 81.40, 86.84, 129.13 (2C), 129.24, 130.92, 132.60, 137.92, 152.51, 154.24, 159.09, 166.95, 171.42

**[M-H]$^-$**: 460.2

Synthesis of **9b**

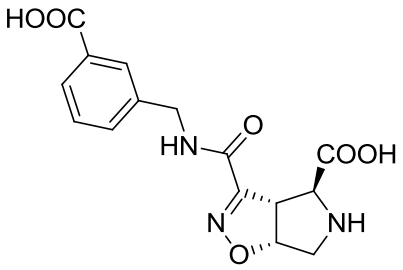


**9b**

1) Derivative **72b** (166 mg, 0.36 mmol) was dissolved in MeOH (1.08 mL) and treated with 1N aqueous NaOH (1.08 mL).The mixture was stirred at room temperature for 3 hours and the disappearance of the starting material was monitored by TLC (cyclohexane/EtOAc 6:4).

After evaporation of MeOH, the aqueous layer was washed with $Et_2O$, made acidic with 2N aqueous HCl and extracted with EtOAc. The organic phase was dried over anhydrous $Na_2SO_4$ and, after evaporation of the solvent, the diacidic intermediate (158 mg, 0.36 mmol,) was obtained as a pale yellow solid.

**Yield**: 94%

**R**$_f$ ($CHCl_3$/MeOH 9:1 + 1% AcOH): 0.24

2) The diacidic intermediate (158 mg, 0.36 mmol) was treated with a 30% $CH_2Cl_2$ solution of trifluoroacetic acid (350 µL,) at 0°C. The solution was stirred at room temperature for 3 hours and the reaction was followed by TLC ($CH_2Cl_2$/MeOH 9:1 + 1% AcOH).

The volatiles were removed under reduced pressure and the solid residue was taken up with MeOH, filtered, washed with MeOH and $Et_2O$ and dried to give **9b** (76 mg, 0.23 mmol) as a white powder.

**Yield**: 64%

**R**$_f$ (*n*-butanol/$H_2O$ /AcOH 4:2:1): 0.44

**M.p.:** dec. T >200°C

**$[\alpha]^{20}_D$**: (–)74.1 (c: 0.20 in $CHCl_3$)

**$^1$H-NMR** (300 MHz, DMSO): 3.19-3.25 (m, 2H); 3.98 (d, *J*= 2.5, 1H); 4.29 (dd, *J*= 2.5, 9.4, 1H); 4.40 (d, *J*= 5.8, 2H); 5.28-5.35 (m, 1H); 7.44 (t, *J*= 7.7, 1H); 7.53 (d, *J*= 7.7, 1H); 7.81 (d, *J*= 7.7, 1H); 7.87 (s, 1H); 9.53 (t, *J*= 5.8, 1H)

**$^{13}$C-NMR** (75 MHz, DMSO): 42.71, 53.72, 56.14, 65.31, 87.87, 128.56, 129.01, 129.24, 131.50, 132.64, 140.25, 154.25, 159.71, 167.95, 171.15

**$[M-H]^-$**: 331.9

Synthesis of **72c**

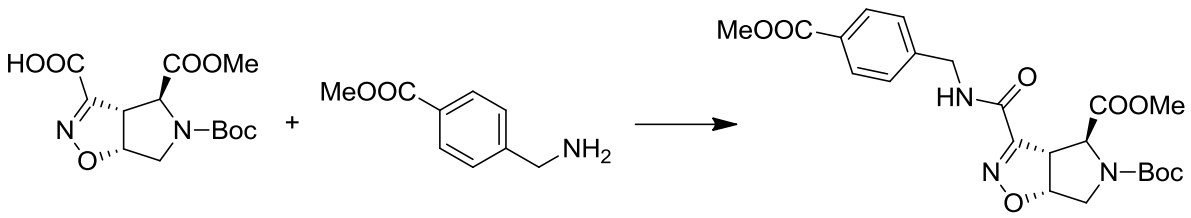


**65** **66c** **72c**

Compound **65** (180 mg; 0.57 mmol) was suspended in $CH_2Cl_2$ (18.8 ml).

HOBT hydrate (185 mg; 1.37 mmol), HBTU (520 mg; 1.37 mmol), DIPEA (496 µl; 2.85 mmol) and **66c** (104 mg; 0.63 mmol ).

The reaction was stirred at r.t. for 24 hours and was monitored by TLC (cyclohexane/EtOAc 6:4).

The organic phase was washed with distilled $H_2O$, dried over $Na_2SO_4$ and filtered.

After removal of the solvent, the crude was purified by flash chromatography (cyclohexane/EtOAc 6:4) to afford **72c** (165 mg; 0.36 mmol)

**Yield** : 63%

**Solid state**: white foam

**$R_f$** (cyclohexane/EtOAc 6:4): 0.22

**$[\alpha]^{20}_D$**: (–)126.2 (c: 0.56 in $CHCl_3$)

**$^1$H-NMR** (300 MHz, DMSO/temp:100°C): 1.37 (s, 9H); 3.65 (dd, *J*= 5.9, 12.9, 1H); 3.71 (s, 3H); 3.79 (d, *J*= 12.9, 1H); 3.87 (s, 3H); 4.33 (d, *J*= 10.3, 1H); 4.45-4.51 (m, 2H); 4.67 (s, 1H); 5.35 (dd, *J*= 5.9, 10.3, 1H); 7.43 (d, *J*= 7.9, 2H); 7.91 (d, *J*= 7.9, 2H); 8.83-8.93 (m, 1H)

**$^{13}$C-NMR** (75 MHz, $CDCl_3$): 28.46 (3C), 43.40, 52.42, 53.04, 54.09, 55.49, 62.78, 81.47, 86.47, 127.89, 130.37 (2C), 142.50, 152.66, 154.03, 158.50, 166.91, 171.41

**$[M-H]^-$**: 460.2

Synthesis of **9c**

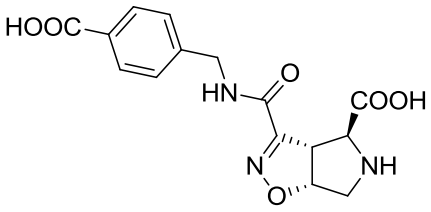


**9c**

1) Derivative **72c** (150 mg, 0.33 mmol) was dissolved in MeOH (0.99 mL) and treated with 1N aqueous NaOH (0.99 mL).The mixture was stirred at room temperature for 3 hours and the disappearance of the starting material was monitored by TLC (cyclohexane/EtOAc 6:4).

After evaporation of MeOH, the aqueous layer was washed with $Et_2O$, made acidic with 2N aqueous HCl and extracted with EtOAc. The organic phase was dried over anhydrous $Na_2SO_4$ and, after evaporation of the solvent, the diacidic intermediate (140 mg, 0.32 mmol,) was obtained as a pale yellow solid.

**Yield**: 94%

**Solid state**: pale yellow solid

**R**$_f$ ($CHCl_3$/MeOH 9:1 + 1% AcOH): 0.24

2) The diacidic intermediate (140 mg, 0.32 mmol) was treated with a 30% $CH_2Cl_2$ solution of trifluoroacetic acid (310 µL,) at 0°C. The solution was stirred at room temperature for 3 hours and the reaction was followed by TLC ($CH_2Cl_2$/MeOH 9:1 + 1% AcOH).

The volatiles were removed under reduced pressure and the solid residue was taken up with MeOH, filtered, washed with MeOH and $Et_2O$ and dried to give **9c** (75 mg, 0.23 mmol) as a white powder.

**Yield**: 70%

**Solid state**: white solid

**R**$_f$ (*n*-butanol/$H_2O$ /AcOH 4:2:1): 0.4

**M.p.:**dec T >200°C

**$[\alpha]^{20}_D$**: not determined

**$^1$H-NMR** (300 MHz, DMSO): 3.22-3.28 (m, 2H); 4.04 (d, *J*= 2.6, 1H); 4.32 (dd, *J*= 2.6, 9.1, 1H); 4.42 (d, *J*= 5.9, 2H); 5.30-5.37 (m, 1H); 7.39 (d, *J*= 8.2, 2H); 7.88 (d, *J*=8.2, 2H); 9.54 (t, *J*= 5.9, 1H)

**$^{13}$C-NMR** (75 MHz, DMSO): 42.73, 53.52, 56.01, 65.18, 87.56, 127.99 (2C), 130.04 (2C), 130.05, 144.81, 154.16, 159.71, 167.87, 170.68

**$[M-H]^-$**: 331.9

Synthesis of **72d**

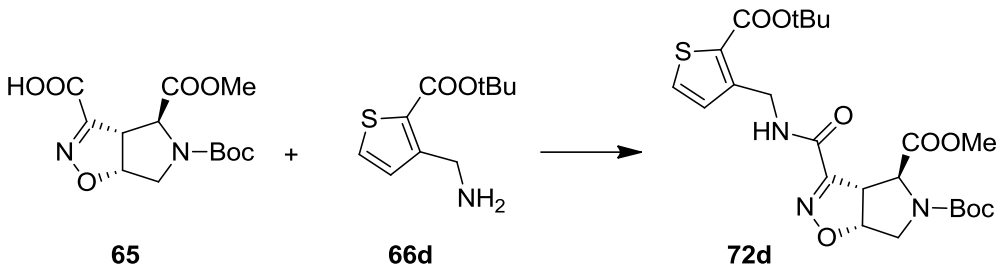


**65** **66d** **72d**

Compound **65** (220 mg; 0.70 mmol) was suspended in $CH_2Cl_2$ (23.1 ml).

HOBT hydrate (227 mg; 1.68 mmol), HBTU (637mg; 1.68 mmol), DIPEA (610 µl; 3.50 mmol) and **66d** (164 mg; 0.77 mmol ).

The reaction was stirred at r.t. for 24 hours and was monitored by TLC (cyclohexane/EtOAc 6:4).

The organic phase was washed with distilled $H_2O$, dried over $Na_2SO_4$ and filtered.

After removal of the solvent, the crude was purified by flash chromatography (cyclohexane/EtOAc 6:4) to afford **72d** (196 mg; 0.38 mmol)

**Yield**: 55%

**Solid state**: white foam

**$R_f$** (cyclohexane/EtOAc 6:4): 0.29

**$[\alpha]^{20}_D$**: (–) 89.2 (c: 0.56 in $CHCl_3$)

**$^1$H-NMR** (300 MHz, DMSO/temp:100°C): 1.42 (s, 9H); 1.60 (s, 9H); 3.69 (dd, *J*= 5.3, 12.9, 1H); 3.75 (s, 3H); 3.83 (d, *J*= 12.9, 1H); 4.38 (dd, *J*= 1.2, 9.4, 1H); 4.71 (d, *J*= 1.2, 1H); 4.75 (d, *J*= 6.2, 2H); 5.40 (dd, *J*= 5.3, 9.4, 1H); 7.12 (d, *J*= 5.0, 1H); 7.72 (d, *J*= 5.0, 1H); 8.65-8.75 (m, 1H)

**$^{13}$C-NMR** (75 MHz, $CDCl_3$): 28.48 (6C), 37.37, 54.14, 54.87, 55.66, 62.62, 81.36, 82.91, 86.59, 130.51 (2C), 130.76, 144.31, 152.58, 154.22, 158.80, 162.10, 171.53

**$[M+H_2O]^+$**: 572.2

Synthesis of **9d**

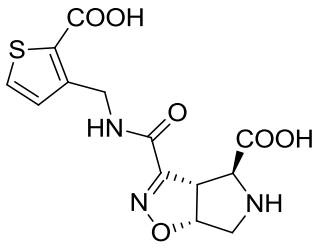


**9d**

1) Derivative **72d** (168 mg, 0.33 mmol) was dissolved in MeOH (0.99 mL) and treated with 1N aqueous NaOH (0.99 mL).The mixture was stirred at room temperature for 3 hours and the disappearance of the starting material was monitored by TLC (cyclohexane/EtOAc 6:4).

After evaporation of MeOH, the aqueous layer was washed with $Et_2O$, made acidic with 2N aqueous HCl and extracted with EtOAc. The organic phase was dried over anhydrous $Na_2SO_4$ and, after evaporation of the solvent, the acidic intermediate (168 mg, 0.33 mmol,) was obtained as a pale yellow solid.

**Yield**: quantitative

**Solid state**: pale yellow solid

**R**$_f$ ($CHCl_3$/MeOH 9:1 + 1% AcOH): 0.63

2) The acidic intermediate (168 mg, 0.33 mmol) was treated with a 30% $CH_2Cl_2$ solution of trifluoroacetic acid (1.1 ml) at 0°C. The solution was stirred at room temperature for 3 hours and the reaction was followed by TLC ($CH_2Cl_2$/MeOH 9:1 + 1% AcOH).

The volatiles were removed under reduced pressure and the solid residue was taken up with MeOH, filtered, washed with MeOH and $Et_2O$ and dried to give **9d** (83 mg, 0.25 mmol) as a white powder.

**Yield**: 77%

**Solid state**: white solid

**$R_f$** (*n*-butanol/$H_2O$ /AcOH 4:2:1): 0.41

**M.p.**: dec. T> 200°C

**$[\alpha]^{20}_D$**: (–) 82.7 (c: 0.14 in $CHCl_3$)

**$^1$H-NMR** (300 MHz, DMSO): 3.18-3.32 (m, 2H); 4.04 (d, *J*= 2.4, 1H); 4.33 (dd, *J*= 2.4, 9.4, 1H); 4.66 (d, *J*= 5.9, 2H); 5.30-5.37 (m, 1H); 7.08 (d, *J*= 5.0, 1H); 7.73 (d, *J*= 5.0, 1H); 9.38 (t, *J*= 5.9, 1H)

**$^{13}$C-NMR** (75 MHz, DMSO): 38.38, 53.64, 56.07, 65.18, 87.67, 128.14, 130.01, 131.78, 147.39, 154.18, 159.71, 164.05, 170.86

**$[M+H]^+$**: 340.0

Synthesis of **72e**

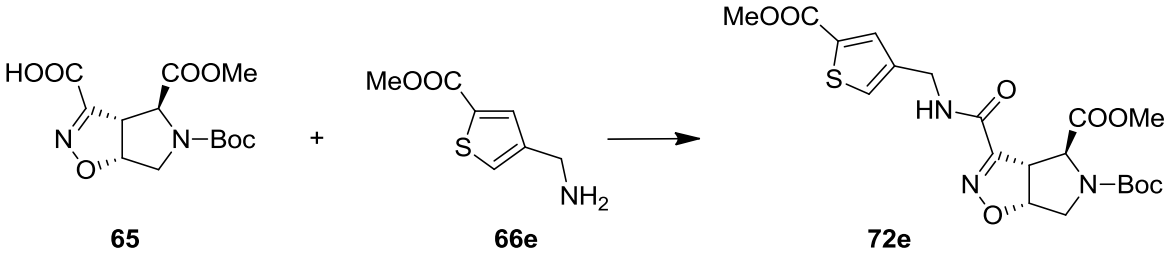


**65** **66e** **72e**

Compound **65** (200 mg; 0.64 mmol) was suspended in $CH_2Cl_2$ (20 ml).

HOBT hydrate (207 mg; 1.53 mmol), HBTU (580 mg; 1.53 mmol), DIPEA (555 µl; 3.18 mmol) and **66e** (131 mg; 0.76 mmol).

The reaction was stirred at r.t. for 24 hours and was monitored by TLC (cyclohexane/EtOAc 6:4).

The organic phase was washed with distilled $H_2O$, dried over $Na_2SO_4$ and filtered.

After removal of the solvent, the crude was purified by flash chromatography (cyclohexane/EtOAc 6:4) to afford **72e** (178mg; 0.38 mmol).

**Yield**: 59%

**Solid state**: pale yellow foam

**R**$_f$ (cyclohexane/EtOAc 6:4): 0.20

**[α]$^{20}_D$**: (–) 108.9 (c: 0.90 in $CHCl_3$)

**$^1$H-NMR** (300 MHz, DMSO/temp:100°C): 1.36 (s, 9H); 3.63 (dd, *J*= 5.0, 12.6, 1H); 3.70 (s, 3H); 3.75 (d, *J*= 12.6, 1H); 3.81 (s, 3H); 4.32 (dd, *J*= 1.8, 9.4, 1H); 4.34-4.41 (m, 2H); 4.65 (d, *J*= 1.8, 1H); 5.33 (dd, *J*= 5.0, 9.4, 1H); 7.64 (s, 1H); 7.72 (s, 1H); 8.74-8.85 (m, 1H)

**$^{13}$C-NMR** (75 MHz, $CDCl_3$): 28.41, 38.62, 52.47, 54.07, 54.71, 55.50, 62.79, 81.41, 86.79, 129.92, 133.55, 134.59, 139.17, 152.57, 154.01, 158.89, 162.58, 171.36

**[M-H]$^-$**: 466.1

Synthesis of **9e**

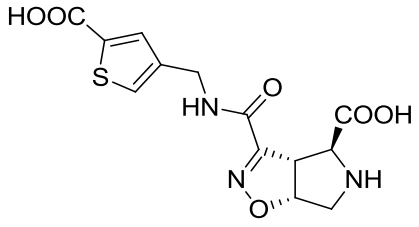

**9e**

1) Derivative **72e** (160 mg, 0.34 mmol) was dissolved in MeOH (1.03 mL) and treated with 1N aqueous NaOH (1.03 mL).The mixture was stirred at room temperature for 3 hours and the disappearance of the starting material was monitored by TLC (cyclohexane/EtOAc 6:4).

After evaporation of MeOH, the aqueous layer was washed with $Et_2O$, made acidic with 2N aqueous HCl and extracted with EtOAc. The organic phase was dried over anhydrous $Na_2SO_4$ and, after evaporation of the solvent, the diacidic intermediate (150 mg, 0.34 mmol,) was obtained as a white solid.

**Yield**: quantitative

**Solid state**: white powder

**R**$_f$ ($CH_2Cl_2$/MeOH 8:2 + 1% AcOH): 0.30

2) The diacidic intermediate (150 mg, 0.34 mmol) was treated with a 30% $CH_2Cl_2$ solution of trifluoroacetic acid (330 µL,) at 0°C. The solution was stirred at room temperature for 3 hours and the reaction was followed by TLC ($CH_2Cl_2$/MeOH 9:1 + 1% AcOH).

The volatiles were removed under reduced pressure and the solid residue was taken up with MeOH, filtered, washed with MeOH and $Et_2O$ and dried to give **9e** (79 mg, 0.23 mmol) as a white powder.

**Yield**: 69%

**Solid state**: white solid

**R**$_f$ (*n*-butanol/$H_2O$ /AcOH 4:2:1): 0.36

**M.p.**: dec. T >195°C

**$[\alpha]^{20}_{D}$**: not determined

**$^{1}$H-NMR** (300 MHz, DMSO): 3.23-3.30 (m, 2H); 4.04 (d, *J*= 2.5, 1H); 4.28-4.36 (m, 3H); 5.28-5.37 (m, 1H); 7.63 (s, 1H); 7.65 (s, 1H); 9.50 (t, *J*= 6.1, 1H)

**$^{13}$C-NMR** (75 MHz, DMSO): 38.39, 53.51, 56.02, 65.15, 87.58, 129.97, 134.02, 135.32, 141.35, 154.18, 159.49, 163.54, 170.73

**$[M-H]^{-}$**: 337.9

Synthesis of **72f**

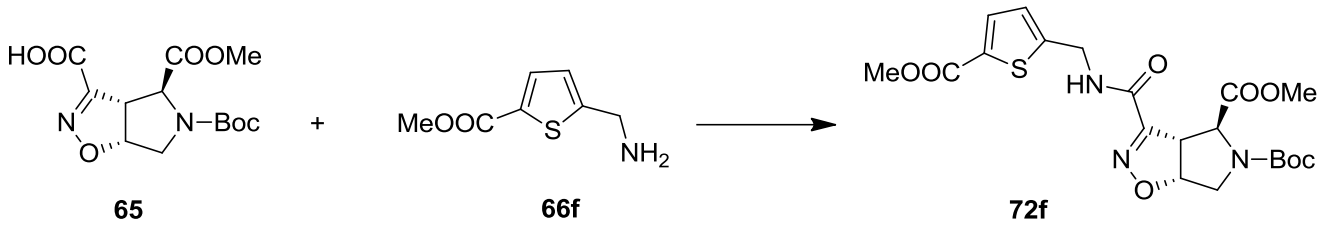


**65** **66f** **72f**

Compound **65** (180 mg; 0.57 mmol) was suspended in $CH_2Cl_2$ (18.8 ml).

HOBT hydrate (185 mg; 1.37 mmol), HBTU (520 mg; 1.37mmol), DIPEA (496 µl; 2.85 mmol) and **66f** (120 mg; 0.70 mmol).

The reaction was stirred at r.t. for 24 hours and was monitored by TLC (cyclohexane/EtOAc 6:4).

The organic phase was washed with distilled $H_2O$, dried over $Na_2SO_4$ and filtered.

After removal of the solvent, the crude was purified by flash chromatography (cyclohexane/EtOAc 6:4) to afford **72f** (178 mg; 0.38 mmol) as a white foam.

**Yield**: 53%

**Solid state**: white foam

**$R_f$** (cyclohexane/EtOAc 6:4): 0.17

**$[\alpha]^{20}_D$**: (–) 105.8 (c: 0.90 in $CHCl_3$)

**$^1$H-NMR** (300 MHz, DMSO/temp:100°C): 1.36 (s, 9H); 3.63 (dd, *J*= 5.3, 12.9, 1H); 3.69 (s, 3H); 3.74 (d, *J*= 12.9, 1H); 3.80 (s, 3H); 4.33 (dd, *J*= 1.8, 9.4, 1H); 4.57 (d, *J*= 5.9, 2H); 4.65 (d, *J*= .8, 1H); 5.35 (dd, *J*= 5.3, 9.4, 1H); 7.05 (d, *J*= 3.8, 1H); 7.62 (d, *J*= 3.8, 1H); 8.92-9.04 (m, 1H)

**$^{13}$C-NMR** (75 MHz, $CDCl_3$): 28.44 (3C), 38.56, 52.44, 54.05, 54.60, 55.39, 62.64, 81.46, 87.02, 127.10, 133.31, 133.82, 147.54, 152.39, 154.21, 158.86, 162.61, 171.35

**$[M-H]^-$**: 466.1

Synthesis of **9f**

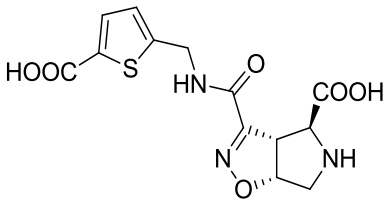


**9f**

1) Derivative **72f** (178 mg, 0.38 mmol) was dissolved in MeOH (1.1 mL) and treated with 1N aqueous NaOH (1.1 mL).The mixture was stirred at room temperature for 3 hours and the disappearance of the starting material was monitored by TLC (cyclohexane/EtOAc 6:4).

After evaporation of MeOH, the aqueous layer was washed with $Et_2O$, made acidic with 2N aqueous HCl and extracted with EtOAc. The organic phase was dried over anhydrous $Na_2SO_4$ and, after evaporation of the solvent, the diacidic intermediate (130 mg, 0.30 mmol,) was obtained as a white solid.

**Yield**: 79%

**Solid state**: white solid

**R**$_f$ ($CH_2Cl_2$/MeOH 8:2 + 1% AcOH): 0.34

2) The diacidic intermediate (130 mg, 0.30 mmol) was treated with a 30% $CH_2Cl_2$ solution of trifluoroacetic acid (285 µL,) at 0°C. The solution was stirred at room temperature for 3 hours and the reaction was followed by TLC ($CH_2Cl_2$/MeOH 9:1 + 1% AcOH).

The volatiles were removed under reduced pressure and the solid residue was taken up with MeOH, filtered, washed with MeOH and $Et_2O$ and dried to give **9f** (60 mg, 0.18 mmol) as a white powder.

**Yield**: 60%

**Solid state**: white solid

**R**$_f$ (n- butanol/$H_2O$ /AcOH 4:2:1): 0.44

**M.p.**: dec. T >200°C

**$[\alpha]^{20}_{D}$**: not determined

**$^{1}$H-NMR** (300 MHz, DMSO): 3.25 (s, 2H); 4.01 (d, *J*= 2.5, 1H); 4.31 (dd, *J*= 2.5, 9.4, 1H); 4.52 (d, *J*= 5.8, 2H); 5.30-5.37 (m, 1H); 7.02 (d, *J*= 3.9, 1H); 7.55 (d, *J*= 3.9, 1H); 9.69 (t, *J*= 5.8, 1H)

**$^{13}$C-NMR** (75 MHz, DMSO): 38.39, 53.53, 55.94, 65.22, 87.81, 127.21, 133.63, 133.88, 150.15, 154.07, 159.62, 163.55, 170.90

**$[M-H]^{-}$**: 337.9

## 6.3 HPLC CHROMATOGRAMS

### 6.3.1 HPLC chromatograms of (–)-26 and (+)-26

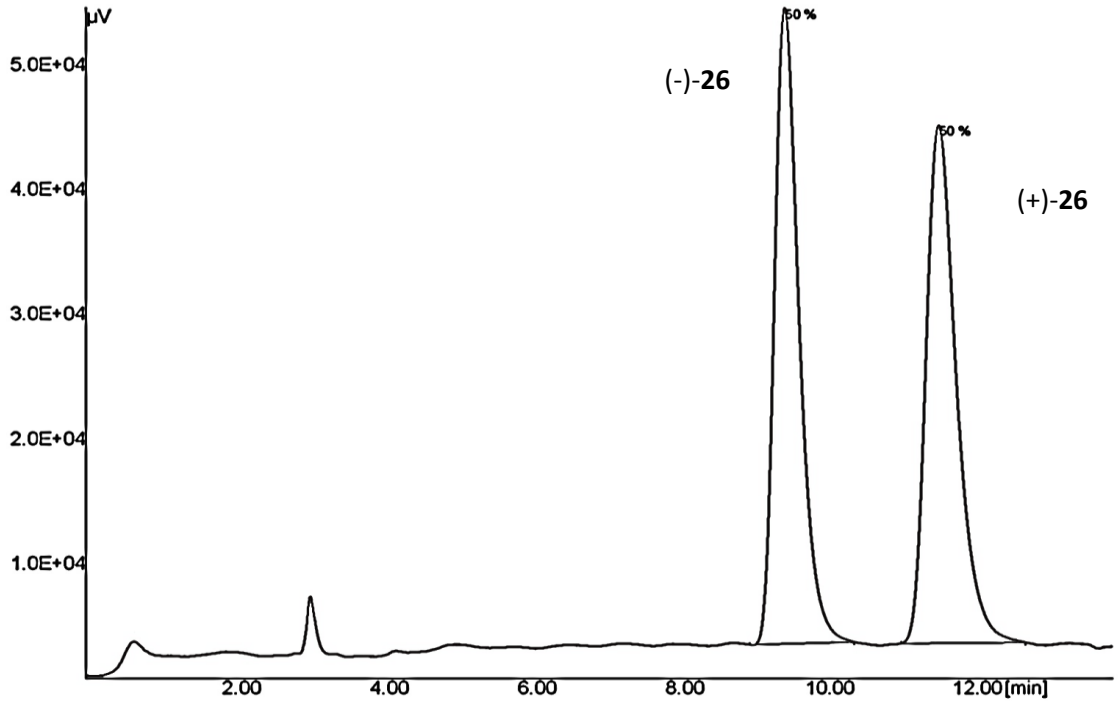


Analytical chiral HPLC condition of the two enantiomers (–)-**26** and (+)-**26**.

Eluent: n-hexane/iPrOH 95:5, Column: Kromasil Amycoat, Flow: 1 ml/min, wavelength; 220 nm.

**$R_t$ I enantiomer:** 9.46 min

**$R_t$ II enantiomer:** 11.55 min

**α** = $(tr_B - t_0) / (t_{rA} - t_0)$: 1.4 ($t_0$ = 3.0 min)

**$R_s$**= $2*[(t_{rb}-t_{ra})/(w_a+w_b)]$: 2.5

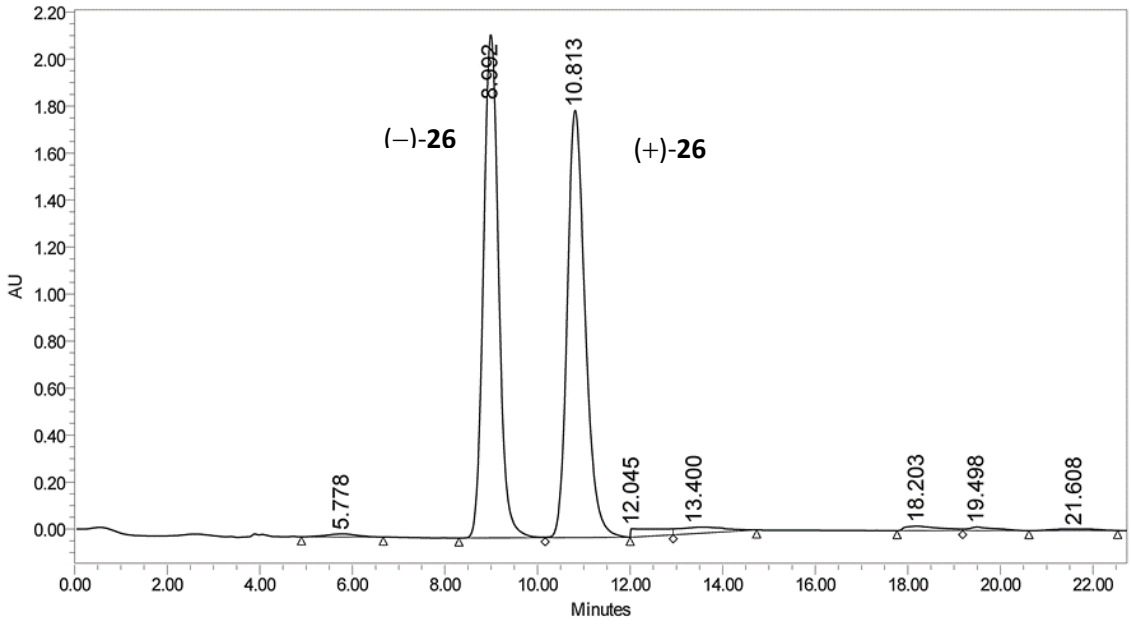


Preparative chiral HPLC condition of the two enantiomers (−)-**26** and (+)**-26**.

Eluent: n-hexane/iPrOH 9:1, Column: Kromasil 5-Amycoat, Flow: 15 ml/min, wavelength; 220 nm.

**$R_t$ I enantiomer:** 8.99 min

**$R_t$ II enantiomer:** 10.81 min

## 6.3.2 HPLC chromatograms of (–)-36 and (+)-36

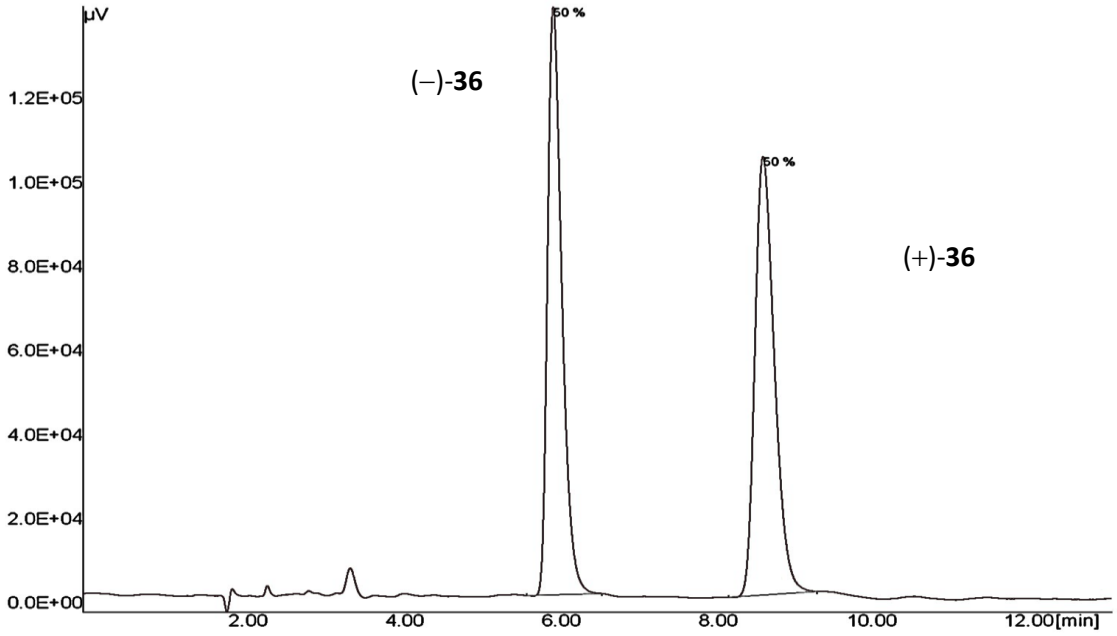


Analytical chiral HPLC condition of the two enantiomers (–)-**36** and (+)-**36**.

Eluent: n-hexane/iPrOH 8:2, Column: Lux-2 amylose, Flow: 1 ml/min, wavelength: 220 nm.

**$R_t$ I enantiomer:** 6.00 min

**$R_t$ II enantiomer:** 8.68 min

**α** = $(tr_B - t_0) / (tr_A - t_0)$: 1.9 ($t_0$ = 2.0 min)

**$R_s$**= $2*[(t_{rb}-t_{ra})/(w_a+w_b)]$: 3.9

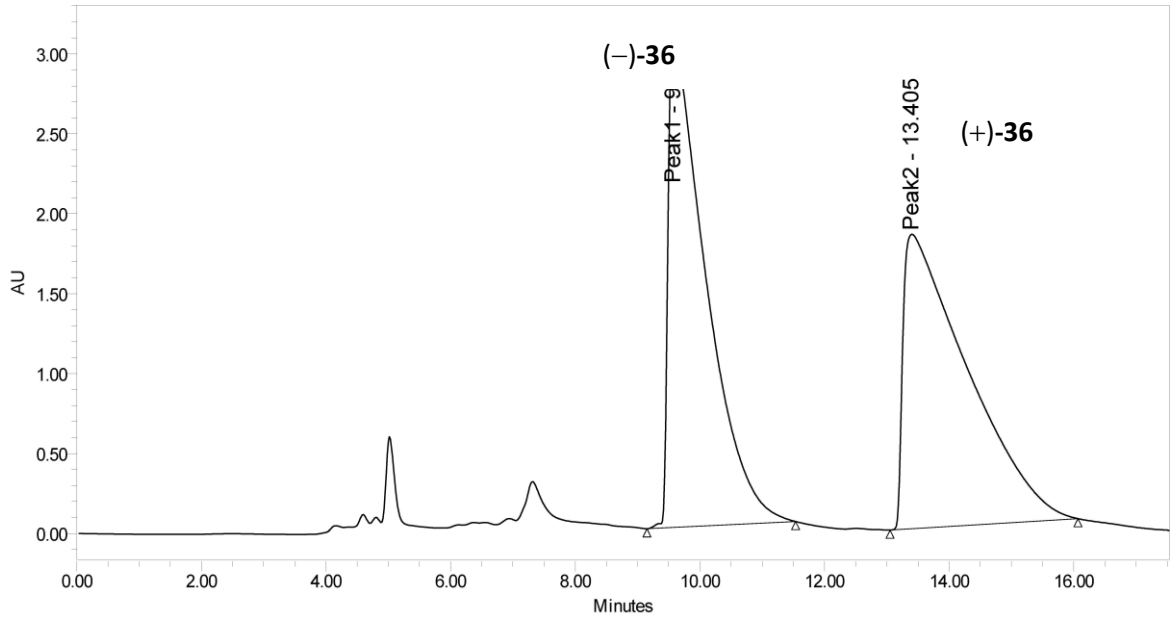


Preparative chiral HPLC condition of the two enantiomers (−)-**36** and (+)-**36**.

Eluent: n-hexane/iPrOH 7:3, Column Lux-2 amylose, Flow: 15 ml/min, wavelength; 220 nm.

**$R_t$ I enantiomer:** 9.58 min

**$R_t$ II enantiomer:** 13.40 min

## 6.3.3 HPLC chromatograms of (–)-32 and (+)-33

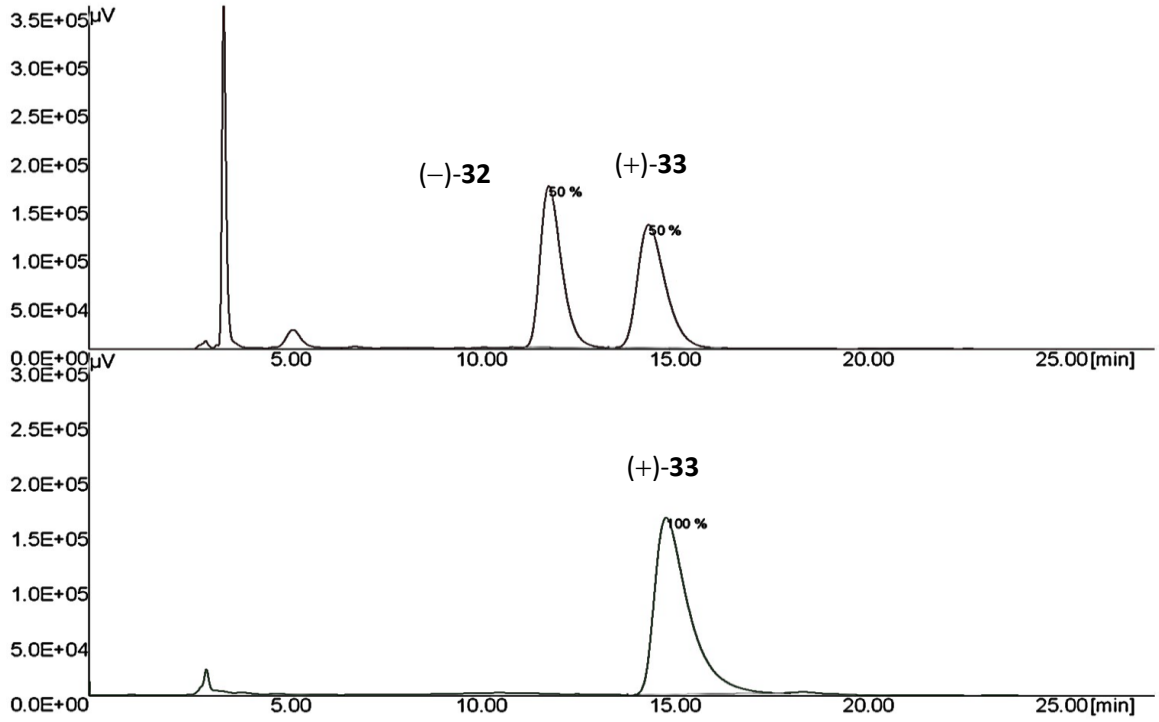


Analytical HPLC condition of (–)-**32** and (+)-**33** compared with enantiopure standard (+)-**33**: Eluent: n-hexane/iPrOH 7:3, Kromasil Amycoat, Flow: 1 ml/min, wavelength: 220 nm.

**$R_t$ I enantiomer** (+)-**33:** 11.88 min

**$R_t$ II enantiomer** (–)-**32:** 14.46 min

**α** = $(tr_B - t_0) / (tr_A - t_0)$: 1.3 ($t_0$ = 3.0 min)

**$R_s$**= $2*[(t_{rb}-t_{ra})/(w_a+w_b)]$: 2.0

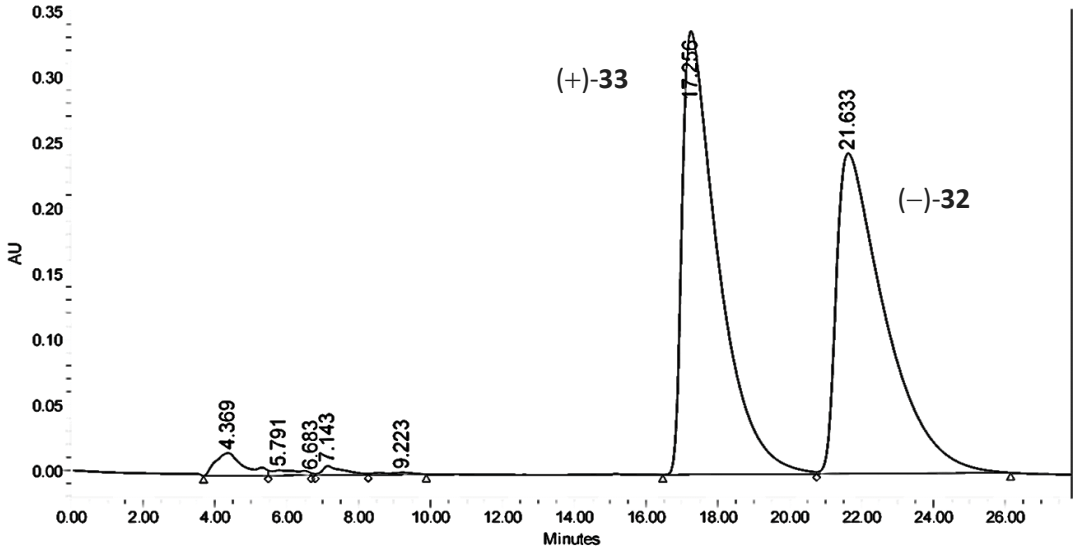


Preparative chiral HPLC condition of (–)-**32** and (+)-**33**. Eluent: n-hexane/iPrOH 1:1, Kromasil Amycoat, Flow: 15 ml/min, wavelength: 220nm.

**$R_t$ I diastereoisomer** (+)-**33:** 6.68 min

**$R_t$ II diastereoisomer** (–)-**32:** 7.14 min

## 6.3.4 HPLC chromatograms of (–)-38 and (+)-39

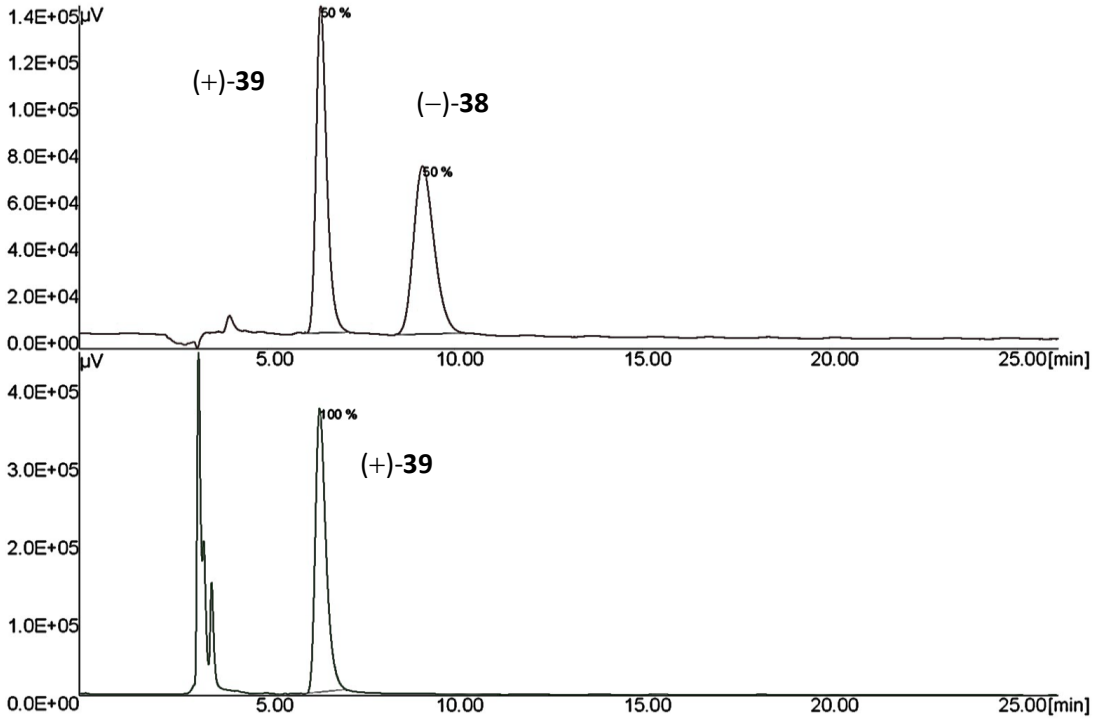


Analytical HPLC condition of (–)-**38** and (+)-**39** compared with enantiopure standard (+)-**39**.

Eluent: n-hexane/iPrOH 1:1, Kromasil, Flow: 1 ml/min, wavelength: 220 nm.

**$R_t$ I diastereoisomer** (+)-**39**: 6.43 min

**$R_t$ II diastereoisomer** (–)-**38:** 9.15 min

**α =** $(tr_B - t_0) / (tr_A - t_0)$: 1.9 ($t_0$ = 3.0 min)

**$R_s$=** $2*[(t_{rb}-t_{ra})/(w_a+w_b)]$: 3.0

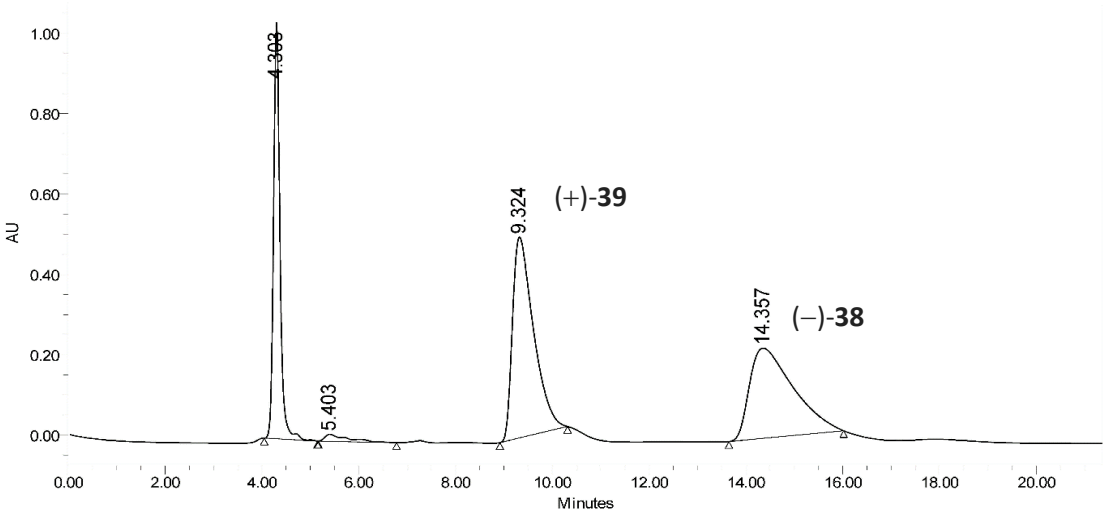


Preparative chiral HPLC condition of (–)-**38** and (+)-**39**. Eluent: n-hexane/iPrOH 1:1, Kromasil, Flow: 15 ml/min, wavelength: 220 nm.

**$R_t$ I diastereoisomer**: (+)-**39:** 9.32 min

**$R_t$ II diastereoisomer:** (-)-**38:** 14.36 min

## 6.3.5 HPLC chromatograms of (3α*R*,6*R*,6α*S*)-**62**, (3α*S*,4*S*,6α*R*)-**63** and (3α*S*,6*S*,6α*R*)-**64**

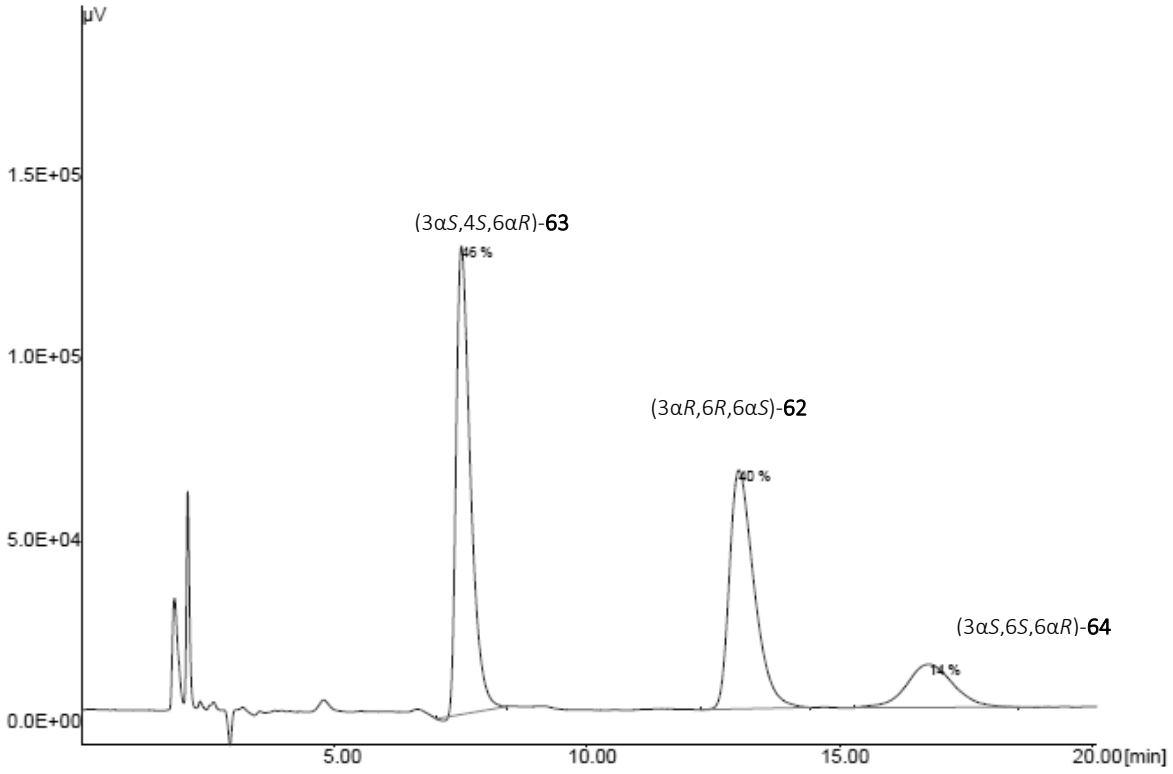


Analytical HPLC condition of (3α*R*,6*R*,6α*S*)-**62**, (3α*S*,4*S*,6α*R*)-**63** and (3α*S*,6*S*,6α*R*)-**64**.

Eluent: n-hexane/i-PrOH 8:2; Column: Lux Amylose; Flux: 1ml/min; wavelength: 220 nm.

**$R_t$ I diasteroisomer** (3α*S*,4*S*,6α*R*)-**63**: 7.51 min

**$R_t$ II diasteroisomer** (3α*R*,6*R*,6α*S*)-**62:** 13.01 min

**$R_t$ III diasteroisomer** (3α*S*,6*S*,6α*R*)-**64:** 16.77 min

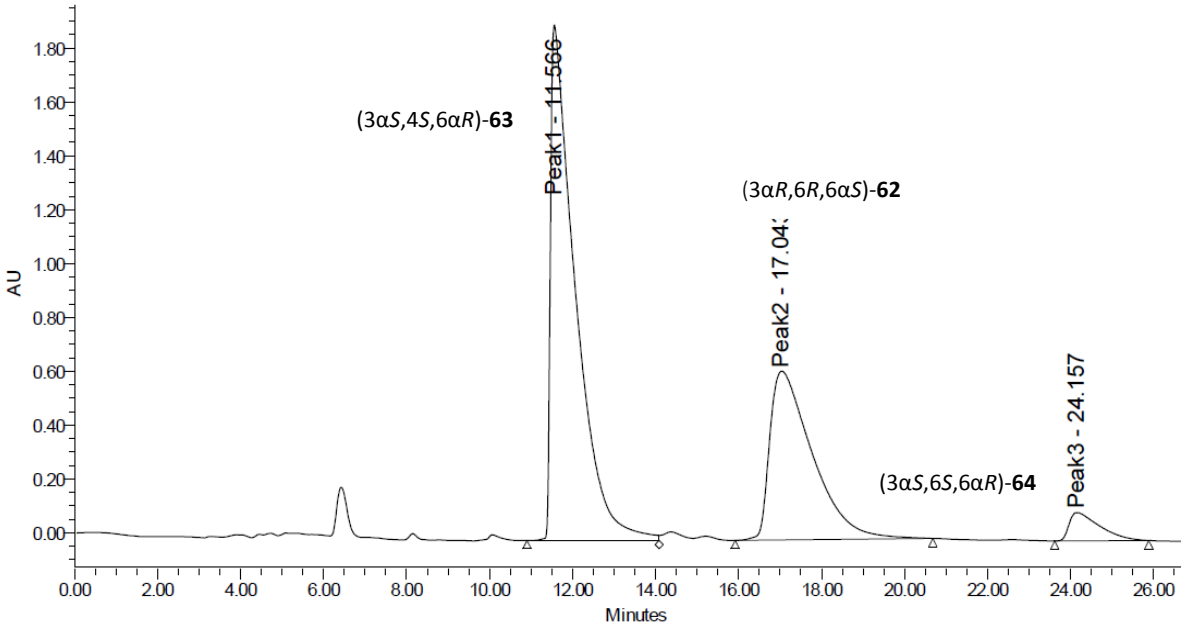


Preparative chiral HPLC condition of (3α*R*,6*R*,6α*S*)-**62**, (3α*S*,4*S*,6α*R*)-**63** and (3α*S*,6*S*,6α*R*)-**64**.

Eluent: n-hexane/iPrOH 7:3, Kromasil, Flow: 15 ml/min, wavelength: 220 nm.

**$R_t$ I diastereoisomer** (3α*S*,4*S*,6α*R*)-**63:** 11.57 min

**$R_t$ II diastereoisomer** (3α*R*,6*R*,6α*S*)-**62:** 17.04 min

**$R_t$ III diastereoisomer** (3α*S*,6*S*,6α*R*)-**64:** 24.16 min

# BIBLIOGRAPHY


[1]Meldrum, B. S. The Journal of nutrition **2000**, 130(4S Suppl), 1007S–1015S.

[2] McEntee, W. J.; Crook, T. H. *Psychopharmacology* **1993**, *111*, 391–401.

[3] Cooke, S. F.; Bliss T. V. *Brain* **2006**, *129*, 1659–73.

[4] Bliss, T. V.; Collingridge, G. L. *Nature* **1993**, *361*, 31–39.

[5] Takamori S., *Neurosci Res.*, **2006**, *55*, 343-51.

[6] Featherstone DE.,. *ACS Chem Neurosci.*, **2010**, *1*, 4-12.

[7] Beart P.M., O'Shea R.D., *Br J Pharmacol*; **2007**, *150*, 5–17.

[8] Olney, J. W.; Lodge, D. Ed., John Wiley, New York. **1988**, 337.

[9] Choi D.W.,. *Neuron*, **1988**, *1*, 623–634.

[10] Almeida A., Heales S.J., Bolanos J.P., Medina J.M.,. *Brain Res*, **1998**, *790*, 209–216.

[11] Coyle J. T., Tsai G.,. *Psycopharmacology*, **2004**, *174*, 32-38.

[12] Moroni F. **1998**, *1*, 266, Ed. UTET.

[13] Ferraguti F, Shigemoto R., *Cell Tissue Res.*, **2006**, *326*, 483–504.

[14] Wheal H.V.; Thomson A.M., Eds., *Excitatory Amino Acids and Synaptic Transmission*. Academic Press: London **1995**.

[15] Monaghan D.T.; Wenthold R.J.; Eds. *The Ionotropic Glutamate Receptors*; Humana Press: Totowa, New Jersey **1997**.

[16] Bräuner-Osborne H., Egebjer J.; Nielsen E.Ø., Madsen, U.; Krogsgaard-Larsen P., *J. Med. Chem.,* **2000**, *43*, 2609-2645.

[17] Treutlein J., Mühleisen T. W., Frank J., Mattheisen M., Herms S., Ludwig K. U., Treutlein T., Schmael C., Strohmaier J., Bösshenz K. V., Breuer R., Paul T., Witt S. H., Schulze T. G., Schlösser R. G., Nenadic I., Sauer H., Becker T., Maier W., Cichon S., Nöthen M. M., Rietschel M., *Schizophr. Res,* **2009**, *111*, 123–30.

[18] Malenka R.C., Niccol R.A., *Neuron*, **1997**, *19*, 473-476.

[19] Chittajallu R., Braithwaite S.P., Clarke V.R.J., Henley J.M., *Trends pharmacol. Sci*., **1999**, *20*, 26-35.

[20] Rodriguez-Moreno A.; Lerma J., *J. Neuron.* **1998**, *20*, 1211-1218.

[21] Kuusinen A., Arvola M., Keinänen K., *EMBO J.*, **1995**, *14*, 6327-6332.

[22] Mayer M.L., *Nature*, **2006**, *440*, 456-462.

[23] Hansen K.B., Furukawa H., Traynelis S.F., *Mol Pharmacol.*, **2010**, *78*, 535-549.

[24] Karakas E., Simorowski N., Furukawa H., *EMBO J.*, **2009**, *28*, 3910-3920.

[25] Armstrong N., Sun Y., Chen G.Q., Gouaux E., *Nature*, **1998**, *395*, 913-917.

[26] Kawamoto S., Uchino S., Xin K.Q., Hattori S., Hamajima K., Fukushima J., Mishina M., Okuda K., *Mol. Brain Res.*, **1997**, *47*, 339-344.

[27] Naur P., Vestergaard B., Skov L.K., Egebjerg J., Gajhede M., Kastrup J.S., *FEBS Lett.*, **2005**, *579*, 1154-1160.

[28] Armstrong N., Gouaux E., *Neuron*, **2000**, *28*, 165-81.

[29] Dean R. Madden, *Nat. Rev. Neurosci.*, **2002**, *3*, 91-101.

[30] Sun Y., Olson R., Horning M., Armstrong N., Mayer M., Gouaux E., *Nature*, **2002**, *417*, 245-53.

[31] Armstrong N., Jasti J., Beich-Frandsen M., Gouaux E., *Cell*, **2006**, *6*, 85-97.

[32] Traynelis S.F., Wollmuth L.P., McBain C.J., Menniti F.S., Vance K.M., Ogden K.K., Hansen K.B., Yuan H., Myers S.J., Dingledine R,. *Pharmacol Rev.*, **2010**, *62*, 405-496.

[33] Zhorov B. S., Tikhonov D. B., *J. Neurochem*, **2004**, *88*, 782–799.

[34] Jackson A.C., Nicoll R.A., *Neuron*, **2011**, *70*, 178-199.

[35] Johnson J.W., Kotermanski S.E., *Curr. Opin. Pharmacol.*, **2006**, *6*, 61-67.

[36] Johnson J.W., Ascher P., *Nature*, **1987**, *325*, 529-531.

[37] Nowak L., Bregestovski P., Ascher P., Herbet A., Prochiantz A., *Nature*, **1984**, *307*,462-5.

[38] Karakas, E.; Simorowski, N.; Furukawa, H. *The EMBO Journal*, **2009**, *28*, 3910–3920.

[39] Collingridge, G. L., Watkins, J. C., *Oxford University Press*: Oxford **1994**.

[40] Wong E. H. F., Kemp J., *Rev. Pharmacol. Toxicol*., **1991**, *31*, 401-425.

[41] Kyle D. J., Patch, R. J.; Karbon, E. W.; Ferkany, J. W.; Krogsgaard- Larsen, P., Hansen, J. J., Eds.; Ellis Horwood: Chichester, **1992**, 121-161.

[42] Shinozaki H.; Ishida M.; Shimamoto K.; Ohfune Y. *Brain Res*., **1989**, *480*, 355-359.

[43] Curry K.; Peet M. J.; Magnuson D. S. K.; McLennan H., *J. Med. Chem*., **1988**, *31*, 864-867.

[44] Allan R. D.; Hanrahan J. R.; Hambley T. W.; Johnston G. A. R.; Mewett K. N.; Mitrovic A. D., *J. Med. Chem*., **1990**, *33*, 2905-2915.

[45] Ornstein P. L.; Klimkowski V. J.; Krogsgaard-Larsen P., Hansen J. J., Ellis Horwood: Chichester, **1992**, 183-200.

[46] Lehmann J., Schneider J., McPherson S., Murphy D. E., Bernard P., Tsai C., Bennett D. A., Pastor G., Steele D. J., Boehm C., Cheney D. L., Liebermann J. M., Williams M., Wood P. L., *J. Pharmacol. Exp. Ther*. **1987**, *240*, 737-746.

[47] Hutchison A. J., Williams M., Angst C., De Jesus R., Blanchard L., Jackson R. H., Wilusz E. J., Murphy D. E., Bernard P. S., Schneider J., Campbell T., Guida W., Sills M., *J. Med. Chem*. **1989**, *32*, 2171-2178.

[48] Meldrum B. S., *Blackwell: Oxford*, **1991**.

[49] Ornstein P. L., Schoepp D. D., Arnold M. B., Leander D., Lodge D., Paschal J. W., Elzey T., *J. Med. Chem*. **1991**, *34*, 90-97.

[50] Chenard B. L., Menniti F. S, *Curr. Pharm. Des*. **1999**, *5*, 381-404.

[51] Mott D. D., Doherty J. J., Zhang S., Washburn M. S., Fendley M. J., Lyuboslavsky P., Traynelis S. F., Dingledine R., *Nat. Neurosci*. **1998**, *1*, 659-667.

[52] Williams K., *Mol. Pharmacol*. **1993**, *44*, 851-859.

[53] Bleakman D., Lodge D., *Neuropharmacology*, **1998**, *37*, 1187-1204.

[54] Benke T.A., Lüthi A., Isaac J.T., Collingridge G.L., *Nature,* **1998**, *393*, 793.

[55] Terashima A., Cotton L., Dev K. K., MeyerG., Zaman S., Duprat F., Henley J. M., Collingridge G. L., Isaac J. T., *Nat. Neurosci.*, **2006**, *9*, 602.

[56] Plant K., Pelkey K.A., Bortolotto Z. A., Morita D., Terashima A., McBain C. J., Collingridge G. L., Isaac J. T., *J. Neurosci.* **2004**, *24*, 5381**.**

[57] Hollmann M. and Heinemann S. *Ann. Rev. Neurosci*., **1994** *17*, 31–108. Cui C.H., Mayer M.L., **1999**. *J. Neurosci*., *19*, 8281–8291.

[58] Alt A., Weiss B., Ogden A.M., Knauss J.L., Oler J., Ho K., Large T.H., Bleakman D., *Neuropharmacology,* **2004**, *46*,793-806.

[59] Schiffer H.H., Swanson G.T., Heinemann S.F. *Neuron*, **1997**, *19*,1141-6.

[60] Ren Z., Riley N.J., Garcia E.P., Sanders J.M., Swanson G.T., Marshall J., *J. Neurosci*., **2003**, *23*,6608-16.

[61] Bowie D. *CNS Neurol Disord Drug Targets*, **2008**, 7,129-43.

[62] Chittajallu R., Braithwaite S.P., Clarke V.R., Henley J.M., *Trends Pharmacol Sci.*, **1999**, *20*, 26-35.

[63] Wisden W., Seeburg P.H., *J Neurosci*., **1993**, 13,3582–3598.

[64] Smolders I., Bortolotto Z.A., Clarke V.R., Warre R., Khan G.M., O'Neill M.J., Ornstein P.L., Bleakman D., Ogden A., Weiss B., Stables J.P., Ho K.H., Ebinger G., Collingridge G.L., Lodge D., Michotte Y., *Nat Neurosci*., **2002**, 5,796-804.

[65] Simmons R. M., Li D. L., Deverill M., Ornstein P.L. and Iyengar S. *Neuropharmacology*, **1998**, *37*, 25–36.

[66] Strutz-Seebohm N., Korniychuk G., Schwarz R., Baltaev R., Ureche O.N., Mack A.F., Ma Z.L., Hollmann M., Lang F., Seebohm G., *Cell Physiol. Biochem*., **2006**, *18*,287-94.

[67] Strutz N., Villmann C., Thalhammer A., Kizelsztein P., Eisenstein M., Teichberg V.I., Hollmann M., *J. Neurosci*., **2001**, *21*, 401-11.

[68] Pinheiro P.S., Perrais D., Coussen F., Barhanin J., Bettler B., Mann J.R., Malva J.O., Heinemann S.F., Mulle C., *Proc. Natl. Acad. Sci. U S A*., **2007**, *104*, 12181-6.

[69] Schiffer H.H., Heinemann S.F., *Am. J. Med. Genet. B. Neuropsychiatr. Genet*., **2007**, *144B*, 20-6.

[70] Hirbec H., Francis J.C., Lauri S.E., Braithwaite S.P., Coussen F., Mulle C., Dev K.K., Coutinho V., Meyer G., Isaac J.T., Collingridge G.L., Henley J.M., *Neuron*., **2003**, *37*,625-38.

[71] Zhang W., St-Gelais F., Grabner C.P., Trinidad J.C., Sumioka A., Morimoto-Tomita M, Kim KS, Straub C, Burlingame AL, Howe JR, Tomita S., *Neuron.*, **2009**, *61*,385-96.

[72] Lerma J., Marques J.M., *Neuron.* **2013**, *80*, 292-311.

[73] Lerma J., *Neurosci.* **2006**, *6*, 89-97.

[74] Rozas J. L., Paternain A. V., Lerma J.,. *Neuron*, **2003**, *39*,543-553.

[75] MacLean D. M., Wong A. Y. C., Fay A.M. and Bowie D., 2011. *The Journal of Neuroscience*. **2003**, *31*, 2136 –2144.

[76] Plested A.J., Vijayan R., Biggin P.C., Mayer M.L., *Neuron*, **2008**, *58*,720-35.

[77] Castillo P. E., Malenka R. C., Nicoll R. A. *Nature*, **1997**, *388*, 182-6.

[78] Pinheiro P. S., Lanore F., Veran J., Artinian J., Blanchet C., Crépel V., Perrais D., Mulle C., *Cortex*, **2013**, *23*,323-31.

[79] Rodríguez-Moreno A., Herreras O, Lerma J., *Neuron*., **1997**, *19*, 893-901.

[80] Kamiya H., Ozawa S., *J Physiol.*, **2000**, *523*,653-665.

[81] Wong L. A., Mayer M. L., Jane D. E. and Watkins J. C. *J. Neurosci*. **1994**, *14*, 3881–3897.

[82] Jane D. E., Hoo K., Kamboj R., Deverill M., Bleakman D. and Mandelzys A., *J. Med. Chem*. **1997**, *40*, 3645–3650.

[83] Campiani G., Morelli E., Nacci V., Fattorusso C., Ramunno A., Novellino E., Greenwood J., Liljefors T., Griffiths R., Sinclair C., Reavy H., Kristensen A.S., Pickering D.S., Schousboe A., Cagnotto A., Fumagalli E., Mennini T., *J Med Chem*., **2001**, *44*, 4501-4.

[84] Butini S., Pickering D.S., Morelli E., Coccone S.S., Trotta F., De Angelis M., Guarino E., Fiorini I., Campiani G., Novellino E., Schousboe A., Christensen J.K., Gemma S., *J Med Chem*., **2008**, *51*, 6614-8.

[85] Toms N. J., Reid M. E., Phillips W., Kemp. M. C. and Roberts P. J., *Neuropharmacology*, **1997**, *36*, 1483–1488.

[86] Dolman N.P., More J.C., Alt A., Knauss J.L., Troop H.M., Bleakman D., Collingridge G.L., Jane D.E., *J Med Chem*., **2006**, *49*,2579-92.

[87] Dolman N.P., More J.C., Alt A., Knauss J.L., Pentikäinen O.T., Glasser C.R., Bleakman D., Mayer M.L., Collingridge G.L., Jane D.E, *J Med Chem*., **2007**, 50, 1558-70.

[88] Mayer M.L., Ghosal A., Dolman N.P., Jane D.E., *J Neurosci*., **2006**, *26*,2852-61.

[89] O'Neill M. J., Bond A., Ornstein P. L., Ward M. A., Hicks C. A., Hoo K. et al. *Neuropharmacology* **1998**, *37*, 1211–1222.

[90] P.Wellendorph; H.Brauner-Osborne, *Br. J. Pharmacol*., **2009**, *156*, 869–884.

[91] Schoepp, D.D.; Jane, D.E.; Monn, J.A. *Neuropharmacology*, **1999**, 38, 1421-1477.

[92] Pin, J.P.; Duvoisin, R. *Neuropharmacology*, **1995**, *34*, 1-26.

[93] Romano, C., Yang, W. L., O'Malley, K.L, *J. Biol. Chem.*, **1996**, *271*, 28612-28616**.**

[94] Suzuki Y.; Moriyoshi E.; Tsuchiya D.; Jingami H; *J. Biol. Chem.,* **2004**, *279*, 35526-35534.

[95] Gregory K. J., Dong E. N., Meiler J., Conn P. J., *Neuropharmacology*, **2011**, *60*, 66-81

[96] Gregory K. J., Nguyen E. D., Malosh C., Mendenhall J. L., Zic J. Z., Bates B. S., Noetzel M. J., Squire E. F., Turner E. M., Rook J. M., Emmitte K. A., Stauffer S.R., Lindsley C. W., Meiler J. and Conn P.J., *ACS Chem. Neurosci.*, **2014**, *5*, 282-295.

[97] Shimamoto K.; Ohfune Y., *J. Med. Chem*. **1996**, *39*, 407-423.

[98] Monn J.A., Valli M.J., Massey S.M., Wright R.A., Salhoff C.R., Johnson B.G., Howe T., Alt C.A., Rhodes G.A., Robey, R.L., Griffey K.R., Tizzano J.P., Kallman M.J., Helton D.R., Schoepp D.D., *J.Med.Chem.*, **1997**, *40*, 528-537.

[99] Schoepp D.D., Johnson B.G., Wright R.A., Salhoff C.R., Mayne N.G., Wu S, Cockerham S.L.;, Burnett J.P., Belegaje R., Bleakman D., Monn J.A., *Neuropharmacology*, **1997**, *36*, 1-11.

[100] Monn J.A., Valli M.J., Massey S.M., Hansen M.M., Kress T.J., Wepsiec J.P., Harkness A.R., Grutsch J.L. Jr., Wright R.A., Johnson B.G., Andis S.L., Kingston A., Tomlinson R., Lewis R., Griffey K.R., Tizzano J.P., Schoepp D.D., *J. Med. Chem.*, **1999**, *42*, 1027-1040.

[101] Thomsen C.; Hansen L.; Suzdak P. D., *J. Neurochem*. **1994**, *63*, 2038-2047.

[102] Bräuner-Osborne, H.; Nielsen B., Krogsgaard-Larsen P., *Eur. J. Pharmacol*. **1998**, 350, 311-316.

[103] Pinto A., Conti P.,De Amici M., Tamborini L., Madsen U., Nielsen B., Christensen T., Bräuner Osborne H. and De Micheli C., *J. Med. Chem*., **2008**, 51, 2311-2315.

[104] Conti P., De Amici M., De Sarro G., Rizzo M., Stensbøl, Bräuner-Osborne H., Madsen U., Toma L., De Micheli C., *J.Med.Chem* **1999**, *42***,** 4099-4107.

[105] Assaf Z., Larsen A. P., Venskutonytė R., Han L., Abrahamsen B., Nielsen B., Gajhede M., Kastrup J. S., Jensen A. A., Pickering D. S., Frydenvang K., Gefflaut T. and Bunch, L. *J.Med.Chem*., **2013**, *56*, 1614-1628.

[106] Nielsen B. S., Banke T. G., Schousboe A. and Pickering D. S*., Eur. J Pharmacol.* **1998**, *360*, 227-238.

[108] Jensen A.A., Bräuner-Osborne H., *Biochem. Pharmacol*. **2004**, *67*, 2115-2127.

[109] Pinto A., Conti P., De Amici M., Tamborini L., Madsen U., Nielsen B., Christesen T., Bräuner-Osborne H. and De Micheli C., *J. Med. Chem.*, **2008**, *51*, 2311–2315.

[110] Dondoni A., Massi A., Minghini E., Sabbatini S., Bertolasi V., *J. Org. Chem.* **2003**, *68*, 6172-6183.

[111] Pinto A., Tamborini L., Mastronardi F., Ettari R., Safoz Y., Bunch L., Nielsen B., Jensen A.A., De Micheli C. and Conti P., *Eur. J. of Med. Chem*. **2014**, *75*, 151-158.

[112] Tamborini L., Pinto A., Smith T. K., Major L. L., Iannuzzi M.C., Cosconati S., Marinelli L., Novellino E., Lo Presti L., Wong P.E. et al., *ChemMedChem* **2012**, *7*, 1623-1634.

[114] Dolman N. P., More J. C. A.;, Alt A., Knauss J. L., Troop H. M., Bleakman D., Collingridge G. L., Jane D. E., *J. Med. Chem,* **2006***, 49,* 2579-2592.